Plant photosynthesis and productivity on Earth in the high CO_2 21st century.
Informing simulations with experimental data.

Anthony P Walker

April 2012

PhD Thesis
Department of Animal and Plant Sciences
University of Sheffield

Supervisors:

Professor F. Ian Woodward
University of Sheffield

Dr Chris Huntingford
Centre for Ecology and Hydrology

Acknowledgements

I'd like to start at the beginning by thanking Rosie Fisher for her willing help in answering all my questions the early days of this PhD. Her advice and suggestions very much helped to put me on track. Many, many thanks are necessary to Joanna Scales who volunteered her summer in 2010 to help with experimental work. There is no way that I could have done all of the work that I had set myself in that year without her.

Thanks to Katie Field for loaning me her greenhouse space, thanks to Janice Lake and Colin Osborne for support with the experimental design, thanks to John Shutt and Steve Fletcher for their help with experimental equipment and Ian Wraith for the loan of a signal generator from the Electrical and Electronic Engineering Dept. Additional thanks go to Darren Rose, Stuart Pearce and Greg Nicholson for running the growth chambers and to Keith Parkinson for helping to optimise the IRGA.

Many thanks to my second supervisor Chris Huntingford, for his enthusiasm, interest, useful comments and encouragement. Thanks to Andrew Beckerman for help with understanding mixed-model multiple regressions and Peter Mitchell for help with ANOVA. Thanks are in order to Jayne Young for support and navigating the University finance system for me. Thanks to Hazel Basford and Sue Carter for additional support with finances and admin.

Many thanks go to my parents, Richard and Dominique Walker, for their whole hearted support. The friends that have helped me along the way are too numerous to name individually but a few need to be named for their advice, care and support through some dark days, those people are Rob Lowe, Emilie Taylor, Moira Walker, Robin Dobson, Tina Basi, Angus Hunter, Jagroop Pandhal, Emma Reynolds and Geoff Gibson.

Of course, many thanks are due to my supervisor, Ian Woodward for his support all the way through this PhD. Thanks for your door always being open and many thanks for providing me with opportunities; supporting me and encouraging me in all the travels, conferences and external activities that I have been lucky enough to have through the course of this PhD. Thanks very much to Rich Norby for his support and provision of many of those opportunities and I look forward to working with you at Oak Ridge in Tennessee. Lastly, huge thanks go to Mark Lomas for his willingness to help and problem solving with SDGVM and JULES, without which I would have struggled a lot, lot harder.

Abstract

Understanding how plant productivity responds to CO_2 is crucial to understanding Earth System dynamics and therefore, predicting the Earth System's response to anthropogenic forcing of atmospheric CO_2. Free Air Carbon dioxide Enrichment (FACE) experiments test the CO_2 response of semi-natural forest stands over the course of a decade of CO_2 enrichment and this Thesis informs and develops global carbon cycle modelling using FACE data.

Meta-analysis of FACE experiments showed maintained productivity gains, and no evidence of photosynthetic acclimate to elevated CO_2, over nine years of enrichment. An artefact of FACE methods is that CO_2 concentrations oscillate at high frequency (1 oscillation per minute) and high amplitude (400–900 μmol mol^{-1}) with the potential to impact carbon assimilation. Chapter three demonstrated that carbon assimilation was increased in *Quercus robur* and *Populus* x *euramericana* compared to steady state CO_2.

Simulation of the Oak Ridge and Duke FACE experiments showed that both the Sheffield Dynamic Global Vegetation Model (SDGVM) and the Joint UK Land Environment Simulator (JULES) could reproduce Net Primary Productivity (NPP) with a reasonable degree of accuracy once V_{cmax} was accurately parameterised. This research highlights the necessity of rigorous model testing with observed data and shows the need to develop a strong, cross model, benchmarking system.

A global meta-analysis assessed the response of V_{cmax} to leaf nitrogen and phosphorus showing that phosphorus reduced the sensitivity of V_{cmax} to nitrogen. Global simulation with the empirical V_{cmax} to leaf nitrogen and phosphorus relationship led SDGVM to over-predict Gross Primary Productivity (GPP) and biomass, yet lowered terrestrial CO_2 sequestration over the course of the 20^{th} and 21^{st} century due to higher rates of soil respiration.

Model bias and compensating factors are highlighted and correction of parameterisation error showed that more explicit process representation is necessary in SDGVM. Areas highlighted for model development were: nitrogen cycle simulation; V_{cmax} and J_{max}; parameterisation; experimental quantification of the effect of soil water stress on forest productivity and the simulation of biomass and mortality. Accurate global datasets of biomass, NPP and leaf traits will help to uncover model bias and compensating factors and will help to develop model processes.

Table of Contents

List of Tables

List of Figures

Chapter 1 Introduction

We face a high CO_2 world. By 2100, with current emission rates (Le Quéré et al. 2009), the atmospheric CO_2 concentration is likely to be between 600 and 1050 µmol mol^{-1}, or two to four-fold higher (Sitch et al. 2008) than the pre-industrial maxima of280 µmol mol^{-1} observed in ice-cores stretching back 800,000 years into the past (Wolff 2011). Given a particular projection of future CO_2 emissions, much of the uncertainty in predicting future atmospheric CO_2 trends has been due to uncertainties in the response of terrestrial ecosystems (vegetation and soils) to increased CO_2 and changing climate (Friedlingstein et al. 2006). Negative feedback from the land surface, as well as negative feedback through physical and biological ocean pumps, has slowed the observed rise in global atmospheric CO_2 concentration over the past 150 years(Canadell et al. 2007). Approximately half the fossil fuel and land use change emissions have been sequestered by the terrestrial biosphere and the ocean's and the majority of the annual variability in the CO_2 sink is due to variability in the sink strength of the terrestrial biosphere (Canadell et al. 2007).

Global climate is intimately linked to atmospheric CO_2 and—if the majority of scientific literature and opinion is correct—consequences of increasing atmospheric CO_2 are increasing global temperatures and changing patterns of climate (Solomon et al. 2007, Allen et al. 2009). Climate change is arguably the most politicised scientific issue of our day as it has the potential to face every person on the planet with changing and potentially unstable weather patterns (Parry et al. 2007). Scientists must provide accurate information, including the limitations of our understanding, to allow the global population, policy makers and businesses to decide on the risks posed to them by climate change and to plan for the future.

An obstacle to understanding the global carbon cycle and climate change is that they are phenomena of the Earth-System as a whole. Principles of the scientific method are redundant when considering how the Earth System will respond to unprecedented change. Repeatable experimental testing of hypotheses using sampling and treatment replication is impossible, making falsification of competing hypotheses difficult. We have one replicate of one treatment – the historical and the future pattern of anthropogenic CO_2 emission within our planetary system, confounded by anthropogenic forcing of other biogeochemical cycles and against a

background of incomplete knowledge of the state and dynamics of the Earth System before the anthropocene (Steffen et al. 2007).

Computer simulation of the Earth-System is the only way that we can attempt to understand and quantify the future impacts of increasing atmospheric CO_2 on Earth. However, the earth-system is hugely complex and while computer modelling efforts have been commendably successful there are still many gaps in our knowledge. The terrestrial biosphere is particularly complex, integrating sub-cellular processes, such as photosynthesis, through the whole organism to the ecosystem and finally to regional scale carbon sequestration. Even for contemporary periods, there is significant uncertainty in precisely how the land surface is interacting with the full global carbon cycle (Le Quéré et al. 2009).

The Earth System, carbon dioxide and humans

The carbon cycle

Human activity has directly increased the carbon flux to the atmosphere by combusting fossil fuels and disturbing natural ecosystems through changing land-use. Anthropogenic modification of the global carbon cycle is by far the most likely cause of observed global climate change (IPCC 2007).

In 2010 anthropogenic carbon emissions from fossil fuels were 9.14 Pg C yr^{-1} (Peters et al. 2012), increasing at a mean rate of 3.4% yr^{-1} between 2000–2008 up from 1% yr^{-1} in the 1990s(Le Quéré et al. 2009). Carbon emissions from land use change, primarily tropical deforestation, were estimated at 0.87 Pg C yr^{-1}in 2010 (Peters et al. 2012) and at 1.5 Pg C yr^{-1} from 1990–2005 (Le Quéré et al. 2009). Total anthropogenic carbon emissions from fossil fuel burning and land-use change, since pre-industrial times to 2000,were estimated at 244 Pg C (Denman and Lohmann 2007) with a total increase in atmospheric carbon estimated at 165 Pg C or 68%, known as the airborne fraction, indicating an increase in the carbon flux from the atmosphere (the carbon cycle is assumed to have been in equilibrium prior to the industrial revolution).

The mean annual airborne fraction was 43% from 1959-2008 (Le Quéré et al. 2009) with mean annual ocean uptake estimated at 2.2±0.4 Pg C yr^{-1} and land uptake estimated at 2.6±0.7 Pg C yr^{-1} between 1990 and 2000. Denman and Lohmann (2007) estimated the total increment of the ocean carbon pool since pre-industrial times at 118 Pg C. Total loss of terrestrial carbon to the atmosphere due to human land use was estimated at 156 Pg C (Houghton 2003). To balance the cycle total atmospheric carbon uptake by the terrestrial biota was estimated at 101 Pg C(Denman and Lohmann 2007), within the range of estimates by Sabine et al. (2004), given as 61 to 141 Pg C. The balance between carbon emissions and the strength of the ocean and land sinks has led to an increase in atmospheric CO_2 concentration from 278 µmol mol^{-1} in the pre-industrial period to 392 µmol mol^{-1} at Mauna Loa, Hawaii in February 2012 (Tans and Keeling 2012).

Plant responses to CO_2 and scaling to the Earth System

CO_2 fertilisation

Atmospheric CO_2 increase has been subject to negative feedback resulting from an increased flux of carbon from the atmospheric pool to the terrestrial and oceanic pools (Canadell et al. 2007). Known as the 'CO_2 fertilisation effect', higher rates of photosynthesis are translated into higher plant growth rates and terrestrial plant biomass (Taylor and Lloyd 1992). Higher levels of atmospheric CO_2 increases photosynthetic carboxylation efficiency by relieving substrate limitation of the enzyme Ribulose 1-5 Bisphosphate Carboxylase/Oxygenase (RuBisCO) and increasing the carboxylation to oxygenation ratio of RuBisCO (Farquhar et al. 1980, Stitt 1991).

Photosynthetic acclimation at elevated atmospheric CO_2

Many enclosure studies on the effect of elevated CO_2 on photosynthesis have identified acclimation of the photosynthetic rate after a prolonged period of exposure to elevated atmospheric CO_2 (Arp 1991, Stitt 1991, Kurasova et al. 2003, Xiao et al. 2008). Acclimation in this context describes down-regulation of the photosynthetic rate so that carbon use efficiency (CUE—carbon assimilation divided by the atmospheric CO_2 concentration) of plants grown at elevated $CO_2$is significantly lower than those of plants grown at ambient CO_2 concentrations (Arp 1991, Woodward 2002).

Experimental evidence has demonstrated that acclimation is related to both the Calvin Cycle and electron transport. Acclimation via the Calvin Cycle occurs via reductions in leaf nitrogen, which is a proxy for leaf RuBisCO concentrations, and carboxylation rates are therefore reduced (Stitt 1991).

In order to incorporate increased carbohydrate due to higher photosynthetic rates under elevated CO_2 into plant biomass, the extra carbon must be stoichiometrically balanced by other elements that are essential components of plant biomass (Elser et al. 2007). In nutrient limited systems it may not be possible for a plant to access more nutrients. Del Pozo et al. (2007) have also shown that nitrogen availability may be reduced at high atmospheric CO_2 due to reduced soil mass flow caused by decreased stomatal conductance and reduced transpiration. Restricted nitrogen availability can limit carbon sink development causing an accumulation of carbohydrate in leaf cells. Accumulated carbohydrate can down-regulate levels of RuBisCO in the leaf (Arp 1991) and nitrogen may be remobilised for use in biomass synthesis in an adaptive

strategy that aims to balance source and sink strength. IndeedRogers and Humphries (2000) showed that acclimation of the photosynthetic rate was strongly correlated with a drop in V_{cmax}—the RuBisCO (i.e. nitrogen) limited maximum rate of photosynthesis, discussed below.

Acclimation via electron transport is caused by increased competition for the reducing products, ATP and NADPH, used in the Calvin Cycle and the nitrite assimilation pathway (Searles and Bloom 2003, Yong et al. 2007). At high nitrogen levels it has been proposed by Yong et al. (2007) that photosynthesis acclimates due to higher nitrogen uptake under elevated CO_2, presumably due to higher nitrogen demand.

The exact processes behind acclimation of photosynthesis to elevated CO_2 have not been fully analysed but a prevalence of nitrogen limitation, and therefore decreased leaf nitrogen concentrations, as a major cause of this phenomenon has been well documented (Arp 1991, Tocquin et al. 2006, Del Pozo et al. 2007). However this correlation did not necessarily mean nitrogen limitation was the cause of photosynthetic acclimation, but that RuBisCO activity was closely tied to the photosynthetic rate.

Climate change

Climate change is expected to impact on terrestrial ecosystems in multiple ways, and that are highly dependent on the particular alterations made by humans to atmospheric gases that are radiatively active (i.e. gases that influence climate but each gas having a different impact). Huntingford et al. (2011) demonstrate in a conceptual study, normalising the effect of each radiative forcing agent to a forcing of +1 Wm^{-2}, how the physiological impacts on terrestrial ecosystems vary strongly between changes to CO_2, non-CO_2 greenhouse gases, ozone, decreasing sulphates – and any imposed climate change. In reality, it is radiative forcing associated with CO_2that is the most important.

The impacts of climate change on terrestrial vegetation are different, and often of opposite sign, to the direct impacts of elevated CO_2. Temperature and precipitation change are likely to have the biggest impacts on vegetation through modification of ecosystem processes and characteristics and increases in frequency and magnitude of extreme events (Karl et al. 1995, Easterling et al. 2000, Beniston et al. 2007). Increases in storm severity and extreme climate events in general may have a large impact on mortality events in eco-systems (Fuhrer et al. 2006, McDowell et al. 2011). Chronic changes in temperature are also impacting predation and

pathogen events in forest ecosystems by relieving predators and pathogens from cold mortality during winter months (Cullingham et al. 2011, Sturrock et al. 2011).

Therefore, central to estimating future terrestrial ecosystem carbon stocks is the balance between the often detrimental effects of imposed climate change and photosynthetic fertilisation due to raised atmospheric CO_2 concentrations.

Model predictions of atmospheric CO_2 increase over the 21st century

A key goal of climate research is to accurately predict the link between a range of different CO_2 emissions scenarios, and their impacts in terms of climate change. This link has two components – first, emissions must be balanced by other sources and sinks to determine the atmospheric CO_2 pool and therefore atmospheric carbon dioxide concentrations, and then from here, associated changes in surface meteorology must be estimated. The 5th IPCC report recognises this differentiation and policy recommendations will be based predominantly on the Representative Concentration Pathways (RCPs;Moss et al. 2010).

Translation of the RCPs to amounts of global warming will inform whether a particular pathway is compatible with a target threshold, such as keeping global warming below two degrees. RCPs need translating from emissions to allow socio-economists to state whether rates of decarbonisation required for particular pathways are feasible. Critical to this mapping are accurate predictions of how much CO_2 the natural components of the Earth system (predominantly terrestrial ecosystems and the oceans) can "draw-down" and thus mitigate emissions. Hence, the stronger the natural sink, the higher the amount of "permissible emissions" to achieve a particular concentration pathway.

Given a particular scenario of anthropogenic greenhouse gas emissions from fossil fuel burning, industrial activity and land use change (Nakicenovic et al. 2000), the terrestrial carbon cycle is the major driver of atmospheric CO_2 concentration over the time-scale of decades (Cramer et al. 2001, Canadell et al. 2007). Through its influence on atmospheric CO_2, the terrestrial carbon cycle will be a key driver of future climate change (Huntingford et al. 2009). Models 'forced' with various CO_2 emissions scenarios taken from the Special Report on Emissions Scenarios (SRES - Nakicenovic et al. 2000) have predicted changes in the state and dynamics of atmospheric CO_2 and the global carbon cycle that vary widely (Cramer et al. 2001, Friedlingstein et al. 2006, Denman and Lohmann 2007, Sitch et al. 2008, Huntingford et al. 2009). Predictions of future global change are generated by running these models.

Model uncertainty

Cramer et al. (2001) investigated the outcomes of HadCM2-SUL GCM predictions of climate change to drive six Dynamic Global Vegetation Models (DGVMs) using the IPCC IS92a scenario (Legget et al. 1992), a 'business-as-usual scenario' with regards to emissions. Ten-year mean

net ecosystem productivity (NEP, i.e. terrestrial land carbon uptake) by 2100 ranged from 0.3 Pg y^{-1} to 6.8 Pg y^{-1}.

Sitch et al. (2008) demonstrated that different DGVMs created a range in atmospheric CO_2 prediction for the 21st century that was increased when feedback was considered between terrestrial carbon flux, atmospheric CO_2 and climate change. They also demonstrated that the largest variability in the prediction of atmospheric CO_2 came from the emissions scenario.

Scholze et al. (2006) investigated the outcomes of 16 different GCMs coupled with a single DGVM, the Lund-Potsdam-Jena model (LPJ), under four different SRES scenarios. The models predicted a wide range of land ecosystem carbon uptake by the year 2100. For the A2 SRES the range of predicted carbon flux from the atmosphere to the land was from -4.1 Pg C y^{-1} (PCM model – also the 20 year mean) to 8.2 Pg C y^{-1} (HadCM3 model, although this was rather extreme – the 20 year mean for HadCM3 stood at 1.9 Pg C y^{-1}).

Friedlingstein et al. (2006) investigated the outcomes from 11 coupled earth-system models used by various research groups under the A2 SRES scenario. Each model consisted of one of 11 GCMs, one of nine terrestrial carbon cycle models (4 DGVMs and 5 land surface schemes) and one of nine ocean carbon cycle models. Predicted land carbon uptake in 2100 ranged from -6.0 Pg C y^{-1} to 11.0 Pg C y^{-1}.

Huntingford et al. (2009) used a simple climate carbon-cycle model to investigate the differences in the behaviour of 11 high-profile climate models. They demonstrated that although variability in GCM structure and parameters caused large uncertainty in prediction of future temperature increase, variability in carbon cycle structure and parameterisation also played an important role.

Findings from Cramer et al. (2001), Friedlingstein et al. (2006), Scholze et al. (2006), Sitch et al. (2008) and Huntingford et al. (2011) demonstrate that there was large variability and therefore uncertainty in predictions of terrestrial-ecosystem carbon uptake by the year 2100. The range of terrestrial carbon uptake generated by DVGM or GCM choice was similar, 6.9 Pg y^{-1} (10 year mean) and 6.0 Pg y^{-1} (20 year mean) respectively. However, in the first instance the range was due to variation in predicted response of terrestrial vegetation to a single climate scenario whereas in the second instance the range was due to variation in predicted climate change scenario.

Currently the terrestrial biosphere exerts negative feedback on atmospheric carbon increases (Denman and Lohmann 2007). However, most modelling studies show that following an increase in magnitude, the strength of negative feedback on atmospheric carbon decreases and even has the potential to reverse resulting in runaway increases in atmospheric carbon; caused by forest mortality and loss of soil carbon, and leading to increased global temperatures and climate change (Cox et al. 2000, Cramer et al. 2001).

Simulated carbon uptake should be nitrogen limited

The strength of negative feedback on atmospheric CO_2 rise by the terrestrial biosphere is limited by the capacity of the terrestrial biosphere to sequester more carbon. Stimulation of carbon sequestration by increased photosynthetic rates assumes that plant growth is carbon limited. Millard et al. (2007) propose that this is not the case and that plant growth, in the majority of cases, is nitrogen limited.

Hungate et al. (2003) studied the nitrogen requirements of global vegetative biomass increases predicted by DGVMs, some of them components of the GCMs used in the last IPCC report. Using carbon-to-nitrogen ratios (C:N; tree = 200, soil = 15) they calculated an increased global nitrogen demand of 2.3 to 16.9 Pg by 2100, yet a supply of only 1.2 to 6.1 Pg nitrogen (based on estimates of deposition, volatisation, leaching and fixation). Only two (SDGVM and HYBRID) of six models fell within this range of future nitrogen supply—the two which explicitly simulate nitrogen uptake. Due to the low carbon to nitrogen ratios of the soil, nitrogen requirements to match additional carbon assimilation are sensitive to soil C:N. In the supplementary material, Hungate et al. (2003) qualify that an increase in soil C:N from 15 to 18.3 would be sufficient to bring all models' nitrogen requirements into realistic projections of nitrogen availability. Gill et al. (2002) showed that in a chamber experiment soil C:N ratios and absolute carbon both increase at higher CO_2 concentrations.

A number of models have now been developed to simulate a full, mass-balanced nitrogen cycle (Thornton et al. 2007, Zaehle and Friend 2010) and even nitrogen and phosphorus cycles (Wang et al. 2007b) which show that CO_2 fertilisation is reduced by nitrogen limitation. However, only Zaehle et al. (2010) extend their simulations to 2100 demonstrating that nitrogen limitation reduced CO_2 fertilisation, resulting in atmospheric CO_2 48 μmol mol^{-1} higher in 2100 than simulations without nitrogen limitation.

Model Calibration and Validation

How much confidence can be placed in the predictions of a computer model? In order to be confident in the model predictions Rykiel (1996) emphasised the need to rigorously test ecological models for simulation accuracy within their domain of applicability. Confidence can be gained by looking at the success of the model's calibration and validation. Calibration is the tuning of the processes simulated within the model using experimentally determined relationships between the driving variables and the variables that the model is trying to simulate. Validation is testing the accuracy of model predictions, once the processes have been calibrated, against an observed data set separate from the calibration dataset (Rykiel 1996). The processes of calibration and validation both need to measure the predicted data's goodness of fit (GOF) with the observed data. We can have confidence in a model when these GOF measurements are satisfactory.

Rykiel (1996) stated that:

> Whenever validation is required, the modeller must specify three things: (1) the purpose of the model, (2) the criteria the model must meet to be acceptable for use and (3) the context in which the model is intended to operate.

The purpose of dynamic global vegetation models is to simulate terrestrial carbon cycling. To be acceptable for use they must accurately simulate current terrestrial productivity and carbon stocks based on accurate simulation of carbon fluxes and vegetation biome boundaries. The context in which carbon cycle models are intended to operate is that of increasing atmospheric CO_2 and change in global temperature, precipitation and radiation patterns and therefore models need to be able to simulate the response of terrestrial productivity and biomass to increased CO_2 against a background of climate variability.

DGVM validation

There has been progress in developing, parameterising and validating terrestrial carbon cycle models (Pitman 2003). Considerable use has been made at the site scale of eddy correlation data which measure land-atmospheric fluxes of momentum, heat, water vapour and more recently, carbon dioxide, and all simultaneously with meteorological measurements (Blyth et al. 2011). At the global scale various satellite derived products (which often depend upon a model of their own) (Lawrence and Chase 2007), land-cover datasets (Cramer et al. 2001, Woodward and Lomas 2004), and most recently a globally gridded map of GPP from the FLUXNET

community (Bonan et al. 2011b) have been used for validation, providing detailed spatial information on the extent and function of terrestrial ecosystems. CO_2 flask measurements provide a global value of mean atmospheric CO_2 and thus a constraint for carbon cycle models when analysing their ability to depict the contemporary period (Schwalm et al. 2010).

DGVMS can also be forced with local observed climatic data at an individual experimental site. The FLUXNET experimental sites (Baldocchi et al. 2001) using the eddy covariance techniques are particularly useful for this kind of validation. Model outputs are then compared with experimentally observed factors such as net ecosystem CO_2 exchange (NEE), latent heat fluxes and sensible heat fluxes (Mercado et al. 2007, Wang et al. 2007b, Zaehle and Friend 2010, Blyth et al. 2011).

Until recently the effect of elevated CO_2 in terrestrial carbon cycle models has been implicitly validated, rather crudely, on the basis that models reproduce with some degree of accuracy the observed global rise in atmospheric CO_2 from pre-industrial times to the present day (Cramer et al. 2001). Although confounded by other factors, the models' responses to CO_2 were shown to be poorly represented due to the wide divergence of predicted CO_2 concentrations into the future given the same forcing scenario (Friedlingstein et al. 2006, Sitch et al. 2008). Spatial and temporal variability in flask CO_2 measurements contains seasonal and inter-annual information on continental-scale variations in CO_2 fluxes. In a more sophisticated, explicit validation of the global CO_2 flux, Cadule et al. (2010) compared the carbon fluxes of three Earth system models against instrumental atmospheric CO_2 observations using a single atmospheric transport model to generate CO_2 concentrations directly comparable at each measurement station. Their results showed that while models were generally reasonable at simulating the long-term trend in carbon fluxes, the models ranged in their ability to simulate carbon fluxes over seasonal and inter-annual cycles and at different sites. Cadule et al. (2010) results provide an excellent new framework for validating global model carbon fluxes simulated by fully coupled Earth System models. All of these measurements are for contemporary periods and allow only a limited understanding of physiological responses to raised (surface) atmospheric CO_2 concentrations.

Cadule et al. (2010) and Blyth et al. (2011) have set a strong precedent for using statistics of model goodness-of-fit (GOF) in the presentation of their validations, giving quantitative comparison of model accuracy. DGVMs appear to have performed well in some validation exercises but models are often not compared on a like-by-like basis i.e. their accuracy at the

same experimental sites has not been compared. It is clear from the discussion above that models diverge significantly in their prediction of future carbon fluxes in a high CO_2 atmosphere (550+ µmol mol^{-1}) for which validation has been difficult.

Free Air Carbon Dioxide Enrichment (FACE) experiments present the opportunity to validate ecosystem scale CO_2 responses to elevated CO_2, 500-600 µmol mol^{-1}, under the same climate. Laboratory-based experiments have been performed to assess the impact of increased ambient CO_2 on photosynthesis and plant productivity (Arp 1991, Stitt 1991). FACE experiments examine the response of natural, semi-natural and agricultural ecosystems to elevated concentrations of atmospheric CO_2 (Hendrey et al. 1993, Hendrey and Kimball 1994, Norby et al. 2010, Drake et al. 2011) over significant periods of time. For this reason, the emerging results from FACE experiments are essential and provide an unprecedented opportunity to validate components of terrestrial carbon cycle models.

Free Air Carbon Dioxide Enrichment

The majority of research has implicated nitrogen limitation as the major cause of photosynthetic acclimation (Sage et al. 1989, Stitt 1991, Rogers and Humphries 2000). However, nitrogen limitation may well be a feature of experimental design as plants grown in pots are restricted in their capacity to respond to nitrogen limitation (Arp 1991, Woodward 2002). Experiments in the field using enclosures or open top chambers have also demonstrated acclimation of photosynthetic rate under elevated CO_2 (Ceulemans et al. 1997) but have themselves drawbacks and environmental influences mediated by experimental design. Free Air Carbon dioxide Enrichment experiments are designed to analyse the effect of elevated atmospheric CO_2 on plants and the ecosystem in the most natural environment possible.

Free Air Carbon dioxide Enrichment (FACE) experiments (Figure 1-1) enrich the local environment with CO_2. Forest stand and field plots are fumigated with CO_2using a wind-driven controlled release mechanism to disperse the CO_2 and CO_2 detection to feedback on the release mechanism. Atmospheric CO_2 is maintained within 10% of the target concentration 90% of the time (based on one minute averages) at wind-speed above 0.4 ms^{-1} (Hendrey et al. 1993).

FACE experiments can address questions such as how plants respond to elevated levels of atmospheric CO_2 under natural field conditions. Does plant photosynthetic apparatus acclimate to elevated CO_2 in the field? And, how does photosynthetic acclimation affect biomass?

FACE and nitrogen

The theory of progressive nitrogen limitation (PNL) states that as woodland systems develop, an increasingly larger fraction of ecosystem nitrogen is locked up in the woodland biomass and therefore the system becomes progressively nitrogen limited (see Gill et al. 2006 for a comprehensive review of PNL). Increased growth under elevated atmospheric CO_2could lead to accelerated PNL (Luo et al. 2006a) and Norby et al. (2010) and Garten et al. (2011) have shown that, in a forest system under going PNL, PNL is accelerated by elevated CO_2.

Gill et al. (2006) showed that in several temperate forests, nitrogen within forest system biomass often increases over and above that attributable to atmospheric deposition. Nitrogen increases in these forest systems have been attributed to biological fixation, uptake from deep soil zones and increased nitrogen scavenging efficiency.

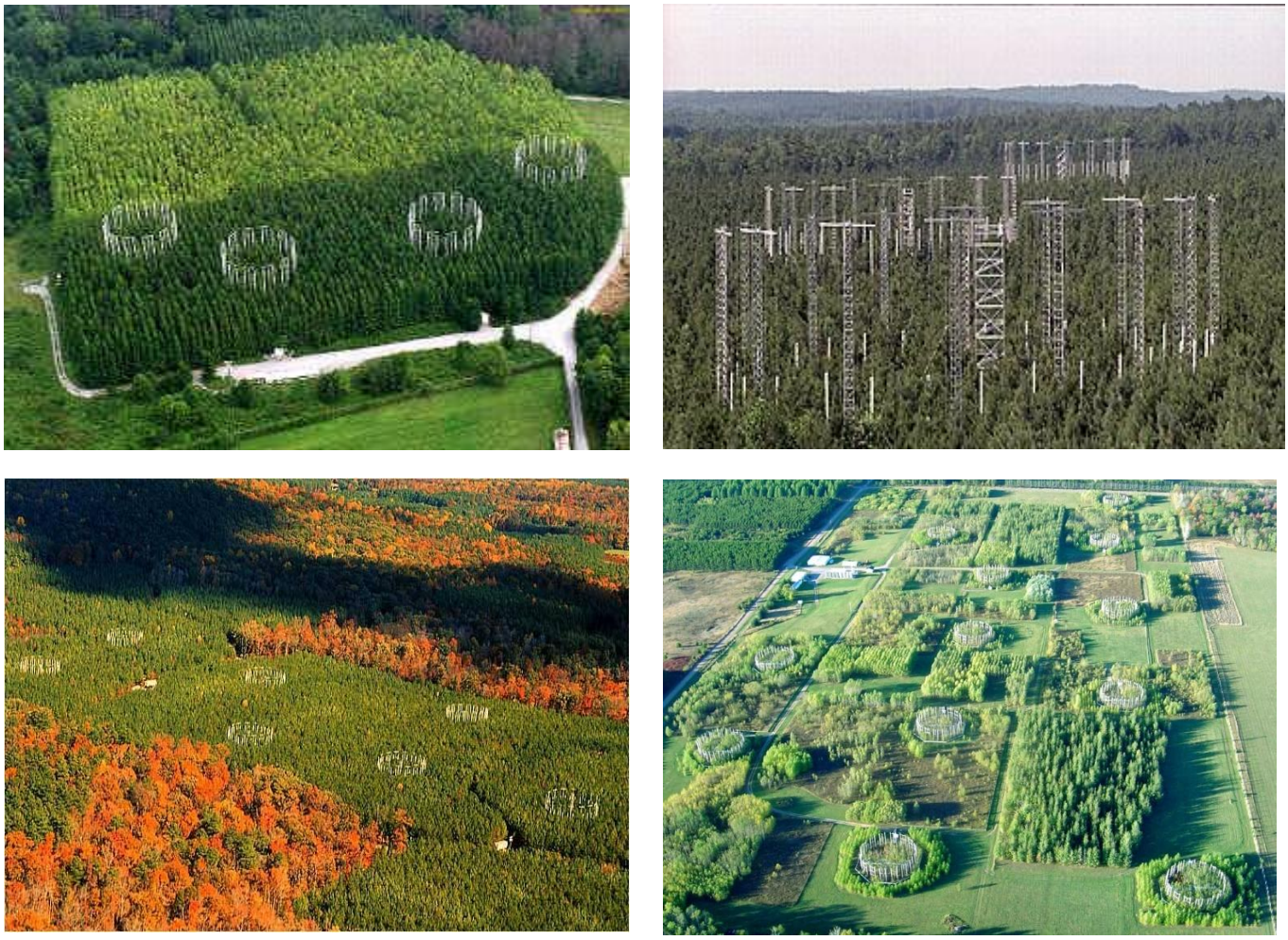

Figure 1-1. Clockwise from topleft: The *Liquidamabar styraciflua* FACE experiment at Oak Ridge, Tennesse ©Oak Ridge National Laboratory, Oak Ridge, Tennessee. Two FACE rings at DukeFACE near Chapel Hill, North Carolina ©Duke FACE project, Duke University, Durham, North Carolina. Layout of FACE rings at ASPENFACE in *Populus tremuloides* stands at Harshaw Experimental Forest near Rhinelander, Wisconsin ©David F. Karnosky. The *Pinus teada* stand surrounded by mixed hardwood forest at DukeFACE ©Will Owens. All photographs reproduced with permission.

In some forest FACE systems increased biomass has been supported by increased nitrogen-use-efficiency or increased nitrogen-scavenging-efficiency (Drake et al. 2011, Zak et al. 2011) and it could be that elevated CO_2 increases a plant's capacity to access nitrogen.

In a synthesis of data from four tree-based FACE sites which all had significantly higher biomass at elevated CO_2, Finzi et al. (2007) showed that at all but one site biomass nitrogen content per-unit-area was increased at elevated atmospheric CO_2 and NPP increased at all four sites. Interestingly the site which showed no change in tree nitrogen content was the only site not limited by nitrogen, indicating a counter-intuitive increase in nitrogen-use-efficiency (NPP/nitrogen uptake) even though nitrogen was readily available. Probably nitrogen uptake was beyond that necessary for growth at ambient CO_2 and the similar nitrogen contents at both CO_2 treatments show that nitrogen was pooled/accumulated beyond growth requirements at ambient CO_2.

At the other three nitrogen-limited sites nitrogen-use-efficiency did not increase, probably because these trees were already at their upper nitrogen-use-efficiency limit. However, overall nitrogen uptake increased at all three sites indicating that increases in NPP were used to increase the efficiency of nitrogen extraction from the soil. Finzi et al. (2006) demonstrated no significant difference in C:N ratio between ambient and elevated CO_2 levels, a result in contrast to many previous findings (Liberloo et al. 2006, Ainsworth and Rogers 2007) probably due to increased nitrogen uptake at these sites yet no increase in nitrogen-use-efficiency.

In an experimentally manipulated prairie system Reich et al. (2001) demonstrated that the magnitude of biomass responses to elevated CO_2 and nitrogen addition was significantly increased with an increase in community diversity. In the same system Reich et al. (2006a) found a significant interaction between elevated CO_2, nitrogen addition and the year of measurement. They demonstrated in the early years (1-3) of the experiment that the percentage increase in biomass caused by elevated CO_2 was greater under the low nitrogen treatment. However, after several years (years 4-6) this reversed and the CO_2 effect was greater under the high nitrogen treatment, indicating that nitrogen limitation became significant to the system over time.

At current CO_2 levels nitrogen (N) is partitioned to photosynthesis (i.e. RuBisCO) at a higher fraction of total N than under higher CO_2 levels (Crous et al. 2008). That nitrogen is partitioned

away from photosynthesis at high CO_2, indicates that carbon is limiting at current CO_2 concentrations. Also at higher CO_2 levels biomass C:N ratios increase (Liberloo et al. 2006), if higher C:N ratios are non-damaging to plants then why do they not have higher C:N ratios at ambient CO_2 levels? As CO_2 levels rise it may be that plants shift from C limitation to N limitation.

Liberloo et al. (2006) reported significant increases in aboveground and belowground plant nitrogen measured as both per-unit-area and per-unit-mass. In an interesting study relating leaf nitrogen on an area basis to photosynthetic rate (carbon fixation rate) Crous et al. (2008) demonstrated that in terms of nitrogen, carbon fixation efficiency of *Pinus taeda* (Loblolly Pine) increased under higher atmospheric CO_2 levels. They also showed that later in the experiment under elevated CO_2 (measurements at 8-9 years) V_{cmax} was reduced in relation to leaf nitrogen for one year old needles. The reduction in V_{cmax} in relation to leaf nitrogen indicated a larger proportion of nitrogen allocated to leaf structure.

Meta-analyses of FACE experiments have demonstrated that photosynthesis is down-regulated and is related to plant nitrogen dynamics. In a meta-analysis of 124 primary FACE studies Ainsworth and Long (2005) calculated an overall mean increase in photosynthetic rate of 23% while recording a mean drop in V_{cmax} of 20% due to elevated atmospheric CO_2 (although they do not quote the exact increase in CO_2 that stimulates this response, most studies elevate by 200 µmol mol^{-1} above ambient CO_2 levels). A break-down of the V_{cmax} results showed a greater decline for grasses than trees and a particularly marked decline across all low nitrogen treatments. Conflicting results for plant nitrogen from meta-analyses have been reported. Ainsworth and Long (2005) showed a 15% drop in leaf nitrogen per unit mass but only a 5% drop per unit area, a figure which they propose is wholly accountable to a 20% drop in RuBisCO per unit area (assuming RuBisCO accounts for 25% total nitrogen). A meta-analysis of studies using a number of CO_2 enrichment methods Taub et al. (2008) found a general decrease in crop grain protein content at elevated CO_2, a decrease that was less marked under high nitrogen fertilisation treatments and close to insignificant for *Glycine max* (Soybean, a symbiotic biological nitrogen fixer).

Limitations of FACE

A goal of FACE experiments is to assess the impact of rising CO_2 on the planet's forest biomes. FACE experiments cover both agricultural and natural systems and a wide range of species and

plant functional types, however tropical and boreal systems are not represented (Hickler et al. 2008). Also, forest FACE experiments are mostly sited in young forests. Bar one, all of the above mentioned systems are either agricultural, grassland/prairie or early stage forestry—there is only one old growth forest FACE experiment. Both young and old forests will be important in determining the response of the land surface to elevated CO2 although the mechanisms by which CO_2 impacts these different age/successional stage systems will be different. For the only FACE experiment in an established, mixed species woodland, Asshoff et al. (2006) showed that only one of four species, *Fagus sylvatica*, had a significant increase of basal area increment in two out of four treatment years. Due to the nature of their experiment there was only one elevated CO_2 replicate and individual trees were considered separate replicates, making it difficult to compare with other FACE experiments. It is recognised that conclusions on forest responses to elevated CO_2 based on FACE data are limited to relatively young, temperate systems.

FACE experiments simulate well the natural environment but are not without artefact. CO_2 concentrations in FACE experiments are not only raised but they oscillate strongly around the target concentration, 350 – 1100 µmol mol^{-1} in the original Brookhaven system (Nagy et al. 1992). The response of assimilation to oscillating CO_2 conditions has been tested in a few crop and tree species and results were varied. At oscillation frequencies similar to those found in FACE experiments, assimilation was stimulated (Evans and Hendrey 1992), remained the same (Hendrey et al. 1997) and was suppressed in comparison with steady state CO_2 concentrations (Holtum and Winter 2003). Holtum and Winter (2003) found evidence that for seedlings of two tropical tree species, high-frequency (3 & 1.5 cycles per minute) oscillations of atmospheric carbon dioxide, characteristic of FACE experiments, can lead to a lower carbon fixation than when atmospheric CO_2 is maintained constant. Hendrey et al. (1997) investigated this issue and found no reduction in electron transport (used as a surrogate for carbon fixed) under high-frequency (1 cycle per minute) atmospheric CO_2 oscillations.

Whether FACE experiments are underestimating plant responses to CO_2 or not they remain the closest experiment to natural conditions. Results from FACE experiments will be useful in testing the validity of DGVMs and in highlighting processes that are as yet poorly understood and hence poorly simulated.

Earth System modelling

Current knowledge of global physical climatic processes, biogeophysical and biogeochemical processes are defined in empirical and theoretical mathematical relationships, which are synthesised into models that simulate the Earth System. There are three main modules of an earth system model:

1) the General Circulation Model (GCM) describing atmosphere energy balance, ocean energy balance, physical cycles and climate.

2) the land surface scheme describing biotic terrestrial interactions with the GCM and terrestrial carbon cycling.

3) the ocean model describing marine biotic interactions with the GCM and the marine carbon cycle.

These models are continually evolving and a full description of earth system climatic modelling would be too large for this review; see Pitman (2003), Denman and Lohmann (2007) and Randall and Taylor (2007) for an overview. This study focuses on the impacts of elevated CO_2 on the carbon cycle component of the land surface scheme.

Land surface and vegetation modelling

The land surface plays a major role in the Earth System, interacting directly with the climate system (Zaehle et al. 2007, Pongratz et al. 2009, Pongratz et al. 2010) and, as described above, vegetation interacts with atmospheric CO_2 in the global carbon cycle. The strength of terrestrial vegetation's interaction in the global carbon cycle responds to elevated CO_2 in the atmosphere and a number of other environmental factors. Previous generations of land surface schemes simulate carbon fluxes. These old land surface models geographically parameterise many properties of the terrestrial biosphere, such as leaf area index (LAI), plant distribution which restricts the full response of the terrestrial biosphere to CO_2 and climate. The latest models that simulate the terrestrial carbon cycle are known as Dynamic Global Vegetation Models (DGVMs). DGVMs differ from the approach of previous land surface schemes to terrestrial carbon cycle modelling by moving towards a more process-based approach to simulating vegetation dynamics, growth, mortality, competition and distribution in response to climate and ecosystem parameters (Cox 2001, Woodward and Lomas 2004).

SDGVM and JULES

The Sheffield Dynamic Global Vegetation Model (SDGVM) and the Joint UK Land Environment Simulator (JULES) are the UK's primary global vegetation models. JULES (Cox 2001, Best et al. 2011, Clark et al. 2011) is a dynamic vegetation land surface scheme used in the Met Office's Unified Model, the various generations of the Hadley Centre models. SDGVM (Woodward et al. 1995, Woodward and Lomas 2004) is a global dynamic vegetation model used primarily for carbon cycle studies. SDGVM does not have a full land surface radiation scheme and therefore cannot be used in a full Earth System model. However, SDGVM is driven by climate and atmospheric CO_2 concentration allowing it to be coupled in a simple Earth System model with the GCM analogue model IMOGEN (Huntingford and Cox 2000, Huntingford et al. 2010) which uses the pattern-scaling technique to simulate the changing climate.

Modelling the CO_2 response

Net Ecosystem Productivity and carbon sequestration

The global carbon cycle is a system made up of pools and fluxes. Soil, wood, leaves and roots are all carbon pools within the terrestrial carbon cycle and each of these pools has properties which determine the residence time of carbon in the pools. Carbon flows between pools and carbon is sequestered if the flow into a pool exceeds outflow. Carbon fluxes into and out of pools are influenced by characteristics of that pool, the environment, and constraints on the capacity of the pool. Many factors influence these processes as represented in Figure 1-2.

Net ecosystem productivity (NEP) is the balance between gross primary productivity (GPP, carbon fixed) and total ecosystem respiration (the sum of autotrophic and heterotrophic respiration) and carbon loses through disturbance events like fires and is the net value of the atmosphere to terrestrial biosphere flux. Global NEP represents annual carbon sequestration by the terrestrial biosphere and poses a problem to model as it is the sum of four fluxes which are much larger than NEP itself. Any small error in one of the three fluxes can strongly affect predictions of NEP.

Subtracting the respiration terms the respiration terms gives us net primary productivity (NPP), the balance between carbon assimilated by plants and that respired by plants over a given time period:

$$NPP = GPP - R_a$$

and

$$NEP = NPP - R_h - D$$

where R_a is autotrophic respiration, R_h is heterotrophic respiration and D is carbon loses through disturbance. The first step in simulating GPP is calculating leaf-level photosynthesis, then scaling to estimate canopy photosynthesis and respiration. Assimilated carbon is then allocated to different biomass fractions; then processes with a longer temporal scale need to be simulated such as plant growth, mortality, ecological dynamics and disturbance events.

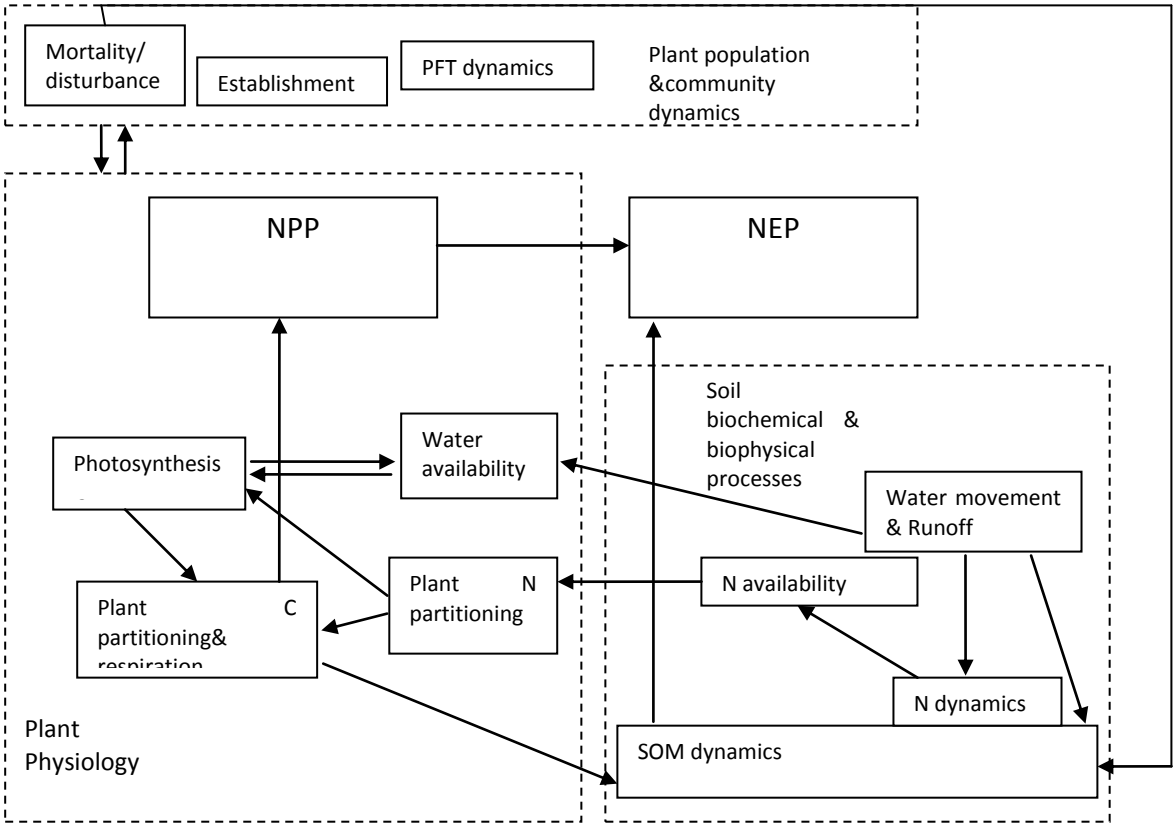

Figure 1-2.A diagram of model processes that influence each other and eventually result in net ecosystem productivity. The dimension of influence not included in this diagram is that of climate, of which the main factors are atmospheric CO_2, temperature and precipitation. We are interested in how changes in these climatic factors, particularly CO_2 affect the relationships of the above system. C partitioning includes the respiratory fraction. PFT – Plant Functional Type.

Leaf carbon assimilation

At the heart of terrestrial carbon cycle models are their leaf-level photosynthesis schemes. Leaf-level photosynthesis is the only route of entry for carbon into the terrestrial biosphere, determining the size of the initial pool which is then distributed to sub-components of the terrestrial carbon cycle. Simulation of leaf level photosynthesis is tightly constrained by biochemical theory and empirical observation (Pachepsky et al. 1996). Most vegetation models use the similar theoretical models of either Farquhar et al. (1980) or Collatz et al. (1992) which mechanistically simulate the biochemical processes of electron transport(Haehnel 1984), the Calvin Cycle and photorespiration (Benson et al. 1950, Calvin 1989). SDGVM uses the Farquhar et al. (1980) formulation while JULES uses the Collatz et al. (1992) formulation.

The models of Farquhar et al. (1980) and Collatz et al. (1992) simulate carbon assimilation as the minimum of three rate limiting processes/factors minus leaf dark respiration: light levels and electron transport; the balance between the rate of carbon (photosynthetic carbon reduction—PCR cycle) and oxygen (photorespiratory carbon oxygenation—PCO cycle) fixation by RuBisCO; and the export rate of photosynthate. Farquhar et al. (1980) simulate carbon assimilation as the minimum of these rates while Collatz et al. (1992) smooth the minimisation of these three rates, effecting a co-limitation where two of the limiting rates are similar. Bonan et al. (2011a) have shown the co-limitation in the Collatz et al. (1992) model to have a significant impact on global Gross Primary Productivity (GPP). Both models simulate the balance between the rate of the PCR and PCO cycle in the same way:

$$A = V_{cmax} \frac{C_i - \Gamma_*}{C_i + K_c(1 + O/K_o)} \tag{1-1}$$

where A is total carbon assimilated (μmol m^{-2} s^{-1}); V_{cmax} is the maximum carboxylation velocity (μmol m^{-2} s^{-1}); C_i is the inter-cellular CO_2partial pressure (μbar) and O is the O_2partial pressure (mbar); K_c is the Michaelis constant for CO_2 (μbar) and K_o is the Michaelis constant for O_2 (mbar) and Γ_* is the compensation point (μbar) of the PCR and PCO cycles where net carbon assimilation is zero.

The Farquhar et al. (1980) and Collatz et al. (1992) models differ in their simulation of the light limited rate of photosynthesis. Light energy is captured by the photosystems of the chloroplast to excite electrons to higher energy status and then these electrons are 'transported' back

down to their energy level at their rest state (Haehnel 1984). Electron transport provides the energy to synthesise the reducing product NADPH and the energy in ATP to regenerate Ribulose 1-5 Bisphosphate (the substrate to which RuBisCO fixes CO_2) in the Calvin Cycle. Farquhar et al. (1980) simulate electron transport as follows:

$$J = 0.5(1 - f)I \tag{1-2}$$

Where *J* is the maximum rate of electron transport (μEq m^{-2} s^{-1}); *f* is the fraction of incident light not absorbed by the chloroplast and *I* is the incident light (μmol m^{-2} s^{-1}). Electron transport is then converted to the light limited rate of carbon assimilation by:

$$J' = \frac{J}{2(2 + 2\phi)} \tag{1-3}$$

where *J'* is the maximum rate of carbon assimilation allowed by electron transport and ϕ is the ratio of oxygenation to carboxylation of the PCR and PCO cycles, which is a saturating function of internal CO_2 concentration (Farquhar et al. 1980). Equation (1-2 simulates electron transport as a linear function of incident light, however Farquhar et al. (1980) assume that the light response of electron transport has a biochemical maximum that saturates at an upper limit, J_{max}. Therefore they assume that J is the minimum of J calculated in equation(1-2 and J_{max} (in practice their model smoothes this minimum function using a quadratic). Collatz et al. (1992) assume that electron transport does not light saturate, simulating light limited carbon assimilation as:

$$J' = a.\alpha.I\frac{C_i - \Gamma_*}{C_i + 2\Gamma_*} \tag{1-4}$$

Where a is leaf absorptance to incident PAR (1-*f*) and α is the intrinsic quantum efficiency for CO_2 uptake.

Both the RuBisCO limited rate of photosynthesis (Equation 1-1) and the light limited rate of photosynthesis (Equations 1-3 & 1-4) are functions of inter-cellular CO_2 concentration. Increasing inter-cellular CO_2 increases substrate availability to RuBisCO and, all else being equal,

RuBisoCO limited carbon assimilation is a saturating function of C_i (Equation 1-1).Increasing inter-cellular CO_2 also increases the efficiency of RuBisCO by increasing the ratio of the PCR cycle to the PCO cycle which reduces the demand for products from electron transport per unit of carbon assimilated (Stitt 1991).Therefore, light limited carbon assimilation is also a saturating function of internal CO_2 concentration (Equations 1-3 & 1-4).

Parameters in Equations 1-1 to 1-4 above are derived from experimental observation and are, in some cases, sensitive to temperature. V_{cmax} is determined as a function of leaf nitrogen (Farquhar et al. 1980, Field and Mooney 1984) and J_{max} is determined as a function of V_{cmax} (Wullschleger 1993, Beerling and Quick 1995).

Water stress also impacts carbon assimilation and JULES and SDGVM simulate water stress in a similar way by determining a water stress multiplier—β, with a range of 0-1—as a function of soil water content below a 'critical' soil water content down to field capacity (Woodward et al. 1995, Clark et al. 2011). In SDGVM V_{cmax} and stomatal conductance are multiplied by β, while in JULES β is applied by multiplying β with assimilation.

Scaling of leaf-level photosynthesis to Gross Primary Productivity

Gross Primary Productivity (GPP) is the carbon assimilation of a whole plant or ecosystem over a given time period. To scale photosynthesis from the leaf level to the whole plant it is necessary to account for assimilation through the canopy(Haxeltine and Prentice 1996). Light is attenuated as it penetrates the canopy. Light levels directly impact the calculation of carbon assimilation through the light limited scheme but also indirectly through the RuBisCO limited scheme. Leaf nitrogen is strongly related to leaf RuBisCO and, as a limiting resource, nitrogen should be distributed through the canopy to maximise carbon gain yet minimise canopy nitrogen allocation. To optimise carbon assimilation it was assumed that nitrogen should be distributed in a linear relationship to the light distribution through the canopy(Chen et al. 1993). SDGVM allocates leaf nitrogen in a particular canopy layer as a proportion of total canopy nitrogen, using the Beer-Lambert law of exponential light attenuation using a coefficient of 0.5 for each canopy layer i.e. leaf nitrogen decreases exponentially through the canopy (Woodward et al. 1995).

However, the Beer-Lambert law describes light attenuation through a homogeneous medium and plant canopies do not conform to this criterion. Through all the layers in a canopy a fraction

of leaves receive direct light from the sun. The Beer-Lambert law is insufficient to describe light coming from the sun passing through the atmosphere, as scattering by atmospheric aerosols splits the sun's radiation into a direct and a diffuse component. Both of these simplifications are considered by SDGVM which uses the Spitters et al. (1986) formulation of canopy light interception. JULES also recognises these complications of canopy light interception and simulates interception using the Sellers et al. (1992) two-stream approach as described and modified by Mercado et al. (2007). Mercado et al. (2009) demonstrated the importance of simulating the diffuse light fraction on the global carbon balance. JULES also recognises that the distribution of nitrogen through the canopy is not according to the Beer-Lambert law and uses an exponential extinction coefficient of 0.78 (Mercado et al. 2007).

Simulation of plant growth responses to nitrogen

Nitrogen interacts with plant growth by stoichiometrically limiting sink production and determining the V_{cmax} (and therefore J_{max} in the Farquhar formulation) parameter via leaf nitrogen. SDGVM simulates canopy nitrogen as a fixed proportion of nitrogen uptake determined by an availability-based function of soil carbon (per-unit-area), soil nitrogen (per-unit-area) and temperature (Woodward and Smith 1994). Nitrogen concentration in the top canopy layer is a fixed input parameter in JULES. SDGVM and JULES do not partition nitrogen to other tissues and therefore nitrogen does not stoichiometrically limit biomass accumulation. Nitrogen directly affects carbon assimilation through its relationship with V_{cmax} (SDGVM and JULES) and J_{max} (SDGVM only).

Thornton et al. (2007) coupled a nitrogen cycle and growth limitation model (Biome BGC) to the Community Land Model 3.0 (CLM3) and found that carbon uptake was 74% less under a nitrogen limited simulation (to 2100, A2 SRES).

Gutschick (2007) has developed a model integrating nitrogen uptake and photosynthesis using it to predict interspecific changes in fitness at elevated atmospheric CO_2. They predict large relative changes in interspecific fitness due to heterogeneity of interspecific changes in nitrogen uptake rates at elevated atmospheric CO_2. Changes in fitness are likely to have significant effects on biogeographic patterns influencing terrestrial carbon cycle dynamics.

While Gutschick (2007) did not investigate global NPP in response to nitrogen and atmospheric CO_2 increase, the results highlight the importance of considering nitrogen in carbon cycle

modelling. The work of Hungate et al. (2003) suggests that quantifying the interaction of carbon and nitrogen dynamics through plants and in particular soils is the major neglected element of terrestrial carbon cycle modelling.

Plant respiration

Simulated respiration is partitioned into maintenance respiration, which supports metabolism and maintains plant function, and growth respiration which provides carbon skeletons and energy as the raw materials for growth. In common with many DGVMs, both SDGVM and JULES simulate growth respiration as 25% of carbon allocated to growth.

Maintenance respiration is simulated separately for each tissue type (leaf, root and sapwood) as a function of tissue nitrogen content, temperature (air or soil) and water stress (not all models). SDGVM simulates night-time leaf respiration (µmol m^{-2} s^{-1}) as 0.17 multiplied by leaf nitrogen (g m^{-2}). Root and stem respiration are taken from their respective biomass pools calculated as a function of their respective biomass and temperature:

$$R = r.\beta.B(0.14e^{0.02t}) \quad (1\text{-}5)$$

Where *R* is respiration (µmol m^{-2} s^{-1}); *r* is the proportion of biomass respired (µmol mol^{-1} s^{-1}); β is the soil water limitation multiplier; *B* is the biomass (mol m^{-2}) and *t* is temperature (^{o}C). JULES simulates maintenance respiration as a function of nitrogen and temperature. Leaf 'dark' respiration (daytime mitochodrial respiration, termed 'dark respiration' to distinguish it from photorespiration as it is equivalent to the respiration that occurs only at night time) is suppressed in JULES when light levels exceed 10 µmol m^{-2} s^{-1}, in line with current theory (Thornley and Cannell 2000). In the version of JULES used in this study (v2.1.2, canopy radiation model 4) dark respiration is simulated as a proportion of V_{cmax} meaning that the temperature sensitivity of respiration is not exponential but has a temperature optimum (Clark et al. 2011):

$$m_t = \frac{2^{0.1(t-25)}}{\left(1+e^{0.3\left(t-t_{upp}\right)}\right)\left(1+e^{0.3(t_{low}-t)}\right)} \quad (1\text{-}6)$$

Where m_t is the temperature sensitive multiplier on the value of V_{cmax} and respiration at 25^{o}C; *t* is temperature and t_{upp} and t_{low} are PFT specific parameters. Whole plant respiration is then

scaled by proportion of root and stem nitrogen to canopy nitrogen, and canopy nitrogen is adjusted for soil water limitation:

$$R_p = 0.012 R_d \left(\beta + \frac{N_r + N_s}{N_c}\right) \quad (1\text{-}7)$$

where R_p is whole plant respiration (kg C m^{-2} s^{-1}); R_d is dark respiration (mol m^{-2} s^{-1}) and N is the nitrogen content (kg m^{-2} s^{-1}) of roots(r), stem(s) and canopy (c). While there is some controversy (Drake et al. 1999, Holtum and Winter 2003) it is generally thought that elevated atmospheric CO_2 concentrations do not directly affect plant respiration rates (Tjoelker et al. 1998) and models do not simulate any direct response of respiration to CO_2.

Carbon partitioning and biomass

Scaling of plant level GPP and NPP to geographical unit level (grid-square level) varies from model to model. Some scale up photosynthesis based on fractional coverage of plant functional types over the whole grid-square (Sitch et al. 2003, Woodward and Lomas 2004). Others simulate all individuals in a small plot (e.g. 30m x 30m) (Friend et al. 1997, Sato et al. 2007) - mean of 10 stochastic plots), known as a gap model, and then multiply this up to grid-square scale. Moorcroft et al. (2001) use partial differential equations to approximate the average of an 'ensemble' of stochastic gap model runs.

NPP must be partitioned to various plant tissue/biomass pools which have various residence times before mortality when they are transferred to the soil carbon pool. Through differing residence times and decomposition rates once part of the soil organic carbon pool the ratios of biomass pools determine the longevity of terrestrial carbon.

NPP can be partitioned to the various biomass pools either proportionally (Cox 2001), allometrically with regards to leaf biomass (Sitch et al. 2003) or certain pools can be prioritized using a demand-based approach (Woodward and Smith 1994). ORCHIDEE (Krinner et al. 2005) allows only 80% of GPP to be allocated to respiration, leaving 20% available to be partitioned to growth. This 20% minimum carbon partition to growth allows the vegetation to respond to resource limitation because ORCHIDEE partitions carbon to various tissues for growth using a resource-limited demand-based approach.

Biomass in SDGVM (and SDGVM-Vc etc) is the result of flows into the biomass pools, namely NPP, and flows out of the biomass pools by mortality. Therefore biomass is determined by the simple equation:

$$B = NPP \times MRT$$

where *B* is biomass and *MRT* is the mean residence time of the biomass pool in question. Wood biomass is the major biomass pool due to the long MRT compared with that of leaves and roots (in SDGVM only fine roots are considered roots) and the MRT of wood is determined by wood mortality.

In SDGVM wood mortality is caused by age and self thinning. Mortality caused by self-thinning is based on two model parameters—a minimum diameter increment (MDI) and wood carbon density, and three state variables—NPP allocation to stem, stem density and stem height. The MDI, current tree diameter and tree stem density is used to calculate the required minimum surface area increment (MSAI). MSAI is multiplied by tree height and wood density to obtain the minimum required carbon allocated to the stem. If there is sufficient labile carbon to meet this demand then there is no mortality, if carbon is insufficient then the stem density is reduced, by killing a fraction of the trees, to a density that will allow the MDI to be satisfied. At a given NPP and tree height, the self thinning algorithm will determine an equilibrium biomass which will be a function of stem density, stem height and the two input parameters (MDI and wood carbon density).

Hypotheses and research questions

The research in this Thesis takes a broad approach to testing and informing global scale carbon cycle models (SDGVM and JULES) with data from FACE experiments. Data from the FACE experiments are analysed, followed by comparisons of the models with data at two FACE sites. Further chapters develop photosynthetic leaf trait relationships and, with findings from previous chapters, scale these relationships to the global land surface using SDGVM.

As discussed above, the relationship between photosynthesis, carbon sequestration and plant nitrogen will be important for predicting terrestrial ecosystem carbon storage and dynamics. Yet the plasticity of plant carbon-to-nitrogen ratios and carbon to nitrogen dynamics over long-term CO_2 enrichment is not well known. In Chapter 2, this Thesis begins with a meta-analysis of FACE experiments to generalise the responses of ecosystems to elevated CO_2. As discussed above, there have been a number of comprehensive meta-analyses; however, up to eight years of FACE experimentation has passed since data were collected for these previous meta-analyses and the responses to FACE enrichment over longer time-scales is of interest. Chapter 2 addresses the research questions:

Does carbon assimilation and sequestration acclimate over long-term CO_2 enrichment (using FACE methods)?

How are model parameters affected by elevated CO_2 (using FACE methods)?

To test the accuracy of assimilation data from FACE experiments, Chapter 3 investigates the effect of oscillating CO_2 concentrations on the temperate forest species *Populus* x e*uramericana* and *Quercus robur*. The oscillations are of a similar frequency to those observed in FACE experiments and the results shed light on experimental artefacts and photosynthetic operation. As discussed above, methods in previous studies have been variable and results from previous studies have been contradictory. The experimental setup in Chapter 3 was designed to be as close to the FACE experiments as possible and it is hypothesised that oscillations in CO_2 concentration will not impact assimilation without a stomatal response. Chapter 3 addresses the research questions:

Is carbon assimilation in trees used in FACE experiments affected by oscillating CO_2 concentrations?

Are hypotheses used to explain previously observed responses to oscillating CO_2 sufficient to explain observations of the assimilation response to oscillating CO_2?

In Chapter 4, the two UK carbon cycle models, SDGVM and JULES, are parameterised and driven with observed climate variables taken from the Oak Ridge and Duke FACE experiments. The ability of the models to capture NPP in response to elevated CO_2 and climate is investigated and compared with observations. The models are run in various configurations to identify areas for model development. Variables governing inter-annual variability in the CO_2 response of the two models are investigated. Results are compared with those from 10 other global carbon cycle models and ecosystem models that have been part of an inter-comparison project funded by the National Centre for Ecological Analysis and Synthesis (NCEAS) in the USA. As discussed above, results from Oak Ridge were affected by progressive nitrogen limitation and it is hypothesised that SDGVM and JULES are less likely to accurately reproduce NPP at Oak Ridge due to their relatively simple simulation of nitrogen dynamics. Chapter four addresses the research questions:

Can SDGVM and JULES reproduce NPP from Oak Ridge and Duke FACE experiments?

How can we develop SDGVM and JULES to improve their simulation accuracy at Oak Ridge and Duke FACE experiments?

As a precursor to the development of SDGVM, Chapter 5 presents the results of a meta-analysis of the empirical relationships between the photosynthetic parameters V_{cmax} and J_{max} and leaf nitrogen, leaf phosphorus and SLA. The Chapter develops these relationships in a global context and investigates the reason for the nature of the coupling between V_{cmax} and J_{max}. It is hypothesised that due to the roles of leaf phosphorus in biochemical processes and machinery and the correlations of leaf functional structure with SLA, both SLA and leaf phosphorus will significantly modify the relationship of these photosynthetic parameters with leaf nitrogen. Chapter 5 addresses the research questions:

Are leaf phosphorus and SLA important co-variates in the empirical relationship between V_{cmax} and leaf nitrogen, and J_{max} and V_{cmax}?

If so, is it possible to develop a single global relationship between V_{cmax} and leaf nitrogen, leaf phosphorus and SLA?

Chapter 6 integrates the findings from chapters 2, 4 and 5 in a global carbon cycle simulation with SDGVM. The relationships of V_{cmax} and J_{max} to leaf nitrogen and leaf phosphorus, developed in Chapter 5, are incorporated into SDGVM. Photosynthetically Active Radiation (PAR) was taken from a dataset rather than calculated from latitude and SDGVM was re-configured to simulate leaf nitrogen and phosphorus using empirical relationships to soil and climatic properties. The study represents an investigation of the impacts of photosynthetic parameters and PAR on the photosynthesis scheme scaled to longer-term ecosystem responses in SDGVM. These impacts are coupled to climate change and atmospheric CO_2 increase using the IMOGEN GCM analogue model. Compared with the standard version of SDGVM, the re-formulation of the simulation of photosynthetic parameters meant that they were revised upwards and it is therefore hypothesised that the modified version of SDGVM would increase GPP and this would be translated into lower rates of atmospheric CO_2 increase over the 21st century. Chapter 6 addresses the research questions:

How do findings and model developments impact the global simulation of the carbon cycle (using SDGVM)?

Does correction of parameter and driving variable biases improve model predictions of the global carbon cycle?

The first Chapters focus on the FACE experiments themselves and Chapter 2 generalises the response to CO_2 with meta-analytical techniques investigating responses over longer time-scales. Chapter 3 investigates potential experimental error in FACE experiments by testing the response of two tree species to oscillating CO_2. Chapter 4 validates SDGVM and JULES with NPP data from Oak Ridge and Duke FACE experiment, identifying areas for model development. To develop the parameterisation of V_{cmax} and J_{max} in SDGVM, Chapter 5 brings together leaf trait data in a meta-analysis of the empirical relationship of V_{cmax} and J_{max} to leaf nitrogen phosphorus and SLA. Chapter 6 integrates findings from many of the previous Chapters into an assessment of their impacts on the simulation of the global carbon cycle.

Chapter 2 Plant and Ecosystem Productivity in Response to Elevated CO_2. A Meta Analysis of Free Air Carbon Dioxide Enrichment (FACE) experiments.

Introduction

Increased atmospheric CO_2 stimulates photosynthetic carbon assimilation over the short to medium terms (Arp 1991, Stitt 1991, Drake et al. 1997, Idso 1999,Norby et al. 2005). Increases in carbon assimilation are often translated into higher plant growth rates and larger biomass pools (Norby et al. 2005), sequestering carbon, creating a negative feedback mechanism in the Earth System which limits the rate of atmospheric CO_2 increase (Taylor and Lloyd 1992, Canadell et al. 2007). The strength of the terrestrial photosynthetic negative feedback varies in response to limiting factors such as nutrient or water availability, climate and other direct and indirect plant responses to CO_2 (Cao and Woodward 1998). Key questions are:

Can increased photosynthesis and growth observed in growth chambers and greenhouse studies (Idso 1999) be maintained over longer time frames and in closed canopy, mature forest systems (Millard et al. 2007)?

Are important carbon cycle model parameters affected by elevated CO_2?

These are not simple questions and they require experimental and modelling approaches. To be fully answered, long term experiments and observations need to be conducted across many ecosystems at early, mid and late successional stages with high replication and a multifactorial approach to treatments which is unrealistic, necessitating the use of models to extrapolate experimental findings. Modelling can be used to integrate observations across temporal and spatial scales but requires well founded parameters and validation based on experimental data. Experimental artefacts need to be minimised and quantified to produce accurate data on plant responses to increased atmospheric CO_2.

Free Air Carbon dioxide Enrichment (FACE) experiments have generated the most natural, medium-term (up to a decade long), large scale results to date on plant and ecosystem responses to an atmosphere enriched in CO_2 (Ainsworth and Long 2005). FACE experiments are conducted in open soil systems allowing roots to grow unrestricted by pots in natural systems, completely in the open air, which removes the interference with radiation and air movement by some kinds of enclosure, minimising experimental artefacts associated with many CO_2

enrichment experiments (Arp 1991, Hendrey 1992). A number of experiments have been conducted in forest plantations, varying from closed-canopy unmanaged systems to short rotation coppice systems (Miglietta et al. 2001b, Norby et al. 2001, Oren et al. 2001, Leuzinger and Korner 2007, Zak et al. 2011).

Previous meta-analyses of FACE experiments and plant responses to CO_2

Meta-analysis is a statistical technique that allows quantitative comparison of a number of primary studies' sample means, standard deviations and replicate number (Gurevitch and Hedges 1999). Meta-analyses aim to generalise the effects of a treatment, such as increased CO_2, by providing a quantitative, cross-study effect-size of an experimental treatment on a dependent variable (Gurevitch and Hedges 1999). Meta-analyses can be used to find the response of model parameters to elevated CO_2 helping to improve the accuracy in simulating a high CO_2 world.

No review of meta-analyses of plant response to elevated CO_2 is complete without mention of Curtis and Wang (1998) who developed the statistical methods to analyse effect sizes categorically in a manner analogous to ANOVA. While the vast majority of their data relates to non-FACE studies it is necessary to discuss their results relating to respiration as they were contrary to some of the findings of this study. In meta-analyses of plant responses to elevated CO_2 Curtis (1996) and Curtis and Wang (1998) both showed a decline in dark respiration under elevated CO_2. Dark respiration has been shown to correlate strongly with plant nitrogen (Ryan 1991, Reich et al. 2006b) and both Curtis (1996) and Curtis and Wang (1998) showed similar declines in respiration and nitrogen when measured on a leaf mass basis. However, Curtis (1996) also observed a decline in respiration when measured on an area basis without an accompanying decline in nitrogen. Ryan (1991) concluded that CO_2 may reduce respiration but that the impact of CO_2, independent of changes in nitrogen were unknown and Tjoelker et al. (1999) showed no effect of CO_2 on respiration in relationship to plant biomass.

In a meta-analysis of *Lolium perenne* at the SwissFACE experiment Ainsworth et al. (2003) found that CO_2 elevated to 600 µmol mol^{-1} stimulated daily carbon assimilation by 35% and increased light-saturated carbon assimilation by over 40%. They observed an 18% reduction in the maximum carboxylation capacity—V_{cmax}—and a 10% reduction in the maximum rate of electron transport—J_{max}. Time after cutting the sward and cutting frequency (i.e. source to sink ratio) was a significant sub-treatment factor influencing V_{cmax} and both light-saturated and daily

carbon assimilation. Treatments that increased the source to sink ratio (carbon producing to carbon consuming tissue ratio) significantly decreased V_{cmax} and reduced carbon assimilation. There appeared to be an interactive effect of low nitrogen exacerbating the effect of high source to sink ratio (i.e. strengthening acclimation), however the results did not appear to be significant. Under a categorical analysis a significant response of J_{max} was only observed at low source to sink ratio and low nitrogen. Nitrogen treatment had a significant effect only on V_{cmax}. Interestingly they found no change in plant responses to elevated CO_2 over the 10 years of the study, presumably due to the fact that the experiment was fertilised and plant responses were not reliant on intrinsic ecosystem nitrogen.

The largest meta-analysis of the Free Air Carbon dioxide Enrichment (FACE) experiments was that of Ainsworth and Long (2005). They covered 15 years of results up to 2003 and used data from 120 published articles covering 12 different large scale FACE sites. The focus of their study was on photosynthetic parameters as well as some plant growth parameters and plant nutrition. They found an increase of 31% in net, light-saturated carbon-assimilation ranging from 11% (C4 plants) to 47% (trees) when analysed by functional group. An actual increase of 28% in diurnal carbon-assimilation was observed, ranging from a no change (C4 plants) to a 46% increase (shrubs, dominated by results from the Nevada desert shrub ecosystem). Increased carbon-assimilation was associated with a 20% reduction in stomatal conductance ranging from a 12% (shrubs, again dominated by results from the water- stressed Nevada desert ecosystem) to 23% (legumes).

Although carbon-assimilation increased at elevated CO_2 concentrations it was accompanied by acclimation of the photosynthetic apparatus, such that both the maximum rate of carboxylation (V_{cmax}) and the maximum rate of electron transport (J_{max}) were reduced by 13% and 5% respectively. Arp (1991) andStitt (1991) argued that optimisation of sink production and carbon gain reduces leaf nitrogen under high CO_2 and is a key factor in the acclimation of photosynthesis to higher levels of atmospheric CO_2. Ainsworth and Long (2005) reported a decrease in leaf nitrogen of 13% on a leaf mass basis and 5% on a leaf area basis. They proposed that the 20% reduction in Ribulose Biphosphate Carboxylase/Oxygenase (RuBisCO) would account for all of the reduction in leaf nitrogen per unit area based on the reasonable assumption that RuBisCO at ambient CO_2 accounts for 25% of leaf nitrogen. Ainsworth and Long (2005) observed a 21% (±18) increase in tree Leaf Area Index (LAI) but no change for C3

grasses or across all PFTs together. They also observed a 6% (±2) decrease in Specific Leaf Area (SLA) with no change in C4 plants.

Luo et al. (2006) conducted a later meta-analysis on carbon and nitrogen pools in elevated CO_2 experiments. Plant carbon was converted from biomass and nitrogen was expressed on a whole plant basis. Both carbon and nitrogen were expressed per unit area. In the FACE experiments they found carbon-pool increases of 12% aboveground, 47% for belowground plant material, but an increase of only 4% on a whole plant basis, illustrating the sometimes contradictory nature of meta-analysis due to each result coming from a different sample of studies. They calculated a 5% increase in root to shoot ratio and a 6% increase in soil carbon. For plant nitrogen they found an increase of 21%, 28% and 26% aboveground, below ground and as a whole, respectively. There was no change in the soil nitrogen pool. These changes in pool sizes were reflected by increased carbon to nitrogen ratios of 10% aboveground and 5% in belowground plant material with no significant change in the soil.

The results of Luo et al. (2006) demonstrated an increase in plant carbon and biomass and an absolute increase in plant nitrogen of similar magnitude. However, the carbon to nitrogen ratios increased, counter to that expected from the absolute increases, which were of similar magnitude.

Ainsworth and Rogers (2007) focused on the photosynthetic response of a range of Plant Functional Types (PFTs) to elevated CO_2. Light-saturated carbon assimilation was stimulated on average by 30%, V_{cmax} reduced by 10% and J_{max} by 5% with significant differences, predominantly in the magnitude of these effects, between functional groups. Notably light-saturated carbon assimilation did not change in C4, non-crop grasses while J_{max} did not change in legumes and trees. Trees had the highest rates of light-saturated carbon assimilation with concurrent lowest reductions in V_{cmax}. They also proposed that the functional types with lower increases in light-saturated carbon assimilation (shrubs, legumes and crops) were Ribulose Biphosphate (RuBP) limited at elevated CO_2 indicating constraints on the up-regulation of the light harvesting biochemical machinery (possibly as a result of an inability to increase LAI) or phosphorus limitation.

The cut-off for inclusion of data in the most comprehensive meta-analysis to date (Ainsworth and Long 2005) was 2003, and later analyses are now also over five years old (Luo et al. 2006,

Ainsworth and Rogers 2007). The majority of data from the Ainsworth and Long (2005) analysis came from crop and grassland FACE experiments and the fate of the carbon cycle in a future high CO_2 world will be dominated by the responses of forests to high CO_2. These reasons prompted the meta-analysis in this chapter, which aims to broaden the meta-analysis of forest responses to FACE enrichment in contrast with other plant functional types. The longevity of FACE experiments at the time of data collection for this study allowed the subdivision of responses by the length of time since CO_2 enrichment began, allowing the detection of any acclimation of the CO_2 response observed in photosynthetic rates, productivity and biomass.

Methods

Primary literature was searched on the Thompson Reuters Web of Knowledge database (Thompson Reuters) and a search of publications pages from each FACE website, or the Principal Investigators website. Data were acquired from tabulated or graphical data in published articles containing means, sample sizes and standard errors or standard deviations under ambient or elevated CO_2. The search resulted in useful data being taken from 233 articles (Appendix I) from 24 different FACE experiments, although 9 experiments yielded only one or two articles (Table 2-1). Of the 233 articles which yielded data, 109 were post 2003, the cut off date for Ainsworth and Long (2005). Graphical data were digitised using digitising software Grab It! (Datatrend Software, Raleigh, NC USA).

Data were recorded in a database and assigned categorical variables based on experimental treatments and types. The variables were Plant Functional Type (PFT); a qualitative assessment of nitrogen addition (a quantitative assessment was not used as it was assumed that the same amount of nitrogen addition would have different effects depending on the system studied); tree canopy level and the number of years after the beginning of CO_2 enrichment. The PFT categorical variable classification was based on that used in land surface models such as the Sheffield Dynamic Vegetation Model SDGVM (Woodward and Lomas 2004). For PFT grasses, forbs and herbaceous legumes were grouped together as a 'grass' in line with how models would simulate this vegetation type. In experiments where improved cultivars of the agricultural pasture C3 grass species *Lolium perenne* were used it was included with the 'crop' PFT as this is used in intensive agricultural systems and pasture is generally viewed as cropland within model land vegetation maps. Contrary to model PFTs, needle leaf trees were included in the 'tree' category with broadleaves as the vast majority of results for needle leaf trees came from the Duke experiment.

Nitrogen treatments were difficult to objectively categorise as nitrogen application, availability and requirements were different in each experiment. A plant focused approach was opted for with a 'normal' category for all unfertilised experiments in semi-natural vegetation and for all standard nitrogen addition rates (assessed in the literature) in the agricultural experiments. The high nitrogen category included any nitrogen addition treatments in semi-natural vegetation or higher than standard application rates in agricultural systems.

Table 2-1. Description of the FACE sites which provided most of the data for this meta-

analysis.

FACE site	Location	lat	lon	CO_2	other treatments	experimental system	year	reference
AspenFACE	Wisconsin USA	45	-89	amb +200	O_3	Aspen +mixed broadleaf	1998	Zak et al 2011
Biocon	Minnesota USA	45	-93	550	N, species diversity	Prairie grassland	1998	Reich et al 2004
China FACE	China	31	120	amb +200		cereals	2001	Chen 2005
Duke FACE	North Carolina USA	36	-71	amb +200	N	Pine forest	1996	Drake et al 2011
ETH FACE	Switzerland	47	8	600	N, cutting	Pasture	1993	Nijs 1996
Maricopa	Arizona USA	33	-112	amb +200	N, irrigation	cereals and cotton	1989	Leavitt et al 1996
NDFF	Nevada USA	36	-116	550		desert	1997	Huxman 1998
NZ FACE	New Zeland	-40	175	475	N, warming	Pasture	1997	Edwards 2001
Oak Ridge	Tennessee USA	36	-84	amb +200		broadleaf plantation	1998	Norby et al 2001
POPFACE	Italy	42	12	amb +200	N	broadleaf plantation	1999	Calfapietra 2001
Rice FACE	Japan	39	141	amb +200		rice	1998	Koizumi 2001
miniFACE	Italy	43	11	600	N	crops	1994	Miglietta 1996
SCC	Switzerland	47	7	520		mature broadleaf forest	2001	Cech 2003
SOYFACE	Illinois USA	40	-88	550		agriculture	2000	Kimbal 1995

Years after commencement of the experiment were divided into three three year periods in an attempt to identify progressive features in plant responses to elevated CO_2. Photosynthetic mode was divided into C3 and C4 photosynthesis and legumes. Although leguminous plants operate in the C3 mode, a major response of C3 plants to increased CO_2 is a drop in leaf nitrogen which interacts with photosynthesis and we wanted to separate the effect of symbiotic nitrogen fixation on C3 photosynthesis. Any differences may be justification for including legumes as a separate PFT in the next generation of land surface vegetation models that will include nitrogen cycling.

As discussed previously, meta-analyses require the data to be independent. After Ainsworth and Long (2005) we considered responses from different treatments (e.g. species, nitrogen addition, irrigation etc) and different years within a particular FACE experiment to be independent. However, in the case of ecophysiological responses, data from different days/months could possibly be considered independent due to environmental differences.

Tissue concentrations expressed as a percentage and as milligrams per gram were analysed together as they are directly comparable when converted to proportional effect-sizes. A_{sat} at a high (550 µmol mol^{-1} and above) common CO_2 concentration was tested for any differences between the effect size when the CO_2 was at the elevated concentration (550 – 600 µmol mol^{-1}) or at saturating concentration (800+ µmol mol^{-1}) and there was no significant difference,

therefore the results under both levels of CO_2 were combined into the single analysis of A_{sat} at a common elevated CO_2 concentration. Leaf respiration per unit area was analysed for any differences when measured either as the daytime respiration (calculated using the Bernacchi et al. 2009 model) or when measured by gas exchange at night time and there was no significant difference. Hence results of leaf respiration per unit area were also combined into a single analysis.

The meta-analytical software package METAWIN (Version 2.1 [release 4.8], Rosenberg et al. 1997) was used to conduct the meta-analysis. The effect-size metric used was the natural logarithm of the response ratio (rr) (Gurevitch and Hedges 1999). The response ratio is calculated as the treatment mean divided by the control mean. This metric was chosen as it has commonly been used in ecological studies and is easy to convert to a meaningful percentage change of dependent variable in response to a treatment. In all cases the number of plot replicates was used as the sample size for the meta-analysis but where it was necessary to convert standard error to standard deviation the reported sample size was used. The effect sizes were weighted in the standard METAWIN method as a function of the inverse of the standard deviation across sample plots. Confidence intervals were generated parametrically using the standard error of the weighted mean response ratio and by bootstrapping (re-sampling with replacement). Confidence intervals were unbalanced around the mean response ratio due to anti-logging. A mixed effects model was assumed (Gurevitch and Hedges 1999).

METAWIN provides tools for a categorical analysis similar to a one-way ANOVA after the methods of Curtis and Wang (1998) which was used to examine the significance of variation between factors within a single categorical variable. Categorical variables PFT and photosynthetic mode were analysed as random effects and nitrogen level, year, canopy and water were analysed as fixed effects.

In the text results are reported as mean effect size percentage change ([rr-1] x 100) to zero decimal places. 95% confidence intervals are expressed in the text as percentages as the mean of the upper and lower bound. A significant effect of elevated CO_2 on a particular dependent variable was determined at the 95% confidence level based on whether the span of the confidence intervals contained the 0% value. A significant effect of a categorical treatment was expressed based on the partitioning of variance method of Curtis and Wang (1998). ‘k’ is used to refer to the number of data points or sample size used in the meta-analysis, often referred to

as number of studies. However the number of studies is misleading as data were not always from separate studies or experiments.

Results

Carbon Assimilation and Biomass Partitioning

Instantaneous, light-saturated carbon assimilation (A_{sat}) was stimulated by 28% ±3.3 on average and Plant Functional Type (PFT) and nitrogen were significant factors modifying the response. Trees had the highest increase in A_{sat} at 38% ±10.6 with C4 grass and shrubs not significantly affected by elevated CO_2, although only C4 grasses had a mean effect size near 0% and a reasonable sample size (k = 16). A_{sat} was lower in plants under high nitrogen treatments (nitrogen added in natural systems or higher than normal nitrogen addition rates in agricultural systems) than in zero (natural systems) or standard (agricultural systems) nitrogen addition treatments. Respiration expressed on a leaf area basis and also on a mass basis increased significantly by 10% ±6.8 and 15% ±7.6 respectively. PFT significantly (significance expressed always at the $P<0.05$ level) affected the CO_2 effect of respiration with tree respiration unaffected but crop and grass respiration increased by 21% ±12.7 and 41% ±38.6 respectively, although the sample size was small (k = 9 & 4 respectively).

Daily integrated carbon assimilation (A') increased by 23% ±4.7 (Table 2-3). Increases in carbon assimilation translated to increases in production and biomass of a similar magnitude. Net Primary Productivity (NPP) increased 21% ±4.0 and, as with carbon assimilation, there was no significant influence of year and no apparent trend in the data. Total biomass increased by 22% ±7.1 and the magnitude of increase was significantly different according to PFT. Trees had the largest total biomass gains at 41% ±9.8 while grasslands (mixed species grasslands) only increased total biomass by 9% ±7.1.

Aboveground biomass was stimulated 16% ±2.5 by elevated CO_2 and there were significant differences in this stimulation of aboveground biomass for different modes of photosynthesis. Legume aboveground biomass was stimulated the most highly at 48% ±12.4 while the biomass of C4 grasses and cereals was not significantly affected by elevated CO_2. Aboveground biomass of C3 plants was stimulated by only 14% ±2.4, a markedly different response to nitrogen fixing C3 plants. By year, stimulation of aboveground biomass increased as the length of enrichment increased, an effect opposite to expectations.

Aboveground tree biomass changes were composed of a 26% ±5.4 increase in canopy biomass; no change but wide confidence intervals in litter biomass and a 23% ±4.5 increase in wood

biomass. Wood biomass was significantly influenced by site/species (breakdown not shown) and the mean effect size was dominated by the 33% ±6 increase at AspenFACE (k = 31 of 46) with the rest of the results coming from the Duke FACE site. Canopy biomass increases were accompanied by a 10% ±2.9 increase in LAI and a 5% ±1.6 decrease in specific leaf area (SLA—leaf area divided by leaf mass) indicating that the canopy has both increased in leaf layers and leaf thickness or density. The response of neither LAI nor SLA were significantly affected by PFT or nitrogen.

Total belowground biomass increased 26% ±6.6 while fine root biomass increased 32% ±6.2. Root biomass (both total and fine) was significantly influenced by PFT with trees and crops showing the largest response and shrubs (the Nevada Desert site) showing no significant change. Root to shoot ratios were unchanged supporting the effect sizes of CO_2 on aboveground and belowground biomass but contrary to findings at specific sites.

Table 2-2. The probability of ecological factor affecting the natural log of the response ratio of a plant/ecosystem response variable to elevated CO_2 using the method of (Curtis and Wang 1998). The number of independent datapoints used in an analysis is represented by k; k total datapoints were used in the factorial analysis of PFT, C3/C4/C3 legume, nitrogen and year; while k canopy and k water datapoints were used in the factorial analysis of canopy and water respectively. The factors analysed for the effect on a particular variables response to elevated CO_2 were PFT, mode of photosynthesis (C3), nitrogen, years after the beginning of CO_2 enrichment (yr), canopy level and soil water. See method section for a description of the categories within each factor. *** represents significance at the $P < 0.001$ level; ** represents significance at the $P < 0.01$ level; * represents significance at the $P < 0.05$ level; - represents significance at the $P < 0.1$ level and n.s. represents $P > 0.1$. A blank cell means that there were insufficient studies for the factorial analysis or the factor was irrelevant to the variable. A' – integrated daily carbon assimilation; A_{sat} – instantaneous rate of light saturated carbon assimilation; J_{max} – maximum rate of electron transport, $V_{c\,max}$ – maximum rate of carboxylation by RuBisco; g_s – stomatal conductance; NPP – net primary productivity; LAI – leaf area index; SLA – specific leaf area; TNC – total non-structural leaf carbon; C – carbon; N – nitrogen, PFT.

		K			factor					
dependent variable		total	canopy	water	PFT	C3/C4	nitrogen	year	canopy	water
Gas Exchange	A'	44	4		n.s.	n.s.	n.s.		n.s.	
	A_{sat}	238	87	33	***	**	*	n.s.	n.s.	n.s.
	A_{sat} common $CO_{2(ambient)}$	26	12		n.s.		n.s.	n.s.	n.s.	
	A_{sat} common $CO_{2(elevated)}$	60	11		***	*	n.s.	***	n.s.	
	J_{max}	91	59	8	**	n.s.	n.s.	n.s.	n.s.	n.s.
	V_{cmax}	99	61	12	n.s.	n.s.	n.s.	*	n.s.	n.s.
	J_{max}/V_{cmax}	15			n.s.	n.s.	n.s.			
	$Chlorophyll_{(area)}$	32	31		n.s.	n.s.			n.s.	
	$Respiration_{(area)}$	41			**	n.s.	n.s.	n.s.		
	$RuBisco_{(area)}$	25	12		n.s.		n.s.	n.s.	n.s.	
	g_s	174	50	24	**	n.s.	n.s.	n.s.	n.s.	**
Biomass	NPP	41		6	*		n.s.	n.s.		n.s.
	Total Biomass	73			***		n.s.	*		
	Aboveground Biomass	366		6	n.s.	***	*	**		n.s.
	Wood Biomass	47			n.s.			n.s.		
	Belowground Biomass	80			**		n.s.	*		
	Fine Root Biomass	110			***		n.s.	n.s.		
	Root:Shoot	28			n.s.		n.s.			
	Agricultural Yield	42		12			*			**
	LAI	84		14	n.s.	n.s.	n.s.	n.s.		n.s.
	SLA	115	69		n.s.	n.s.	n.s.	n.s.	n.s.	
Carbon & Nitrogen	$Total\ Nitrogen_{(ground\ area)}$	58			**		n.s.	n.s.		
	$Leaf\ Nitrogen_{(area)}$	111	45		**	n.s.	n.s.	n.s.	n.s.	
	$Leaf\ Nitrogen_{(mass)}$	195	87	18	*	n.s.	n.s.	n.s.	n.s.	n.s.
	$Leaf\ Protein_{(mass)}$	13			n.s.	n.s.	n.s.			
	$Leaf\ Protein_{(area)}$	13			n.s.	n.s.				
	$Leaf\ Carbon_{(mass)}$	32			n.s.		**	*		
	$TNC_{(mass)}$	26	12		n.s.	n.s.	n.s.	n.s.	n.s.	
	$TNC_{(area)}$	20			n.s.	*	n.s.			
	$Starch_{(area)}$	34		4	*		*	n.s.		n.s.
	$Starch_{(mass)}$		7						n.s.	
	$Sugar_{(area)}$	21		4	***			n.s.		n.s.
	Leaf C:N	81	32	8	***	n.s.	***	n.s.	n.s.	n.s.
	$Litter\ Nitrogen_{(mass)}$	61		8	n.s.		n.s.	n.s.		n.s.
	$Wood\ Nitrogen_{(mass)}$	17					n.s.	n.s.		

Wood Nitrogen$_{(ground\ area)}$	11						*	
Wood C:N	17						n.s.	
Root Nitrogen$_{(mass)}$	8						n.s.	
Plant Phosphorus	41	17		n.s.	n.s.	n.s.	**	**
Litter Phosphorus	22			**				

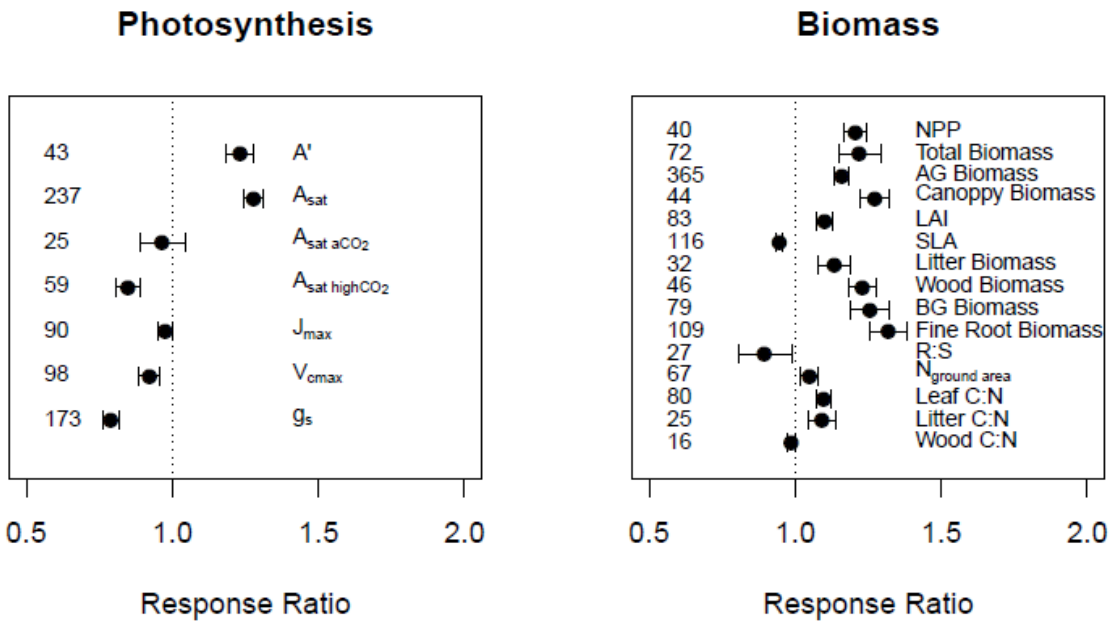

Figure 2-1.The response ratio of photosynthetic parameters and biomass to elevated CO_2. The number of samples in the meta-analyses (k) is shown on the left hand side of the plots. R:S is the root to shoot ratio; A' is daily integrated carbon assimilation; A_{sat} is carbon assimilation at saturating light and growth CO_2; $A_{sat\ aCO2}$ is carbon assimilation at saturating light and low CO_2; $A_{sat\ aCO2}$ is carbon assimilation at saturating light and at saturating CO_2.

Table 2-3. Mean effect size (response ratio) and confidence intervals of gas exchange variables in response to elevated CO_2. Confidence intervals are expressed as the 95% interval based on the normal distribution (parametric) or from re-sampling with replacement (bootstrap). 'k' represents the number of data points used in each analysis. A red background in the low confidence interval column signifies that the lower boundary of the 95% confidence interval is above one and therefore the variable in question was significantly increased under elevated CO_2 treatment. A blue background in the high confidence interval column signifies that the upper boundary of the 95% confidence interval is below one and therefore the variable in question was significantly decreased under elevated CO_2 treatment.

					95% Confidence Interval			
					Low	High	Low	High
Variable	Factor	Group	k	Mean	Parametric	Parametric	Bootstrap	Bootstrap
A'	-		43	1.23	1.186	1.280	1.185	1.287
A_{sat}	-		237	1.28	1.245	1.312	1.236	1.316
	PFT	tree	111	1.38	1.328	1.427	1.313	1.436
		grass	55	1.21	1.149	1.280	1.147	1.294
		C4grass	16	1.01	0.907	1.130	0.929	1.116
		crop	45	1.25	1.182	1.314	1.189	1.307
		shrub	10	1.13	0.962	1.322	0.903	1.450
	C3	C3	199	1.31	1.272	1.346	1.260	1.348
		legume	22	1.21	1.112	1.318	1.123	1.310
		C4	16	1.01	0.903	1.137	0.926	1.109
	nitrogen	normal	184	1.31	1.276	1.351	1.267	1.357
		high	44	1.14	1.069	1.206	1.059	1.211
		mean	3	1.39	0.898	2.162	1.280	1.524
		low	6	1.27	1.032	1.551	1.151	1.401
A_{sat} (ambient CO_2)	-		25	0.96	0.889	1.046	0.904	1.039
A_{sat} (elevated CO_2)	-		59	0.85	0.807	0.892	0.799	0.895
	PFT	tree	10	1.01	0.927	1.106	0.951	1.088
		grass	28	0.73	0.678	0.781	0.680	0.775
		C4grass	16	0.85	0.773	0.938	0.785	0.916
		crop	5	0.95	0.838	1.086	0.862	1.040
	C3	C3	35	0.89	0.834	0.940	0.823	0.943
		legume	8	0.72	0.615	0.832	0.610	0.794
		C4	16	0.85	0.763	0.946	0.782	0.917
	year	7 to 9	2	0.96	0.322	2.851	0.917	0.990
		4 to 6	8	1.06	0.946	1.182	1.002	1.123
		1 to 3	49	0.80	0.757	0.839	0.754	0.839
J_{max}	-		90	0.98	0.949	1.004	0.949	1.004
	PFT	tree	63	1.00	0.968	1.032	0.970	1.033
		grass	16	0.95	0.883	1.014	0.890	1.020
		crop	6	0.97	0.870	1.092	0.904	1.009
		shrub	5	0.77	0.650	0.911	0.685	0.893
$V_{c\ max}$	-		98	0.92	0.887	0.959	0.884	0.961
	year	7 to 9	9	0.96	0.832	1.107	0.885	1.062
		4 to 6	25	1.00	0.931	1.077	0.938	1.060
		1 to 3	64	0.88	0.840	0.924	0.827	0.934
$J_{max}/V_{c\ max}$	-		15	1.00	0.951	1.046	0.955	1.044
$Chlorophyll_{(area)}$	-		31	1.00	0.964	1.043	0.963	1.042
$Chlorophyll_{(mass)}$	-		19	0.83	0.778	0.884	0.777	0.899
$Respiration_{(area)}$	-		40	1.10	1.036	1.172	1.044	1.171
	PFT	tree	26	1.01	0.949	1.078	0.959	1.064
		crop	9	1.21	1.086	1.340	1.095	1.324
		grass	4	1.41	1.073	1.845	1.211	2.290
$Respiration_{(mass)}$	-		15	1.15	1.080	1.231	1.060	1.233
$RuBisco_{(mass)}$	-		5	0.85	0.715	1.012	0.743	0.930
$RuBisco_{(area)}$	-		24	0.83	0.716	0.954	0.728	0.939
G_s	-		173	0.79	0.762	0.816	0.762	0.816
	PFT	tree	74	0.85	0.806	0.889	0.812	0.883

		grass	45	0.77	0.720	0.831	0.726	0.831
		C4grass	16	0.74	0.605	0.900	0.639	0.843
		crop	33	0.72	0.670	0.767	0.666	0.763
		shrub	5	0.75	0.570	0.995	0.634	0.908
	water	dry	8	0.80	0.660	0.980	0.695	0.935
		wet	16	0.63	0.560	0.716	0.578	0.679
Sap flux$_{(ground\ area)}$	-		6	1.15	0.947	1.397	1.012	1.276
Sap flux$_{(wood\ area)}$	-		4	1.01	0.808	1.260	0.873	1.121

Table 2-4. Mean effect size (response ratio) and confidence intervals of growth variables in response to elevated CO_2. Confidence intervals are expressed as the 95% interval based on the normal distribution (parametric) or re-sampling with replacement (bootstrap). 'k' represents the number of data points used in each analysis. A red background in the low confidence interval column signifies that the lower boundary of the 95% confidence interval is above one and therefore the variable in question was significantly increased under elevated CO_2 treatment. A blue background in the high confidence interval column signifies that the upper boundary of the 95% confidence interval is below one and therefore the variable in question was significantly decreased under elevated CO_2 treatment.

					95% Confidence Intervals			
					Low	High	Low	High
Variable	Factor	Group	k	Mean	Parametric	Parametric	Bootstrap	Bootstrap
NPP	-		40	1.21	1.166	1.246	1.169	1.239
	PFT	tree	34	1.20	1.158	1.237	1.162	1.231
		shrub	6	1.72	1.264	2.352	1.554	2.002
Total Biomass	-		72	1.22	1.150	1.292	1.163	1.284
	PFT	tree	32	1.39	1.299	1.493	1.301	1.482
		bogmoss	4	1.03	0.743	1.418	0.874	1.161
		grass	30	1.09	1.024	1.167	1.047	1.139
		crop	6	1.43	1.166	1.760	1.123	1.817
	year	7 to 9	12	1.21	0.987	1.491	1.064	1.344
		4 to 6	13	1.38	1.214	1.567	1.216	1.556
		1 to 3	47	1.18	1.105	1.257	1.116	1.247
Aboveground Biomass	-		365	1.16	1.136	1.184	1.133	1.186
	C3	C3	322	1.14	1.117	1.165	1.116	1.166
		legume	37	1.48	1.363	1.609	1.357	1.624
		C4	6	1.13	0.870	1.459	0.973	1.281
	nitrogen	normal	315	1.14	1.119	1.171	1.117	1.173
		high	43	1.23	1.159	1.305	1.170	1.319
		low	5	1.18	0.977	1.435	1.059	1.300
		mean	2	1.57	0.389	6.340	1.190	2.072
	year	7 to 9	62	1.28	1.207	1.366	1.189	1.384
		4 to 6	137	1.15	1.115	1.190	1.116	1.189
		1 to 3	166	1.14	1.103	1.173	1.101	1.177
Canopy Biomass	-		44	1.27	1.225	1.320	1.220	1.333
Litter Biomass	-		32	1.13	1.081	1.188	1.092	1.179
Wood Biomass	-		46	1.23	1.183	1.277	1.152	1.319
Total Belowground Biomass	-		79	1.26	1.191	1.324	1.184	1.320
	PFT	tree	35	1.32	1.232	1.422	1.229	1.425
		grass	23	1.05	0.950	1.160	0.960	1.140
		crop	21	1.40	1.249	1.574	1.259	1.561
	year	7 to 9	21	1.38	1.214	1.570	1.242	1.540
		4 to 6	28	1.32	1.231	1.426	1.208	1.437
		1 to 3	30	1.16	1.086	1.249	1.075	1.271
Fine Root Biomass	-		109	1.32	1.258	1.382	1.248	1.393
	PFT	tree	59	1.46	1.384	1.533	1.377	1.547
		grass	23	1.05	0.955	1.154	0.969	1.148
		crop	21	1.40	1.258	1.567	1.263	1.560
		shrub	6	0.83	0.656	1.042	0.763	0.940
Root:Shoot ratio	-		21	1.01	0.943	1.072	0.955	1.068
Agricultural Yield	-		41	1.13	1.097	1.173	1.101	1.174
	nitrogen	normal	29	1.10	1.058	1.142	1.058	1.141
		high	7	1.21	1.110	1.308	1.141	1.278
		low	5	1.21	1.076	1.371	1.124	1.318
	water	dry	5	1.21	1.107	1.318	1.199	1.217
		wet	7	1.05	1.000	1.113	1.001	1.100
LAI	-		83	1.10	1.071	1.130	1.072	1.129
SLA	-		115	0.94	0.932	0.958	0.931	0.959

Table 2-5. Mean effect size (response ratio) and confidence intervals of carbon, nitrogen and phosphorus variables in response to elevated CO_2. Confidence intervals are expressed as the 95% interval based on the normal distribution (parametric) or re-sampling with replacement (bootstrap). 'k' represents the number of data points used in each analysis. A red background in the low confidence interval column signifies that the lower boundary of the 95% confidence interval is above one and therefore the variable in question was significantly increased under elevated CO_2 treatment. A blue background in the high confidence interval column signifies that the upper boundary of the 95% confidence interval is below one and therefore the variable in question was significantly decreased under elevated CO_2 treatment.

					95% Confidence Interval			
					Low	High	Low	High
Variable	Factor	Group	k	Mean	Parametric	Parametric	Bootstrap	Bootstrap
Total $N_{(ground\ area)}$	-		58	1.05	1.015	1.080	1.006	1.091
	PFT	tree	40	1.07	1.039	1.108	1.034	1.119
		crop	18	0.90	0.836	0.975	0.846	0.958
Leaf $N_{(area)}$	-		110	0.96	0.932	0.980	0.937	0.976
	PFT	tree	48	0.99	0.960	1.023	0.966	1.020
		grass	32	0.89	0.846	0.940	0.853	0.935
		C4grass	16	0.97	0.862	1.092	0.881	1.048
		crop	14	0.92	0.869	0.982	0.888	0.954
Leaf $N_{(mass)}$	-		194	0.93	0.904	0.959	0.919	0.942
	PFT	tree	131	0.95	0.918	0.976	0.934	0.960
		grass	19	0.87	0.801	0.953	0.818	0.919
		crop	37	0.92	0.870	0.971	0.896	0.938
		shrub	6	0.87	0.713	1.058	0.781	0.931
$Protein_{(mass)}$	-		12	0.85	0.803	0.901	0.798	0.886
$Protein_{(area)}$	-		12	0.91	0.799	1.032	0.809	1.011
Plant $Carbon_{(mass)}$	-		32	1.00	0.997	1.004	0.997	1.004
	year	4 to 6	10	1.01	1.001	1.013	1.001	1.012
		1 to 3	21	1.00	0.995	1.002	0.996	1.001
			31	1.00	0.998	1.004	0.998	1.004
$TNC_{(mass)}$	-		26	1.13	1.030	1.231	1.081	1.180
$TNC_{(area)}$	-		20	1.05	0.947	1.169	0.958	1.158
$TNC_{(area)}$	C3	C3	17	1.01	0.907	1.122	0.926	1.098
$TNC_{(area)}$		legume	3	1.48	0.792	2.783	1.183	1.822
$Starch_{(mass)}$	-		31	1.08	1.004	1.167	0.993	1.174
$Starch_{(area)}$	-		34	1.45	1.267	1.653	1.256	1.665
$Starch_{(area)}$	PFT	tree	26	1.29	1.120	1.483	1.107	1.507
$Starch_{(area)}$		crop	6	2.25	1.550	3.264	1.600	2.972
$Starch_{(area)}$		grass	2	1.72	0.083	35.846	1.325	2.280
$Starch_{(area)}$	nitrogen	normal	31	1.53	1.326	1.758	1.317	1.775
$Starch_{(area)}$		low	3	0.88	0.352	2.187	0.809	0.977
$Sugar_{(mass)}$	-		11	1.04	0.993	1.090	0.994	1.073
$Sugar_{(area)}$	-		21	2.76	1.342	5.680	1.658	4.520
$Sugar_{(area)}$	PFT	tree	17	1.73	1.141	2.634	1.195	2.425
$Sugar_{(area)}$		crop	4	19.58	5.404	70.932	15.032	26.685
Leaf C:N ratio	-		80	1.10	1.072	1.122	1.077	1.119
	PFT	tree	47	1.04	1.022	1.068	1.024	1.065
		grass	18	1.18	1.140	1.217	1.140	1.216
		crop	8	1.14	1.083	1.207	1.090	1.216
		shrub	6	1.16	1.073	1.249	1.115	1.222
	nitrogen	normal	70	1.08	1.055	1.099	1.057	1.098
		high	9	1.19	1.131	1.248	1.141	1.242
Litter $N_{(mass)}$	-		60	0.93	0.899	0.963	0.899	0.962
Litter C:N ratio	-		25	1.09	1.046	1.140	1.045	1.138

Wood $N_{(mass)}$	-		16	0.95	0.912	0.994	0.920	1.005
Wood $N_{(area)}$	-		10	1.09	1.078	1.105	1.074	1.102
Wood C:N ratio	-		16	0.99	0.972	1.002	0.978	0.998
Root $N_{(mass)}$	-		7	1.03	0.931	1.137	0.969	1.108
Root $N_{(area)}$	-		3	0.98	0.748	1.278	0.932	1.148
Leaf $Phosphorus_{(mass)}$	-		40	1.02	0.977	1.069	0.991	1.054
	year	4 to 6	8	1.10	1.039	1.173	1.065	1.136
		1 to 3	32	0.99	0.953	1.024	0.954	1.029
	canopy	upper	8	1.11	1.039	1.185	1.058	1.184
		lower	5	1.03	0.900	1.179	1.000	1.063
		understorey	5	1.06	0.921	1.231	1.012	1.115
Litter $Phosphorus_{(mass)}$	-		23	1.07	0.964	1.185	0.965	1.165
	PFT	tree	11	1.20	1.040	1.392	1.107	1.291
		grass	10	0.95	0.765	1.175	0.861	1.051
		bogmoss	5	0.79	0.504	1.248	0.666	1.026

Photosynthetic acclimation and nitrogen stoichiometry

Light saturated photosynthesis at a common CO_2 concentration was unchanged when the common concentration was at ambient levels, but decreased by 15% ±4.3 at saturating CO_2levels. At saturating CO_2 concentrations; PFT, photosynthetic mode and years of enrichment all influenced the effect size. Trees and crops showed no reduction in assimilation, but assimilation was significantly reduced in C3 and C4 grasses with legumes showing the strongest reduction of 27% ±5.1. V_{cmax} decreased 8% ±3.6 and J_{max} was not significantly decreased although J_{max} was reduced in shrubs. Both results were dominated by results from the tree PFT (65 of 98 and 63 of 90 data points respectively). J_{max}/V_{cmax} was not significantly affected by elevated CO_2 concentration. RuBisCO per unit leaf area decreased by 17% ±11.9.

Leaf nitrogen per unit leaf area was significantly decreased by 4% ±2.5 and the response was significantly affected by PFT but neither trees nor C4 grasses showed a significant decrease in leaf nitrogen per unit area. Leaf nitrogen per unit mass decreased by 7% ±1.1, less of a decrease than in many previous studies, and was significantly affected by PFT ranging from a 5% ±1.4 decrease for trees to a 17% ±10.4 for grasses. The decrease in leaf nitrogen per unit mass was reflected by an increase in leaf carbon to nitrogen ratio of 10% ±2.5 also significantly influenced by PFT ranging from a 4% ±2.3 increase for trees to a 17% ±3.9 increase for grasses. Unsurprisingly nitrogen addition treatment significantly affected the effect size, however as with A_{sat} at saturating CO_2 concentration, the effect was opposite from that expected. 'Normal' nitrogen levels caused an 8% ±2.2 increase in leaf carbon to nitrogen ratio under elevated CO_2 while high nitrogen caused a 19% ±5.9 increase.

Both leaf chlorophyll concentration and protein concentration were significantly reduced by 17% ±5.3 and 15% ±4.9 respectively, under elevated CO_2, but were not significantly reduced on a leaf area basis. The lack of change in chlorophyll supports the results of no change in J_{max}.

Wood nitrogen concentration was reduced by 5% ±4.1 but this was not reflected by a change in the wood carbon to nitrogen ratio which was unaffected. Litter nitrogen decreased 7% ±3.4 and litter carbon to nitrogen ratio increased by 9% ±4.7. Root nitrogen concentration was not significantly affected by elevated CO_2. Most plant nitrogen parameters decreased or remained unchanged while total plant nitrogen per unit of ground area significantly increased by 5% ±3.2.

Leaf percentage carbon significantly increased four to six years after the beginning of the experiment by 1% ±0.6. On a mass basis total non-structural carbon in the leaf increased 13% ±10.0, leaf starch increased 8% ±8.1 and sugar concentration was unchanged. Overall there was no change in leaf phosphorus concentration however in the later years of an experiment or in the upper canopy (studies mostly cross over both categories) leaf phosphorus was significantly increased by 10% ±6.7. There was a 20% ±17.6 increase in litter phosphorus under elevated CO_2.

Water Balance

Stomatal conductance (g_s) was decreased by 21% ±3 and was significantly influenced by PFT and water levels. g_s of trees was reduced by 15% ±4.2 while the g_s of grasses and shrub crops (cotton and soy) reduced 28% ±9.8 and 29% ±8.4. The g_s of C4 grasses were also reduced by 26% ±14.8. Soil water also influenced the effect size of g_s, somewhat counter intuitively g_s was more strongly reduced under irrigated or wet conditions, perhaps due to it being a relative effect and not an absolute effect. Sap flow expressed per unit of sapwood or ground area was unaffected by increased CO_2. However, due to the low sample size, an effect may have gone undetected as the response of sap flow per unit of ground area appeared to have increased but the confidence intervals were wide.

Discussion

Carbon Flux and Partitioning

The increase in A_{sat} and A' were similar to those calculated by Ainsworth and Long (2005). The effect size on daily carbon assimilation and wood biomass were 23%, exactly the same as the number derived by Norby et al. (2005) for increases in NPP under elevated CO_2. We calculated a similar mean increase in NPP at 19% ±4.0 and total biomass was increased by 22% ±7.1. These results indicate a consistent stimulation of the net drawdown of atmospheric carbon and sequestration in biomass although there were significant differences in total biomass by PFT.

Respiration was increased under elevated CO_2 on both a mass and leaf area basis. Respiration is strongly correlated with nitrogen concentration (Papale et al. 2006) and the calculated increases in respiration were unexpected as a drop in leaf nitrogen under elevated CO_2 is a common phenomenon, a phenomenon backed up by the results of this meta-analysis and others (Medlyn and Jarvis 1999, Ainsworth and Long 2005, Taub et al. 2008). It is possible that respiration was increased due to the increases in leaf sugar and starch concentrations and Thornley and Cannell (2000) argued that carbon supply was an important driver of respiration. Increased quantities of labile carbon could be used by the plant if energy requiring processes are restricted and respiration has been shown to increase in a number of species when labile carbon has been increased (Farrar 1985). The results presented here indicate that respiration was not tied to nitrogen concentration and that increased labile carbon may stimulate respiration. This has implications for modelling; plant labile carbon should be tied to sink limitation and respiration. For example, as with many carbon cycle models SDGVM and JULES simulate respiration as a function of plant nitrogen, and temperature (Woodward et al. 1995, Woodward and Lomas 2004, Best et al. 2011), with no consideration of the labile carbon pool. Labile carbon needs to be linked to sink limitation, for example, CLMCN (Thornton et al. 2007) reduces Gross Primary Productivity (GPP) according to soil nitrogen limitation rather than restricting plant growth, causing an increase in labile carbon.

Consistent with previous studies (Arp 1991, Ainsworth and Long 2005,Iversen 2010) patterns of carbon allocation shifted under elevated CO_2. Fine roots in particular had higher increases in biomass under elevated CO_2 than aboveground biomass. Non-nitrogen fixing C3 plants had smaller increases in aboveground biomass than legumes, with trees and crops showing large increases in both total below ground biomass and fine root biomass, indicating that growth was

limited by soil resources and that plants were foraging for these resources. By contrast grasses showed no change in belowground biomass and had the largest decreases in leaf nitrogen, on both a mass and area basis indicating that grasses were unable to adapt allocation patterns in order to acquire additional nitrogen. Legumes showed the highest increases in aboveground biomass consistent with their nitrogen-fixing bacterial symbionts allowing them to avoid nitrogen limitation and further indicating that observed increases in root mass of non-legumes could be due to nitrogen limitation. Not enough data were available to quantify root allocation in legumes.

The analysis of root to shoot ratio indicated no significant change, contrary to the analyses of biomass partitioning. Contradictions, like the one here between root and shoot biomass effect-sizes and root to shoot ratio effect-sizes, are possible in meta-analysis due to each effect-size metric coming from a potentially different sample of studies. As with the biomass effect-size, it was likely that the root to shoot ratio response was variable across PFTs and there were insufficient root to shoot ratio data to subdivide the responses. Also sampling methods may have missed changes in the distribution of roots in the soil profile. Iversen (2010) showed that for trees there was an overall increase in root to shoot ratio under elevated CO_2 but there was also a redistribution of roots in the soil profile with plants in many experiments having greater root mass at depth.

Photosynthetic acclimation, plant nitrogen and sustainability of increased biomass production

In this meta-analysis the responses of A_{sat}, A', biomass and NPP were not significantly affected by the time passed since the beginning of the experiment (Table 2-2). To maintain increased biomass production increased photosynthesis must be maintained. Down-regulation of the photosynthetic system in acclimation to elevated CO_2 has been well researched and documented yet its causes are debated (Arp 1991, Stitt 1991, Woodward 2002) due to the multiple processes at several levels of organisation that interact with and regulate the photosynthetic system.

Carbon assimilation at a common CO_2 concentration was not affected by ambient measurement concentrations but was significantly reduced at elevated or saturating CO_2 measurement concentrations. This was an unexpected result as the effect sizes of $V_{c\,max}$ and J_{max} suggest that assimilation would be reduced at low CO_2 ($V_{c\,max}$ limited photosynthesis) and

remain the same at saturating CO_2 (J_{max} limited). These contrasting results were presumably due to the data coming from different studies, highlighting that photosynthetic acclimation to high CO_2 was a result of species and ecosystem-specific interactions that were difficult to generalise with meta-analytical techniques. Acclimation of photosynthesis was less significant in trees, also observed by Ainsworth et al. (2007), probably due to the fact that leaf nitrogen per unit area was not decreased while in grasses there was a significant decrease.

Overall we calculated a decrease in V_{cmax} (8%) and no change in J_{max} yet no change in the J_{max}/V_{cmax} ratio. Ainsworth and Long (2005) observed a larger decrease in V_{cmax} (14%), a slight decrease in J_{max} (5%) and a decrease in V_{cmax}/J_{max} ratio. The results from this meta-analysis were dominated by trees whereas the results of Ainsworth and Long (2005) were weighted towards results from grasses. This study showed a decrease in RuBisCO of similar magnitude as Ainsworth and Long (2005) and a decrease in chlorophyll was only significant when measured on a leaf mass basis (Figure 2-2). The decrease in chlorophyll only on a mass basis was consistent with no response in J_{max} given the decrease in SLA under elevated CO_2 as J_{max} was measured on an area basis. Reductions in leaf nitrogen were also observed only on a mass basis for the tree PFT suggesting that changing SLA may be a strategy in maintaining leaf photosynthetic apparatus scaled to the leaf area, and therefore to incoming radiation. It could be argued that observed decreases in SLA were due to increases in leaf carbon, however increase in leaf sugar and starch were far greater on a leaf area than on a leaf mass basis (Figure 2-2).

These results lend weight to the theory of controlled down-regulation of the photosynthetic apparatus, in particular RuBisCO, due to accumulation of photosynthetic products in the leaf as a result of low sink demand (Arp 1991, Stitt 1991). Indeed Ainsworth and Long (2005) observed a 17% increase in above-ground dry matter production, 10% lower than the observed increase in diurnal carbon assimilation. Optimisation theory suggests that a plant would adjust to these higher levels of carbohydrate and match carbon assimilation to sink demand, and if sinks were nitrogen limited, reallocating nitrogen locked in RuBisCO to sink production. Sink production may not always be nitrogen limited, Körner et al. (2005) show limited response to elevated CO_2 despite their forest system having been ‘well supplied by mineral nutrients’ (Asshoff et al. 2006).

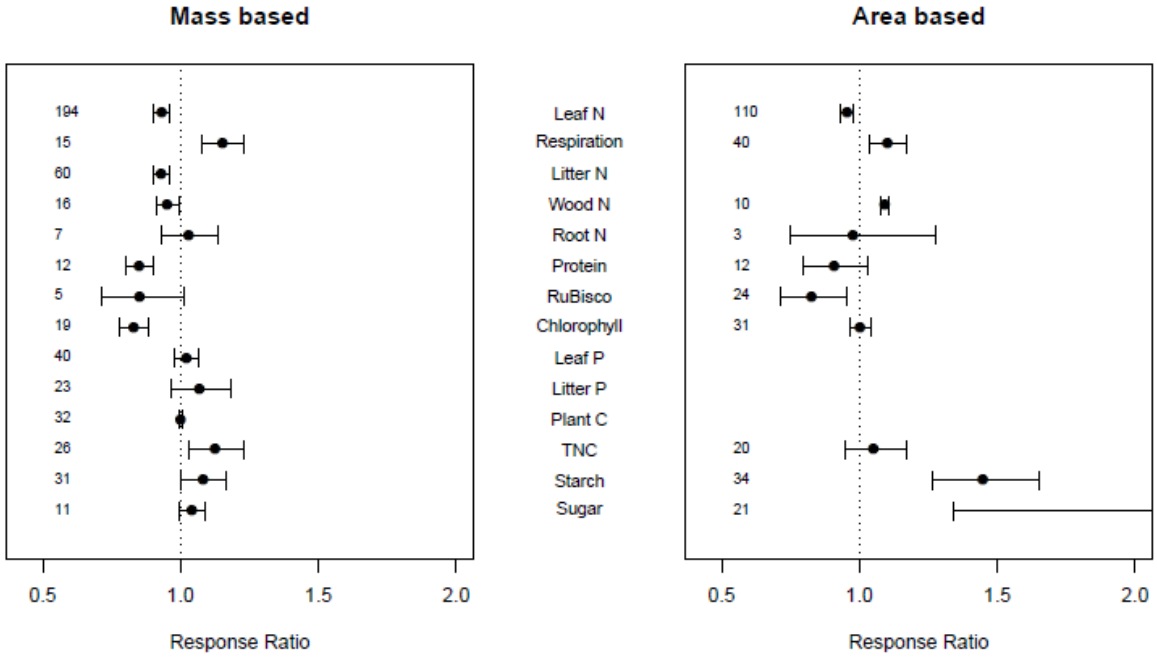

Figure 2-2. The response of plant traits to elevated CO_2 when expressed on either a mass or area basis. The number of samples in the meta-analyses (k) is shown on the left hand side of the plots.

The dominant theory for the cause of photosynthetic acclimation is that of limited sink production caused by nitrogen limitation (Arp 1991) although this is biased towards higher latitudes where phosphorus limitation is not significant (McGroddy et al. 2004, Mercado et al. 2011). Sink limitation causes a decrease in the fraction of photosynthate exported from the leaf allowing carbon compounds to accumulate in the leaf. The accumulation of photosynthate under high CO_2 was demonstrated by this analysis which showed increases in leaf concentrations of sugar, starch and total non-structural carbohydrates. The increase in leaf concentration of soluble carbohydrates is known to reduce the expression of RuBisCO genes causing a drop in the concentration of leaf RuBisCO (VanOosten and Besford 1996). If this is then translated into a drop in active RuBisCO concentration, V_{cmax} and photosynthesis would decrease. The drop in RuBisCO per unit of leaf area was accompanied by a drop in total leaf protein concentration (there were too few studies to find a significant decrease in protein per unit leaf area).

Interestingly high nitrogen treatments caused a significantly smaller increase in A_{sat} than under 'normal' nitrogen treatments. Stronger acclimation of photosynthesis under high nitrogen is in line with the mechanisms proposed by Searles and Bloom (2003) who ascribe the reduction in carbon assimilation to competition from nitrogen assimilation pathways for reducing products generated by electron transport through the photosystems. Competition between carbon assimilation and nitrogen assimilation (specifically nitrite assimilation which occurs in the chloroplast) for reducing products may account for some of the decrease in leaf nitrogen under high CO_2 and would suggest that the decrease in leaf nitrogen may not be wholly adaptive. If competition between the carbon and nitrogen reducing cycles was significant one would expect the capacity for electron transport (J_{max}) to be maintained and this was observed in this study.

Results indicate that there was little flexibility in plant tissue stoichiometry other than in leaves. The proportional nitrogen requirements of roots in particular were relatively fixed. To optimise growth in situations where sink production is limited by nitrogen it appears logical to reduce nitrogen resources allocated to non-sink limiting carbon acquisition. Shifts in leaf stoichiometry suggest that nitrogen could have been re-mobilised. If the re-mobilisation was to wood which has a much higher C:N ratio then the ecosystem may be able to store more carbon per unit of nitrogen leading to increased carbon sequestration under elevated CO_2 (Hungate et al. 2003).

Long term sequestration of carbon in tree biomass requires increases in wood production. Wood production significantly increased by 23% overall demonstrating the potential for increased carbon storage in terrestrial vegetation in a high CO_2 Earth. No changes in wood stoichiometry overall were observed. In contrast to this, wood nitrogen concentration decreased although the upper bound of the confidence interval was very close to one.

Overall, total plant nitrogen actually increased per unit of ground area by 5% indicating that plants under elevated CO_2 were accessing nitrogen either unavailable or accessed at a later date by plants under ambient CO_2 conditions. This would be expected from the observations of increased fine root biomass which may reduce leaching from the system and mine nitrogen in the lower soil layers (Iversen 2010). Where does the extra nitrogen in plant biomass come from and does it come from a source that would normally become available to a plant growing at ambient CO_2 at a later date? If the answer is yes, then increased biomass production in the early stages of forest succession maybe at the expense of biomass production as a forest system matures and may make age related decline in NPP (Hickler et al. 2006) more severe.

Indeed, a severe decline in NPP was observed at the Oak Ridge FACE experiment under both CO_2 treatments (Iversen et al. 2011) and the decline was exacerbated by elevated CO_2 (Garten et al. 2011). By contrast, Drake et al. (2011) observed continued CO_2 enhancement of growth for over 12 years of CO_2 enrichment at Duke and the results of the meta-analysis presented here show no sign of declining growth for up to a decade of CO_2 enrichment.

Results presented here show that neither leaf phosphorus nor litter phosphorus were reduced under elevated CO_2 demonstrating that these systems were nitrogen limited. There are currently no FACE experiments in tropical ecosystems, which are predominantly phosphorus limited (McGroddy et al. 2004, Mercado et al. 2011). As with nitrogen in nitrogen limited systems, phosphorus limits biomass production stoichiometrically and the interaction of elevated CO_2 with phosphorus will be important in determining the impact of CO_2 fertilisation on ecosystem carbon sequestration. Cernusak et al. (2011) found that tropical seedling phosphorus concentration was correlated with transpiration and they proposed that elevated CO_2 may reduce plant phosphorus due to reductions on stomatal conductance. A search of the Thompson Reuters database found no studies of the interaction of elevated CO_2 and phosphorus on plant growth. While leaf nitrogen is of fundamental importance to photosynthesis, a number of studies have begun to show the importance of phosphorus in photosynthesis (Ordonez et al. 2009, Domingues et al. 2010, Cernusak et al. 2011) and any CO_2 interactions with phosphorus may also feedback directly on carbon assimilation.

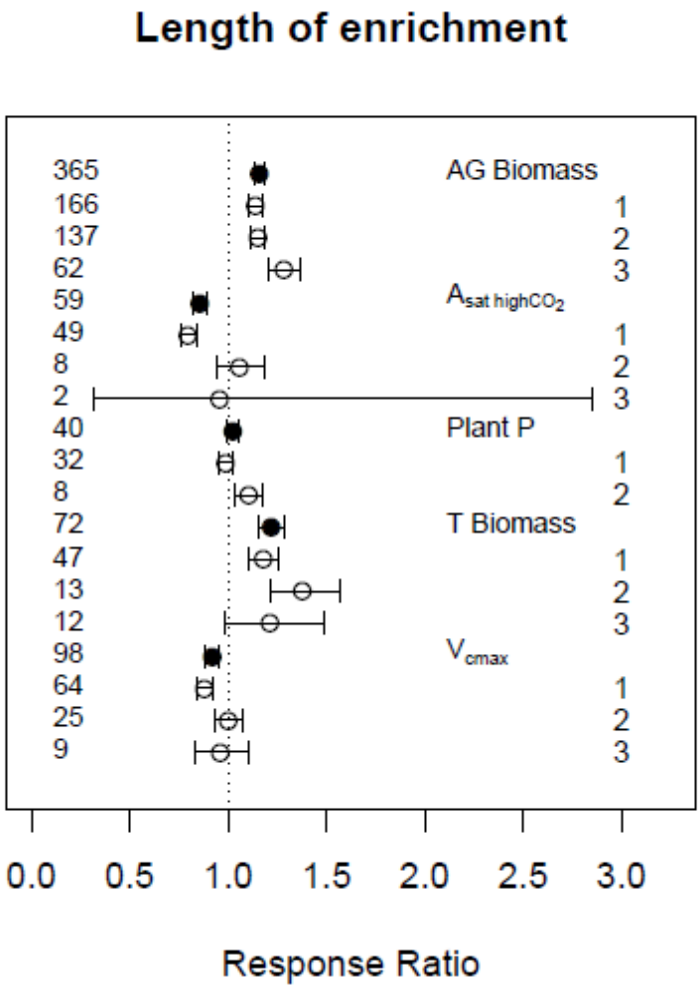

Figure 2-3.The impact of time since the beginning of the experiment on the response to elevated CO_2. Years since the beginning of the experiment were binned into three time periods of three years each (bin 1—years 1 to 3, bin 2—years 4 to 6, bin 3—years 7 to 9). The overall response is shown by solid symbols and the responses binned by year are shown by open symbols. The number of samples in the meta-analyses (k) is shown on the left hand side of the plots. T Biomass—total biomass, AG Biomass—above-ground biomass.

Potential effects of CO_2 on long-term biomass

Where length of time since the beginning of the experiment significantly affected CO_2 responses, it was often counter to expectations based on acclimation (down-regulation) of the CO_2 response over time (Figure 2-1 and Figure 2-3). The response of aboveground biomass was higher in years 7–9 than in the earlier years. Also any photosynthetic acclimation appeared to be reduced in the later years of the experiments. A_{sat} at high CO_2 and V_{cmax} were both decreased under elevated CO_2 in the early years of the experiments but these reductions were

not apparent in the later years. The results presented here show evidence for acclimation of photosynthesis over only the short term (1–3 years) after which acclimation was not apparent.

Only if increased NPP under elevated CO_2 is sequestered in plant biomass or soil organic matter will the negative feedback on atmospheric CO_2 be maintained. In a nitrogen-limited system and assuming stoichiometric shifts are sustainable, biomass will be higher under elevated CO_2 atmospheres as increased carbon to nitrogen ratios should allow vegetation to contain higher levels of carbon per unit nitrogen in the canopy and in woody tissues (suggested by wood nitrogen concentrations but not wood carbon to nitrogen ratios). If elevated CO_2 also helps plants to access ecosystem nitrogen unavailable to plants at lower CO_2 concentrations (Iversen 2010, Drake et al. 2011) then these effects will be synergistic, promoting higher ecosystem biomass than in equivalent systems with lower atmospheric CO_2.

The data used in this meta-analysis were from relatively young forest systems which had not yet reached maturity. The effect size of elevated CO_2 on basal area increment at the Swiss Canopy Crane (SCC) site (Körner et al. 2005), the only FACE experiment in a mature forest system, showed no significant change. The SCC site is unique in a number of ways in that it uses a unique CO_2 enrichment method and only has a single replicate at the plot scale. However, the results are interesting as they suggest mature, fertile ecosystems cannot increase production in response to elevated CO_2., although assimilation was increased at the SCC site and they cannot account for this additional carbon (Zotz et al. 2005). In mature systems the stoichiometry of longer lived plant tissues will only shift on generational timescales. Worth noting is that the SCC forest was growing on soil only 30 cm deep and this will limit the capacity of the soil as a nutrient and water reservoir, which could strongly limit any CO_2 response.

The data from Oak Ridge showed a general decline in NPP with the age of the experiment accompanied by a reduction of the proportional increase in NPP under elevated CO_2 (Garten et al. 2011, Iversen et al. 2011). However, nitrogen limitation will give a competitive advantage to biological nitrogen fixers and these have been observed to increase in the understorey at Oak Ridge (Souza et al. 2010). Over generational timescales ecological shifts will become important and must be considered when modelling even though there is little experimental data for calibration and validation.

The availability of water to plants in closed canopy, equilibrium ecosystems is fundamental to canopy height (Ryan and Yoder 1997) and therefore the biomass that the system can support. Although stomatal conductance was strongly reduced at elevated CO_2, with the implication of higher water use efficiency, plant sap flow was not reduced by high CO_2 according to our results. Sap flow was not reduced at Duke as increases in LAI partly compensated reductions in stomatal conductance (Schafer et al. 2003). Elevated CO_2 is known to enhance drought tolerance (Leakey et al. 2009) and our results for agricultural yield support this. However, Warren et al. (2011) has observed that reductions in stomatal conductance under elevated CO_2 caused leaves to senesce and abscise sooner in *Liquidambar styraciflua* in response to an extreme heat-wave in 2007.

Conclusions

The results presented here demonstrate that higher rates of photosynthesis were translated into higher rates of productivity and subsequently higher accumulation of biomass under high CO_2. However, respiration was increased probably as a result of higher levels of labile leaf carbon. The results suggest that the nature of carbon partitioning under elevated CO_2 was particular to PFTs and ecosystems and the nature of the limitations within those systems. Factors limiting to plant growth other than carbon may mean that initial biomass increases may not be maintained although longer term responses to elevated CO_2 showed no evidence of acclimation. In later years of FACE experiments, photosynthetic rates and parameters were no different under ambient or elevated CO_2, indicating a release from apparent acclimation in earlier years. The response of above-ground and total biomass in years 6-9 of FACE showed no evidence of decreasing.

The results presented in this Chapter showed that LAI, a key parameter for scaling photosynthesis, responded to elevated CO_2 and therefore accurate prognostic simulation of LAI and its response to elevated CO_2 is necessary for carbon cycle simulation in a changing atmospheric environment. As with previous studies, leaf nitrogen was shown to decrease as was the important photosynthetic parameter V_{cmax}. As described by Ainsworth and Long (2005) the decrease in V_{cmax} was likely to be wholly attributable to the decrease in leaf nitrogen. Interestingly, V_{cmax} showed no response to elevated CO_2 in the later years of FACE experimentation. SLA decreased under elevated CO_2, possibly in response to decreasing leaf nitrogen concentration in order to maintain leaf nitrogen per unit area.

Processes requiring further investigation for carbon-cycle modelling are nutrient (both nitrogen and phosphorus) limited sink production; shifts in plant stoichiometry in response to elevated CO_2 and the subsequent effects of changing nitrogen and phosphorus concentrations on photosynthesis; carbon allocation patterns and photosynthetic and respiratory responses to increased labile carbon.

Chapter 3 The effect of high frequency oscillations of atmospheric CO_2 concentration on plant carbon assimilation in *Populus* x *euramericana*, *Quercus robur* and *Vicia faba*

Introduction

Plant photosynthesis and respiration couple the biota of the Earth's land surface and atmospheric CO_2 (Denman and Lohmann 2007). Understanding plant responses to increased atmospheric CO_2 is crucial to prediction of the trajectory of future atmospheric CO_2 concentration and climate change (Friedlingstein et al. 2006). It is also crucial to farmers, foresters, conservationists and those involved in land and biological resource management to understand how natural and managed ecosystems will respond to future changes in atmospheric CO_2.

Free Air Carbon dioxide Enrichment (FACE) (Hendrey and Kimball 1994) experiments have generated the most natural results to date on plant and ecosystem responses to an atmosphere enriched in CO_2 (Ainsworth and Long 2005). FACE experiments have minimised experimental artefacts associated with many CO_2 enrichment experiments. They are conducted in open soil systems allowing roots to grow unrestricted by pots which have affected many CO_2 enrichment experiments. They are subjected to all the elements, completely in the open air, which removes the interference with radiation and air movement that is caused by open top chambers (Evans and Hendrey 1992).

However, FACE experiments have their own artefacts. Some artefacts are due to the cost of the CO_2 itself - $1 million per year at the Oak Ridge site (Norby, pers. comm.) - and minimising its use such as often turning off the enrichment at night and enriching only the tree canopy in woodland ecosystems. Another artefact is related to the control of the elevated CO_2 concentration. CO_2 concentrations are not only increased on average they also fluctuate strongly: 350 – 1100 μmol mol^{-1} in the original Brookhaven system (Nagy et al. 1992); 350 – 750 μmol mol^{-1} at the Nevada Desert FACE Facility (Jordan et al. 1999); 350 – 850 μmol mol^{-1} for the MiniFACE system (Miglietta et al. 2001a); 350 – 1000 μmol mol^{-1} at the Japanese RiceFACE experiment (Okada et al. 2001) and 350 – 800 μmol mol^{-1} in the WebFACE system at the Swiss Canopy Crane site (Pepin and Körner 2002). The oscillations were of relatively high frequency as one minute integrals significantly reduced the range of CO_2 concentrations and increased the

frequency of CO_2 samples within ±10% of the mean concentration (Nagy et al. 1994). Oscillations may have been of a lower frequency at the Swiss WebFACE site as one minute integrals had less impact on the distribution of sampled CO_2 concentrations (Pepin and Körner 2002).

High frequency oscillations in atmospheric CO_2 concentration may influence plant carbon assimilation by altering the efficiency of assimilation (assimilation divided by CO_2 concentration) and could therefore bias the results of FACE experiments (Hendrey et al. 1997). Evans and Hendrey (1992) investigated the response of carbon assimilation (using labelled C^{14} techniques) in cotton (*Gossypium hirsuitum* [L.]) leaves to a square wave oscillation (switching between two concentrations, 360 and 1090 µmol mol^{-1}) in CO_2 at oscillation periods of one, two, five and ten minutes. Plants were exposed to the oscillation treatments for two hours prior to a dose of labelled CO_2 being added during the last oscillation cycle.

For oscillation periods of two minutes and over Evans and Hendrey (1992) found an increase in the radioactivity of leaves exposed to oscillating CO_2 concentration over those exposed to steady state CO_2 concentration (700 µmol mol^{-1}). They speculated that at 360 and 700 µmol mol^{-1} leaf carbon assimilation was limited by RuBisCO activity while at 1090 µmol mol^{-1} assimilation was limited by availability of inorganic phosphate or ribulose- 1,5-bisphosphate (RuBP) regeneration. They proposed that the switching between the two states of limitation may have had a synergistic effect, boosting carbon assimilation under oscillating CO_2 conditions.

Evans and Hendrey (1992) also investigated the response to 5 – 60 second pulse lengths of increased and decreased CO_2 concentrations from 700 µmol mol^{-1}. Carbon assimilation rates were unchanged at three pulse concentrations: 450, 750 and 1150 µmol mol^{-1} for pulse lengths up to 15 seconds and for pulse lengths up to 30 seconds in the 450 and 750 µmol mol^{-1} treatments. At longer pulse lengths, assimilation rates increased with increasing pulse length. Assimilation rates at 1800 µmol mol^{-1} were significantly higher for pulse lengths between 5 and 60 seconds and increased steadily with increasing pulse time. These results suggest that there may have been a diffusion-regulated lag-time between the change in atmospheric CO_2 concentration and the internal CO_2 concentration at the chloroplast. Increasing the CO_2 differential would have reduced the lag-time before changes in assimilation were detectable.

Cardon et al. (1995) showed that in maize (*Zea mays* [L.]) oscillation in CO_2 concentration between 150 – 500 µmol mol^{-1} with a six minute period did not affect mean carbon assimilation but increased transpiration compared with steady state CO_2 concentration. Cardon et al. (1995) also showed that in the common bean (*Phaseolous vulgaris* [L.]) oscillation in CO_2 concentration between 235 – 430 µmol mol^{-1}, with a six minute period, slightly (their statistics were not presented) reduced both mean carbon assimilation and transpiration compared with steady state CO_2 concentration.

Hendrey et al. (1997) used chlorophyll fluorescence and electron transport as a proxy for carbon assimilation in *Triticum aestivum* (L.) seedlings. They tested a square wave oscillation between 425 and 850 µmol mol^{-1} with periods ranging between 2 and 240 seconds. They observed an oscillation of chlorophyll fluorescence (F_t) in phase with the oscillations in CO_2 at periods above eight seconds. The oscillation in F_t reached its maximum amplitude at periods of 32 seconds and above. At 32 second periods the oscillation in F_t was a triangle wave and not square wave. Both these results suggest that while oscillation in CO_2 concentration was detectable at periods of eight seconds and above, there was a time lag between a change in atmospheric CO_2 and its full influence upon the light harvesting systems in the thylakoid membranes of the chloroplast.

In a low O_2 atmosphere (to eliminate photorespiration) Hendrey et al. (1997) used rates of electron transport through photosystem II (*J*) as a proxy for carbon assimilation rates. They found that at oscillation periods of 60 seconds and below, carbon assimilation was not significantly affected. At periods of two minutes and four minutes they found that *J* (carbon assimilation) was significantly reduced by about 18%.

Holtum and Winter (2003) tested the effect of oscillating CO_2 concentrations (435 – 765 µmol mol^{-1}) on the seedlings of two tropical tree species: teak (*Tectonia grandis* [L. f.]) and barrigon (*Pseudobombax septenatum* [Jacq.] Dug.). Carbon assimilation was calculated using an infra-red gas analyser (IRGA). They separated, in time, the reference measurement and the analysis measurement by conducting an experimental run once in the absence of plant material and then once in the presence of plant material. The recorded CO_2 concentrations of the two runs were then used to calculate the mean carbon assimilation rate. A modified version of this approach has been used here. Holtum and Winter (2003) found a significant reduction in carbon assimilation under oscillating CO_2 compared with steady state. For teak the reduction

was 7.6% and 4.1% under oscillation periods of 40 seconds and 80 seconds respectively. For barrigon, oscillating CO_2 caused a reduction in carbon assimilation of 10.5% at an oscillation period of 40 seconds.

The prevailing hypothesis for reduced assimilation was that oscillating atmospheric CO_2 drives assimilation rates up and down the A-C_i /C_a curve (Hendrey et al. 1997, Holtum and Winter 2003). When CO_2 concentrations increase to levels where the regeneration of RuBP becomes the limiting factor and the curve approaches the asymptote then carbon assimilation is lower per unit of atmospheric CO_2. This reduction in efficiency causes a reduction in mean carbon assimilation under oscillating CO_2. Both these experiments switched CO_2 from steady state to oscillation and elevated the CO_2 concentration simultaneously. Therefore they were not testing simply oscillating CO_2, they were testing the response to a step change in CO_2 and then either steady state or oscillating CO_2. This step change may have impacted stomatal activity and perhaps the stomatal response to a step change in CO_2 concentration may have been different under oscillating CO_2 compared to steady state.

Understanding the potential bias caused by oscillating CO_2 is necessary for proper interpretation of FACE results and for use of FACE results in model validation. To date, the literature has provided contradictory results. At oscillation frequencies similar to FACE experiments, some studies found a stimulation of photosynthesis (Evans and Hendrey 1992), others found no impact of oscillating CO_2 (Hendrey et al. 1997) while others found decreases in assimilation rates (Holtum and Winter 2003).

To date no tree species used in FACE experiments has been assessed under oscillating CO_2 and results from previous experiments are mixed. Therefore, the responses of photosynthetic rates in trees to oscillations in atmospheric CO_2 concentration have been investigated here using at least one species that has also been used in FACE experiments. The selected species were *P*. x *euramericana* (Dode), an amphistomatous, hybrid poplar used in the POPFACE (Calfapietra et al. 2001) experiment; *Q*. *robur* (L.) a hypostomatous, temperate, deciduous species and *Vicia faba* (L.) an amphistomatous annual crop. To our knowledge these are the only temperate trees to be investigated for their sensitivity to oscillating atmospheric CO_2 concentration.

As discussed above, previous experiments on the impact of oscillating CO_2 did not pre-treat plants to elevated CO_2 so were investigating the difference between a step change in CO_2 to

either steady state CO_2 or oscillating CO_2. The method in this Chapter pre-treated plants to elevated atmospheric CO_2 and so only the effect of oscillation in CO_2 concentration was tested. It was assumed that this was more in keeping with the nature of the FACE experiments as plants would be acclimated to elevated CO_2.

This Chapter aims to quantify the impacts of oscillating CO_2 on carbon assimilation in temperate tree species used in FACE experiments. *Populus* x *euramericana* (Dode) and *Quercus robur* (L.) were subjected to an atmosphere that oscillates in CO_2 concentration and carbon assimilation, stomatal conductance and transpiration were measured with an Infra-Red Gas Analyser (IRGA). It was hypothesised that a stomatal response to oscillating CO_2 would be key to understanding the assimilation response, therefore the two species used in the experiment presented in this Chapter were chosen for their contrasting stomatal characteristics.

Hendrey et al. (1997) and Holtum and Winter (2003) proposed that oscillating CO_2 caused reductions in assimilatory carbon use efficiency which were the cause of their observed reductions in assimilation under oscillating CO_2. To test this hypothesis, an empirically determined A-C_a or A-C_i curve was used as a simple model to determine carbon assimilation at a given CO_2 concentration. Using this A-C_i model with a time series of CO_2 concentrations, oscillating as in this experiment and in that of Holtum and Winter (2003), gave quantifiable predictions of the Hendrey et al. (1997) hypothesis to compare with experimental data.

Methods

Plant material and growth

Hardwood cuttings of *Populus* x *euramericana* (Dode) (Salicaceae) were taken from 2-3 year old wood in June 2009 and again in June 2010. Cuttings were soaked in water for three days and were then transplanted, otherwise they were untreated. On 22nd June 2010, *V. faba* seeds were planted after soaking in water for 12 hours. Cell grown *Q. robur* plants were bought from a nursery and transplanted on the 23rd June, transplanted plants were selected by eye for uniformity in height and leaf mass. All plants were grown in 17.5 cm pots filled with a 1:1:1 M3 peat based compost/sand/vermiculite mixture.

Plants were grown at the University of Sheffield, Professor Sir David Read Controlled Environment Facility on a day/night cycle of 16/8 hours, 20/18 ^{o}C at a constant relative humidity of 60% and a constant CO_2 concentration of 550 µmol mol^{-1} in 2009 and 620 µmol mol^{-1} in 2010. The plants were grown in a controlled environment growth chamber (Sanyo-Gallenkamp PG1700H, Sanyo Electric Co. Ltd., Moriguchi, Japan) under eight 250w metal halide bulbs (MHN –TD Pro, Koninklijke Phillips Electronics N.V., Amsterdam, Netherlands) giving a photon flux density of 450-600 µmol m^{-2} s^{-1} in the upper canopy. Plants were moved around every two or three days to homogenise their light environment. Plants were tray watered every other day with half strength Rorison's solution (Heinen et al. 2009) to eliminate water stress and nutrient stress.

Oscillating CO_2 system

An airstream oscillating in its CO_2 concentration was generated by mixing two air streams – one at a high CO_2 concentration (1140 µmol mol^{-1} in the first experiment) and the other CO_2-free air. The high CO_2 stream was generated by mixing pure CO_2 and CO_2-free air in a gas mixer (GMA-2, Heinz Walz GmbH, Effeltrich, Germany). The CO_2-free air supply to the Walz mixer was supplied by the in-house compressed air supply as the internal pump in the mixer was not capable of maintaining the required flow rate of 5 l min^{-1}. The CO_2-free air stream was also supplied from the in-house compressed air supply, filtered and passed through soda lime. Where practical all gas tubing was made of Teflon© (Polytetrafluoroethylene, PTFE) to minimise adsorption of CO_2 in the gas path.

The high CO_2 air stream was maintained at a flow rate of 5 l min^{-1} and the CO_2-free air stream was mixed into it, at a variable flow rates of 2 – 8 l min^{-1}, by a proportional solenoid valve (PSV; Christian Burkeart GmbH & Co KG, Ingelfingen, Germany) controlled by an AC signal generator (Thandar TG501, Thurby Thandar Instruments Ltd., Huntingdon, UK). The mixing of a variable flow rate air stream with one of constant flow rate created an asymmetric wave-pattern with the CO_2 concentration below the mean concentration for proportionally more time but the departure from the mean was less. As discussed above, the asymmetric wave pattern made the experimental conditions similar to those at the FACE sites. Similar to many of the FACE experiments, the oscillation amplitude was 430 – 770 µmol mol^{-1} in the first experiment, 500 – 900 µmol mol^{-1} in the second and third experiments.

Prior to mixing, the two air-streams were humidified by being bubbled through water and then passed through a cold trap built using a cold bath (HC & F40 Ultratemp 2000, Julabo Labortechnik GmbH, Seelbach, Germany) set at 12 ^{o}C to set the dew points of the air-streams and to maintain an RH of about 60% at the experimental temperatures (see Figure 3-1 for photos of the full system). In the growth chamber the two airstreams were mixed and then vented to atmosphere. An infra-red gas analyser (IRGA; CIRAS-1, PP Systems, Amesbury, MA, USA) was connected to the air-stream oscillating in its CO_2 concentration just before the vent ensuring that the IRGA cells did not become pressurised. The IRGA's external air supply pump was used to draw a constant flow rate air-stream at 500 ml min^{-1}. The IRGA was internally modified to bypass its automatic control system for CO_2 and water vapour in order to minimise the gas path length and hence minimise damping in the peaks of the CO_2 oscillations. Within the IRGA a 100 ml min^{-1} air-stream was drawn from the supply to the reference cells and the remaining air-stream of 400 ml min^{-1} was pumped to the leaf cuvette (PLC4[n], PPSystems, Amesbury, MA, USA). Air within the leaf cuvette was mixed by an impeller to ensure the changing atmospheric CO_2 concentration was experienced by the leaf. From the cuvette a sample of air was drawn and analysed by the analysis cell of the IRGA. The difference in time between analysis by the reference cell and the analysis cell was estimated at 5 seconds by aligning the peaks of the reference cell and analysis cell CO_2 measurements and this agreed closely with the calculated time to flush the gas path between the outlet and inlet of the IRGA which was 4.3 seconds.

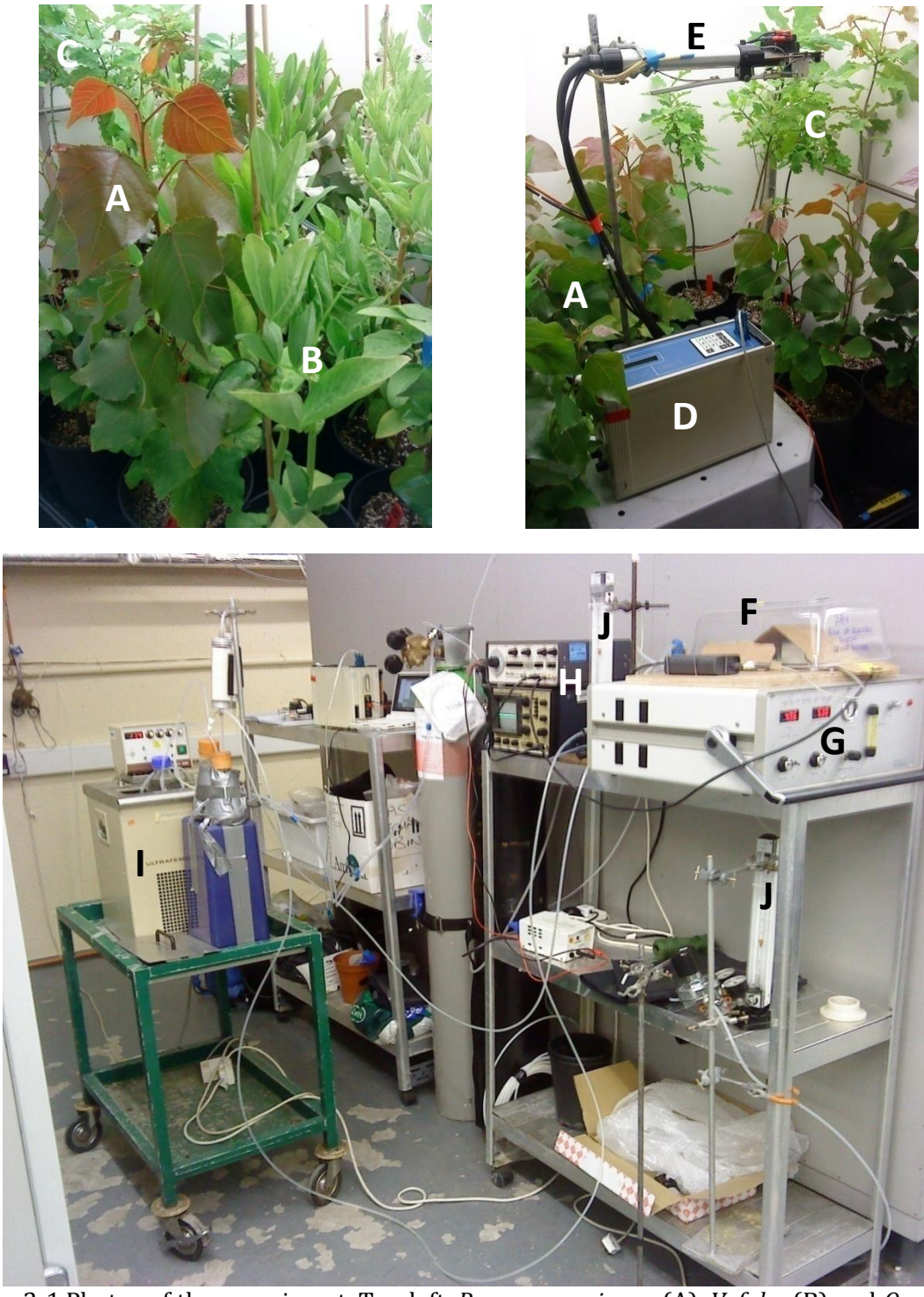

Figure 3-1.Photos of the experiment. Top left, *P*. x *euramericana* (A), *V. faba* (B) and *Q. robur* (C) in the growth cabinet. Top right, the IRGA (D) with a *Q. robur* leaf in th cuvette (E). Bottom, experimental equipment: Proportional solenoid valve (F), Walz gas mixer (G), signal generator and oscilloscope (H), cold bath and dew trap (I), flow meters (J).

Calculation of carbon assimilation

IRGAs calculate carbon assimilation using the difference in the CO_2 concentration of reference (pre leaf cuvette) IRGA cell and the analysis (post leaf cuvette) IRGA cell. In steady state studies the difference between these two cells is due mostly to CO_2 removal by the plant. There is a certain amount of random error in the measurement of the IRGA cells. The IRGA was checked against certified standard gases (BOC, Linde AG, Munich, Germany) at two concentrations of 264 and 807 µmol mol^{-1}. Flow rates were verified using flow meters (Solartron Mobrey 1100, Emerson Electric Company, Ferguson, MO, USA).

Additionally, the non-steady state nature of these experiments created a number of additional causes of the difference between the two cells which needed correction. There was a time-lag in the measurement between the two cells and diffusion of CO_2 occurred during the measurement interim, reducing the amplitude of the oscillation. There was also some drift in the calibration between the two cells.

To correct for diffusion between the two cells the relationship between the two cells based on a control run of oscillating CO_2 with an empty cuvette (for either the increasing or decreasing wave) was determined. Firstly, the data from the analysis cell were timeshifted three measurement timesteps (each 1.6 s) to match the wave pattern of the reference cell. This generated a near linear fit between the concentrations measured in the analysis cell and the reference cell dependent on whether the concentration was increasing or decreasing (Figure 3-2). The relationship between the two cells was then described using the loess curve fitting function in R.

Random error and slight drift in measurement calibration between the two cells caused some points to lie off the curve (Figure 3-2). To correct for the random error and drift, the curve was fit repeatedly over 4 iterations, at each step eliminating points from the analysis that were more than a given distance from the relationship and then re-fitting the curve. Typically less than 5% of points were removed and this gave an improved representation of the relationship between the two cells (Figure 3-2). The removal of these outliers was necessary, demonstrated by its application to control runs with no plant. Without this outlier removal step, the range of calculated assimilation for four control runs (assimilation should have been zero) was -0.745 to 0.315 µmol m^{-1} s^{-2}, with the outlier correction this range was reduced 37 fold to: -0.004 to 0.025 µmol m^{-1} s^{-2}.

The corrected relationship of CO_2 in the analysis cell to CO_2 in the reference cell in a control run enabled prediction of pre-plant exposed CO_2 in the analysis cell from the reference cell values of an experimental run with a leaf in the cuvette. No-plant control runs were conducted at the beginning of the day and after every two experimental runs.

Finally, random error and calibration drift had to be corrected in the experimental run. Again reference cell measurements were timeshifted so the wave patterns matched. Random error and drift were corrected using the method above. The analysis cell to reference cell relationship was described by iteration of the loess function and removal of outliers. To clean random error and drift from the data any points more than ±8 µmol mol^{-1} from the loess relationship were recalculated using the loess relationship. That these outliers were caused by error and not caused by the plant was demonstrated by the need to control for these outliers in a control run conducted in the absence of plant material as described above.

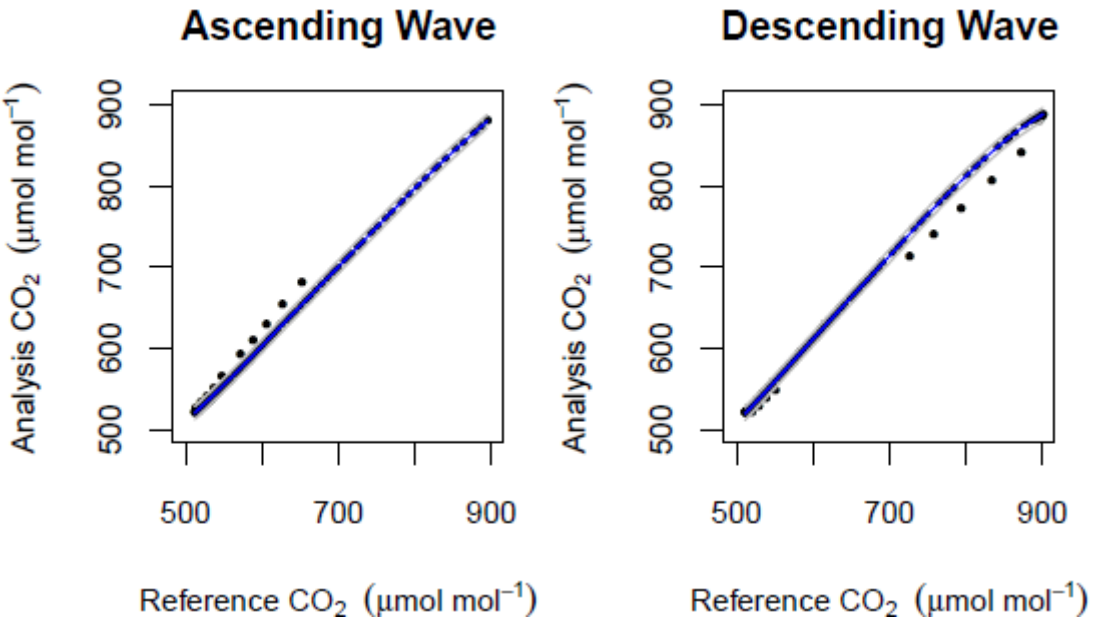

Figure 3-2. The relationship of CO_2 concentration in the IRGA analysis cell (timeshifted) to that in the reference cell for a run with no plant material in the cuvette (runs with plant material in the cuvette looked qualitatively very similar). Points more than ±8 µmol mol^{-1} off the loess line (points outside the grey lines) were excluded (<5%) from the line fitting to accurately portray the line upon which most (>95%) of the data lie.

These correction steps gave reference cell CO_2 concentrations and analysis cell CO_2 concentrations with diffusion error, random machine error and calibration drift minimised allowing the best estimate of plant carbon assimilation. Carbon assimilation was calculated using the same formulas as the IRGA uses to calculate carbon assimilation (PPSystems 2003) and the above described corrections allowed us to make an accurate measurement of carbon assimilation almost instantaneously under oscillating CO_2.

Measurements of carbon assimilation and transpiration under experimental treatments

All experiments were conducted in the centre of the growth chambers in the upper canopy of the plants at a photon flux density of 500 µmol m^{-2} s^{-1}. Exploratory experiments were carried out: 1) to test the constancy of carbon assimilation over a day; 2) to test whether oscillation in CO_2 affected subsequent assimilation at steady state; 3) to test for any changes in carbon assimilation over longer (one hour) runs of oscillating CO_2 and 4) to see how quickly CO_2 assimilation reached steady state once a leaf was clamped in the cuvette.

Assimilation rates peaked about 90 minutes after lights on and were relatively constant over the next four hours. Oscillating CO_2 concentrations did not affect subsequent carbon assimilation rates at steady state CO_2 concentration, implying that the order of measurement of control or experimental treatments was not critical. Assimilation rates were the same at the beginning of an hour long run of oscillating CO_2 as they were at the end and therefore plants were not pre-treated to oscillating CO_2. Under steady state CO_2 concentration at 550 µmol mol^{-1} (the same concentration as the growth chamber) assimilation rates of *P*. x *euramericana* reached steady state within two minutes of the leaf entering the cuvette. However, assimilation rates of *Q*. *robur* took 20 minutes to stabilise after entering the cuvette, so leaves were left in the cuvette for 20 minutes prior to the beginning of any treatment.

Experiments were conducted in the four hour window of constant assimilation rates beginning 90 minutes after lights on. In the first experiment, and on each day, 3-4 leaves on two *P*. x *euramericana* plants were investigated for assimilation rates at steady state $CO_2$of 550 µmol mol^{-1}. After 1 hour they were then tested again for assimilation rates under oscillating CO_2 concentrations with a mean of 550 µmol mol^{-1} and a range of 430 – 770 µmol mol^{-1}. The hour time lag was necessary to reset the system from steady state to oscillating CO_2 and to wait for the system to stabilise. Each oscillating run was conducted for 12 minutes.

The first experiment tested a single factor at four levels. Carbon assimilation under oscillation periods of 60, 120 or 300 seconds and a steady state control (with no oscillation). Plants were allocated to a treatment at random. Over three weeks leaf carbon assimilation was measured on a total of 78 leaves on 21 plants. The steady state measurements on each leaf were taken for two reasons; to ensure that there was no trend in carbon assimilation over the course of the experiment and to provide paired measurements. There was no trend in assimilation rates at steady state CO_2 over the course of the experiment.

The second and third experiments were designed to minimise the time-lag between the oscillating measurements and the steady state measurements that was a consequence of allowing the Walz gas-mixer to stabilise once the concentration had been reset. The stabilisation time of the Walz mixer was avoided by using it only for the oscillating CO_2 apparatus and using a bottle of gas at fixed CO_2 concentration for the steady state air stream. After 20 minutes of stabilisation in the cuvette, leaves of either *P*. x *euramericana*, *Q*. *robur* or *V*. *faba* were subjected to five minutes of CO_2 at 622 µmol mol^{-1}; then 12 minutes of oscillating CO_2 with a mean of 620 µmol mol^{-1} and a range from 500 – 850 µmol mol^{-1}; followed by another 5 minutes of steady state CO_2 at 620 µmol mol^{-1}. The third round of experiments was conducted only on *Q*. *robur*. The two oscillations in the third round of experiments were of a period of 60 seconds (for 12 minutes) and 300 seconds (for 20 minutes) and the order of these oscillating periods alternated.

A-C_i curves for *P*. x *euramericana* and *Q*. *robur* were generated in 2010 using a single leaf on three different plants. Assimilation rates were measured once steady state assimilation had been achieved. Assimilation measurements began at the growth CO_2 concentration of 620 µmol mol^{-1} increasing in steps of 100 µmol mol^{-1} to 1000 µmol mol^{-1}, then to 1200 and 1400 µmol mol^{-1}. CO_2 was decreased to 1000, then to 750 µmol mol^{-1} and then in steps of 100 µmol mol^{-1} until 150 µmol mol^{-1}. Stomatal conductance and transpiration were also recorded.

Modelling assimilation rates

A Michaelis-Menton equation was fit to experimentally determined A-C_i data, using non-linear least squares regression fitting, creating a formula for assimilation as a function of C_i:

$$A = \frac{V_{max}\, C_i}{k_m + C_i} + i$$

where A is assimilation, C_i is internal CO_2 concentration, i is the intercept, V_{max} is the asymptote minus the intercept and k_m is the value of C_i when A, minus the intercept, is half V_{max}. This equation, with the non-linear least squares derived coefficients, was used to predict carbon assimilation under oscillating CO_2 from observed values of CO_2. C_i was calculated from observed CO_2 values, assimilation, stomatal conductance and transpiration.

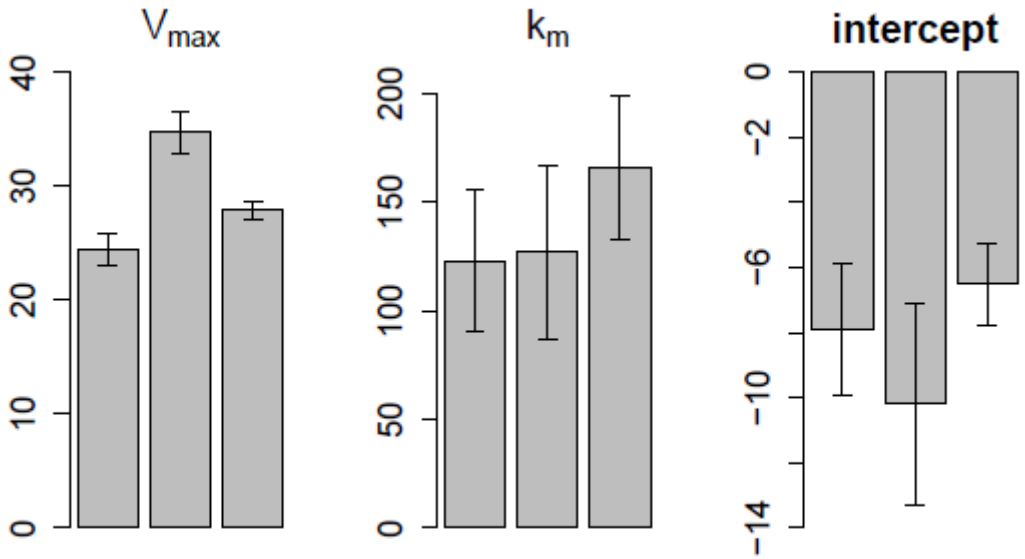

Figure 3-3. Comparison of coefficients (±SE) from a non-linear least squares regression of assimilation with internal leaf CO_2 using a Michaelis-Menton curve. The three values of each coefficient are for curves for three Q. robur plants. The overlap of error bars in all coefficients but V_{max} suggests that the A-C_i relationship from plant to plant changes only in V_{max} and not K_m nor the intercept.

To account for the difference between the A-C_i curve of the leaves on which the A-C_i model was calculated and the A-C_i curve of the leaf in the experimental run, the V_{max} coefficient was adjusted. The adjusted V_{max} was calculated for the leaf by rearranging the Michaelis-Menton equation and using the mean assimilation and CO_2 concentration from the experimental run to

calculate V_{max}. It was assumed that k_m and the intercept did not change compared with that in the A-C_i model. This assumption was verified by comparison of the parameters of the non-linear regressions of the three A-C_i curves fitted separately for each *Q. robur* leaf; only for the V_{max} parameter did standard errors not overlap (Figure 3-3).This method was used to predict instantaneous assimilation rates. The A-C_i curve was also used to calculate assimilation under oscillating CO_2 at different mean concentrations when driven by changes in C_i observed in an example experimental run. The A-C_a data of Holtum & Winter (2003) were digitised using Grabit XP (Build 10, Datatrend Software) in order to predict assimilation under oscillating CO_2 from their A-C_a data and for their experiments. The oscillation in CO_2 concentration generated by their experimental setup was a symmetrical sawtooth wave and to drive their model the oscillation in CO_2 concentration was approximated by the trigonometric function:

$$C_a = \left(\frac{1}{3} r \left(\sin^{-1}.\sin\left(t\left(\frac{0.5p}{\pi}\right)^{-1}\right)\right)\right) + \overline{C_a}$$

Where, C_a and $\overline{C_a}$ are atmospheric CO_2 concentration in µmol mol^{-1} and the mean respectively; $r$is the peak to peak amplitude and p is the period of the oscillation in seconds.

Statistics

All analyses were carried out using R version 2.13.0 (R Core Development Team et al. 2012). The first experiment was designed to be analysed with a one-way ANOVA on plant means. Leaf to leaf variation in carbon assimilation was high and a statistical power analysis (of a *t*-test) to detect a 10% change in carbon assimilation indicated that the number of required replicates would be impractical. Assimilation at steady state CO_2 concentration for each leaf was measured so paired *t*-tests within each treatment were also conducted. There were 6 replicate plants in each treatment apart from the 120 second treatment which had 5. A total of 84 leaves had carbon assimilation measured, once at steady state CO_2 and once under CO_2 oscillating at one of the three treatment frequencies. To account for the high between leaf variation in assimilation rates and to take advantage of the full set of leaf measurements a mixed effects ANOVA model was also applied to the data (Pinheiro et al. 2011). The experiment was not designed for this kind of analysis and hence had many missing factor (treatment by plant) combinations as each plant was subjected to only the control treatment and a single oscillating

treatment. There are no clear methods to estimate the degrees of freedom using a mixed model ANOVA with missing treatment combinations so we were unable to calculate *P* values for the mixed model analysis of the first experiment.

The second and third rounds of experiments were designed with a mixed model ANOVA in mind and hence all treatment combinations were analysed using mixed model analyses using the lme function, part of the nlme package (Pinheiro et al. 2011) which can calculate degrees of freedom and hence generate *P*-values.

Results

The experiments in 2009 (Figure 3-4) suggested that carbon assimilation was not significantly affected (P>0.05) by oscillations in CO_2 concentration between 430 and 770 µmol mol^{-1} when analysed by fixed-effects ANOVA on plant means (Table 1). Due to the high error variance we analysed the data using paired t-tests based on plant means and a mixed-effects ANOVA. Paired t-tests were also not significant.

The mixed-effects ANOVA model analysed oscillation frequency as the fixed effect and leaf nested within plant as a random effects (Table 1). The experiments were designed for a fixed-effects ANOVA and therefore there were missing treatment and plant leaf combinations meaning that degrees of freedom of the analysis could not be calculated. However, the F-statistic of 3.6 and the largest t-value (between the control and 300 second oscillation) of -3.03 (Table 3-2) suggests the possibility of an effect. This result, along with the high error variance motivated the experiments in 2010 that were designed for a mixed-effects analysis and to minimise the error variance caused by the experimental setup. Results for plant transpiration were non-significant when analysed by a fixed-effects ANOVA on plant means and a mixed-effects ANOVA (data not shown).

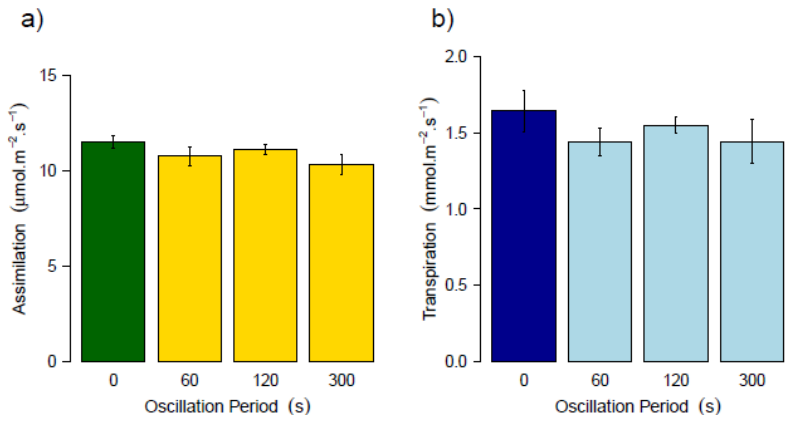

Figure 3-4. Mean (±1 SEM; based on plant means) assimilation and transpiration for Poplar at steady state CO_2 concentration (green and dark blue) and CO_2 oscillating with periods of 60, 120 and 300 seconds (yellow and light blue). An ANOVA on plant means showed that none of the treatments had a significant effect on either assimilation or transpiration.

Table 3-1. Fixed and mixed-effects ANOVA of plant carbon assimilation explained by the oscillation treatment. Data for each plant replicate in the fixed-effect model calculated as the mean of 3-5 measured leaves.

Model type	Term	df	Sum Sq	Mean Sq	*F* statistic	P(>F)
fixed	Frequency	3	4.62	1.54	1.4783	0.2522
	Residuals	19	19.78	1.04		
mixed	Frequency	3	11.61	3.88	3.6001	na

Chapter 1 Table 3-2.Parameters from the mixed-effects ANOVA on carbon assimilation (Table 3-1). Oscillation frequency as the fixed-effect and leaf nested within plant as the random-effects. Student's *t* values are given for the contrasts of the control treatment with zero and for each frequency with the control treatment. Note that despite the inability to estimate *P*-values, the *t*-values for the contrasts of the 60 second and 120 second oscillating treatments with the control treatment are too low to give a significant *P* value even with very large degrees of freedom.

	Mean	Std. Error	*t* value	*P*
Control	11.18	0.208	53.8	na
60 seconds	10.77	0.303	-1.35	na
120 seconds	11.27	0.297	0.31	na
300 seconds	10.09	0.359	-3.03	na

Results from the cross species experiment (Figure 3-5) showed that there was a significant effect ($P<0.001$) of oscillation on carbon assimilation but not on transpiration or stomatal conductance (Table 3-3). There was a significant effect of species on mean rates of assimilation, stomatal conductance (g_s) and transpiration (Table 3-3). There was no significant interaction between species and treatment for any of the response variables and so the results in Table 3-3 are for additive models of treatment and species. Closer investigation of the effect of treatment on carbon assimilation (Table 3-4) showed that for Oak and Poplar carbon assimilation was significantly ($P<0.001$) higher (1.97 µmol m^{-2} s^{-1}) under oscillation than under the first constant CO_2 treatment but that there was no significant difference between the oscillating treatment and the second constant treatment. This effect was consistent across both Oak and Poplar. It was not possible to assess this effect for *V. faba* because of equipment malfunction. Consistent with the results for Oak and Poplar however, was that there was no difference in carbon assimilation (or any other response variable) between the oscillation CO_2 treatment and the second constant CO_2treatment.

The variable frequency experiment on Oak showed that neither carbon assimilation, transpiration nor stomatal conductance were affected (Table 3-5). There was no difference between either oscillating treatment and no difference between either constant CO_2 treatment.

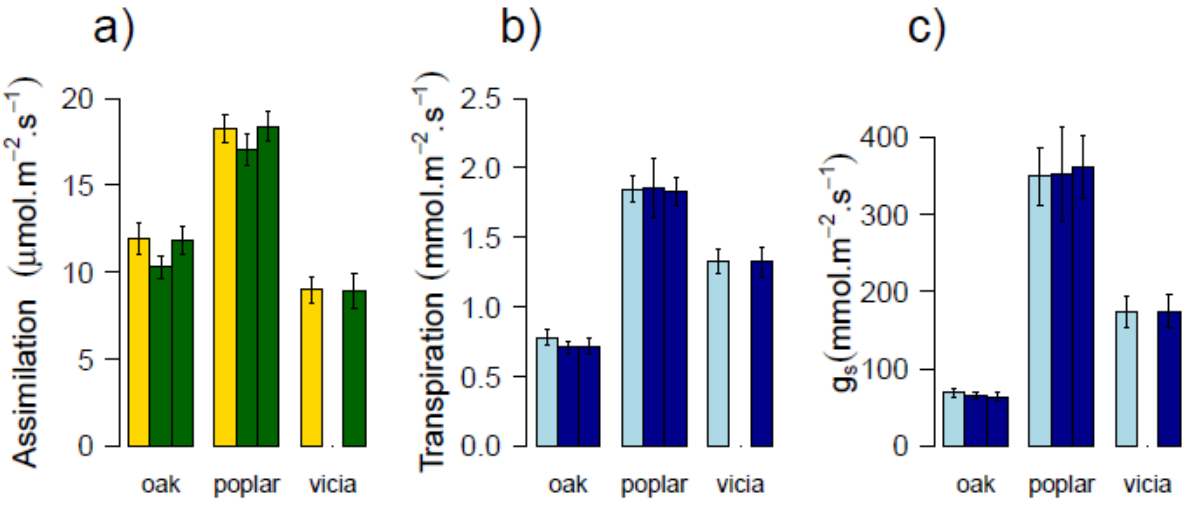

Figure 3-5. Mean (±1 SEM; based on plant means) assimilation (a), transpiration (b) and stomatal conductance (c) at steady state CO_2 concentration (green and dark blue) and CO_2 oscillating with a period of 60 seconds (yellow and light blue) for *Q. robur*, *P.* x *euramericana* and *V. faba*. Each group of three bars represents, from left to right, oscillating CO_2, the first constant CO_2 treatment (measured before the oscillating treatment) and the second oscillating treatment (measured after the oscillating treatment).

Table 3-3.Mixed-effects ANOVAs of carbon assimilation, transpiration and stomatal conductance explained by oscillation treatment and species. Due to the missing data for the first constant CO_2 treatment of *V. faba*, these results are for only Oak and Poplar.

Dependent variable	term	df_n	df_d	*F* statistic	*P*
Assimilation	Intercept	1	68	729.22	<0.001
	Oscillation	2	68	11.55	<0.001
	Species	1	13	33.55	<0.001
Stomatal Conductance	Intercept	1	68	104.38	<0.001
	Oscillation	2	68	0.11	0.895
	Species	1	13	42.34	<0.001
Transpiration	Intercept	1	68	394.62	<0.001
	Oscillation	2	68	0.14	0.865
	Species	1	13	66.43	<0.001

Table 3-4.Parameters from the ANOVA of assimilation shown in Table 3-3. The overall mean, the difference between the means of Poplar and Oak, the difference between the mean under oscillating CO_2 and the first steady state run (Osc vs st1) and the difference between the mean under oscillating CO_2 and the second steady state run (Osc vs st2).

	Estimate	se	df	*t* statistic	*P*
Overall mean	11.26	0.854	68	13.19	<0.001
Poplar vs Oak	6.52	1.126	13	5.79	<0.001
Osc vs st1	1.972	0.205	68	4.81	<0.001
Osc vs st2	-0.974	0.205	68	-2.73	0.026

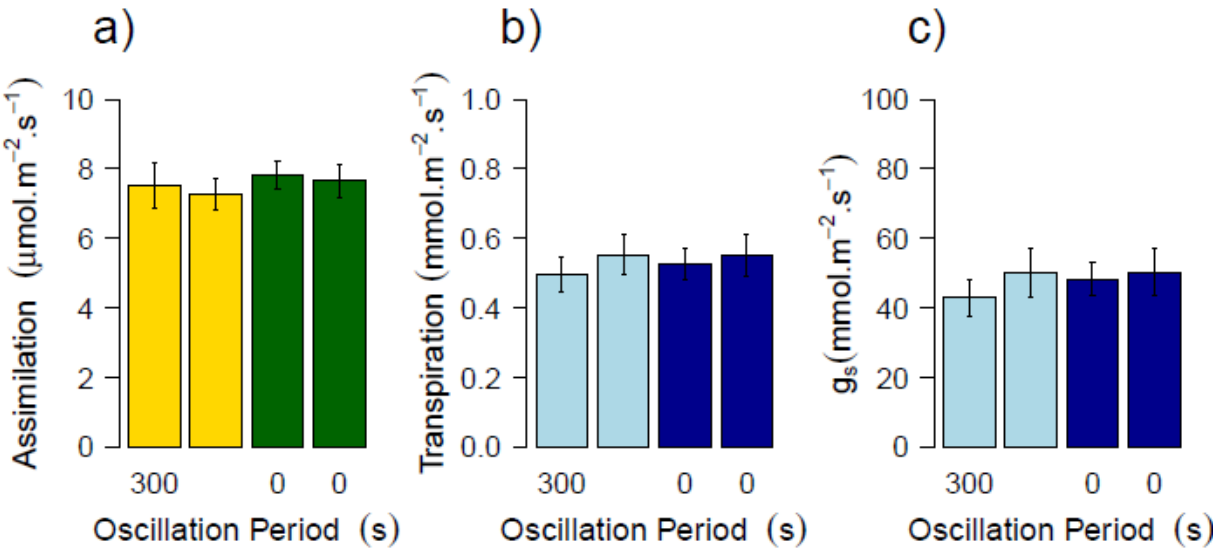

Figure 3-6. Mean (±1 SEM; based on plant means) assimilation (a), transpiration (b) and stomatal conductance (c) at steady state CO_2 concentration (green and dark blue) and CO_2 oscillating with a period of 60 seconds or 300 seconds (yellow and light blue) for Oak. From left to right the constant CO_2 treatments are the first treatment (measured before the first oscillating treatment) and the second treatment (measured in between the two oscillating treatments).

Table 3-5.Mixed-effects ANOVAs of carbon assimilation, transpiration and stomatal conductance explained by oscillation treatment.

Dependent variable	term	df_n	df_d	*F* statistic	*P*
Assimilation	Intercept	1	45	179.04	<0.001
	Frequency	3	45	1.77	0.166
Stomatal Conductance	Intercept	1	45	96.67	<0.001
	Frequency	3	45	1.32	0.277
Transpiration	Intercept	1	45	166.29	<0.001
	Frequency	3	45	1.37	0.264

Discussion

Results from the original experiment in 2009 suggested that there may be a reduction in carbon assimilation by *P*. x *euramericana* at oscillation periods of 300 seconds (Table 3-1). The suggested reduction in assimilation was not accompanied by any reduction in transpiration. These results were contradicted by the results from the third experiment where assimilation in Oak was not affected at oscillations of 300 seconds. The suggested reduction in assimilation in the first experiments was not detected by an ANOVA of plant means but came from a mixed-effects analysis for which the experiment was not designed.

There were a number of sources of error in the first experiment. Plants exhibited high variability in assimilation rates (although this was also the case in the second and third experiments). There was separation in time between assimilation measured under constant CO_2 and oscillating CO_2 which may have allowed error through diurnal variation in assimilation rates. Also the calculation of assimilation was not considered as good as for the second round of experiments as drift in the calibration between the two IRGA cells was not explicitly accounted for in each run. The first round of experiments really only suggested a possible effect that the second round was designed to investigate. Therefore conclusions are drawn from the second and third rounds of experiments.

The second experiment showed an increase in assimilation under oscillating CO_2 and for the following constant CO_2 treatment. In preliminary experiments, changes in assimilation and g_s were observed in relation to the time after enclosing the leaf in the cuvette, exhibiting first a drop and then a recovery of rates after enclosure in the cuvette. The observed increase in assimilation may have been due to this recovery of leaf physiological rates after an initial decline post enclosure in the cuvette. However, the leaf response to cuvette enclosure was accounted for in the method by maintaining leaves in the cuvette until steady states had been reached, including for g_s (the major leaf response to cuvette enclosure) indicating that enclosure was not the cause of increased assimilation rates. If the increase in assimilation was a response to cuvette enclosure it should also have been observed in the third experiment.

It was hypothesised that changes observed in assimilation may be due to non-steady state responses of stomata. However, there was no evidence to suggest stomatal responses were affected by oscillating CO_2 and hence increased assimilation must have been due to factors not related to stomatal conductance. Non-stomatal responses could include changes in internal

conductance (g_i) to CO_2 diffusion (Flexas et al. 2008), uncoupled with changes in conductance (Heinen et al. 2009). It may be that for increases in assimilation under oscillating CO_2 there was a synergistic effect of switching between carbon limited and light limited photosynthesis, as proposed by Evans and Hendrey (1992). The stimulation of assimilation by this synergy would have to last for more than five minutes after oscillation ceased to explain the higher rate of assimilation under steady state CO_2 immediately after the experiment.

The obvious difference between the two experiments was that assimilation was lower for all treatments in the third experiment. The drop in assimilation was likely a result of leaf age as the third experiment was conducted after the second and leaves were older. The leaves were also subject to powdery mildew which progressed as the plants aged and probably stressed the leaves reducing the photosynthetic potential.

Due to the inverse relationship of C_i to assimilation, low assimilation rates meant that the lower bound of the C_i oscillation was higher at low assimilation rates than at high assimilation rates. It is proposed that assimilation rates were increased under oscillating CO_2 due a synergy caused by switching between V_{cmax} and J_{max} limited assimilation rates. Given lower assimilation rates, the lower bound of C_i under oscillating CO_2 would be higher and perhaps not low enough to switch between the two rates. This effect could be exacerbated as lower assimilation rates suggest a lower V_{max} of the simple Michaelis-Menton curve meaning a lower value of C_i at the knee of the curve, i.e. the point at which assimilation switches from V_{cmax} limitation to J_{max} limitation.

At medium to high rates of assimilation (>10 mol m^{-2} s^{-1}) in healthy leaves, oscillating CO_2 appears to increase carbon assimilation in *Q*. *robur* and *P*. *euramericana*, probably by switching the photosynthetic rate limiting process between the PCA cycle and electron transport. Increases in carbon assimilation were observed by Evans and Hendrey (1992) in *G*. *hirsuitum* in response to oscillating CO_2. These increases in carbon assimilation may occur in the field in FACE experiments and may influence carbon assimilation at the leaf level and with no change in stomatal conductance would also increase leaf level water use efficiency. However, when integrated at the ecosystem scale leaf-level changes are not necessarily translated into ecosystem level changes. For example, NPP at Oak Ridge FACE was strongly affected by ecosystem nitrogen dynamics (Garten et al. 2011, Iversen et al. 2011) and WUE response to increased CO_2 at Duke FACE was balanced by the leaf area index response (Schafer et al. 2002).

Lag time

Hendrey et. al. (1997) observed evidence to suggest that there was a diffusion-related timelag which damped the effect of oscillations in CO_2 of high frequency. Hendrey et al. (2007) observed damping and smoothing of chlorophyll fluorescence (F_t) in comparison with the CO_2 oscillation at periods below 32 seconds indicating that the diffusion-related time lag under these conditions was significant. Diffusion-related lag times appeared not to be significant for teak and barrigon at oscillation periods of 40 and 80 seconds (Holtum and Winter, 2003). Holtum and Winter (2003) used a smoothly oscillating waveform and their results suggested that for smooth waveforms a diffusion-related timelag was not significant.

Assimilation was calculated over short timesteps (16 seconds) for the course of the oscillation period. If diffusion related lag times were significant then the amplitude of the observed assimilation rates should be damped in comparison with the predicted assimilation rates. However, predictions and observations of instantaneous assimilation rates did not support this (Figure 3-7). The analysis of assimilation during the course of the oscillation show that observed assimilation rates were similar to those predicted by the A-C_i curve suggesting that the lag time was not slow enough to affect assimilation under these oscillation frequencies. The shape of the observed and predicted oscillations in assimilation rates were very similar and, in conjunction with a lack of stomatal response, adds weight to the hypothesis that it was the A-C_i curve driving the response to oscillating CO_2 levels.

Diffusion related lag times were not long enough to damp oscillations in internal CO_2 concentration when the oscillations were gradual and not square-wave. Therefore plants exposed to FACE methods are likely to experience oscillations in CO_2 concentration at the chloroplast. However, given that the predicted reductions caused by the non-linearity of the A-C_i curve were very small, it is concluded that assimilation in FACE experiments would not be reduced by oscillations in CO_2 concentration if the study species have similar A-C_i curves and do not have a direct stomatal response.

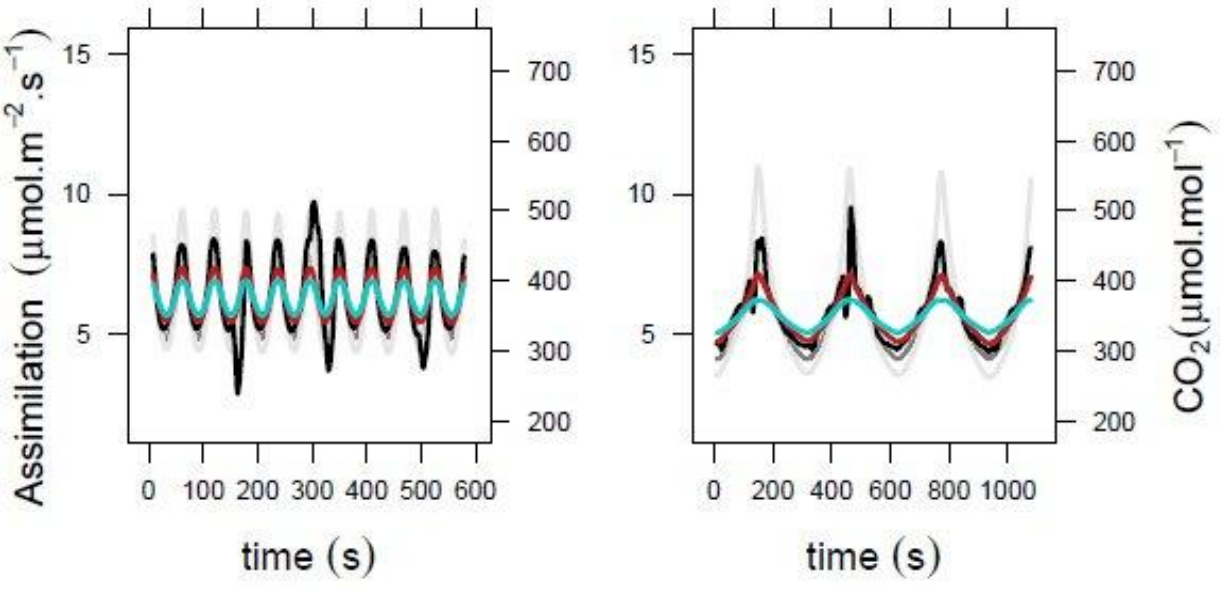

Figure 3-7. Observed (black lines) and predicted assimilation (red and blue lines) smoothed with a moving 16 second average for *Q. robur* under oscillating CO_2 of two periods: 60 and 300 seconds, over a 10 and 20 minute run respectively. Predicted assimilation was based on internal leaf CO_2 concentration (right scale) calculated from observations of stomatal conductance (light grey) and from predictions of stomatal conductance based on its relationship to CO_2 under steady state conditions (darker grey).

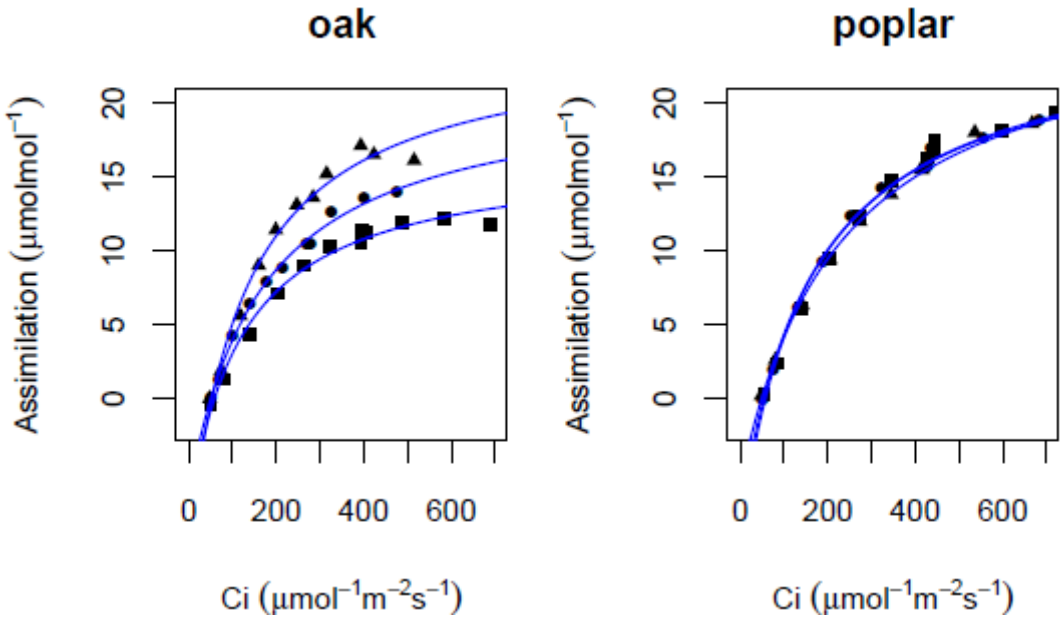

Figure 3-8. Assimilation against leaf internal CO_2 concentration (C_i) measured at steady state for *Q. robur* and *P.* x *euramericana*. A-C_i curves were measured on single leaves of three different plants and these different plants are represented by the different symbols. The blue curves were fit for each individual plant using a non-linear least squares regression on the Michaelis-Menton equation.

Table 3-6. Carbon assimilation of *P.* x *euramericana* and *T. grandis* under steady state (SSA) CO_2 conditions and the mean assimilation under oscillating (OA) CO_2 conditions predicted by their respective A-C_a curves driven with the oscillating CO_2 data from each experiment with an intercept term added to shift the mean concentration of the oscillation. There are no data for *T. grandis* for a mean of 750 µmol mol^{-1} and above as no A-C_a curve was available above 870 µmol mol^{-1}.

	P. x *euramericana*			*T. grandis*		
Mean CO_2 µmol mol^{-1}	SSA µmol m^{-2} s^{-1}	OA	Difference %	SSA µmol m^{-2} s^{-1}	OA	Difference %
350	8.14	7.91	-2.82	4.86	4.74	-2.47
450	10.27	10.04	-2.24	5.66	5.58	-1.41
550	11.97	11.76	-1.75	6.31	6.23	-1.27
650	13.29	13.09	-1.50	6.80	6.72	-1.18
750	14.23	14.06	-1.19	-	-	-
850	14.82	14.72	-0.67	-	-	-
950	15.19	15.15	-0.26	-	-	-
1050	15.49	15.43	-0.39	-	-	-
1150	15.67	15.62	-0.32	-	-	-

Changing carbon efficiency by changing CO_2 concentration

Hendrey et al (1997) and Holtum & Winter (2003) observed reductions in carbon assimilation under oscillating CO_2, proposing that oscillating CO_2 shifts assimilation rates up and down the A-C_i/C_a curve leading to a reduction in mean assimilation efficiency (carbon assimilated per unit of CO_2) due to the non-linearity of the relationship.

Hendrey et al. (1997) saw what looked like significant decreases in electron transport at oscillation periods of 60 seconds and above. They did not publish A-C_a curves nor assimilation rates (electron transport through photosystem II) at any of the mean, low or high steady state CO_2 concentrations for the wheat used in their experiments. However, using A-C_a data from both this experiment and from Holtum and Winter (2003) the predicted relative reduction in assimilation was much less than the observed relative reduction in electron transport (results not shown).

Integrated predicted assimilation rates based on the A-C_i/C_a curves of *P.* x *euramericana* in this experiment and teak from Holtum and Winter (2003) under oscillating and steady state CO_2 conditions are shown in Table 3-6. Under the respective amplitudes of the oscillations in CO_2 experienced by the plants in these studies, oscillations in CO_2 concentration had only a minor

effect on carbon assimilation across a wide range of mean CO_2 concentrations. For Poplar, oscillating CO_2 conditions were predicted to reduce carbon assimilation by a maximum of 0.23 µmol m^{-2} s^{-1} or under 3% compared to assimilation at steady state. The data from Holtum and Winter (2003) show that the reduction in assimilation rate that they observed cannot be predicted by their A-C_a curve. The predicted reduction was only 0.08 µmol m^{-2} s^{-1} compared to the 0.57 µmol m^{-2} s^{-1} reduction observed. Using the A-C_a model with Holtum and Winter's (2003) data, mean predicted assimilation rates under oscillating CO_2 were reduced but by much less than they observed.

These predicted results indicate that the hypothesis relating reduction in assimilation under oscillating CO_2 to reduced efficiency caused by shifting up and down the A-C_a curve is not sufficient to explain the reductions observed by Holtum and Winter (2003) and Hendrey et al (2007).

The shape of the A-C_a curve and the stomatal response to translate the A-C_a curve into an A-C_i curve will form the major components of the response of plants to oscillations in atmospheric CO_2. Assuming the response of stomata to oscillations in CO_2 is unaffected or similar to the integrated response to CO_2 under steady state conditions, the mean and amplitude of the oscillation will determine assimilation. Three species were chosen with very different stomatal characteristics to test this and no stomatal response was observed in any of them and concurrently with no reduction in carbon assimilation. For this reason, and the minimal reductions predicted by A-C_a curves it is concluded that previously observed reductions in assimilation under oscillating CO_2 may have been caused by a differential stomatal response to a step change in CO_2 when the step is to either steady state or oscillating CO_2.

Conclusions

Under oscillating CO_2 (with a 60 second period), a consistent increase in carbon assimilation of nearly 2 µmol $m^{-2}s^{-1}$ across both *P.* x *euramericana* and *Q. robur* was observed compared to assimilation under steady state CO_2. This increase of over 15% in Poplar and nearly 20% in Oak has been observed by others (Evans and Hendrey 1992) and could significantly increase assimilation in FACE experiments. Evidence in this Chapter suggests that oscillations in CO_2 may stimulate carbon assimilation, perhaps by switching between electron transport limitation and carboxylation limitation, although further work is needed to test the nature and causes of this stimulation. There was no response of stomatal conductance or transpiration to oscillating CO_2.

Testing the hypothesis of Hendrey et al. (1997), that oscillating CO_2 reduced assimilatory carbon use efficiency and hence reduced assimilation; assimilation rates were predicted to decrease based on modelling assimilation with A-C_i/C_a curves driven with CO_2 data from the experiments, but only by a small percentage. Reductions in assimilation efficiency caused by non-linearity in the A-C_i curve appeared insufficient to explain previously observed reductions in assimilation under oscillating CO_2. The data presented in this Chapter show no stomatal response to a switch from steady state CO_2 to oscillating CO_2 with the same mean CO_2 concentration. We propose that previously observed reductions in assimilation under oscillating CO_2 may have been caused by a different stomatal response to a step change in CO_2 from steady state to either steady state or oscillating CO_2, although this remains to be tested.

Chapter 4 The performance of carbon cycle models against Net Primary Productivity at Oak Ridge and Duke FACE

Introduction

There has been significant progress in developing, parameterising and validating terrestrial carbon cycle models. Considerable use has been made at the site scale of eddy co-variance data which measure land-atmospheric fluxes of momentum, heat, water vapour and more recently, carbon dioxide, and all simultaneously with meteorological measurements see Schwalm et al. (2010) and Lawrence et al. (2011) for examples. At the global scale various satellite derived products (Running et al. 2004), land-cover datasets (Woodward and Lomas 2004), and most recently a globally gridded product from the FLUXNET community (Beer et al. 2010) have been used for validation, providing very detailed spatial information on the extent and function of terrestrial ecosystems. Finally CO_2 flask measurements provide a global value of mean atmospheric carbon dioxide and thus a constraint for carbon cycle models when analysing their ability to depict the contemporary period (Cadule et al. 2010). Until recently the effect of elevated CO_2 in terrestrial carbon cycle models had been implicitly validated rather crudely on the basis that the models reproduce with some degree of accuracy the observed global rise in atmospheric CO_2 over the long term. Although confounded by other factors, the models' responses to CO_2 were shown to be poorly constrained by the huge divergence of predicted CO_2 concentrations into the future given the same forcing scenario (Friedlingstein et al. 2006).

Differences in flask values at different points in space and time contain seasonal and inter-annual information on continental-scale variations in CO_2 fluxes. In a more sophisticated, explicit validation of the global CO_2 flux, Cadule et al. (2010) compared the carbon fluxes of three Earth system models against instrumental atmospheric CO_2 observations using a single atmospheric transport model to generate CO_2 concentrations directly comparable at each measurement station. Their results showed that while models were generally reasonable at simulating the long-term trend in carbon fluxes, the models ranged in their ability to simulate carbon fluxes over seasonal and inter-annual cycles and at different sites. Cadule et al. (2010) results provide an excellent new framework for validating global model carbon fluxes simulated by fully coupled Earth System models. All of these measurements are for contemporary periods and allow only a limited understanding of physiological responses to raised (surface) atmospheric CO_2 concentrations.

Free Air Carbon dioxide Enrichment (FACE) experiments present the opportunity to validate ecosystem scale CO_2 responses to elevated CO_2, 500-600 µmol mol^{-1}, under the same climate. Laboratory-based experiments have been performed to assess the impact of increased ambient CO_2 on photosynthesis and plant productivity (Arp 1991, Stitt 1991). However, these do not provide information on the long-term effects of such increase, and the applicability to natural systems of any acclimation of the CO_2 response (a decrease over time of the initial boost to productivity) observed in these laboratory experiments has been questioned (Arp 1991, Stitt 1991). FACE experiments examine the response of natural, semi-natural and agricultural ecosystems to elevated concentrations of atmospheric CO_2 (Evans and Hendrey 1992, Hendrey and Kimball 1994) over significant periods of time. For this reason, the emerging results from FACE experiments are essential and provide an unprecedented opportunity to validate terrestrial carbon cycle models.

Most forest FACE experiments are fully replicated at the stand scale. With the acknowledgement that global carbon cycle models are point models running at the stand level and scaled to a region, FACE experiments are suitable for direct comparison with large scale terrestrial carbon cycle models. While the impact of elevated CO_2 will be important in both young and old growth forest and the mechanisms by which CO_2 affects carbon sequestration in different age systems are likely to be quite different, the only FACE experiment in a mature system (Körner et al. 2005) was conducted at the individual tree scale and as such was less comparable with stand-scale carbon-cycle models. The FACE experiments used in this study represent the most natural, and oldest forest systems tested with FACE technology to date. This study uses data from the Oak Ridge (Iversen et al. 2011) and Duke (McCarthy et al. 2010, Drake et al. 2011) FACE experiments located in the South Eastern USA. They are both in relatively young but closed canopy and maturing, unmanaged plantation ecosystems. The two FACE sites are very similar climatically and the primary difference between these two sites is that Oak Ridge is deciduous broadleaf while Duke is evergreen needleleaf. McCarthy et al. (2010) found that the primary drivers of variability in the CO2 response of NPP at Duke FACE were nitrogen and the water balance.

The two major UK DGVMs/LSMs are used in this study: the Sheffield Dynamic Global Vegetation Model (SDGVM; Woodward et al. 1995, Woodward and Lomas 2004) which is a stand-alone global carbon cycle model; and the Joint UK Land Environment Simulator (JULES; Best et al.

2011) which is the LSM used in the Hadley Centre's Earth System model and is the updated version of the MOSES/TRIFFID model. SDGVM and JULES are the focus of the research in this Chapter due to access and to determine the ability of DGVMs to capture NPP dynamics under elevated CO_2 with only a simple nitrogen model (SDGVM) or parameterisation of canopy nitrogen. JULES parameterises leaf nitrogen as a single value per PFT (Clarke et al. 2011) while SDGVM simulates canopy nitrogen as a function of soil decomposition rates (Woodward et al. 1995). The focus on the UK models was due to access and time constraints in modifying the models; ideally multiple variants of the models would be used to assess the importance of the nitrogen cycle in these experiments and simulations.

Results are also presented from another 10 LSMs/DGVMs and ecosystem models. Along with SDGVM, these models were part of a US National Centre for Ecological Analysis and Synthesis (NCEAS) project and detailed comparisons of the water and nitrogen dynamics of these different models is the subject of (De Kauwe et al. In Prep, Zäehle et al. In Prep).

This study was primarily a benchmarking/validation exercise, addressing the question: can a range of DGVMs reproduce NPP under ambient and elevated CO_2 at the Oak Ridge and Duke FACE experiments? Furthermore, can models reproduce the response of NPP to elevated CO_2? Models are compared using measures of model skill in reproducing the observed NPP at the FACE sites. To test whether models can also reproduce the relationship of NPP to climatic and biological drivers of NPP, models and observations are further compared using multiple linear regressions of NPP on precipitation, temperature, photosynthetically active radiation (PAR), canopy nitrogen and nitrogen uptake.

SDGVM and JULES have simple nitrogen dynamics and it was hypothesised that using observed values of canopy nitrogen and the observed relationship of V_{cmax} to leaf nitrogen in the models would improve simulations of NPP. To test this, SDGVM and JULES were modified to be driven with observations of canopy nitrogen and the observed relationship of V_{cmax} to leaf nitrogen. SDGVM was also modified to take PAR as a driving variable as opposed to internal calculation of PAR based on latitude and time of year (the default SDGVM method).

It was also hypothesised that soil water limitation would play a key role in the simulated CO_2 response and the impact of soil water limitation in the two models was assessed by running the models without soil water limitation.

This Chapter sheds light on what model process and parameter improvements are necessary for improved confidence in the ability of the models to inform policy-relevant questions, such as: how will terrestrial ecosystems respond to raised surface CO_2 concentrations?

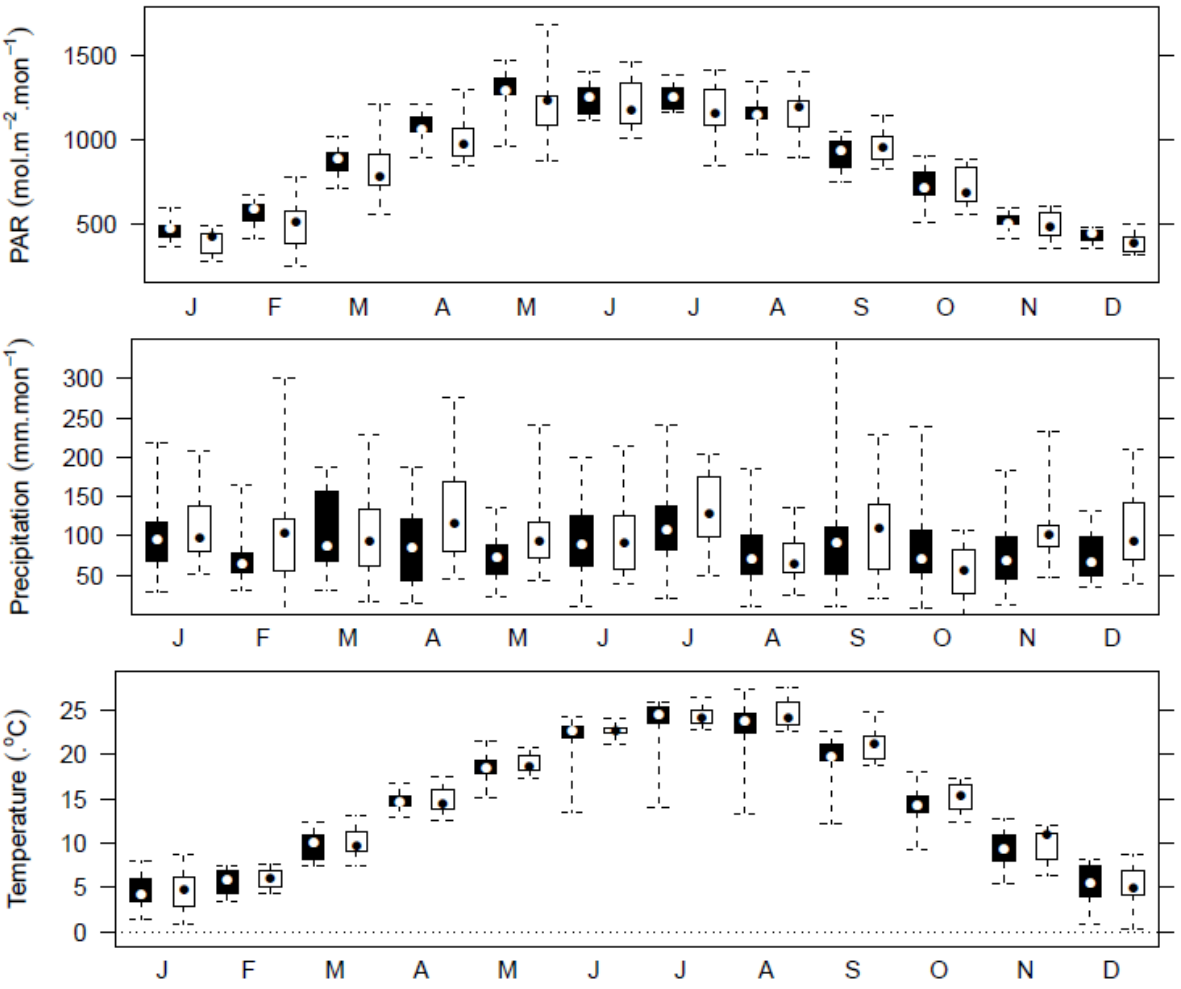

Figure 4-1. Box and whisker plots showing the distribution of monthly climate values over the course of the Duke (black bars) and Oak Ridge (white bars) FACE experiments. Temperatures are expressed as the monthly means and precipitation and Photosynthetically Active Radiation (PAR) are monthly sums. Dots in the box represent the median of the monthly values, boxes are the inter-quartile range (IQR) and whiskers extent to the full range.

Methods

FACE sites

This study uses data from the Oak Ridge (Norby and Iversen 2006) and Duke (McCarthy et al. 2007) FACE experiments over the long periods of years, 1998–2008 and 1997–2007 respectively. The sites are in similar locations in the South Eastern USA. Oak Ridge FACE, Tennessee (35°54' N; 84°20' W) was composed of Sweetgum (*Liquidambar styraciflua* [L.]), planted in 1988 at the high density of 2800 trees ha^{-1} with the original purpose of biomass production. The plantation was unmanaged since establishment and showed little understory growth. The soil is an Aquic Hapludult (Wolftever Series) and the rooting depth is up to 2 m. Duke FACE, North Carolina (35°58' N; 79°06' W) was composed of Loblolly Pine (*Pinus taeda* [L.]), also unmanaged since establishment in 1983 but with a significant understory of native hardwoods, in some cases emerging into the canopy. Planting density was 1713 pines ha^{-1} and hardwoods established at 2589 trees ha^{-1}. The soil is an Ultic Hapludalph (Enon series) with a depth of 0.75 m. Annual meteorological data and other site characteristics are presented in Table 4-1 and the monthly meteorological data is presented in Figure 4-1.

Observed NPP and relative responses are shown in Figure 4-2. McCarthy et al. (2010) have shown that the mean magnitude of NPP (by block—replicate plots were blocked by soil fertility) was most strongly correlated with a soil nitrogen availability index with inter-annual variability determined by precipitation minus potential evapo-transpiration (P-PET) and disturbance events. The linear regression in this study showed that only temperature was a significant correlate with NPP (Table 4-2) suggesting that temperature was driving P-PET.

In this study we use annual NPP to validate our models which was measured using detailed, on-the-ground, inventory style methods (McCarthy et al. 2007, Norby RJ et al. 2008). At both sites NPP was calculated as the sum of wood and coarse root production, leaf production and fine root production. Wood and coarse root production was measured using trunk diameter allometrics and wood density measurements; leaf production was calculated from litter fall and fine root production was measured using mini-rhizotrons. NPP is the remainder of GPP once plant respiration has been subtracted and this is how the models simulate NPP. At the FACE sites, NPP allocated to plant biomass production was measured but not NPP allocated to root exudation and mycorhizal symbionts was not measured nor were changes in stored plant

carbon. Measured NPP represents annual plant growth, which is the major component of NPP, rather than NPP in its strictest sense.

Table 4-1.Comparison of driving data and some input parameters at Duke and Oak Ridge. Data are the annual mean (1 SD).

		Duke		ORNL	
Location		North Carolina, USA 35° 58' N, 79° 05' W		Tennessee, USA 35° 54' N, 84° 20' W	
CO_2 enrichment (ppmv)		550		565	
Species		*Pinus taeda*		*Liquidambar styraciflua*	
Plant Functional Types		80% Evergreen Needleleaf 20% Deciduous Broadleaf		100% Deciduous Broadleaf	
Soil depth (m)		0.75		2	
Precipitation (mm)		1080	(180)	1230	(220)
Temperature (°C)		14.8	(0.63)	14.8	(0.90)
PAR (mol m^{-2} yr^{-1})		10600	(440)	10000	(1200)
RH (%)		74.7	(3.7)	75.9	(2.5)
Maximum canopy nitrogen	amb	9.07	(0.72)	6.95	(0.71)
(g m^{-2} ground area)	elv	11.26	(1.55)	no sig diff	

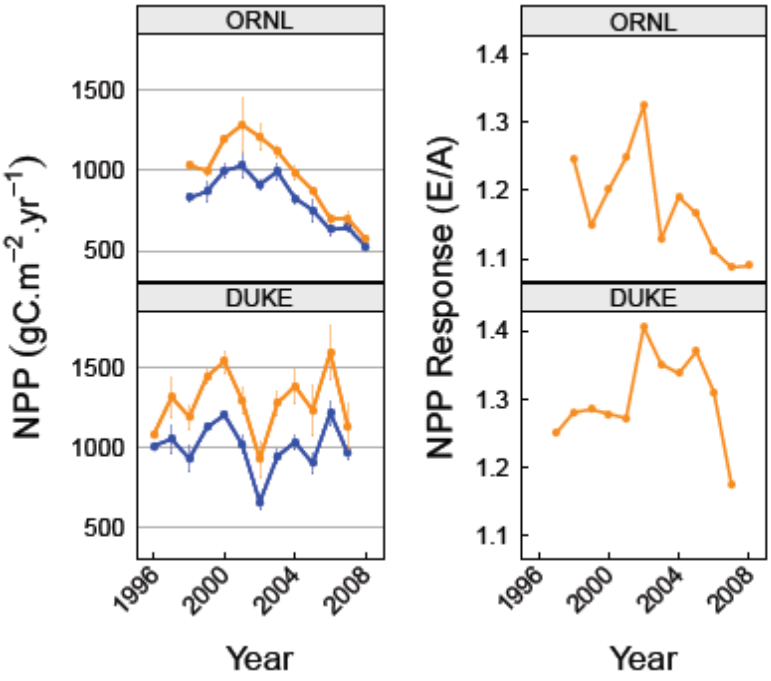

Figure 4-2. Observations of mean annual NPP (±1 SEM, right plot) and relative response of NPP to elevated CO_2 (left plot) at Duke and Oak Ridge FACE experiments, ambient CO_2 treatment (blue lines) and elevated CO_2 treatment (orange lines).

Models

The latest version of SDGVM from the 7th June 2007 and JULES v2.1.2 were used as the baseline models in these simulations. Both SDGVM and JULES represent similar fundamental processes that determine carbon cycling and water cycling but as yet neither of them explicitly model nitrogen or phosphorus cycling which are known to place limitations on NPP. SDGVM and JULES represent differently processes of water and carbon cycling, in particular plant mediated carbon cycling.

Ten other models were run by their respective modelling groups as part of the US National Centre for Ecological Analysis and Synthesis model inter-comparison project. The models were: CABLE (Wang et al. 2007a), CLMCN (Thornton et al. 2007), DAYCENT (Del Grosso et al. 2009), EALCO (Wang et al. 2007a), ED2.1 (Moorcroft et al. 2001), GDAY (Medlyn et al. 2000), ISAM (Jain and Yang 2005), LPJ-GUESS (Hickler et al. 2004), OCN (Zaehle and Friend 2010) and TECO (Bell et al. 2007); and they represent a wide range of processes at various scales of application. Many of these models have a mass balance nitrogen cycle. As described below JULES and SDGVM were modified to take the observed maximum canopy nitrogen as a driving variable.

Maximum annual canopy nitrogen was used as a driving variable. Maximum canopy nitrogen was scaled to daily canopy nitrogen using the following equation:

$$N_{can,m} = \frac{LAI_m}{\mathrm{LAI}_{\mathrm{max,m}}} \left(N_{can,max} \times \frac{LAI_{max,m}}{LAI_{max,o}}\right) \quad (4\text{-}1)$$

Where $N_{can,m}$ is the model canopy nitrogen in gm^{-2}; $N_{can,max}$ is the observed annual maximum canopy nitrogen in gm^{-2}; LAI_m is the modelled LAI; $LAI_{max,m}$ is the maximum modelled LAI and $LAI_{max,o}$ is the annual maximum observed LAI. The purpose of this scaling was twofold. One, to scale maximum canopy nitrogen, which occurs at maximum LAI, to canopy nitrogen at the LAI on a given day.Two, to maintain the ratio of maximum canopy nitrogen to maximum LAI, observed at the FACE sites. It was important to maintain the ratio of canopy nitrogen to LAI as nitrogen distribution through the canopy is a function of LAI and as such is an important factor in determining V_{cmax} and J_{max} at each layer in the canopy.

The observed relationship of V_{cmax} (µmol m^{-2} s^{-1}) to leaf nitrogen on an area basis was included in the models and in SDGVM the relationship of J_{max} to V_{cmax} (µmol m^{-2} s^{-1}) was also coded into the model (both taken from the NCEAS protocol), as follows:

Duke:

$$V_{cmax\,,i} = 22.29N_{a\,i} + 8.450 \quad (4\text{-}2)$$

$$J_{max\,,i} = 1.860V_{cmax\,,i} \quad (4\text{-}3)$$

Oak Ridge:

$$V_{cmax\,,i} = 20.497N_{a\,i} + 8.403 \quad (4\text{-}3)$$

$$J_{max\,,i} = 1.974V_{cmax\,,i} + 13.691 \quad (4\text{-}4)$$

Replacing the functions for:

SDGVM:

$$V_{cmax\,,i} = 11N_{a\,i} \quad (4\text{-}5)$$

$$J_{max\,,i} = 1.64V_{cmax\,,i} + 29.1 \quad (4\text{-}6)$$

JULES:

$$V_{cmax\,,i} = 800N_{c\,i} \quad (4\text{-}7)$$

Where N_a refers to leaf nitrogen on a ground area basis (gm^{-2}) and N_c the leaf nitrogen to carbon ratio (top leaf N:C ratio nl0 in JULES—0.046 for broadleaved trees and 0.033 for needleleaf trees), the subscript *i* refers to canopy layer. The J_{max} terms were not relevant to the JULES simulations as the equations for photosynthesis are based on the Collatz et al. (1991) scheme which does not assume a biochemical limit to electron transport.

At Duke, canopy nitrogen for each PFT was reported on a plot area basis while the models assumed canopy nitrogen values were per the area occupied by the PFT, therefore observed canopy nitrogen values were scaled by the total plot area divided by the fraction of area occupied by a PFT, i.e. in the case of the broadleaved PFT, measured canopy nitrogen values were scaled by 1.0/0.2 to drive the model.

SDGVM normally calculates Photosynthetically Active Radiation (PAR) based on latitude and time of year. SDGVM was also modified to take daily observed measurements of PAR as a driving variable.

Simulations

SDGVM and JULES were initialised using the site-specific parameters (from the ambient treatment where relevant) presented in Table 4-1. Both models were spun up over 500 years using site-specific land-use histories, historical CO_2 records (Boden 2011) and randomly repeated years of the driving variables measured during the experimental treatments. The simulations proper were started at the time of planting to the year prior to CO_2 enrichment, 1983-1996 and 1988-1997 at Duke and Oak Ridge respectively. In neither model were the land-cover fractions dynamic (i.e. TRIFFID was turned off in JULES) and they were driven with 80% evergreen needleleaved trees and 20% deciduous broadleaved trees at Duke and 100% broadleaved trees at Oak Ridge. Two simulations, representing the two CO_2 treatments, were then run over the years for which data were available, 1996-2007 and 1998-2008.

As described above the models were able to be run with a number of additional driving variables. Initial simulations were run in the models' standard configurations (hereafter referred to as just SDGVM or the standard run), as they would be in a global run, with the exception of soil depth, soil texture, field capacity and wilting point taken from the NCEAS protocol.

Four additional versions of SDGVM were run, all driven with observed annual maximum canopy nitrogen, the first with canopy nitrogen and the standard SDGVM V_{cmax} and J_{max} to nitrogen parameterisations (canN). The second parameterised with the observed relationships of photosynthetic parameters (V_{cmax} and J_{max}) to nitrogen (canN Vc) (Equation 4-2 to 4-5). The third and fourth simulations built on canN Vc using observed PAR (canN Vc PAR) and one with mean observed PAR (canN Vc xPAR). For JULES two simulations (additionally to the standard run) were driven with canopy nitrogen and with observed V_{cmax} and J_{max} relationships, these simulations were run with both observed PAR (canN Vc – as using observed PAR is standard for JULES, the comparable SDGVM runs were termed canN Vc PAR) and mean observed PAR (results are not presented for the mean PAR as it differed very little from the inter-annually varying PAR run).

The above simulations were also run with soil water limitation in the models turned off. Both models apply a soil water stress multiplier (β in JULES, kg in SDGVM—for consistency referred to as β hereafter) (Woodward et al. 1995, Best et al. 2011). β is reduced proportionally from one, when soil water drops below a critical volumetric soil water content (set as an input

parameter in JULES—known as the critical point, and determined by soil texture in SDGVM), to zero when the soil water content reaches wilting point (set as an input parameter in both SDGVM and JULES). In JULES, potential carbon assimilation is then multiplied by β to yield actual carbon assimilation. While in SDGVM, V_{cmax}, J_{max} and stomatal conductance (g_s) are multiplied by β. In the non-soil water stressed simulations β was maintained at 1 regardless of soil water content.

Statistics

All statistical tests were carried out in R (R Core Development Team 2011) using internal R functions. 'Goodness of fit' metrics were the coefficient of determination (R^2 - the square of Pearson's correlation coefficient); the single, absolute maximum error (ME); the root of the mean squared error (RMSE) and model efficiency (EF), a measure of how the simulated data compares with the mean of the observed values as a predictor of the observed values, calculated:-

$$EF = \left(\sum_{i=1}^{n}(\bar{O} - O_i)^2 - \sum_{i=1}^{n}(P_i - O_i)^2\right) \Big/ \sum_{i=1}^{n}(\bar{O} - O_i)^2 \qquad (4\text{-}8)$$

where P_i are the model predicted values, O_i are the observed values and *n* is the number of data. An EF value above zero indicates that the model predictions are a better fit to the observed data than the mean of the observations, with a value of one indicating a perfect fit. Below zero EF is un-bounded and indicates that the mean of the observations is a better descriptor of the observations than the predicted data.

In a sensitivity analysis, multivariate linear regressions were used to detect correlations between annual values of NPP and climatic and biological driving variables—annual precipitation, mean annual temperature, mean annual relative humidity, annual PAR, annual maximum canopy nitrogen and for the models (NCEAS intercomparison 10) that simulated it – annual nitrogen uptake.NPP under elevated CO_2 was detrended by the difference in mean between the two CO_2treatments. Canopy nitrogen was also detrended in the same way to eliminate any differences in canopy nitrogen caused by the treatments. Interactions between driving variables were left out of the models due to the low number of data available (number of years by two treatments, n=22). The effect of CO_2 as an interaction term was investigated and was found to be insignificant (results not shown) although there were perhaps insufficient

data (n=22 at each site) to detect any subtle interactions of CO_2 concentration and driving variables on NPP. Statistical models (linear fixed-effects multiple regressions) were fitted to the data using all driving variables. If the regressions were significant then they were simplified by removing insignificant driving variables one by one until all driving variables were significant (P<0.1).

Statistics presented were again the coefficient of determination for the entire statistical model (R^2) and the corresponding P value; p values for each individual variable and a measure of the coefficient of determination (r^2) for each individual variable. The coefficient of determination—R^2—measures the variance in the response variable explained by variance in the explanatory variables of a multiple regression. To tease out the contributions of each explanatory variable to the R^2, a coefficient of determination—r^2—can be calculated for each explanatory variable. Type I sums of squares coefficients of determination (Type I r^2) (Sokal and Rohlf 1995) are calculated as the increase in R^2 of the full regression model with the addition of the explanatory variable in question. The type I r^2 value depends upon the order in which the explanatory variables are added to the model and, particularly for those variables added to the model first, could also include variance correlated with other explanatory variables. For this reason, when calculating Type I r^2, variables were added to the model in reverse order of their correlation to other explanatory variables.

Type II sums of squares coefficients of determination (Type II r^2) (Sokal and Rohlf 1995) measure the variance in the response variable accountable to variance in the explanatory variable that is uncorrelated with the other explanatory variables. Type II r^2 is the decrease in the R^2 of the full regression when removing the explanatory variable in question and is independent of the order in which the variables are fitted to the statistical model. It is calculated as follows:

$$r(II)_y^2 = r_y^2 \times t_y \qquad (4\text{-}9)$$

Where $r(II)^2_y$ is the Type II r^2 of the explanatory variable y; r_y is the Pearson correlation coefficient between explanatory variable y and the response variable and t_y is the tolerance of explanatory variable y calculated:

$$t_y = 1 - R_{y,z}^2 \qquad (4\text{-}10)$$

Where $R^2_{y,z}$ is the coefficient of determination of explanatory variable y regressed against the remaining set of explanatory variables.

Results

At Duke, a multiple-regression of annual NPP on climatic driving variables (annual precipitation, mean annual temperature and PAR) and peak canopy nitrogen was not significant (Table 4-2). At Oak Ridge however, the multiple-regression of annual NPP was significant (P<0.001) with the multiple-regression explaining 79% of the inter-annual variation in NPP. The variable that accounted for the majority of the explained variation was canopy nitrogen (Table 4-2).

Table 4-2.Results from multivariate linear regressions of the observed data. Detrended NPP was regressed on the measured driving variables at a site. r is the Pearson correlation coefficient. Tolerance is a measure of the independence of a driving variable from the other driving variables and is calculated as one minus the R^2 from a multiple linear regression of the driving variable in question against all the other driving variables. The driving variables in the table are listed in order of tolerance. Part r^2 (also known as semi-partial r^2) is a measure of the variation in NPP explained by the driving variable in question. The p value, R^2 and P are all taken from the multiple regression.

run	var	explanatory variable	r	tolerance	part r^2 (II)	part r^2 (I)	p value	multiple R^2	P of model
Duke	npp	precipitation	0.23	0.88	0.05	0.03	0.308	0.30	0.175
		temperature	-0.52	0.79	0.22	0.12	0.036		
		canopy nitrogen	0.38	0.77	0.11	0.06	0.118		
		PAR	0.35	0.76	0.09	0.09	0.154		
ORNL	npp	temperature	-0.29	0.89	0.07	0.14	0.016	0.82	0.000
		canopy nitrogen	0.64	0.65	0.26	0.62	0.000		
		precipitation	0.06	0.62	0.00	0.03	0.646		
		PAR	-0.26	0.47	0.03	0.03	0.097		
	npp	canopy nitrogen	0.77	0.99	0.58	0.63	0.000	0.79	0.000
		temperature	-0.29	0.90	0.07	0.12	0.018		
		precipitation	0.18	0.89	0.03	0.03	0.120		

SDGVM

In its standard release, SDGVM under-predicted NPP at both sites (Figure 4-4), severely so at Duke (RMSE 455 gC $m^{-2}y^{-1}$), such that the mean of the observations was a better predictor of the observations than simulated NPP, indicated by a negative model efficiency (EF = -3.63). SDGVM captured the inter-annual variability in NPP at Duke with an R^2 of 0.54 (P<0.001) and less well at Oak Ridge with an R^2 of 0.36 (P<0.01).

Adding canopy nitrogen and PAR as driving variables to the simulations and modifying photosynthetic parameters had a considerable impact on both the absolute values of NPP and the inter-annual variability of NPP. Using observed canopy nitrogen as a driving variable (canN) improved the R^2 and EF at both sites (Table 4-3). At Duke, EF was strongly improved due to higher absolute values of NPP. The subsequent addition to the model of the observed relationships of V_{cmax} and J_{max} to leaf nitrogen led to a marked over prediction of NPP at both sites, decreasing EF. The R^2 at Oak Ridge was strongly increased in the canN Vc run as the observed photosynthetic parameters strongly increased model sensitivity to canopy nitrogen, shown to correlate strongly with NPP in the experiment (Iversen et al. 2011).

The over-prediction of NPP when driving the model with observed nitrogen and photosynthetic relationships was corrected by using observed daily PAR as a driving variable. SDGVM over-predicted the levels of photosynthetically active radiation (PAR) at the two sites (46% on an annual basis at Oak Ridge although the over-prediction was higher in the winter). At Oak Ridge however, the improved simulation accuracy of absolute values was at the cost of accurate simulation of inter-annual variability. Using the mean of the observed PAR (i.e. no inter-annual variability in PAR) as a driving variable improved both the R^2 and model efficiency (although it remained below zero) at Oak Ridge. The mean PAR simulation at Duke had little impact on the R^2 yet improved the model efficiency due to better simulation of absolute values. Unlike the Oak Ridge simulation, there was little change in simulation of inter-annual variability due to less inter-annual variation in PAR at Duke over the course of the experiment (Figure 4-1).

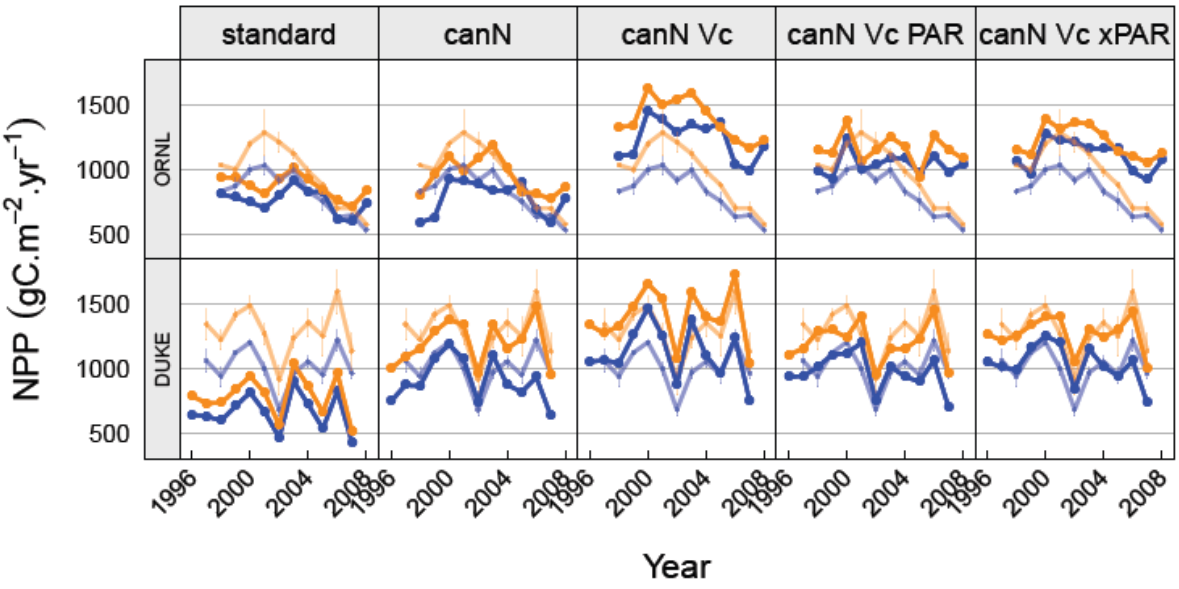

Figure 4-4. SDGVM simulations (solid lines) and observations (mean ± 1 SEM; faded lines) of NPP at Duke and Oak Ridge FACE experiment, ambient CO_2 treatment (blue lines) and elevated CO_2 treatment (orange lines). The results of five different configurations of the model are shown: the standard SDGVM release; using annual maximum canopy nitrogen as a driving variable (canN); using annual canopy nitrogen as a driving variable and observed relationships of V_{cmax} and J_{max} to leaf nitrogen (canN Vc); using canopy nitrogen, V_{cmax} etc and observed PAR (canN Vc PAR); and using canopy nitrogen, V_{cmax} etc and the mean of observed PAR (canN Vc PAR).

Table 4-3.Model skill statistics for SDGVM NPP at Oak Ridge and Duke FACE. The R^2 and P value are from a linear regression of modelled NPP on observed NPP. The absolute maximum error [abs(ME)] and root mean square error (RMSE) are presented as well as model efficiency (ME), a measure of the models accuracy for both the variability and absolute values. A model efficiency of one indicates a perfect fit, while a value below zero indicates that the mean of the observations is a better predictor of the observations than the model predictions.*P*-values are colours from yellow to red with warmer colours indicating increasing significance. EF values are colour coded from yellow to red from zero to one, i.e. increasing model skill; and from yellow to blue from zero to minus one, i.e. decreasing model skill, and all values below minus one are coloured blue.

Site	run	CO_2	R^2	*P*	abs(ME)	RMSE	EF
Duke	Standard	all	0.54	0.000	633	455	-3.63
	canN	all	0.67	0.000	330	154	0.47
	canN Vc	all	0.68	0.000	405	183	0.25
	canN Vc PAR	all	0.67	0.000	263	138	0.57
	canN Vc xPAR	all	0.68	0.000	233	120	0.68
ORNL	Standard	all	0.36	0.003	479	188	0.19
	canN	all	0.48	0.000	295	155	0.44
	canN Vc	all	0.68	0.000	652	435	-3.35
	canN Vc PAR	all	0.12	0.108	559	284	-0.86
	canN Vc xPAR	all	0.64	0.000	546	297	-1.04

The

relationship of NPP to driving variables represents an *ad hoc* sensitivity analysis, highlighting variables that are important drivers of NPP in the models. The assumption was that if inter-annual variability in a model's NPP prediction was sensitive to a particular driving variable then that variable was an important driver of NPP. This assumption holds where there was significant variability in NPP and the driving variable in question, however if there was little variability in either then this assumption breaks down. It is quite possible that the main driver of the absolute value of NPP may vary little over the course of the simulations and that inter-annual variability was driven by a different variable which appears to have been the case for some of the models (results presented below) in this study. With this caveat in mind the relationship of NPP to driving variables is explored.

Precipitation and temperature were significant correlates with detrended NPP for SDGVM throughout most of the model runs (Table 4-4) indicating that SDGVM was a model that responded to climate. Canopy nitrogen and PAR were significant correlates of NPP suggesting that the core photosynthesis model in SDGVM was a key driver of NPP. No correlation was found between canopy nitrogen and NPP in the canN run but the correlation in the canN Vc run suggests that it was light that limited photosynthesis and hence NPP in the canN run. There was a switch in NPP sensitivity from precipitation to temperature from the standard to the canN run at Oak Ridge.

JULES

Similar to SDGVM, the standard release of JULES (with vegetation dynamics—TRIFFID—turned off) strongly under-predicted NPP at Duke (Figure 4-5) with an RMSE of 423gC $m^{-2}y^{-1}$. At Oak Ridge JULES captured the mean NPP but significantly over-predicted NPP in the later years of the experiment (Table 4-5). Similar to SDGVM, JULES simulated the inter-annual variability in NPP more accurately at Duke (R^2 = 0.61, P<0.001) than at Oak Ridge (R^2 = 0.27, P<0.05). However, at neither site were the JULES simulations a better predictor of the observations than the mean of the observations themselves (EF = -2.99 & 0.00 at Duke and Oak Ridge respectively).

Driving JULES with canopy nitrogen had little impact on NPP at Oak Ridge. At Duke the mean NPP was strongly increased bringing the simulated values in line with the observed values (EF = 0.47). Unlike SDGVM, driving JULES with mean short wave radiation (which JULES linearly converts to PAR) had little impact on the inter-annual variability in simulated NPP (results not

shown). PAR was not an important driving variable of NPP in JULES, as seen in the Duke simulations where, although observed PAR was used as a driving variable, PAR was never a significant correlate of NPP (Table 4-4). Although PAR was a significant variable in the JULES simulations of Oak Ridge it was a significant variable even in simulation where mean PAR was used (results not shown). This was because PAR was correlated with precipitation at Oak Ridge, shown by the low tolerance of the two variables.

Precipitation was the driving variable most correlated with NPP across the JULES runs. Comparison to simulations without soil water stress (β = 1) showed that soil water stress reduced NPP in JULES by 27% at DUKE and 25% at Oak Ridge (Figure 4-6). By contrast, the magnitude of soil water limitation in SDGVM was 5% at DUKE and 2% at Oak Ridge (Figure 4-6). The strength of soil water limitation in JULES indicates that inter-annual variability in, and to a large extent absolute, NPP was a product of soil water limitation. Soil water is the difference between precipitation and evapotranspiration. The strong correlation to precipitation indicates that precipitation was a major driver of soil water limitation at both sites. At Duke, temperature was also a major negative correlate with NPP and given the strength of soil water limitation in JULES it is likely that temperature driven changes in evapo-transpiration were important at Duke.

Simulated inter-annual variability was strongly improved in the CanN Vc simulation at Duke but there was also a marked over-prediction of NPP in 2003, removal of the 2003 data improved the R^2 to 0.68(P<0.001) and increased EF to 0.68. 2003 was a peculiar year for JULES due to an absence of soil water limitation which had a strong effect on NPP in other years (Figure 4-6). It was likely that the combination of low temperature (third lowest mean annual temperature—14.3 ^{o}C) and high rainfall (second highest mean annual precipitation—1346 mm) maintained high levels of soil water in JULES during 2003 leading to an over-prediction of NPP.

Table 4-4.Multivariate linear regressions of SDGVM NPP on driving variables (annual values). See Table 4-2 for an explanation of the metrics.

site	Run	CO_2	R^2	P	abs(ME)	RMSE	EF
Duke	Standard	all	0.61	0.000	705	423	-2.99
	canN Vc	all	0.49	0.000	645	215	0.47
	canN Vc -2003	all	0.68	0.000	363	155	0.68
ORNL	standard	all	0.27	0.014	430	208	0.00
	canN Vc	all	0.26	0.015	549	280	-0.20

Table 4-5.Model skill statistics for JULES NPP at Oak Ridge and Duke FACE. See Table 4-3 caption for further description.

site	run	variable	*r*	tolerance	Part r^2 (II)	Part r^2 (I)	*p*	R^2	*P*
Duke	Standard	temperature	-0.46	0.98	0.21	0.28	0.008	0.56	0.000
		precipitation	0.54	0.98	0.28	0.28	0.002		
	canN	temperature	-0.51	0.96	0.25	0.25	0.000	0.75	0.000
		precipitation	0.65	0.89	0.37	0.22	0.000		
		canopy nitrogen	0.57	0.88	0.28	0.28	0.000		
	canN Vc	temperature	-0.54	0.96	0.28	0.28	0.000	0.74	0.000
		precipitation	0.64	0.89	0.36	0.22	0.000		
		canopy nitrogen	0.52	0.88	0.23	0.23	0.001		
	canN Vc PAR	precipitation	0.47	0.88	0.20	0.13	0.002	0.75	0.000
		temperature	-0.62	0.79	0.31	0.07	0.000		
		canopy nitrogen	0.60	0.77	0.27	0.09	0.000		
		PAR	0.78	0.76	0.46	0.46	0.000		
	canN Vc AR	temperature	-0.53	0.96	0.27	0.28	0.003	0.59	0.001
		precipitation	0.54	0.89	0.25	0.17	0.004		
		canopy nitrogen	0.40	0.88	0.14	0.14	0.023		
ORNL	Standard	temperature	-0.15	0.90	0.02	0.13	0.382	0.50	0.001
		precipitation	0.64	0.90	0.37	0.37	0.001		
	canN	canopy nitrogen	0.12	0.99	0.01	0.03	0.473	0.52	0.004
		temperature	-0.47	0.90	0.20	0.35	0.014		
		precipitation	0.39	0.89	0.13	0.13	0.039		
	canN Vc	canopy nitrogen	0.67	0.99	0.45	0.51	0.000	0.84	0.000
		temperature	-0.44	0.90	0.18	0.27	0.000		
		precipitation	0.25	0.89	0.06	0.06	0.022		
	canN Vc PAR	temperature	-0.14	0.89	0.02	0.06	0.386	0.62	0.002
		canopy nitrogen	0.52	0.65	0.18	0.01	0.011		
		precipitation	0.86	0.62	0.46	0.16	0.000		
		PAR	0.92	0.47	0.39	0.39	0.001		
	canN Vc xPAR	canopy nitrogen	0.29	0.99	0.08	0.11	0.056	0.65	0.000
		temperature	-0.53	0.90	0.25	0.42	0.002		
		precipitation	0.36	0.89	0.11	0.11	0.026		

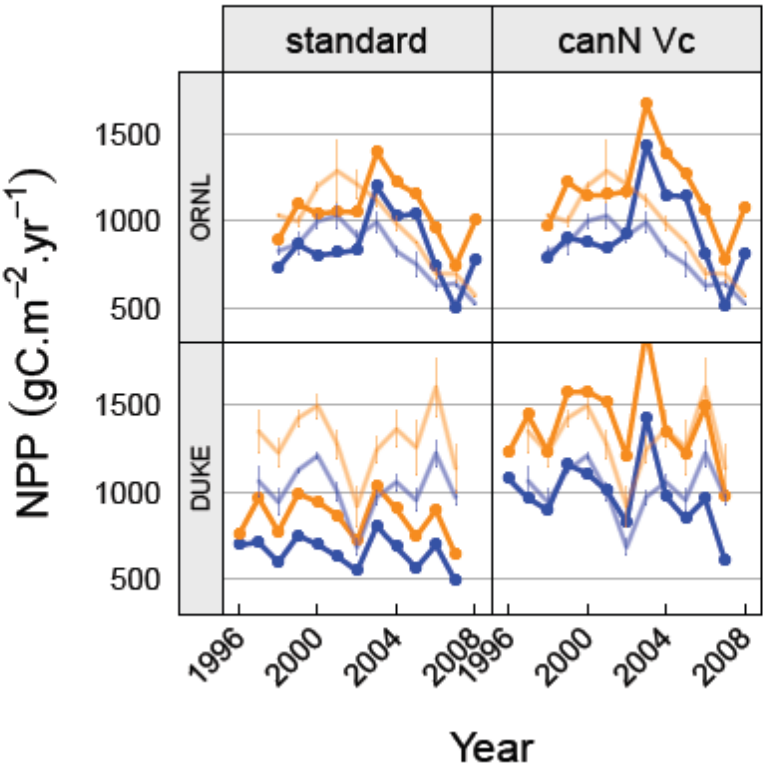

Figure 4-5. JULES simulations of NPP at Duke and Oak Ridge FACE experiments. See Figure 4-4 for a description of the plots. The results of two configurations of the model are shown: the standard JULES release and JULES driven with observed annual canopy nitrogen and observed relationship of V_{cmax} to leaf nitrogen (canN Vc).

Table 4-6.Multivariate linear regressions of JULES NPP on driving variables (annual values). SeeTable 4-2 for an explanation of the metrics.

site	run	variable	*r*	tolerance	Part r^2 (II)	Part r^2 (I)	*p*	R^2	*P*
Duke	Standard	temperature	-0.62	0.98	0.38	0.48	0.000	0.79	0.000
		precipitation	0.56	0.98	0.31	0.31	0.000		
	canN Vc	temperature	-0.58	0.96	0.32	0.40	0.000	0.87	0.000
		precipitation	0.72	0.89	0.46	0.41	0.000		
		canopy nitrogen	0.24	0.88	0.05	0.05	0.017		
ORNL	Standard	PAR	-0.48	0.72	0.17	0.50	0.009	0.63	0.000
		precipitation	0.42	0.72	0.13	0.13	0.019		
	canN Vc	PAR	-0.40	0.72	0.11	0.45	0.025	0.64	0.000
		precipitation	0.52	0.72	0.19	0.19	0.005		

All Models

The broad range of ecosystem and dynamic vegetation models of the NCEAS inter-comparison project simulated NPP at the two FACE sites with a wide range of accuracy (Figure 4-7&Table 4-7). With the exception of GDAY all models captured, with some degree of significance, the inter-annual variability at Duke while five out of the ten models failed to capture any of the inter-annual variability at Oak Ridge. The mean R^2 at Duke was 0.46±0.23 (1 standard deviation) compared with 0.25±0.27 (1 SD) at Oak Ridge. Mean model efficiency was -3.04±4.95 (1 SD) at Duke while at Oak Ridge it was -6.77±6.53 (1 SD).

With the exception of ISAM at Duke, simulated NPP of all models was significantly correlated to the models' driving variables (Table 4-8). Important driving variables differed from model to model, but there were similarities, providing a criterion for grouping the models. The most strongly correlated variable was often the same at both sites for a particular model. This was counter to the observations where inter-annual variability was related to the water-balance and disturbance events at Duke (McCarthy et al. 2010) and declining nitrogen availability at Oak Ridge (Garten et al. 2011, Iversen et al. 2011). The propensity of the models to be dominated by the same process at both sites indicates that the models were not flexible enough to switch limiting factors as observed in nature.

With the exception of DAYCENT, the central core of all the models used in this study is the Farqhuar et al. (1980) or Collatz et al. (1991) photosynthesis scheme, up-scaled to the canopy (Spitters et al. 1986, Sellers et al. 1992, Haxeltine and Prentice 1996). These models are effectively photosynthesis models with abiotic and biotic ecological factors directly acting on photosynthetic parameters and influencing allocation of the assimilated carbon to pools of various residence times. With strong correlation to PAR and/or canopy nitrogen, GDAY, LPJ-GUESS, OCN, TECO (at Oak Ridge) and SDGVM (canN, canN Vc, canN Vc PAR) were primarily driven by their photosynthesis schemes. OCN showed little variability and the primary driver of NPP may be the tightly constrained simulation of nitrogen uptake (see Appendix A for canopy nitrogen values across the models).

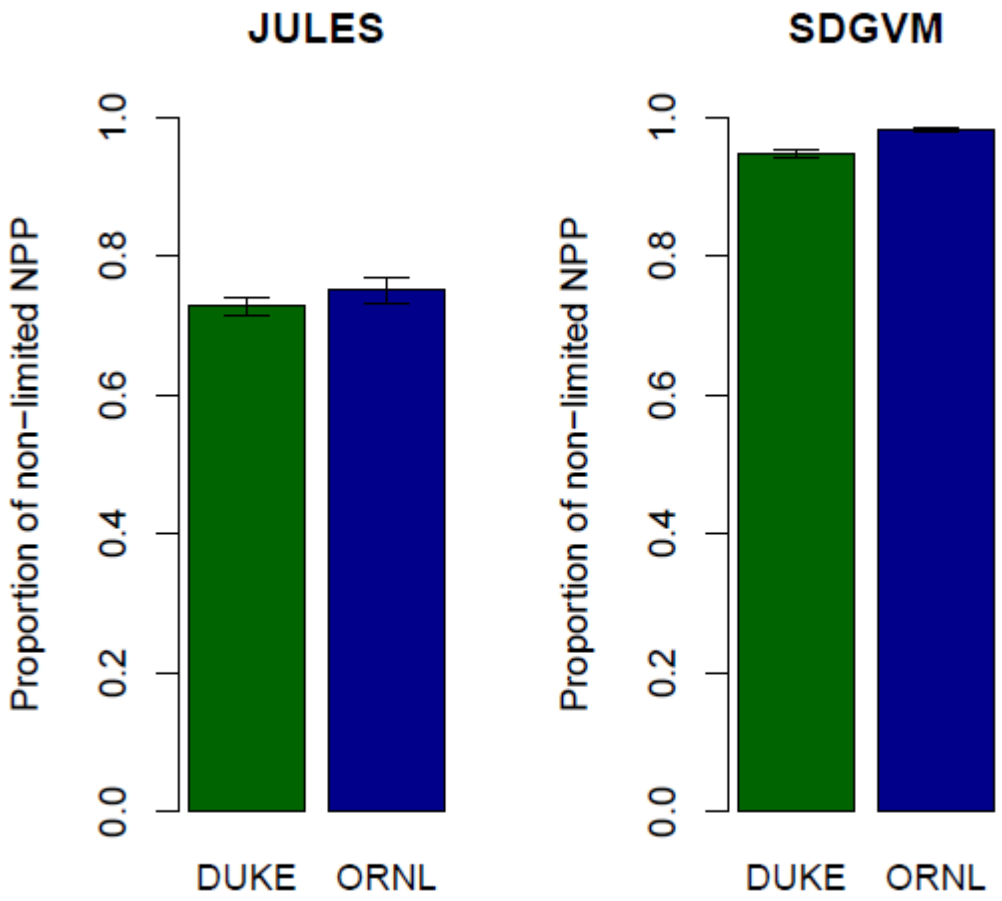

Figure 4-6. The proportional reduction in mean annual NPP ($\pm$1 SEM) caused by soil water limitation. Means were calculated across simulation years and CO_2 treatments. The reduction in NPP was calculated by dividing NPP in a soil water limited simulation by NPP in a simulation with soil water limitation turned off.

The most important variable for the majority of models was nitrogen uptake, those models were: CABLE, CLMCN and ED2.1 at both sites; and DAYCENT, EALCO and TECO at Duke. The strong relationship to nitrogen uptake indicates that these models were driven by stoichiometric constraints on NPP. For the simulations nitrogen uptake was more important at Duke than at Oak Ridge whereas observations suggested that nitrogen limitation was more dominant at Oak Ridge. Interestingly, many of the models that were correlated with nitrogen uptake displayed reasonable prediction of NPP at Duke, indicating that simulated nitrogen uptake must have been driven to some extent by climate.

At Oak Ridge, where we expected nitrogen uptake to be the key driving variable, DAYCENT, EALCO, SDGVM and ISAM were most correlated to temperature, indicating a strong role for respiration in these models. DAYCENT is a growth driven model, not carbon assimilation driven model and temperature has a positive effect on growth, however the negative relationship with temperature indicates that respiration was more important. Temperature could also have been important in the water balance of these models although precipitation was only a correlate of NPP in SDGVM and JULES. These models could be considered more climatically driven.

The decline in NPP at Oak Ridge

ED2.1 was the only model that was driven by nitrogen uptake (Table 4-8) and that captured some of the decline in NPP at Oak Ridge. All of the other models that captured some of the inter-annual variability at Oak Ridge—EALCO, ISAM, OCN, SDGVM and JULES—were driven by other factors, primarily temperature.

With the exception of EALCO, GDAY and perhaps OCN all models failed to capture the strong decline in NPP observed at Oak Ridge. EALCO captured the decline in NPP at Oak Ridge very well however, and as with the SDGVM simulation most consistent with observations (canN), by far the strongest correlate with simulated NPP was temperature.

GDAY and OCN captured a decline in NPP at Oak Ridge but missed most of the inter-annual variability. Both models achieved accurate values of NPP in the final years of the experiment, indicating that their long-term response may be accurate but that the timing of the decline and the plant response to decreased nitrogen availability may be inaccurate. The decline at Oak Ridge was extreme and is perhaps unlikely to be seen in nature due to the very high planting density (the stand was originally planted as a biomass crop). The exact timing of the decline would be very hard to reproduce accurately within the models as it depends on accurate site management histories (Zäehle Pers. Comm.) and perhaps un-represented strategies of Sweetgum in coping with nitrogen stress like responsive root dynamics(Franklin et al. 2009, Iversen 2010). It appears that GDAY and OCN may have captured the more sustainable value of NPP at Oak Ridge, although they both under-predicted NPP at Duke and GDAY simulated a negative response to CO_2 over most of the course of the experiment.

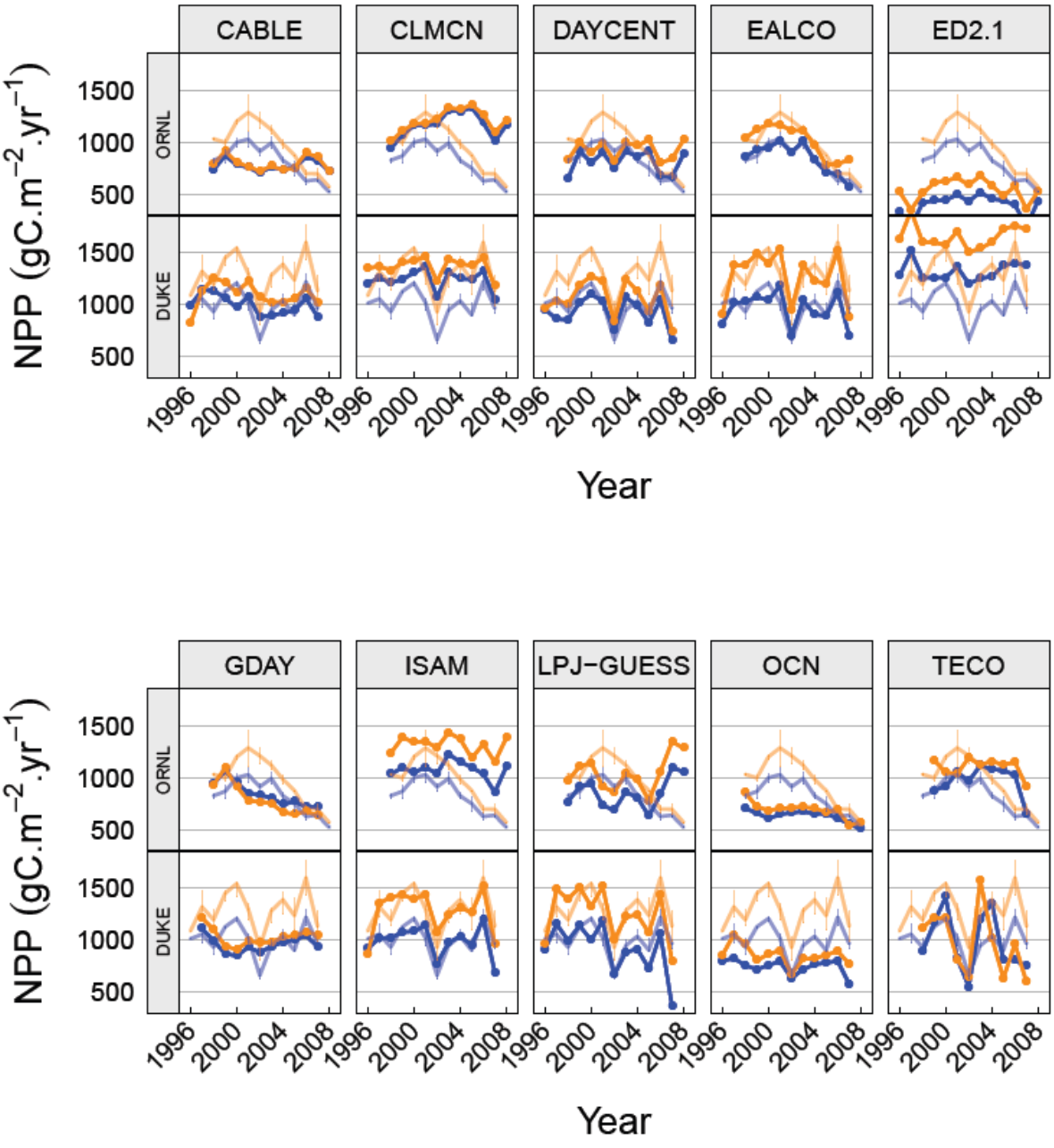

Figure 4-7. Simulations of NPP at Duke and Oak Ridge FACE experiment by ten LSMs. See Figure 4-4 for a description of the plots.

Table 4-7.Model skill statistics of the ten LSMs in simulating NPP at Duke and Oak Ridge. See Table 4-3 for further explanation.

model	site	r2	p	me	rmse	ef
CABLE	DUKE	0.32	0.004	442	205	-2.27
	ORNL	0.02	0.562	517	250	-16.69
CLMCN	DUKE	0.64	0.000	411	210	-2.79
	ORNL	0.01	0.613	639	367	-9.65
DAYCENT	DUKE	0.60	0.000	407	202	-0.52
	ORNL	0.10	0.157	449	204	-2.50
EALCO	DUKE	0.70	0.000	266	139	0.68
	ORNL	0.87	0.000	132	68	0.83
ED2.1	DUKE	0.44	0.000	593	377	-2.79
	ORNL	0.45	0.001	626	428	-14.61
GDAY	DUKE	0.07	0.219	630	270	-9.13
	ORNL	0.10	0.178	507	222	-1.98
ISAM	DUKE	0.72	0.000	273	121	0.70
	ORNL	0.22	0.029	807	354	-4.76
JULES	DUKE	0.49	0.000	645	215	0.47
	ORNL	0.26	0.015	549	280	-0.20
LPJGUESS	DUKE	0.58	0.000	595	194	0.52
	ORNL	0.04	0.367	711	306	-1.91
OCN	DUKE	0.40	0.001	705	386	-14.38
	ORNL	0.46	0.001	580	288	-14.73
SDGVM	DUKE	0.61	0.000	399	180	0.20
	ORNL	0.49	0.000	277	151	0.02
TECO	DUKE	0.16	0.079	636	334	-0.38
	ORNL	0.18	0.081	449	211	-1.71

Table 4-8.Multivariate linear regressions of simulated NPP on driving data of the ten LSMs. See Table 4-2 for an explanation of the metrics.

Model	Site	variable	*r*	tolerance	Part r^2 (II)	Part r^2 (I)	*p*	R^2	*P*
CABLE	Duke	temperature	0.13	1.00	0.02	0.02	0.002	0.97	0.000
		nitrogen uptake	0.98	1.00	0.95	0.95	0.000		
	ORNL	temperature	-0.19	0.60	0.02	0.19	0.044	0.92	0.000
		canopy nitrogen	-1.28	0.10	0.16	0.33	0.000		
		nitrogen uptake	2.14	0.09	0.39	0.39	0.000		
CLMCN	Duke	nitrogen uptake	0.88	0.91	0.71	0.92	0.000	0.98	0.000
		canopy nitrogen	0.25	0.91	0.06	0.06	0.000		
	ORNL	canopy nitrogen	0.67	0.88	0.40	0.42	0.000	0.93	0.000
		nitrogen uptake	0.63	0.88	0.35	0.48	0.000		
		temperature	-0.19	0.80	0.03	0.03	0.013		
DAYCENT	Duke	temperature	-0.41	0.86	0.15	0.46	0.000	0.89	0.000
		nitrogen uptake	0.71	0.86	0.43	0.43	0.000		
	ORNL	nitrogen uptake	0.38	0.89	0.13	0.08	0.025	0.64	0.001
		temperature	-0.59	0.88	0.30	0.34	0.002		
		precipitation	-0.39	0.65	0.10	0.01	0.047		
		PAR	-0.56	0.65	0.21	0.21	0.006		
EALCO	Duke	temperature	-0.59	0.80	0.28	0.08	0.000	0.71	0.000

		nitrogen uptake	0.50	0.79	0.20	0.47	0.001		
		PAR	0.51	0.65	0.17	0.17	0.003		
	ORNL	temperature	-0.69	0.82	0.39	0.68	0.000	0.84	0.000
		canopy nitrogen	0.43	0.80	0.15	0.09	0.001		
		precipitation	0.30	0.70	0.06	0.06	0.022		
ED2.1	Duke	nitrogen uptake	0.97	0.62	0.58	0.75	0.000	0.89	0.000
		precipitation	-0.29	0.58	0.05	0.02	0.009		
		temperature	-0.59	0.33	0.11	0.03	0.000		
		canopy nitrogen	-0.52	0.31	0.08	0.08	0.001		
	ORNL	precipitation	0.42	0.82	0.15	0.32	0.006	0.73	0.000
		canopy nitrogen	-0.62	0.75	0.28	0.10	0.000		
		nitrogen uptake	0.69	0.65	0.31	0.31	0.000		
GDAY	Duke	canopy nitrogen	0.99	0.93	0.85	0.90	0.000	0.90	0.000
		PAR	0.24	0.93	0.05	0.05	0.004		
	ORNL	canopy nitrogen	na	na	na	na	na	0.98	0.000
ISAM	Duke	temperature	-0.10	0.98	0.01	0.02	0.627	0.11	0.308
		precipitation	0.29	0.98	0.08	0.08	0.174		
	ORNL	temperature	-0.41	0.88	0.15	0.33	0.026	0.51	0.001
		precipitation	0.45	0.88	0.18	0.18	0.016		
LPJGUESS	Duke	canopy nitrogen	-0.24	0.69	0.04	0.24	0.010	0.91	0.000
		temperature	-0.63	0.64	0.25	0.11	0.000		
		PAR	0.72	0.61	0.32	0.54	0.000		
		nitrogen uptake	0.23	0.52	0.03	0.03	0.024		
	ORNL	PAR	0.95	0.94	0.85	0.70	0.000	0.91	0.000
		canopy nitrogen	-0.18	0.85	0.03	0.00	0.028		
		temperature	-0.51	0.81	0.21	0.21	0.000		
OCN	Duke	PAR	0.44	0.75	0.15	0.02	0.015	0.63	0.002
		canopy nitrogen	0.31	0.69	0.07	0.39	0.086		
		precipitation	-0.33	0.67	0.07	0.00	0.078		
		temperature	-0.35	0.49	0.06	0.14	0.107		
		nitrogen uptake	0.42	0.44	0.08	0.08	0.065		
	ORNL	temperature	0.38	0.95	0.14	0.04	0.012	0.66	0.000
		PAR	-0.81	0.95	0.62	0.62	0.000		
TECO	Duke	canopy nitrogen	0.37	0.91	0.13	0.35	0.003	0.83	0.000
		nitrogen uptake	0.72	0.91	0.47	0.47	0.000		
	ORNL	precipitation	0.29	0.75	0.06	0.42	0.051	0.79	0.000
		canopy nitrogen	0.71	0.75	0.37	0.37	0.000		

NPP Response

The proportional response of NPP to elevated CO_2 (elevated NPP divided by ambient NPP) at Oak Ridge was lower and showed wider variability than at Duke. The magnitude of the response declined over the years of the experiment at Oak Ridge while there was no trend over the years at Duke (Figure 4-2). The models exhibited a very wide range of responses compared to the observations (Figure 4-8).

At both sites, and as with all configurations of the model, SDGVM captured the mean response in NPP to elevated CO_2. JULES over-predicted the NPP response to $CO_2$and driving JULES with observed canopy nitrogen further increased the simulated response to CO_2.As with SDGVM, JULES was unable to capture any of the inter-annual variability in the response to CO_2.

ED2.1 over-predicted the response at Oak Ridge, while many of the models under-predicted the response. CABLE and CLMCN showed practically no response at Oak Ridge. TECO and GDAY predicted a significant number of negative responses and CABLE, CLMCN and GDAY were so strongly dominated by nitrogen uptake or canopy nitrogen that there was virtually no response to elevated CO_2 at Oak Ridge and a lower than observed response at Duke.

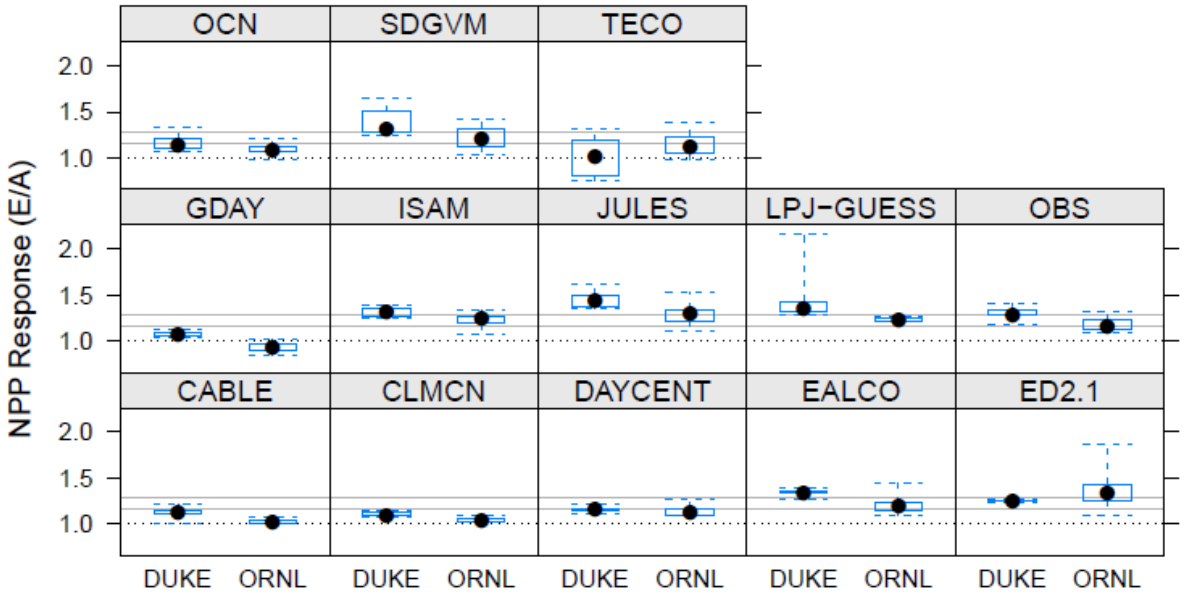

Figure 4-8. Range of annual NPP responses observed at each site and for each model. No response is shown by the dotted line and the median observed response for each site is shown by the grey lines. The SDGVM and JULES simulations presented are the canN Vc xPAR and canN Vc respectively.

Few of the models could simulate the inter-annual variability in the relative response (Table 4-9). GDAY, EALCO, JULES, DAYCENT, ISAM and CASA captured some of the inter-annual variability in the absolute response at Duke. Only LPJ approached capturing (R^2 = 0.32, P = 0.068) any of the inter-annual variability in the absolute response at Oak Ridge. Given the difficulty in simulating NPP in absolute terms, poorly simulated responses were to be expected. Of those models which did capture some of the inter-annual variability in response, half were unable to capture the absolute values of NPP indicating that perhaps the drivers of NPP were different to the drivers of the models' response. Of the models that captured some of the inter-annual variability in the response, only EALCO, ISAM and JULES simulated the absolute values of NPP with any accuracy, all at Duke. The models which captured the NPP response and absolute values of NPP were all correlated to different driving variables (Table 4-8).

Table 4-9. Model skill statistics in reproducing the proportional response of NPP to elevated CO_2. SDGVM and JULES results are for the canN Vc xPAR and the canN Vc runs respectively.

		relative		absolute	
model	site	R^2	P	R^2	P
CABLE	DUKE	0.55	0.005	0.43	0.021
	ORNL	0.01	0.836	0.00	0.927
CLMCN	DUKE	0.00	0.904	0.00	0.872
	ORNL	0.08	0.397	0.20	0.168
DAYCENT	DUKE	0.21	0.136	0.53	0.007
	ORNL	0.08	0.406	0.25	0.114
EALCO	DUKE	0.68	0.001	0.76	0.000
	ORNL	0.03	0.662	0.05	0.546
ED2.1	DUKE	0.27	0.083	0.06	0.456
	ORNL	0.09	0.363	0.02	0.686
GDAY	DUKE	0.24	0.124	0.77	0.000
	ORNL	0.01	0.753	0.00	0.875
ISAM	DUKE	0.39	0.030	0.51	0.009
	ORNL	0.05	0.514	0.01	0.732
JULES	DUKE	0.10	0.328	0.57	0.005
	ORNL	0.07	0.419	0.00	0.955
LPJ-GUESS	DUKE	0.00	0.906	0.34	0.045
	ORNL	0.19	0.180	0.32	0.068
OCN	DUKE	0.10	0.312	0.03	0.607
	ORNL	0.07	0.418	0.09	0.366
SDGVM	DUKE	0.04	0.548	0.18	0.166
	ORNL	0.00	0.964	0.02	0.647
TECO	DUKE	0.08	0.434	0.00	0.921
	ORNL	0.04	0.592	0.03	0.671

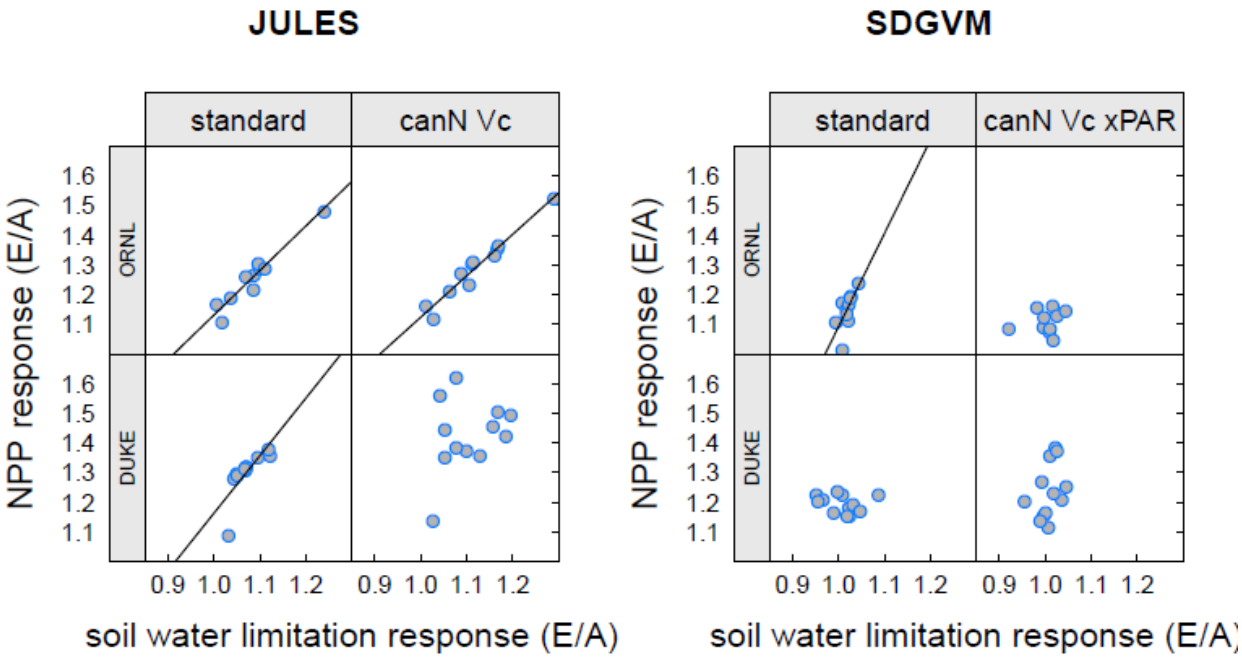

Figure 4-9. The response of NPP (elevated divided by ambient values) in relation to the response of soil water limitation. Where significant (P<0.05), linear regression lines are plotted. Soil water limitation values are based on the reduction of NPP from an unlimited state caused by soil water limitation (as shown in Figure 4-6). As such elevated divided by ambient values over 1 represent a release from, not an increase in, soil water limitation under elevated CO_2.

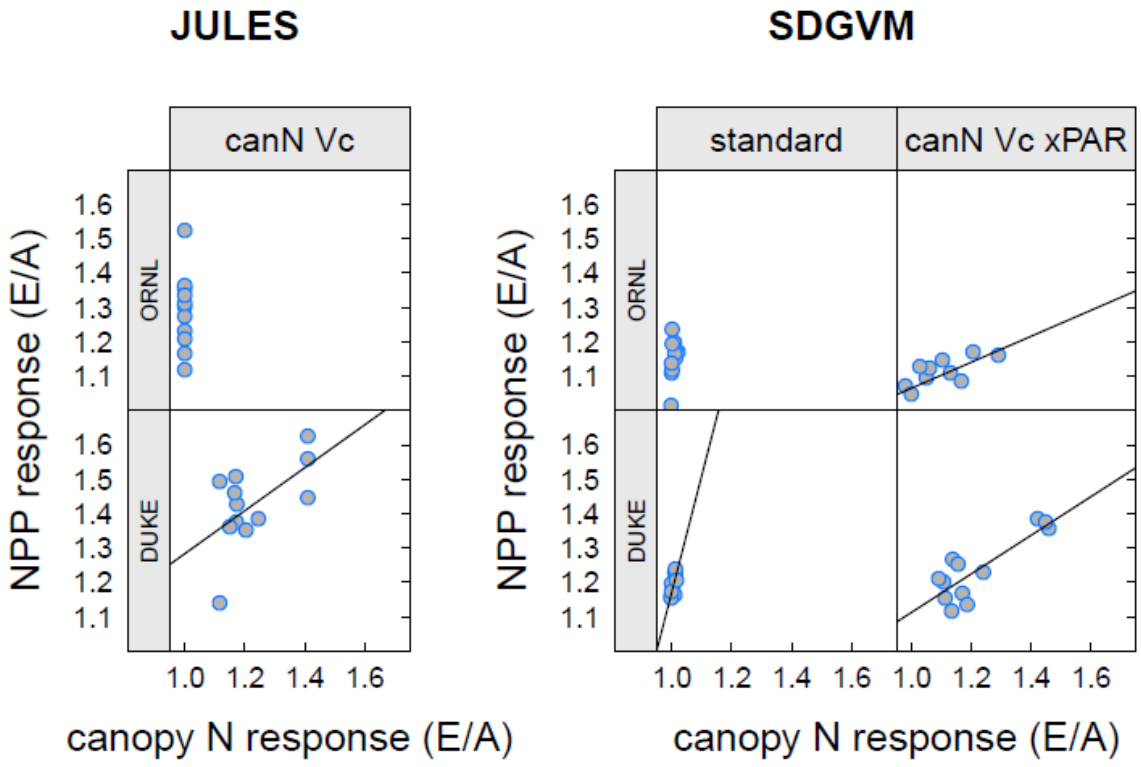

Figure 4-10.The response of NPP in relation to the response of canopy nitrogen. Where significant (P<0.05), linear regression lines are plotted.

Drivers of the CO_2 response in JULES and SDGVM

For SDGVM and JULES there were two drivers of the simulated NPP response—the response of soil water limitation and the response of canopy nitrogen. The response of NPP to elevated CO_2 in JULES and SDGVM was positively correlated to the response of soil water limitation to elevated CO_2 (Figure 4-9). In general, NPP was released from soil water limitation by elevated CO_2 and the proportional release from soil water limitation was positively correlated to the NPP response. The correlation was significant for all JULES simulations other than canN Vc at Duke, while the correlation was only significant for the standard SDGVM simulation at Oak Ridge. For those simulations where the NPP response was not correlated to the soil water limitation response, the NPP response was correlated with the canopy nitrogen response (Figure 4-10). Drivers of the response were effectively the same as drivers of NPP, but it was the response of these drivers to elevated CO_2 that was crucial.

JULES NPP was strongly affected by soil water which translated through a release of soil water limitation by elevated CO_2 and the magnitude of this release was directly correlated with the magnitude of the NPP response. For SDGVM, where soil water limitation was much weaker, the NPP response was only related to the release from soil water limitation at Oak Ridge in the standard run. The NPP response of SDGVM was more determined by the response of canopy nitrogen.

Differences between the two models were down to structural differences in model process representation. JULES was only affected by the canopy nitrogen response at Duke when driven with observed canopy nitrogen as this was the only simulation in which canopy nitrogen was different between the two treatments. TRIFFID was turned off in JULES and therefore LAI was a constant for the needle-leaf PFT and a function of temperature for the broadleaf PFT (Best et al. 2011). In contrast, SDGVM calculates LAI to optimise carbon assimilation (Woodward et al. 1995). Elevated CO_2 increased assimilation in the lower canopy while respiration was left unchanged, leading to higher LAI under elevated CO_2 and a consequent impact on NPP.

Discussion

As discussed in the methods, root exudates, plant-derived mycorrhizal carbon and changes in the labile and stored carbon pool were not measured at the FACE sites. Therefore observed NPP was more a measurement of growth. The observed values of NPP are GPP minus autotrophic respiration, minus root exudates, minus changes in stored carbon etc (McCarthy et al. 2007, Iversen et al. 2011),while the model calculations of NPP are the difference between GPP and autotrophic respiration. Therefore, observed NPP and modelled NPP were not expected to be exact. Notably, modelled NPP ought to have been higher than measured NPP, however there was no general over-prediction of NPP by the 12 models.

NPP at Oak Ridge was driven mainly by (declining) nitrogen availability (Garten et al. 2011, Iversen et al. 2011) as a result of progressive nitrogen limitation (PNL) caused by stand development (Gill et al. 2006). PNL occurs as progressively more ecosystem nitrogen is immobilised in woody plant biomass reducing the amount of mobile nitrogen available for new plant growth and leading to a progressive reduction in NPP (Gill et al. 2006). As described in Norby et al. (2010) we found that the major correlate of NPP was canopy nitrogen. We also found that temperature was negatively correlated to NPP, albeit less strongly, indicating a role of the water balance, or respiration, in NPP.

While SDGVM and JULES in their standard versions were sensitive to the important drivers of the inter-annual variability at Duke, both under-estimated NPP for these warm temperate sites in the south eastern US. The other LSMs demonstrated a wide range of NPP simulation accuracy (Figure 4-7&Table 4-7) and differential sensitivity to driving variables (Table 4-8) as we would expect from the widely ranging predictions of future atmospheric and land surface change (Cramer et al. 2001, Friedlingstein et al. 2006, Blyth et al. 2011).

It was encouraging that under the conditions in which we would expect SDGVM and JULES to perform (i.e. the non-stoichiometrically nitrogen limited system at Duke), with several additional driving variables, observed photosynthetic parameters and no arbitrary tuning, NPP was simulated with a good level of accuracy. At Duke, where NPP was driven primarily by climate, SDGVM, JULES and many of the other models simulated the inter-annual variability in NPP with a reasonable degree of accuracy. At Oak Ridge this did not appear to be the case, and most models tended to poorly simulate NPP at Oak Ridge.

SDGVM & JULES development

At both sites, marked improvements were made to the simulation of NPP by SDGVM with the inclusion of extra, site-specific driving variables and parameters to the model (Figure 4-4 & Table 4-3). Canopy nitrogen was under-predicted by SDGVM and, with the default parameter set, was limited to an unrealistically narrow range. Using measured canopy nitrogen improved the simulation of NPP and the correlation with canopy nitrogen showed that nitrogen was clearly an important determinant of NPP. Leaf nitrogen was an important parameter for simulating carbon assimilation as most models simulate the Farqhuar et al. (1980) or Collatz et al. (1991) model parameter V_{cmax} (and consequently J_{max} in the Farquhar model) as a linear function of leaf nitrogen (Evans 1989). The linear function is not always explicitly declared in modelling papers, often does not vary by PFT and has perhaps been used as a model tuning parameter (Bonan et al. 2011b). Kattge et al. (2009) have shown that the linear function of V_{cmax} and nitrogen varies by biome and Bonan et al. (2011b) have demonstrated the high sensitivity of global carbon cycle simulations with CLM4 to the V_{cmax} parameter.

The results here demonstrate the sensitivity of carbon dynamics to the V_{cmax} and J_{max} parameters and their relationship to leaf nitrogen. Using observed values of nitrogen and relationships to V_{cmax} strongly increased NPP at Oak Ridge with a mean error of 435 gC $m^{-2}yr^{-1}$ (49%) above the observations. Similar increases were obtained by Bonan et al. (2011b) in a global study, using more realistic values of V_{cmax} in CLM4, simulated GPP was 40% higher than FLUXNET observations. Bonan et al. (2011b) determined that low V_{cmax} values, when compared with those from Kattge et al. (2009), were compensating for canopy scaling of light that over-predicted carbon assimilation (Bonan et al. 2011a).

PAR at the FACE sites was over-predicted by SDGVM, possibly as a result of the simple cloud cover parameterisation employed by SDGVM. At Duke, the addition of PAR as a driving variable significantly reduced NPP, improving SDGVM's performance. At Oak Ridge mean values of NPP were very much improved. However, all skill was lost due to a strong model response to the inter-annual variability in PAR, probably due to the higher variance in PAR at Oak Ridge. In the standard version of SDGVM, low parameterisation of V_{cmax} was compensating the over-prediction of PAR at these sites, highlighting model biases and compensating factors that are inherent in every model. Uncovering these errors and compensations is necessary for model development and should help to make models more realistic in their simulations.

To improve the simulation accuracy of absolute values and inter-annual variability of NPP, simulation of canopy nitrogen needs to be more accurate. Simulation of canopy nitrogen in SDGVM could be improved using either a process based approach as has been done by a number of groups (Thornton et al. 2007, Wang et al. 2007a, Migliavacca et al. 2011) or an empirical approach using global regressions of leaf nitrogen against climatic and edaphic variables such as those determined by Reich et al. (2007) and Ordonez et al. (2009).

The way that clouds interact with solar radiation is complex and is influenced by the type of cloud, the elevation of the cloud and the sun, and the density and water droplet size within the cloud (Kazantzidis et al. 2011) which makes the simulation of the effect of cloud on radiation from simply cloud cover data difficult. Instead of attempting the simulation of the interaction of cloud with radiation, SDGVM could be driven directly with fields of PAR taken from an observed dataset, such asNew et al. (1999), and this is developed in a later chapter. Correct parameterisation of V_{cmax} and its relationship to nitrogen (and other leaf traits) will be a key improvement to SDGVM and later chapters investigate this further.

Driving JULES with observed canopy nitrogen increased values of NPP closer to observed values of NPP at Duke. But in contrast to SDGVM, driving JULES with observed canopy nitrogen (and observed photosynthetic parameter relationships to nitrogen) had little effect on the inter-annual variability in NPP at both FACE sites. The effect of declining canopy nitrogen was masked by the strong effect of soil water limitation (as discussed below) suggesting that perhaps high soil water limitation was compensating for overly high potential carbon assimilation in JULES, as highlighted by the extremely high value of NPP in 2003 when soil water limitation was very low. The switch in NPP sensitivity of SDGVM from precipitation to temperature in the standard to the canN run at Oak Ridge shows that model projections in response to climate change could be very different given the photosynthetic parameterisation of that model.

The decline in NPP at Oak Ridge

The poorer performance of SDGVM and JULES at Oak Ridge indicated that under certain circumstances growth at Oak Ridge was not limited by carbon assimilation (Körner 2009, Muller et al. 2011). At Oak ridge both the absolute NPP and the NPP response to elevated CO_2 declined over the years of the experiment. Using leaf litter ^{15}N as an indicator of soil nitrogen availability (Garten et al. 2011) show that the decline in absolute values of NPP and the response was likely to have been a result of progressive nitrogen limitation (PNL) caused by stand development

(Johnson 2006), which was accelerated by CO_2 enrichment (Luo et al. 2006b). PNL occurs as progressively more ecosystem nitrogen is immobilised in woody plant biomass reducing the amount of mobile nitrogen available for new plant growth and leading to a progressive reduction in NPP (Johnson 2006).

Of the models that were capable of simulating nitrogen limitation, NPP was again poorly simulated at Oak Ridge. Given that Duke and Oak Ridge shared very similar climates, neither of the major differences in simulations between Duke and Oak Ridge—Plant Functional Type and soil depth—were expected to so strongly affect the simulation of NPP that there could be such a difference in accuracy between the two sites. The poor representation of the inter-annual variability by almost all of the models at Oak Ridge yet accurate prediction at Duke suggests that the difference in simulation accuracy between the two sites was likely a result of missing, or poorly representing, nitrogen supply to the plant.

Reduced nitrogen limits growth in two ways; one, there is less nitrogen available to stoichiometrically balance carbon fixed by photosynthesis hence there are not the resources available to construct the amino acid components of new tissue (Elser et al. 2007) and; two, as a consequence, leaf nitrogen is reduced leading to lower photosynthetic capacity and hence lower CO_2 assimilation (optimisation theory suggests that nitrogen should be freed from the biochemical photosynthetic machinery in order to balance nitrogen limitation with carbon limitation) although there are likely to be physiological constraints on full optimisation (Lloyd et al. 2010).

Neither SDGVM nor JULES simulate a full, mass-balanced nitrogen cycle and therefore could not reproduce the decline in NPP at Oak Ridge caused by progressive nitrogen limitation. Many of the other models do have, in one form or another, a process based approach to the nitrogen cycle, yet the other LSMs produced varying predictions of NPP and canopy nitrogen and few of them simulated a decline at Oak Ridge.

Of the models that did simulate a decline in NPP, NPP was not necessarily correlated with nitrogen. Temperature was the major correlate for EALCO and SDGVM where a slight decline was simulated. Many of the other models showed a strong correlation of NPP to canopy nitrogen or nitrogen uptake. However, many of these models also lacked any skill in matching the observed NPP, indicating that although many of the models were strongly sensitive to

nitrogen, the simulation of the nitrogen cycle and its interaction with the carbon cycle were inaccurate. However, capturing the exact timing of the decline would require exact prediction of the dynamics of plant available nitrogen (PAN) which is partly dependent on accurate site history representation. In a modelling study and using an empirically derived estimate of PAN, Franklin (2007) showed that much of the variability in NPP at both Oak Ridge and Duke could be explained by variability in PAN and the different allocation strategies and parameters, particularly root lifespan, of the different species at the two sites. The models which captured NPP in the later few years of the experiment—OCN, GDAY and CABLE—also captured the response of NPP in the later years and perhaps give an accurate representation of a stable equilibrium between the carbon and nitrogen cycle.

The scale and cost of the FACE experiments meant that only one factor was tested—CO_2—and its interaction with temperature was not tested. However, the radiative forcing of CO_2 in the atmosphere makes rising atmospheric CO_2 a causal agent of rising surface temperatures (Allen et al. 2009). The FACE experiments can tell us little about the interaction of CO_2 with temperature although the negative correlation of NPP with temperature at both sites indicates that increasing temperature is likely to reduce the stimulation of NPP by rising CO_2. However, consistently warmer temperatures are likely to lead to higher rates of nitrogen mineralisation from organic matter in the soil (Beier et al. 2008) which could have compensated some of the nitrogen limitation at Oak Ridge, softening the observed decline.

In systems that are nitrogen limited such as the Oak Ridge FACE experiment, over the longer term, ecological processes may also lead to increased nitrogen availability. Nitrogen fixers would be expected to have a competitive advantage leading to their establishment in the community. Indeed, the nitrogen fixer *Elaeagnus umbellata* (Thunb.) has been shown to be increasing in numbers in the Oak Ridge under-storey (Souza et al. 2010) although these did not have a significant impact on the NPP of the system by the end of the experiment. The under-storey development at Oak Ridge and temperature related increases in nitrogen mineralisation highlight the timescale mismatch between models and even relatively long-term experiments.

For SDGVM, the closest representation of the decline at Oak Ridge was when driven with observed canopy nitrogen. This was not surprising considering that NPP at Oak Ridge was strongly correlated with canopy nitrogen (Table 4-2).However, SDGVM did not capture the full extent of the decline. Canopy nitrogen drives gross carbon assimilation—the driver of growth in

the model—while at the site it is thought that growth was limited stoichiometrically, causing both the decline in NPP and reduced canopy nitrogen (Norby et al. 2010). NPP and canopy nitrogen were well correlated but the reduced NPP by photosynthetic nitrogen limitation was likely to be the secondary, not the primary cause as suggested by SDGVM.

Abramowitz et al. (2008) describe a good method for generating a benchmark to assess model output. The benchmark is a neural-network based, best-prediction of a state variable using the information contained in the driving variables. However, if we used this benchmarking method on these FACE sites we would assume that models should be better able to simulate Oak Ridge than Duke, due to the stronger correlation of NPP to driving variables at Oak Ridge. In fact the opposite is the case due to the state variable (NPP) being strongly correlated with a driving variable (canopy nitrogen) but not strongly causally related. The strong correlation arises due to the correlation of both variables with the causal driving variable (nitrogen availability). To benchmark our models considering only canopy nitrogen as a driving variable and not nitrogen availability would make little sense at Oak Ridge and may lead to inaccurate conclusions.

Sensitivity of NPP to soil water

Annual precipitation was a consistently significant correlate with NPP in the JULES simulations (Table 4-4). To test the impact of soil water stress on NPP, SDGVM and JULES simulations were run with β always set at 1 (i.e. no soil water stress). The release from soil water limitation in JULES strongly increased NPP and reduced the amount of inter-annual variability across all simulations and at both sites. Regression analysis of the no β runs showed that precipitation was no longer a significant correlate of NPP (results not shown). The β factor explains the sensitivity of JULES to precipitation with soil water limitation being the main driver of inter-annual variability. The strong correlation of JULES and observed NPP at Duke (standard & canN), indicates that annual NPP at Duke was sensitive to soil water status. The correlation of observed NPP at Duke to temperature indicates that it was vapour pressure deficit (VPD) that was the bigger driver of soil water status, while both temperature and precipitation were important for JULES.

Duke was simulated with a shallower soil than Oak Ridge (0.75m as opposed to 2m), and given the very similar temperature climates at the two sites, the temperature correlation at Duke but not Oak Ridge indicated that it was temperature's role in the water balance, and not respiration, that was key for JULES. However, temperature was still a major correlate of NPP

when the β stress multiplier was removed, indicating that temperature was impacting NPP other than through the water balance—most likely via respiration.

The strong correlation of JULES NPP with precipitation in these simulations and only limited correlation with temperature contrasts with the results of Cadule et al. (2010) which showed that NPP simulated by HADCM3 (of which MOSES/TRIFFID i.e. JULESv1.0 is the LSM) in the South and South Eastern US correlated strongly with temperature during El Niño and La Niña events. This was likely due to the sensitivity of JULESv1.0 to temperature due to the Q_{10} relationship used to describe canopy 'dark' respiration as a function of temperature (Mercado et al. 2007), (Huntingford et al. Submitted). The Q_{10} relationship makes 'dark' respiration increase exponentially in response to temperature as opposed to JULESv2.1.2 (canopy radiation model 4—as used in these experiments) which simulates canopy 'dark' respiration as a function of V_{cmax} (i.e. has a temperature maximum and not exponentially increasing with temperature) and suppresses 'dark' respiration over 10 μmol $m^{-2}s^{-1}$ PAR (Mercado et al. 2007).

The strong sensitivity of JULES to inter-annual variability in precipitation has implications for the prediction of Cox et al. (2000) andHuntingford et al. (2008) that the Amazon will die-back under realistic climate change scenarios. Given the sensitivity to precipitation of JULESv2.1.2, predicted Amazon dieback using JULESv1.0 (MOSES/TRIFFID) could have been extreme although predicted die-back has been shown to be far smaller when modelling respiration as a function of V_{cmax} (and therefore has a temperature optimum) rather than using an exponential Q_{10} style relationship (Huntingford et al. Submitted). Due to the precipitation sensitivity of JULESv2.1.2 there is a need to address the uncertainty and validate the strength of soil water limitation in models.

The discrepancy between SDGVM and JULES of the strength of soil water limitation indicates that there is a large difference between the photosynthesis and respiration schemes of the models which is then balanced by the different magnitudes of soil water limitation. Either SDGVM was under-predicting potential carbon available for growth or JULES was over-predicting. It is likely that the explanation is somewhere in between. There was evidence to suggest that JULES soil water limitation was too high. Model skill of the canN Vc run at Duke was improved by the removal of 2003 because there was practically no soil water limitation in 2003 allowing the very high NPP set by the canopy photosynthesis and respiration scheme. Canopy nitrogen was expected to decrease NPP in the later years of the simulation at Oak Ridge

however NPP in JULES was not correlated with canopy nitrogen, only precipitation, again indicating that soil water limitation may have been overly strong. With realistic values of canopy nitrogen (and therefore V_{cmax}) it appears that JULES over-predicted carbon available for growth and that this was compensated by over-sensitivity to soil water stress. In contrast, Mercado et al. (2007) found that in non-water stressed simulations of the Amazon carbon assimilation was under-predicted when compared to observations. They ascribed this to reduction of respiration in the light, which was modelled in these FACE simulations and could have accounted for the over-prediction of carbon available for growth. To obtain V_{cmax} Mercado et al. (2007) used observations of leaf nitrogen concentration and observed relationships of area based $V_{cmax}$to leaf nitrogen concentration in similar, local forest which could have been confounded by differences in SLA between the two forests.

NPP Response

McCarthy et al. (2010) showed that the main driver of the response, and NPP in general, observed at Duke was an index of nitrogen availability although the response to CO_2 was associated with increased access to soil nitrogen under elevated CO_2 (Drake et al. 2011). The absolute response, and NPP in general, was further modified by soil water status (measured as precipitation minus potential evapo-transpiration), although the relative response was little affected by soil water. Soil water status was unaffected by CO_2 although the reasons for this were unclear (Schafer et al. 2002). There was evidence at Duke for increased soil nitrogen mobilisation under elevated CO_2 (Drake et al. 2011) which maintained the NPP response to CO_2. Unlike at Duke, Garten et al. (2011) showed the declining NPP and response to CO_2 at Oak Ridge to be related to declining soil nitrogen availability as indicated by leaf $\delta^{15}N$ concentrations. Garten et al. (2011) showed that the declining soil nitrogen status was accelerated by high CO_2. Both these studies showed that the NPP response was directly related to drivers of NPP in general. At Oak Ridge the response of the drivers was important, while at Duke it was the overall values of these drivers that determined the response (i.e. CO_2 did not affect these drivers).

For SDGVM and JULES the modelled responses of NPP to elevated CO_2 were driven by the response of the main drivers of NPP, i.e. canopy nitrogen/LAI and soil water respectively. The evidence from Oak Ridge supported this sensitivity of NPP response to driver response, while the evidence from Duke was a little more complex showing that the overall magnitude of the

NPP response was governed by soil nitrogen status (McCarthy et al. 2010) and that the NPP response was maintained over the course of the experiment by increased mobilisation of nitrogen under elevated CO_2. Results from the simulation showed that soil water was the key driver of the NPP response in JULES, while the SDGVM response was mostly driven by increased LAI and canopy nitrogen. Results from the experiments suggest that soil nitrogen was the most important driver of the NPP response.

Neither SDGVM nor JULES simulate stoichiometric nitrogen limitation and their inability to capture the decline at Oak Ridge suggests that a mass balanced nitrogen cycle is necessary. JULES's general over-prediction of the NPP response suggests that the absence of a J_{max} term in the Collatz et al. (1991) formulation may over-estimate CO_2 responses. A number of models captured low values of NPP and the NPP response in the final years at Oak Ridge, however they also under-predicted the response at Duke. Many of the other models with stoichiometric nitrogen limitation could not capture the response at either site. Stoichiometric nitrogen limitation can only be represented using a full process-based nitrogen cycling model to predict plant available nitrogen—a model that is very hard to validate due to no available method for measuring plant available nitrogen, independent of plant growth. The processes which govern nitrogen availability are complex and have been shown to differ across both of these FACE sites with the associated mechanisms behind the differences still under investigation (Iversen 2010, Drake et al. 2011, Iversen et al. 2011). Stoichiometric growth limitation has been shown to be a major limitation to potential terrestrial carbon uptake over the 21st century (Hungate et al. 2003) and the results of this study suggest that more work needs to be done before we can accurately predict the interaction of the carbon and nitrogen cycles. Specifically, the mechanisms governing mineralisation of soil nitrogen and strategies that plants use to influence mineralisation need to be formalised into mathematical functions and algorithms suitable for use in computer models.

Conclusions

Simulations of NPP in both JULES and SDGVM were improved by calibrating them with observed values of canopy nitrogen and the V_{cmax} to leaf nitrogen relationships (although SDGVM also required accurate values of PAR to achieve improved simulations of NPP). Furthermore, the process of adding canopy nitrogen, the V_{cmax} relationship to leaf nitrogen, PAR and running simulations without soil water limitation, demonstrated biases and

compensation of these biases in SDGVM and JULES. At the FACE sites, the default, low values of canopy nitrogen and V_{cmax} in SDGVM compensated over-prediction of PAR. While, JULES appeared to over-predict potential carbon assimilation (with correct V_{cmax} values), perhaps compensating this by having strong soil water limitation. Investigation of these biases and compensating factors is key to model process development and validation of these compensating factors, like the strength of soil water limitation in terrestrial ecosystems, presents a significant challenge calling for collaboration between modellers and experimentalists.

Most models reproduced, with some degree of accuracy, NPP at the two FACE sites. However, there was a consistent difference across models in the simulation accuracy of NPP at the Oak Ridge and Duke FACE experiments. The poorer accuracy of the models at Oak Ridge was to be expected due to the progressive nitrogen limitation at that site (Garten et al. 2011) highlighting the difficulties in simulating plant available nitrogen. The need to accurately represent nitrogen dynamics is still a priority for terrestrial carbon cycle modelling and depends on site history and plant allocation strategies as well as soil nitrogen dynamics.

Models were consistently better at reproducing the absolute values of NPP, under both elevated and ambient CO_2, than the response to elevated CO_2 (i.e. the absolute or proportional difference in NPP under ambient and elevated CO_2). In this Chapter, the large range of predicted NPP responses to elevated CO_2 across 12 models (most with a nitrogen cycle), suggests that the next generation of LSMs is unlikely to reduce the range of predicted future atmospheric CO_2 seen in previous studies using models with a limited, or no, nitrogen cycle (Cramer et al. 2001, Friedlingstein et al. 2006, Sitch et al. 2008, Huntingford et al. 2009).

However, we can have confidence in the fact that some models reproduced the average and range of responses and to increase confidence in future predictions, benchmarking methods to assess model performance should be used to give more weight to predictions from 'better' models. The responses to elevated CO_2 at the FACE experiments provide unique data, suitable for benchmarking models as part of a wider benchmarking framework.

Chapter 5 A global meta-analysis of the photosynthetic traits V_{cmax} and J_{max}in relation to leaf traits nitrogen, phosphorus and SLA.

Introduction

Terrestrial photosynthesis is the proximal driver of the global carbon cycle over sub-daily to seasonal timescales (Canadell et al. 2007, Cadule et al. 2010) and is the core process of terrestrial carbon cycle models. The Farquhar et al. (1980) model of integrated photosynthetic processes is used in the majority of global carbon cycle models or Dynamic Global Vegetation Models (DGVMs – the acronym will be used below to refer to both global carbon cycle models with fixed and dynamic vegetation) with some models such as JULES (Clark et al. 2011) and CLM(Oleson et al. 2010) using the adaptation of the Farquhar model by Collatz et al. (1991). In the Farquhar model the rate of photosynthesis at the scale of a leaf is primarily determined by two physiological parameters and two environmental variables: the maximum rate of carboxylation by RuBisCO (V_{cmax}); the maximum rate of electron transport (J_{max}); the concentration of CO_2inter-cellular air space of the leaf (C_i) and the fraction absorbed of incident photosynthetically active radiation (*f*APAR) (Farquhar et al. 1980). The Collatz et al. (1991) formulation does not include the J_{max} term. Both models have a third physiological variable which limits carbon assimilation rate at high C_i and *f*APAR levels.

DGVMs are highly sensitive to the parameterisations of V_{cmax} and to a lesser extent J_{max} (Chapter 4, Bonan et al. 2011b) yet their parameterisation in individual models varies widely suggesting that they may have been used as tuning parameters for the models (Chapter 4, Bonan et al. 2011b). The new generation of models now include a full nitrogen cycle (Calvin 1989, Oleson et al. 2010, Zaehle and Friend 2010) and in some cases a phosphorus cycle (Wang et al. 2007b) so it will be important to apply realistic scaling relationships of photosynthetic parameters with leaf nutrient concentrations to these models.

Many studies have shown the relationship of maximum photosynthetic rates (A_{max}) and photosynthetic parameters to leaf traits (Wullschleger 1993, Niinemets 1999, Wright et al. 2004, Reich et al. 2007, Kattge et al. 2009, Reich et al. 2009). V_{cmax} in a leaf is determined by the active amount of the protein RuBisCO (Farquhar et al. 1980). As RuBisCO is such a large proportion of leaf protein the response of V_{cmax} to leaf nitrogen has been well researched and documented(Wullschleger 1993, Kattge et al. 2009). In a comprehensive study, Field and

Mooney (1984) showed the relationship of photosynthesis to leaf nitrogen in wild plants. Perhaps the focus on leaf nitrogen in relation to photosynthesis has also been due to the research bias in northern latitudes and the acknowledgement of nitrogen as the major limiting nutrient in northern ecosystems. Traditionally J_{max} has been related to V_{cmax} on the basis that optimisation of resources allocated to photosynthesis would closely maintain the ratio of these two parameters (Wullschleger 1993). Many studies have been conducted measuring V_{cmax} and J_{max} in individual species (Wullschleger 1993, Beerling and Quick 1995), in different environments (Kattge et al. 2009, Reich et al. 2009), and synthesised at higher taxonomical/functional scales (Kattge et al. 2009).

Phosphorus is also a significant limiting factor in many biomes across the globe (Elser et al. 2007, Reich et al. 2009, Quesada et al. 2011) and while leaf nitrogen slowly increases with latitude, phosphorus strongly increases with latitude driving a broad scale change in leaf N:P ratios (McGroddy et al. 2004, Reich and Oleksyn 2004). McGroddy et al. (2004) showed that in general terrestrial forest leaf phosphorus and leaf nitrogen scaled isometrically with carbon and with each other but that in some cases nitrogen and phosphorus increased in proportion to carbon at higher rates of primary production. In a broader study, Reich et al. (2010) showed that relationships of nitrogen to phosphorus follow a 2/3 scaling law across biomes and functional types. Phosphorus was shown to scale at a greater rate than nitrogen to growth rate proxies such as Specific Leaf Area (SLA – the ratio of leaf area to leaf mass) and A_{max}. They proposed that this relationship is driven by area to volume scaling and the coupling of nitrogen to leaf area while phosphorus is coupled to leaf mass(Reich et al. 2010).

Research has begun to investigate the effect of leaf phosphorus on the two photosynthetic parameters. Phosphorus is the limiting nutrient across much of the tropics (Reich and Oleksyn 2004, Wang et al. 2007a, Quesada et al. 2010, Quesada et al. 2011) and has roles in photosynthesis as a major component of Ribulose 1,5 Bisphosphate (RuBP), the sugar with which CO_2 is compounded in the PCR cycle, and Adenosine Triose-Phosphate (ATP) necessary for transferring the energy captured from electron transport to the PCR cycle. Phosphorus also plays a role in more general cell metabolism, such as membrane function, which could also influence the rate of photosynthesis.

Reich et al. (2009) showed that A_{max} (maximum photosynthetic rates) became increasingly sensitive to nitrogen at increasing levels of leaf phosphorus. Phosphorus was shown to be the

only nutrient of significance in a regression model with V_{cmax} while nitrogen was found to be the only nutrient of significance in a regression model with J_{max} in tropical species of West Africa (Meir et al. 2007). In a factorial N and P addition to *Pinus radiata* (D. Don) experiment, Bown et al. (2007) introduced a regression framework based on the concept that photosynthetic parameters were limited by either N or P, dependent upon the leaf tissue being above or below a critical N:P ratio. They calculated the critical ratio to be 23 on a molar basis (a ratio of 10.4 on a mass basis), showing that at higher ratios P was a better correlate with photosynthetic parameters. In a conceptually similar analysis considering either N or P to be the sole limiting nutrient, Domingues et al. (2010) demonstrated that leaf phosphorus and SLA, along with leaf nitrogen, were important predictors of V_{cmax} and J_{max} in seasonally dry forests of West Africa. They calculated a critical N:P ratio that varied between 13 and 20 on a mass basis depending chiefly on SLA. These results point at the need to simulate V_{cmax} and J_{max} dynamically in response to leaf nitrogen, leaf phosphorus and SLA. No similar studies have been conducted for temperate biomes although N:P and A_{max} have been investigated by a number of authors (Wright et al. 2001, Reich et al. 2009).

SLA (and its inverse Leaf Mass Area – LMA) is related to leaf nitrogen and phosphorus but more strongly on a mass basis (Niinemets 1999, Wright et al. 2004, Reich et al. 2007,Ordonez et al. 2009). In a meta-analysis of 597 species, Niinemets (1999) demonstrated a strong relationship between LMA, leaf nitrogen and light-saturated carbon assimilation rates (A_{max}) on both mass and area based measurements. While in an analysis of the GLOPNET database, Wright et al. (2004) showed that the correlation of LMA to A_{max} was only significant for mass based measurements. Niinemets (1999) showed that the mass based relationship of V_{cmax} with leaf nitrogen was modified by leaf density (a component of LMA), due to a decreasing fraction of leaf nitrogen allocated to RuBisCO with increasing leaf density. SLA has also been shown to modify the ratio at which either leaf nitrogen or leaf phosphorus became limiting to V_{cmax} and J_{max} (Domingues et al. 2010). Poorter et al. (2009) demonstrated the heterogeneous nature of LMA across biomes, plant functional types, and both spatially and temporally. LMA responds strongly to a number of environmental variables such as integrated radiation, temperature and water availability (Wright et al. 2005, Reich et al. 2007, Ordonez et al. 2009,Poorter et al. 2009).

Several analyses of multivariate relationships between photosynthesis and leaf traits have taken an approach which assumes that either nitrogen or phosphorus is the limiting nutrient

and therefore only one of these nutrients limits V_{cmax} and J_{max} in their model. While there is good reason to assume that a limiting nutrient will play a dominant role in determining V_{cmax} and J_{max}, due to the nitrogen requirements of RuBisCO there is likely to be a relationship between V_{cmax} and nitrogen even at low levels of phosphorus and that a release from phosphorus limitation will manifest as a more sensitive coupling of V_{cmax} to nitrogen as demonstrated for A_{max} by Reich et al. (2009). For this reason our approach has been more similar to that of Reich et al. (2009) than that of Meir et al. (2007) and Domingues et al. (2010).

There is some difference in the way that these leaf traits are measured and presented – either as a concentration or on a per unit leaf area basis. Concentration indicates the maximum carboxylation capacity per unit of leaf mass, while a leaf area basis indicates the leaf capacity per unit area which is a proxy for light absorption—an environmental factor which one would expect a plant to optimise photosynthetic resources against. At a given stomatal conductance and internal conductance (g_i—which may relate to SLA), SLA indicates the diffusion rate of CO_2 to the site of carboxylation. Indeed, in West African tree species, SLA was shown to be the only significant correlate of V_{cmax} and J_{max} in a multiple regression of these terms in conjunction with leaf nitrogen and phosphorus concentration (Meir et al. 2007). However, it was also shown that mass based measurements of leaf nutrients explained more variation in photosynthetic parameters than area based measurements, even when regressed in conjunction with LMA in West African species (Domingues et al. 2010).

Across a broad range of plant species, many studies have demonstrated a positive, linear relationship between V_{cmax}, J_{max} and leaf nitrogen (Wullschleger 1993, Beerling and Quick 1995) and that the slope and intercept of this relationship varies by biome (Kattge et al. 2009). More recent studies have demonstrated the significance of leaf phosphorus and SLA in relation to V_{cmax} at sites in tropical West Africa (Domingues et al. 2010) and Australia (Cernusak et al. 2011). Using a broad database of plant traits, Reich et al. (2009) demonstrated that carbon assimilation became less sensitive to leaf nitrogen as leaf phosphorus decreased.

Kattge et al. (2009) showed that in tropical biomes, where leaf phosphorus is expected to be lower, the slope of the V_{cmax} to nitrogen relationship was lower. The results from Reich et al. (2009) suggest that the variability observed by Kattge et al. (2009), in the V_{cmax} against N slope, may be due to leaf phosphorus. A global relationship between V_{cmax}, leaf nitrogen, leaf

phosphorus and SLA may exist and could explain the different relationships to leaf nitrogen by biome.

Previous studies investigating the effect of leaf phosphorus on V_{cmax} have adopted a limiting factors approach, assuming that only leaf nitrogen or leaf phosphorus determines V_{cmax} depending on which is the more limiting nutrient. We propose that due to the high fraction of leaf nitrogen that is in RuBisCO, leaf nitrogen will always have a relationship to V_{cmax} and so an approach that considers interactions between phosphorus and nitrogen was opted for in this Chapter.

This Chapter aims to answer the question: is there a global relationship between V_{cmax} or J_{max} and leaf nitrogen, leaf phosphorus and SLA? The approach was to collect data published in the literature, analysing either V_{cmax} or J_{max} against leaf nitrogen, leaf phosphorus and SLA with mixed-model multiple regressions that include all interaction terms of the explanatory variables. More than a single data point was taken from each study and mixed-models were used to take account of the non-independence of the data taken from an individual study.

J_{max} has been shown to correlate strongly with V_{cmax} and the study in this Chapter assessed whether the J_{max} to V_{cmax} relationship was modified by leaf nitrogen, leaf phosphorus or SLA. Mixed-model multiple regressions were used to assess this. It was hypothesised that the tight relationship between J_{max} and V_{cmax} was due to optimal allocation of resources between these two parameters to optimise carbon assimilation. To test this hypothesis, biochemical models of photosynthesis were employed to assess the impact of the J_{max} to V_{cmax} slope on carbon assimilation.

The new generation of DGVMs now include a full nitrogen cycle (Calvin 1989, Oleson et al. 2010, Zaehle & Friend 2010) and in some cases a phosphorus cycle (Wang, Houlton & Field 2007) and empirical scaling relationships of the photosynthetic parameters V_{cmax} and J_{max} with leaf nutrient concentrations will allow prognostic determination of these parameters by DGVMs in a changing environment. This Chapter makes a first attempt, to our knowledge, at a global meta-analysis of the relationships of V_{cmax} and J_{max} with leaf N, P and SLA.

Methods

Literature review & data collection

In July 2011 the Thompson Reuters Web of Science database was searched for 'photosynthesis' or 'carboxylation' and either 'nitrogen', 'phosphorus' or 'SLA' as well as a number of other related search terms. The aim was to find papers that had simultaneously measured as many of the following parameters on a single leaf or for a species: V_{cmax}, J_{max}, leaf nitrogen, leaf phosphorus and specific leaf area (SLA) or leaf mass to area ratio (LMA). Where LMA was reported, SLA was calculated as the reciprocal of LMA. While this is not a perfect conversion for mean values this error would have contributed to the residual error of the model which, while undesirable, was not a serious problem. There was a significant difference (P<0.05, Student's t) in the means of SLA reported as SLA, or SLA calculated as the inverse of LMA. However, there was a large overlap in their ranges and there was no difference in their relationship to J_{max} (results not shown). Data were copied from tables or digitised from graphics using Grab It! (Datatrend Software, Raleigh, NC USA). Minimum requirements for inclusion in this study were that either V_{cmax} or J_{max} were measured along with two of the three leaf traits yielding data from 26 papers (Appendix J) and 118 species distributed globally (Figure 5-1). Some of these data were collected from trees in their natural environment and subject to natural environmental variation while other data were collected from lab grown plants (mostly tree species) subjected to experimental treatments. The majority of the species used in the greenhouses and labs were native to the area of the research centre. While we acknowledge that using data from lab experiments may push the range of traits outside those found in nature (Kattge et al 2009), we felt that the value of a larger dataset outweighed these concerns. Either species means or treatment means were collected leading to a dataset of 388 species/treatment combinations.

Statistics

Our goal was to estimate the coefficients of a multiple regression between the photosynthetic parameters and several leaf traits, with data collected from numerous studies in the literature. To do this we used a novel method in the field of trait based relationships, similar to that of Ordonez et al. (2009), employing a linear mixed-model regression framework with leaf traits as fixed effects and the author of the paper from which the data were digitised (rather than geographical location) as the random effect. Using author as the random effect accounted for

the non-independence of data within a study. We acknowledge that in this study we did not account for the heteroscedasticity of sampling variances between different studies and therefore we did not weight the data. As the data from the papers are neither correlation coefficients nor results from experiments that allow a response ratio to be calculated, traditional methods of meta-analysis were not employed.

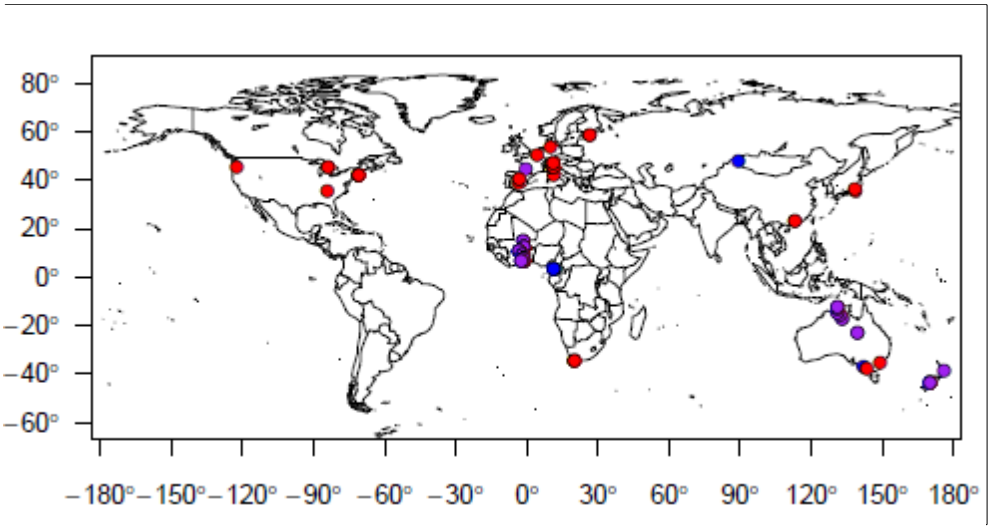

Figure 5-1. Map of locations from which data for the original research were collected. Colouring of the points represents collection of leaf nitrogen data (red), leaf phosphorus data (blue) or both (purple).

All statistical analyses were carried out using the open-source software package R, version 2.13.0 (R Core Development Team 2011). Maximal models were fit to the data with the 'lme' function of the 'nlme' library (Pinheiro et al. 2011) using the author of the paper as a random effect and the leaf traits as fixed effects. All data were natural log transformed to achieve normality within each group and to eliminate heteroscedasticity in model residuals. Models were then simplified using the 'dropterm' function of the 'MASS' library (Venables and Ripley 2002) to conserve marginality and the minimum adequate model was fine-tuned using *t*-test *p*-values of the model coefficients and comparison of alternative models using the Akaike Information Criterion (AIC) and ANOVAs. The model with the lowest AIC value is the 'best', maximising the amount of information contained within the data accounted for by the model while minimising the number of parameters in the model. Each model was fit to a subset of the full dataset as mixed model analyses are unable to deal with missing values. As there is no

mixed-model equivalent of the fixed-effects model coefficient-of-determination a number of methods were used to indicate the variance explained by the fixed-effects in the model. The coefficient-of-determination (R^2) of a linear regression of fitted values of a model against the response variable was calculated. Decreases in the intercept and residual variance from a null model represent increases in variance explained by the fixed effects. The intercept (between group) variance and residual (within group) variance are shown for each model along with the percentage decreases in these variances from a null model which includes only random effects (i.e. the response variable fit only to the intercept and the random effect of author).

Modelling carbon assimilation

Carbon assimilation was modelled using the equations from Farquhar et al. (1980) for perfectly coupled electron transport and Calvin cycles. The Sheffield Dynamic Vegetation model (SDGVM) canopy photosynthesis module was re-coded as a stand-alone model in R (R Core Development Team 2011). As with the current version of SDGVM, partitioning of light into direct and diffuse was based on (Spitters et al. 1986) and nitrogen was scaled through the canopy using Beer's Law scaling. Leaf Area Index was kept constant at a value of five. Coefficients of the equations relating V_{cmax} to leaf nitrogen and J_{max} to V_{cmax} were taken from the bivariate relationships presented in Table 5-4 and 5-5.

Results

On an area basis, values of V_{cmax} and J_{max} both varied roughly 25 fold ranging from 6.4 to 163.2 and 18.0 to 429.1 µmol $m^{-2}s^{-1}$ respectively, while on a concentration basis, V_{cmax} and J_{max} varied 130 and 68 fold, respectively, from 0.09 to 11.71 and from 0.27 to 18.43 µmol $g^{-1}s^{-1}$. SLA ranged nearly 100 fold from 0.0025 to 0.2360 m^2g^{-1}. On an area basis leaf nitrogen and phosphorus ranged from 0.12 to 4.69 and from 0.004 to 0.535 g m^{-2}, respectively, and on a concentration basis, from 0.012 to 0.059 and from 0.0004 to 0.0043 g g^{-1}. Values of leaf phosphorus ranged 134 fold measured on an area basis but only 12 fold on a mass basis, while leaf nitrogen varied 39 fold on an area basis and 49 fold on a concentration basis. The large range of phosphorus on a leaf area basis while relatively low range on a concentration basis suggests that phosphorus was far more tightly coupled to leaf mass than leaf area, as noted by Reich et al. (2010). There was a suggestion that nitrogen may scale more closely with leaf area than mass although the difference was relatively small.

On average, 13% more variation (measured using the R^2 of model fitted values against observed values) in V_{cmax} and J_{max} was described by leaf nitrogen and SLA when measurements were made on a leaf concentration basis compared with a leaf area basis (Table 5-1). Much of this difference in explained variation was due to the data from Meir et al (2007) which had especially high values of SLA (an order of magnitude higher than the rest of the dataset). Removal of their data from the analysis reduced the variance explained by concentration based measurements to within 2% and 4% of area based measurements for V_{cmax} and J_{max} respectively.

Reporting of V_{cmax} and J_{max} in the literature has been primarily on an area basis and therefore there were less data available to analyse on a leaf concentration basis. The majority of data when analysing on a concentration basis, and including leaf phosphorus as a model term, came from the Domingues et al. (2010) paper. Therefore any concentration based analysis of V_{cmax} and J_{max} on leaf phosphorus represented a less sophisticated reanalysis of the Domingues et al. (2010) data. As the relationship of leaf phosphorus to V_{cmax} and J_{max} was a goal of this paper we focused our analyses on area based measurements.

While the relationship of V_{cmax} to leaf nitrogen has often been expressed in the literature, J_{max} is usually expressed in relation to V_{cmax} (Wullschleger 1993, Beerling and Quick 1995) as theory suggests that J_{max} should be optimised with respect to V_{cmax}. Our data support this, showing

that 16% more variation in J_{max} was described when regressing against V_{cmax} as opposed to leaf nitrogen. For this reason, the analyses of J_{max} presented here include V_{cmax} as a primary explanatory variable.

Table 5-1. Results from mixed-effects models of V_{cmax} and J_{max} regressed on leaf nitrogen and SLA when the leaf traits V_{cmax}, J_{max} and nitrogen were measured on a leaf area basis or leaf mass basis. A model of J_{max} regressed on V_{cmax} and SLA is also shown for comparison. For direct comparison of leaf area based measurements with leaf concentration based measurements, the area or mass based models were applied to the same datasets. Reported are the number of observations used in the regression (N); the number of papers which the observations came from and that were used as the random-effects (N_g); the intercept variance (i.e. the variance associated with the random effect - between group variance) and the residual variance (within group variance) from the model along with the percentage decrease in these variances from a null model in which the response variable was regressed only on the intercept and the random effects; the R^2 of a linear fixed-effect regression of the fitted values from the model compared with the observed values, and the Akaike Information Criterion of the models (AIC).

response variable	explanatory variables	N	Ng	Intercept variance	%age	residual variance	%age	R^2	AIC
log(Vcmax)area	log(N)area	278	22	0.244	-39.694	0.104	25.365	0.71	236.9
log(Vcmax)area	log(N)area+log(SLA)	278	22	0.272	-56.096	0.103	26.451	0.71	237.5
log(Vcmax)area	log(N)area+log(SLA)+int	278	22	0.288	-64.936	0.102	26.788	0.71	239.4
log(Vcmax)conc	log(N)conc	278	22	0.467	36.286	0.104	29.265	0.84	249.4
log(Vcmax)conc	log(N)conc+log(SLA)	278	22	0.267	63.566	0.102	30.172	0.84	236.3
log(Vcmax)conc	log(N)conc+log(SLA)+int)	278	22	0.224	69.422	0.100	31.477	0.84	229.8
log(Jmax)area	log(N)area	226	18	0.208	0.189	0.075	23.744	0.75	123.6
log(Jmax)area	log(N)area+log(SLA)	226	18	0.256	-23.146	0.072	26.880	0.76	120.4
log(Jmax)area	log(N)area+log(SLA)+int	226	18	0.309	-48.450	0.071	28.168	0.76	121.9
log(Jmax)conc	log(N)conc	226	18	0.498	36.513	0.077	29.927	0.88	143.5
log(Jmax)conc	log(N)conc+log(SLA)	226	18	0.251	67.946	0.072	34.946	0.89	118.0
log(Jmax)conc	log(N)conc+log(SLA)+int	226	18	0.195	75.179	0.069	37.321	0.89	107.9
log(Jmax)area	log(Vcmax)area	226	18	0.067	67.996	0.016	83.788	0.95	-219.3
log(Jmax)area	log(Vcmax)area+log(SLA)	226	18	0.067	67.974	0.016	83.942	0.95	-219.3
log(Jmax)area	log(Vcmax)area+log(SLA)+int	226	18	0.070	66.426	0.015	84.410	0.95	-222.6
log(Jmax)conc	log(Vcmax)conc	226	18	0.080	89.818	0.018	83.837	0.97	-194.4
log(Jmax)conc	log(Vcmax)conc+log(SLA)	226	18	0.067	91.505	0.016	85.573	0.97	-219.3
log(Jmax)conc	log(Vcmax)conc+log(SLA)+int	226	18	0.066	91.524	0.016	85.573	0.97	-217.3

V_{cmax} in relation to leaf nitrogen, leaf phosphorus and SLA

As expected, models of V_{cmax} regressed on leaf nitrogen and either SLA or leaf phosphorus explained a significant amount of variation in V_{cmax} (Table 5-3). When V_{cmax} was regressed on nitrogen and SLA, the minimum adequate model—defined as the model with the lowest AIC value—was that of nitrogen alone with an AIC of 236.9. This was not the case for a model using the same dataset and concentration rather than area based measurements of leaf nitrogen.

When nitrogen was measured on a concentration basis both SLA and the interaction of SLA with leaf nitrogen were significant model terms (Table 5-1).

For V_{cmax} regressed on nitrogen and phosphorus, the maximal model—that with both explanatory variables and the interaction between them as model terms—was the minimum adequate model with the lowest AIC value of 42.5. The fitted values of V_{cmax} from these minimum adequate models accounted for, respectively, 71% and 72% of the variation in the observed values of V_{cmax} (measured using a linear fixed-effect regression of the fitted values on the observed values) when regressed on leaf nitrogen (for the nitrogen and SLA dataset) or leaf nitrogen and leaf phosphorus.

Figure 5-2 and Figure 5-3 show that the assumptions of a mixed model analysis were satisfied by both these minimum adequate models; i.e. there was no heteroscedasticity in the model residuals; the observed values of V_{cmax} bore a linear relationship to model fitted values and the residuals, when separated by author, were normally distributed.

J_{max} in relation to V_{cmax}, leaf nitrogen, leaf phosphorus and SLA

Outputs from four way mixed model relationships between J_{max}, V_{cmax}, leaf nitrogen and either SLA or leaf phosphorus are shown in Table 5-4. Figure 5-2 and Figure 5-5 show that the assumptions of a mixed model analysis were satisfied for these minimum adequate models. Based purely on AIC values, minimum adequate models were harder to define as some model terms were often not significant. For J_{max} against V_{cmax}, nitrogen and phosphorus, the model with the lowest AIC (-127.8), was that of V_{cmax} and phosphorus, however the model of J_{max} against V_{cmax} alone had a very similar AIC of -127.6 and the explained variation was not significantly different than that with the lowest AIC (Table 5-2).

For J_{max} regressed against V_{cmax}, nitrogen and SLA, the model with the lowest AIC value (-227.3) was the maximal model, including all interaction terms. The three-way interaction was significant (P<0.01) but this is difficult to interpret and the variation explained by this model when compared with other simpler models was only fractionally higher. However, analysis of variance showed that other models, with similarly low AICs, explained significantly less variation than the maximal model (Table 5-2). Discounting the maximal model from the analysis due to its difficulty in interpretation, the simplest model without loss of explained variance was that of V_{cmax}, SLA and their interaction.

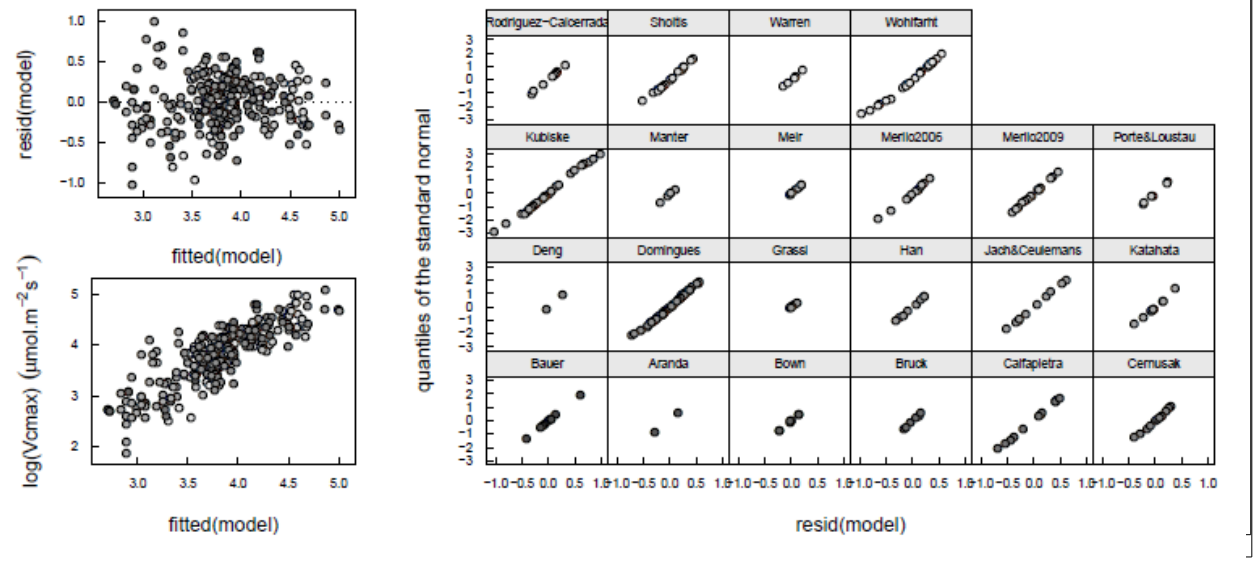

Figure 5-2.Plots showing that the assumptions of a mixed model have been met for the model of V_{cmax} against leaf nitrogen, SLA and the interaction between leaf nitrogen and SLA. Top left—model residuals against fitted values of the model; bottom left—observed values of V_{cmax} against the model fitted values and, right—model residuals plotted against quantiles of the normal distribution for each individual paper (random effect).

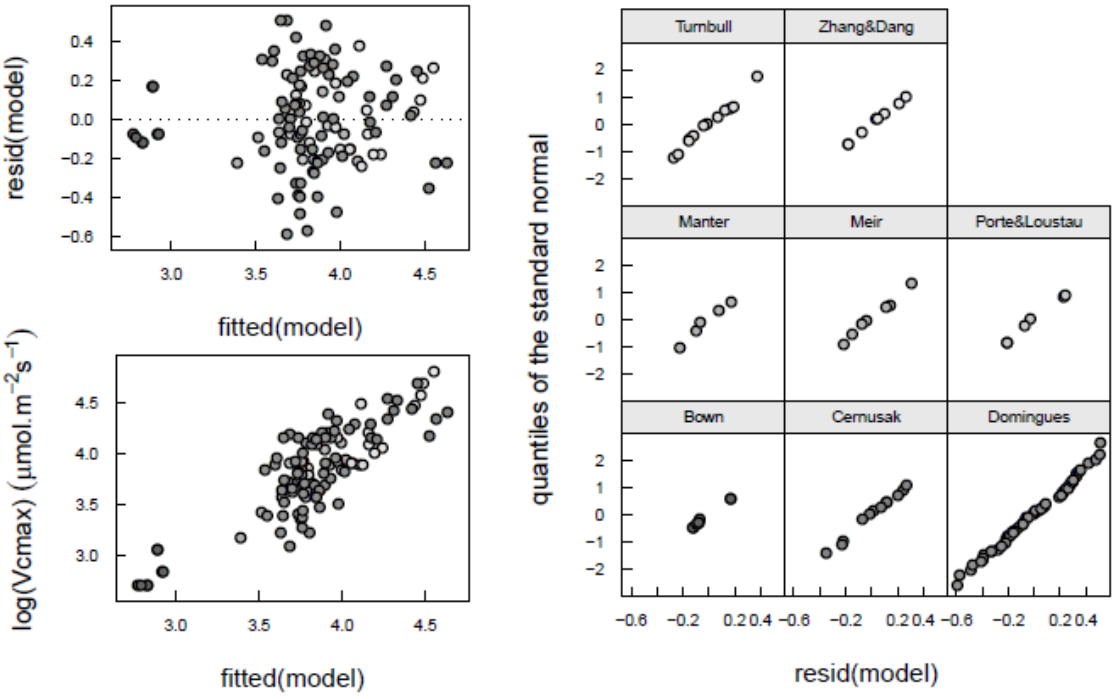

Figure 5-3. Model assumption plots for V_{cmax} against leaf nitrogen, leaf phosphorus and the interaction between leaf nitrogen and leaf phosphorus, all measured on a leaf area basis. Plots as in Figure 5-2.

Table 5-2. ANOVA of variance explained by various models of J_{max} regressed on V_{cmax}, SLA and leaf nitrogen. The Akaike Information Criteria (AIC) is also presented. The models in column one are labelled (a-d) which is used to identify the bi-model comparisons which yield the statistics presented in columns in 7–13.

Model				a		b		c		d	
	df	AIC	logLik	L.Ratio	p-value	L.Ratio	p-value	L.Ratio	p-value	L.Ratio	p-value
V_{cmax}, SLA, N + all interactions (a)	10	-227.3	123.7	NA	NA	NA	NA	NA	NA	NA	NA
V_{cmax}, SLA, N + 2 interactions (b)	8	-223.4	119.7	7.919	0.019	NA	NA	NA	NA	NA	NA
V_{cmax}, SLA, N + 1 interaction (c)	7	-222.9	118.4	10.424	0.015	2.505	0.113	NA	NA	NA	NA
V_{cmax}, SLA + interaction (d)	6	-222.6	117.3	12.716	0.013	4.797	0.091	2.292	0.130	NA	NA
V_{cmax} only	4	-219.3	113.6	20.047	0.003	12.128	0.016	9.623	0.022	7.331	0.026

Table 5-3. Linear mixed model outputs regressing V_{cmax} on two explanatory variables either leaf nitrogen and SLA or leaf nitrogen and leaf phosphorus (both on a unit area basis). All data were log transformed using the natural logarithm. Models using the same dataset are shown in contiguous light grey with the minimum adequate model for that dataset highlighted in darker grey. Shown are the coefficients and standard errors for the model terms; the students t statistics for the model terms; the minimum and maximum values of the model terms; F statistics for the model terms; the intercept and residual variance (and their percentage decrease from a null model); the R^2 of fitted values regressed on the response variable, and the Akaike Information Criterion (AIC).

response variable	explanatory variable	Coefficient	SE	DF	t statistic	p	min	max	numDF	denDF	F statistic	p	N	Ng	Intercept variance	residual variance	R2	AIC
log(Vcmax)area	intercept	3.27	0.35	253	9.38	0.000			1	253	1075.26	0.000	278	22	0.288	0.102	0.71	239.4
	log(N)area	0.64	0.30	253	2.15	0.032	0.12	4.69	1	253	83.03	0.000			-64.9	26.8		
	log(SLA)	-0.10	0.08	253	-1.32	0.188	0.00	0.24	1	253	1.69	0.195						
	log(N)area:log(SLA)	0.01	0.06	253	0.23	0.816			1	253	0.05	0.816						
log(Vcmax)area	intercept	3.29	0.34	254	9.58	0.000			1	254	1137.05	0.000	278	22	0.272	0.103	0.71	237.5
	log(N)area	0.57	0.07	254	7.58	0.000	0.12	4.69	1	254	82.65	0.000			-56.1	26.5		
	log(SLA)	-0.10	0.08	254	-1.25	0.211	0.00	0.24	1	254	1.57	0.211						
log(Vcmax)area	intercept	3.70	0.11	255	33.49	0.000			1	255	1266.85	0.000	278	22	0.244	0.104	0.71	236.9
	log(N)area	0.60	0.07	255	9.00	0.000	0.12	4.69	1	255	81.07	0.000			-39.7	25.4		
log(Vcmax)area	intercept	2.47	0.33	255	7.51	0.000			1	255	1427.64	0.000	278	22	0.212	0.128	0.64	286.6
	log(SLA)	-0.32	0.07	255	-4.48	0.000	0.00	0.24	1	255	20.09	0.000			-21.2	8.4		
log(Vcmax)area	intercept	3.96	0.24	102	16.62	0.000			1	102	663.15	0.000	113	8	0.164	0.061	0.72	42.5
	log(N)area	0.78	0.17	102	4.47	0.000	0.12	3.06	1	102	19.22	0.000			18.7	21.2		
	log(P)area	0.12	0.08	102	1.51	0.133	0.00	0.54	1	102	0.85	0.359						
	log(N)area:log(P)area	0.19	0.06	102	2.98	0.004			1	102	8.90	0.004						
log(Vcmax)area	intercept	4.10	0.28	103	14.48	0.000			1	103	349.40	0.000	113	8	0.320	0.062	0.71	48.1
	log(N)area	0.36	0.10	103	3.75	0.000	0.12	3.06	1	103	19.86	0.000			-58.8	19.3		
	log(P)area	0.11	0.08	103	1.37	0.174	0.00	0.54	1	103	1.87	0.174						
log(Vcmax)area	intercept	3.83	0.18	104	21.24	0.000			1	104	452.01	0.000	113	8	0.248	0.064	0.70	47.8
	log(N)area	0.39	0.09	104	4.36	0.000	0.12	3.06	1	104	19.00	0.000			-22.9	16.5		
log(Vcmax)area	intercept	4.31	0.26	104	16.36	0.000			1	104	438.45	0.000	113	8	0.255	0.071	0.67	59.3
	log(P)area	0.19	0.08	104	2.49	0.014	0.00	0.54	1	104	6.21	0.014			-26.4	7.0		

Table 5-4. Linear mixed model outputs regressing J_{max} on three explanatory variables: V_{cmax} and either leaf nitrogen and SLA or leaf nitrogen and leaf phosphorus (both on a unit area basis). All data were log transformed using the natural logarithm. The table is the same format as Table 5-3.

response variable	explanatory variable	Coefficient	SE	DF	t statistic	p	min	max	numDF	denDF	F statistic	p	N	Ng	Intercept variance	residual variance	R2	AIC
log(Jmax)area	intercept	1.23	0.63	94	1.94	0.055			1	94	1198.17	0.000	108	7	0.106	0.012	0.96	-121.5
	log(Vcmax)area	0.88	0.17	94	5.13	0.000	14.90	123.97	1	94	453.73	0.000			63.454	82.727		
	log(N)area	-0.16	0.79	94	-0.20	0.840	0.12	3.06	1	94	1.54	0.218						
	log(P)area	0.00	0.26	94	-0.01	0.990	0.00	0.23	1	94	1.28	0.260						
	log(Vcmax)area:log(N)area	0.02	0.21	94	0.10	0.917			1	94	0.88	0.352						
	log(Vcmax)area:log(P)area	0.01	0.07	94	0.20	0.845			1	94	0.08	0.781						
	log(N)area:log(P)area	-0.14	0.28	94	-0.51	0.611			1	94	1.74	0.190						
	log(Vcmax)area:log(N)area:log(P)area	0.03	0.08	94	0.33	0.740			1	94	0.11	0.740						
log(Jmax)area	intercept	1.27	0.62	95	2.04	0.044			1	95	1169.03	0.000	108	7	0.110	0.012	0.96	-123.3
	log(Vcmax)area	0.87	0.17	95	5.16	0.000	14.90	123.97	1	95	458.42	0.000			62.153	82.748		
	log(N)area	0.07	0.33	95	0.22	0.828	0.12	3.06	1	95	1.54	0.218						
	log(P)area	0.02	0.25	95	0.10	0.924	0.00	0.23	1	95	1.29	0.258						
	log(Vcmax)area:log(N)area	-0.04	0.08	95	-0.50	0.617			1	95	0.87	0.353						
	log(Vcmax)area:log(P)area	0.01	0.07	95	0.11	0.913			1	95	0.08	0.780						
	log(N)area:log(P)area	-0.05	0.04	95	-1.34	0.182			1	95	1.81	0.182						
log(Jmax)area	intercept	1.33	0.28	96	4.73	0.000			1	96	1194.41	0.000	108	7	0.109	0.012	0.96	-125.3
	log(Vcmax)area	0.86	0.06	96	14.44	0.000	14.90	123.97	1	96	462.67	0.000			62.595	82.732		
	log(N)area	0.07	0.33	96	0.21	0.831	0.12	3.06	1	96	1.56	0.215						
	log(P)area	0.05	0.04	96	1.19	0.235	0.00	0.23	1	96	1.31	0.256						
	log(Vcmax)area:log(N)area	-0.04	0.08	96	-0.50	0.620			1	96	0.88	0.349						
	log(N)area:log(P)area	-0.05	0.04	96	-1.37	0.174			1	96	1.87	0.174						
log(Jmax)area	intercept	1.39	0.25	97	5.48	0.000			1	97	1122.33	0.000	108	7	0.117	0.012	0.96	-127.1
	log(Vcmax)area	0.84	0.04	97	19.01	0.000	14.90	123.97	1	97	467.55	0.000			59.770	82.776		
	log(N)area	-0.09	0.09	97	-0.96	0.339	0.12	3.06	1	97	1.55	0.216						
	log(P)area	0.04	0.04	97	1.11	0.268	0.00	0.23	1	97	1.31	0.255						
	log(N)area:log(P)area	-0.06	0.04	97	-1.62	0.108			1	97	2.64	0.108						
log(Jmax)area	intercept	1.39	0.25	98	5.60	0.000			1	98	1404.22	0.000	108	7	0.094	0.012	0.95	-126.5
	log(Vcmax)area	0.83	0.04	98	18.84	0.000	14.90	123.97	1	98	456.70	0.000			67.633	82.074		
	log(N)area	0.04	0.05	98	0.85	0.395	0.12	3.06	1	98	1.60	0.208						
	log(P)area	0.05	0.04	98	1.14	0.255	0.00	0.23	1	98	1.31	0.255						
log(Jmax)area	intercept	1.37	0.25	99	5.57	0.000			1	99	1406.03	0.000	108	7	0.095	0.012	0.95	-127.8
	log(Vcmax)area	0.84	0.04	99	19.86	0.000	14.90	123.97	1	99	457.90	0.000			67.363	81.950		

	log(P)area	0.06	0.04	99	1.48	0.142	0.00	0.23	1	99	2.19	0.142						
log(Jmax)area	intercept	1.51	0.51	98	2.99	0.004			1	98	1405.10	0.000	108	7	0.094	0.012	0.95	-125.9
	log(Vcmax)area	0.80	0.13	98	6.24	0.000	14.90	123.97	1	98	453.83	0.000			67.657	81.957		
	log(P)area	0.12	0.22	98	0.57	0.572	0.00	0.23	1	98	2.17	0.144						
	log(Vcmax)area:log(P)area	-0.02	0.06	98	-0.31	0.755			1	98	0.10	0.755						
log(Jmax)area	intercept	1.15	0.20	100	5.81	0.000			1	100	1314.23	0.000	108	7	0.103	0.012	0.95	-127.6
	log(Vcmax)area	0.86	0.04	100	21.30	0.000	14.90	123.97	1	100	453.84	0.000			64.723	81.648		
log(Jmax)area	intercept	4.47	0.20	100	21.98	0.000			1	100	481.12	0.000	108	7	0.278	0.058	0.78	35.0
	log(N)area	0.37	0.09	100	4.12	0.000	0.12	3.06	1	100	16.99	0.000			4.513	14.382		
log(Jmax)area	intercept	5.21	0.29	100	17.68	0.000			1	100	441.48	0.000	108	7	0.303	0.060	0.78	38.2
	log(P)area	0.28	0.08	100	3.67	0.000	0.00	0.23	1	100	13.50	0.000			-4.197	12.185		
log(Jmax)area	intercept	3.47	0.94	201	3.70	0.000			1	201	5624.74	0.000	226	18	0.063	0.015	0.95	-227.3
	log(Vcmax)area	0.27	0.24	201	1.14	0.255	6.40	163.22	1	201	1177.63	0.000			69.630	85.209		
	log(N)area	2.94	0.99	201	2.99	0.003	0.12	4.69	1	201	3.16	0.077						
	log(SLA)	0.45	0.22	201	2.03	0.043	0.00	0.24	1	201	0.83	0.364						
	log(Vcmax)area:log(N)area	-0.70	0.25	201	-2.81	0.005			1	201	0.18	0.669						
	log(Vcmax)area:log(SLA)	-0.12	0.06	201	-2.15	0.033			1	201	8.28	0.004						
	log(N)area:log(SLA)	0.61	0.22	201	2.71	0.007			1	201	1.02	0.313						
	log(Vcmax)area:log(N)area:log(SLA)	-0.15	0.06	201	-2.60	0.010			1	201	6.75	0.010						
log(Jmax)area	intercept	4.15	0.91	202	4.55	0.000			1	202	5208.05	0.000	226	18	0.069	0.015	0.95	-222.4
	log(Vcmax)area	0.08	0.23	202	0.37	0.713	6.40	163.22	1	202	1150.57	0.000			66.987	84.820		
	log(N)area	0.44	0.21	202	2.08	0.039	0.12	4.69	1	202	3.05	0.082						
	log(SLA)	0.61	0.22	202	2.83	0.005	0.00	0.24	1	202	0.83	0.364						
	log(Vcmax)area:log(N)area	-0.06	0.05	202	-1.34	0.182			1	202	0.17	0.682						
	log(Vcmax)area:log(SLA)	-0.16	0.05	202	-3.02	0.003			1	202	8.13	0.005						
	log(N)area:log(SLA)	0.03	0.03	202	1.03	0.306			1	202	1.05	0.306						
log(Jmax)area	intercept	3.91	0.88	203	4.43	0.000			1	203	5534.07	0.000	226	18	0.065	0.015	0.95	-223.4
	log(Vcmax)area	0.15	0.22	203	0.70	0.486	6.40	163.22	1	203	1146.97	0.000			68.861	84.668		
	log(N)area	0.34	0.19	203	1.82	0.071	0.12	4.69	1	203	3.09	0.080						
	log(SLA)	0.56	0.21	203	2.66	0.008	0.00	0.24	1	203	0.80	0.372						
	log(Vcmax)area:log(N)area	-0.07	0.05	203	-1.57	0.118			1	203	0.18	0.671						
	log(Vcmax)area:log(SLA)	-0.15	0.05	203	-2.84	0.005			1	203	8.06	0.005						
log(Jmax)area	intercept	3.43	0.83	204	4.14	0.000			1	204	5343.79	0.000	226	18	0.067	0.015	0.95	-222.9
	log(Vcmax)area	0.27	0.21	204	1.33	0.185	6.40	163.22	1	204	1141.09	0.000			67.571	84.536		
	log(N)area	0.05	0.03	204	1.50	0.134	0.12	4.69	1	204	3.05	0.082						
	log(SLA)	0.43	0.19	204	2.21	0.028	0.00	0.24	1	204	0.81	0.370						
	log(Vcmax)area:log(SLA)	-0.11	0.05	204	-2.41	0.017			1	204	5.78	0.017						
log(Jmax)area	intercept	3.23	0.82	205	3.94	0.000			1	205	5189.51	0.000	226	18	0.070	0.015	0.95	-222.6
	log(Vcmax)area	0.31	0.20	205	1.50	0.134	6.40	163.22	1	205	1136.04	0.000			66.426	84.410		

	log(SLA)	0.40	0.19	205	2.05	0.042	0.00	0.24	1	205	2.02	0.157							
	log(Vcmax)area:log(SLA)	-0.11	0.05	205	-2.31	0.022			1	205	5.36	0.022							
log(Jmax)area	intercept	1.48	0.17	205	8.63	0.000			1	205	5622.41	0.000	226	18	0.064	0.016	0.95	-219.1
	log(Vcmax)area	0.76	0.03	205	28.01	0.000	6.40	163.22	1	205	1113.35	0.000			69.124	84.035		
	log(N)area	0.05	0.03	205	1.35	0.178	0.12	4.69	1	205	3.04	0.083						
	log(SLA)	-0.03	0.03	205	-0.87	0.384	0.00	0.24	1	205	0.76	0.384						
log(Jmax)area	intercept	1.56	0.13	205	12.10	0.000			1	205	5804.03	0.000	226	18	0.062	0.016	0.95	-218.5
	log(Vcmax)area	0.77	0.03	205	25.28	0.000	6.40	163.22	1	205	1108.63	0.000			70.133	83.945		
	log(N)area	0.13	0.17	205	0.73	0.465	0.12	4.69	1	205	3.06	0.082						
	log(Vcmax)area:log(N)area	-0.02	0.04	205	-0.41	0.683			1	205	0.17	0.683						
log(Jmax)area	intercept	1.59	0.12	206	13.35	0.000			1	206	5760.32	0.000	226	18	0.063	0.016	0.95	-220.3
	log(Vcmax)area	0.77	0.03	206	28.49	0.000	6.40	163.22	1	206	1113.37	0.000			69.756	83.949		
	log(N)area	0.06	0.03	206	1.75	0.082	0.12	4.69	1	206	3.06	0.082						
log(Jmax)area	intercept	1.51	0.11	207	13.51	0.000			1	207	5477.05	0.000	226	18	0.067	0.016	0.95	-219.3
	log(Vcmax)area	0.79	0.02	207	33.25	0.000	6.40	163.22	1	207	1105.45	0.000			67.996	83.788		
log(Jmax)area	intercept	4.49	0.11	207	40.22	0.000			1	207	1725.78	0.000	226	18	0.208	0.075	0.75	123.6
	log(N)area	0.49	0.06	207	8.03	0.000	0.12	4.69	1	207	64.51	0.000			0.189	23.744		
log(Jmax)area	intercept	3.12	0.31	207	10.04	0.000			1	207	1443.66	0.000	226	18	0.249	0.086	0.71	155.2
	log(SLA)	-0.35	0.07	207	-5.20	0.000	0.00	0.24	1	207	27.00	0.000			-19.578	12.571		

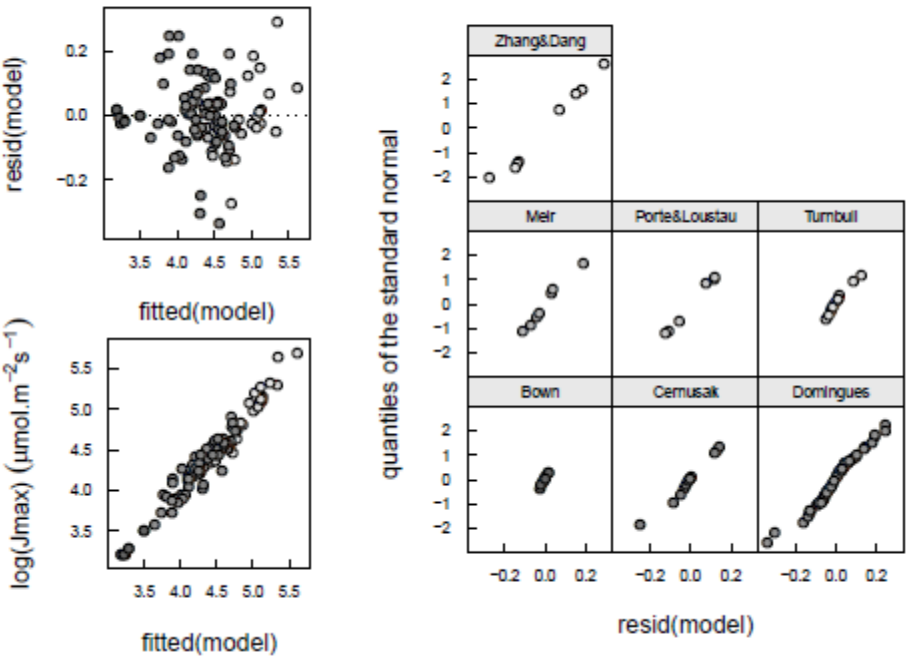

Figure 5-4. Plots showing the assumptions of a mixed model have been met for the model of J_{max} against V_{cmax}, leaf nitrogen, leaf phosphorus and the interaction of both leaf nitrogen and leaf phosphorus with V_{cmax}. All measured on a leaf area basis. Plots as in Figure 5-2.

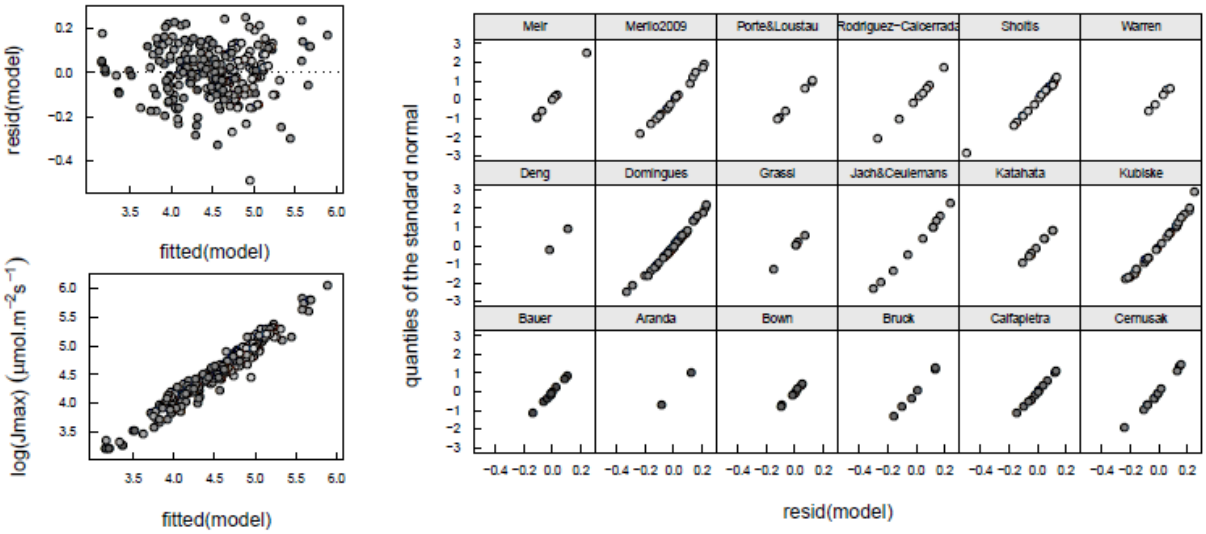

Figure 5-5. Plots showing the assumptions of a mixed model have been met for the model of J_{max} against V_{cmax}, leaf nitrogen, SLA and the interaction of SLA with V_{cmax}. All measured on a leaf area basis. Plots as in Figure 5-2.

Discussion

V_{cmax}, leaf phosphorus and SLA

For the minimum adequate model of V_{cmax} against leaf nitrogen and phosphorus, leaf nitrogen was a significant correlate while leaf phosphorus alone was not. Leaf phosphorus was only significant in interaction with leaf nitrogen, modifying the nature of the correlation between V_{cmax} and leaf nitrogen. That leaf phosphorus was only significant in interaction with leaf nitrogen highlights the importance of considering interaction terms. The analysis of V_{cmax} and J_{max}byDomingues et al. (2010) concluded that leaf nitrogen and leaf phosphorus were best considered in terms of limiting factors; however, their conclusion was based on additive models and did not consider the interaction term between nitrogen and phosphorus in their standard regression model.

The relationship between V_{cmax} and leaf nitrogen, and how it was modified by leaf phosphorus, is shown in Figure 5-8. Increasing phosphorus increases the sensitivity of V_{cmax} to nitrogen. The finding for phosphorus is similar to that of Reich et al. (2009) who found that, in a global analysis, increased leaf phosphorus increased the sensitivity of A_{max} to leaf nitrogen. The data presented in this Chapter show that phosphorus affects the A_{max} to leaf nitrogen relationship by modifying the V_{cmax} to nitrogen relationship, not the J_{max} to V_{cmax} relationship. Due to phosphorus playing several roles in the regeneration of RuBP, it was unexpected that leaf phosphorus would not affect J_{max}, although the lack of affect on the J_{max} to V_{cmax} relationship may represent tight coupling between the two parameters rather than no impact of phosphorus on J_{max}.

Reich et al. (2009)showed this tightening of the relationship between A_{max} and leaf nitrogen to hold true across biomes with different N:P ratios. Kattge et al. (2009) found the relationship of V_{cmax} to leaf nitrogen to have a smaller slope parameter for tropical trees growing on the phosphorus poor oxisols. Although the tropics tend to have lower soil phosphorus (Quesada et al. 2010) and leaf phosphorus (McGroddy et al. 2004, Reich and Oleksyn 2004) than temperate regions, Kattge et al. (2009) calculated an only slightly lower slope for tropical trees on non-oxisols (26.19) than for temperate trees (29.81). The calculated slope parameter did however have a three-fold higher standard deviation for tropical trees on oxisols which may represent slope variation in response to varying leaf phosphorus.

Domingues et al. (2010) showed that SLA was important in models of V_{cmax} and J_{max} on a concentration basis and our results support that finding (Table 5-1). Aranda et al. (2006) showed that SLA was significant when traits were measured on an area basis, reducing V_{cmax} per unit nitrogen as SLA increased. However, our results indicated that the area based relationship between V_{cmax} and leaf nitrogen was not affected by SLA. Alone, SLA was a significant correlate of V_{cmax} but the higher explained variance by leaf nitrogen and the insignificance of SLA when in conjunction with leaf nitrogen suggested that the correlation between SLA and V_{cmax} could be explained away by the covariance of SLA with leaf nitrogen. Also, Niinemets (1999) showed that the components of SLA—leaf thickness and leaf density—showed different relationships to A_{max}. That these two components of SLA were not correlated with each other but both correlated with SLA (Niinemets 1999) indicates that SLA may not have a consistent effect on photosynthesis and is dependent upon which of its components (thickness or density) is changing. SLA (or its inverse LMA) responds to multiple environmental and ecological factors and components of SLA (i.e. density and thickness) strongly correlate with nitrogen (Niinemets 1999, Poorter et al. 2009). It may be that changing SLA is a plant's primary mechanism by which changes in leaf nitrogen are driven and our results suggest that leaf nitrogen is the proximal driver of V_{cmax} as established by many previous studies (Field and Mooney 1984, Wullschleger 1993, Reich et al. 2007, Kattge et al. 2009). Phosphorus also changes with leaf nitrogen and SLA, and as with SLA, in a bivariate relationship with V_{cmax} phosphorus is a significant covariate but that covariation is eroded away when analysed in conjunction with leaf nitrogen. However, and in contrast to SLA, leaf phosphorus modifies the nature of the relationship of V_{cmax} to nitrogen, indicating that as phosphorus limits biochemical processes, V_{cmax} becomes less sensitive to leaf nitrogen.

J_{max} and V_{cmax}

V_{cmax} was the major determinant/covariate of J_{max} accounting for 95% of the variation in J_{max} for both the analyses including nitrogen and either phosphorus or SLA. We found the slope of the regression of log transformed J_{max} on V_{cmax} to be 0.79 and 0.82 for the larger dataset on an area and concentration basis respectively (Table 5-4& Table 5-1). Similar to the analysis of Reich et al. (2010) for the scaling of leaf nitrogen with leaf phosphorus, this could represent the 2/3 scaling relationship expected by the allometric relationship of leaf area to leaf volume. In this case, J_{max} would be more correlated to leaf area and V_{cmax} to leaf mass.

This can be interpreted as light harvesting complexes scaling with light capture and hence area, and carboxylation capacity scaling with the quantity of leaf tissue. Perhaps the higher values of the coefficient than 2/3 represents a more mixed relationship than J_{max} scaling purely with area and V_{cmax} purely with mass, although the difference in the slope from exactly 2/3 could also represent error from the 'true' value due to the sample size (Reich et al. 2010). Indeed, in an early analysis of the relationship between J_{max} and V_{cmax}, Wullschleger (1993) described a slope coefficient of 1.64 for un-transformed data. Digitising Wullschleger (1993) data we natural log-transformed J_{max} and V_{cmax} and re-analysed it with a linear fit. We found that regression assumptions were not violated by the transformation and that the slope coefficient was 0.84 (with an R^2 of 0.87). In an analysis of natural log transformed J_{max} against V_{cmax} from the TRY database (Kattge et al. 2011), J_{max} scaled against V_{cmax} with a slope parameter of 0.77 (and R^2 of 0.81) Our results suggested that J_{max} may be less sensitive to changes in V_{cmax} at higher levels of SLA although little extra variation was explained. The indication was that as SLA increases, the J_{max} to V_{cmax} relationship approaches the pure allometric scaling law. This was somewhat counter-intuitive as we would assume the difference between volume and area to be more apparent in thicker leaves, not thinner ones with high SLA. In this study, in the analysis of the Kattge et al. (2011)data and in the re-analysis of the Wullschleger (1993) data the log transformed J_{max} to V_{cmax} slope was always above the 2/3 slope of area to volume scaling. If the J_{max} to V_{cmax} relationship was determined by area to volume scaling it was expected that increasing SLA (i.e. thinner leaves) would increase the slope as area and volume approached unity. Counter to expectations, increasing SLA decreased the slope. There was no evidence to suggest that the relationship of J_{max} to V_{cmax} was in any way modified by phosphorus, although the data presented here only represent 108 species/treatment combinations.

To analyse the relationship of J_{max} to V_{cmax} in more depth we investigated the effect of the slope parameter on carbon assimilation under various environmental conditions. Figure 6 shows the effect of the slope parameter on a single leaf Farquhar model while Figure 7 shows the effect on a full canopy photosynthesis model used by the Sheffield Dynamic Vegetation Model (SDGVM). The analyses show that the slope parameter, as would be expected, determines the point at which assimilation switches from light limitation to CO_2 and V_{cmax} (nitrogen) limitation. More interestingly, the analysis shows that for contemporary and historical CO_2 concentrations, the value of the slope parameter that we calculated is

well above parameter values (0.6-0.75 dependent on CO_2 and nitrogen) at which carbon assimilation becomes light saturated. Optimisation theory would suggest that the slope parameter should be minimised with respect to the light saturation point, as beyond light saturation J_{max} has no impact on carbon assimilation yet represents higher investment of resources in the biochemical machinery that determine J_{max}. High calculated values (beyond light saturation) of the slope parameter suggests that there may be a functional significance to a higher than expected J_{max}.

The analysis using the canopy model of SDGVM shows that our calculated value of the slope parameter would mean permanent light limitation. This is likely to be unrealistic and perhaps shows that SDGVM is generally light limited, a limitation observed in Chapter 3. However, the higher light limitation of the SDGVM canopy at observed values of the slope parameter may indicate that the higher slope parameter values than expected may be explained by optimisation of canopy carbon assimilation, not leaf level assimilation. Another hypothesis of the higher than expected values of J_{max} is that electron transport is not really limiting, as suggested by Collatz et al. (1991), and that light, when CO_2 and nitrogen are limiting carbon assimilation, can still be used to synthesise ATP and NADPH useful in other biochemical pathways, i.e. nitrite reduction by nitrite reductase which occurs in the chloroplast (Anderson and Done 1978).

Leaf trait relationships by biome

A number of studies have investigated the variation in V_{cmax} and J_{max}, and the relationship of V_{cmax} to nitrogen, due to plant phenology and functional type (Wullschleger 1993, Beerling and Quick 1995, Kattge et al. 2009) and V_{cmax} and J_{max} relationships to nitrogen, phosphorus and SLA by biomes along tropical rainfall gradients (Domingues et al. 2010, Cernusak et al. 2011). The data in this Chapter were too few to investigate the effect of multiple leaf traits on photosynthetic parameters, particularly phosphorus, in different biomes. Also, data were sourced from a mixture of natural environments and experimental studies which meant comparison by biome may have been confounded by experimental manipulation putting trait values outside of the range found in their native biomes. The indication from Kattge et al. (2009) was that there are different slopes of the relationship between V_{cmax} and nitrogen, with biomes that are more likely phosphorus limited (Reich and Oleksyn 2004) showing lower slopes. Our analysis shows that V_{cmax} is less sensitive to nitrogen at low levels of

phosphorus and it is intriguing that these differences by biome may be explained away by the addition of leaf phosphorus to the regression analysis.

The increase in explanatory power of these models

While the analyses showed that leaf phosphorus was a significant addition to the model of V_{cmax} and indicated that SLA may be a significant addition to the model of J_{max}, the analyses also indicated that the increase in explained variation achieved by their addition was minimal, particularly so for SLA in the model of J_{max}.

The dominant covariate of J_{max} was V_{cmax} and the addition of an interaction term with SLA did not increase the variance explained when measured by the R^2 of the fitted values of J_{max} with the observed values, and decreased the residual and intercept variation from that in the null model by only 1%. The increases in variation explained by the addition of SLA to a model of J_{max} appear to be too small to warrant a change in the way that J_{max} is currently simulated in global vegetation models.

For the model of V_{cmax} phosphorus increased the R^2 by 2% when compared with the bivariate model of V_{cmax} and nitrogen, reduced the residual variance by 6% of the null model values and reduced the intercept variance by 42%. This reduction in intercept variance indicated a shift from variance explained by random effects to variance explained by fixed effects. Phosphorus is likely to be an important variable relating to V_{cmax} and is worthwhile to consider it as a variable in global vegetation models.

It was difficult to compare this small increase in explained variation with previous studies as directly comparable metrics have not been published. As demonstrated by (Kattge et al. 2009) for different biomes across the globe and Domingues et al. (2010) in a gradient of biomes from open savannah to semi-deciduous forest in West Africa, V_{cmax} and J_{max} were differentially sensitive to leaf traits in different biomes. It may be that the small increase in explained variation by adding phosphorus and, particularly, SLA to regression models may reflect the fact that these relationships may be more biome specific although there were insufficient data to test this.

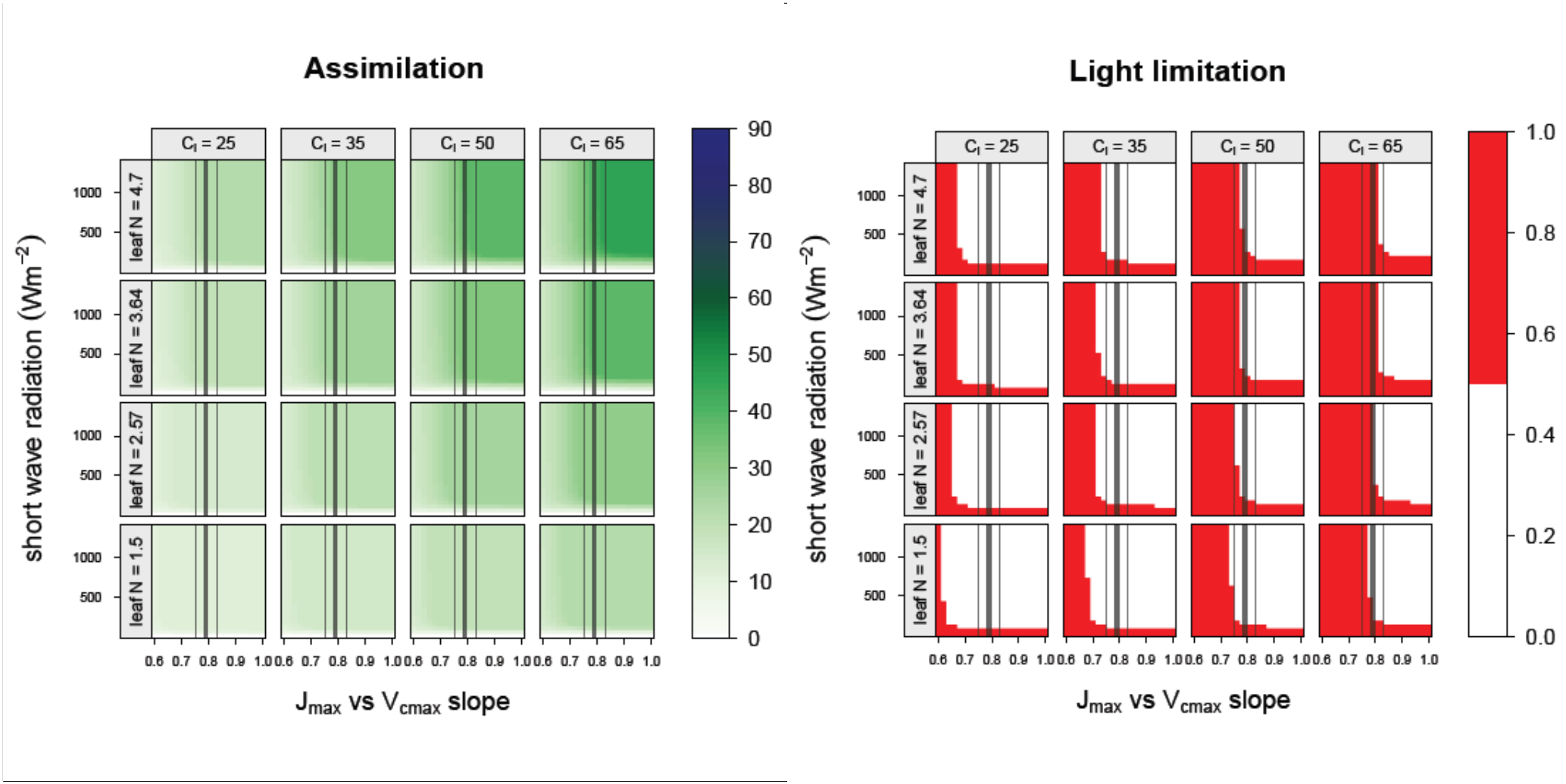

Figure 5-6. The effect of the J_{max} to V_{cmax} (both log transformed) slope parameter on assimilation (left hand plots) and light limitation to photosynthesis (right hand plots) using a single leaf Farquhar model. The slope parameter is on the x-axis and shortwave radiation on the y-axis. The panels are combinations of leaf nitrogen (gm^{-2}—rows, increasing bottom to top) and internal CO_2 partial pressure (Pa—columns, increasing left to right). The value of the slope (thick vertical line) and the 95% confidence bounds (thin vertical lines). Leaf nitrogen effectively sets the log transformed V_{cmax} parameter using the relationships presented above (slope – 0.6 & intercept – 3.7), the J_{max} to V_{cmax} intercept was maintained at 1.51.

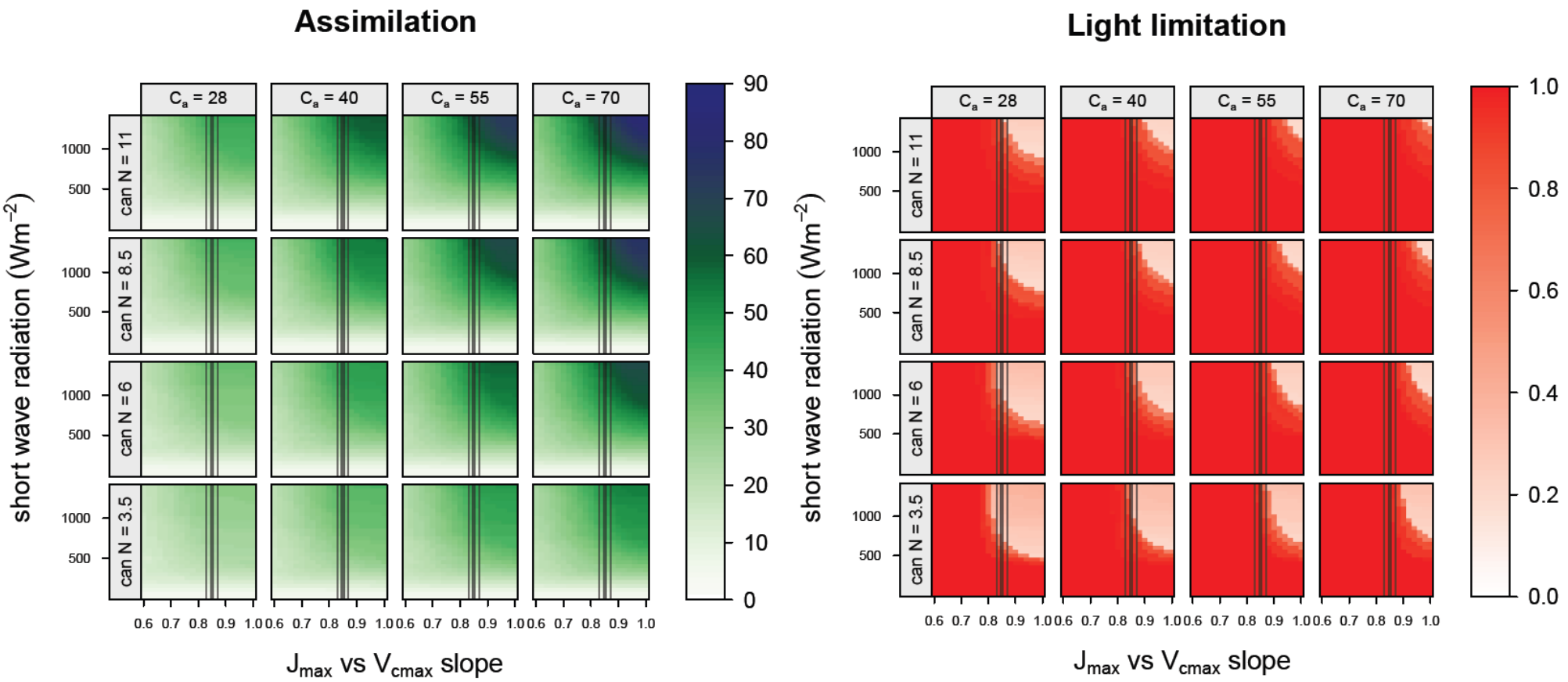

Figure 5-7. The effect of the J_{max} to V_{cmax} slope parameter on assimilation (left hand plots) and light limitation to photosynthesis (right hand plots) using the canopy photosynthesis model of SDGVM. The slope parameter is on the x-axis and shortwave radiation on the y-axis. The panels are combinations of leaf nitrogen (gm^{-2}—rows, increasing bottom to top) and ambient CO_2 partial pressure (Pa—columns, increasing left to right). The value of the slope (thick vertical line) and the 95% confidence bounds (thin vertical lines) are plotted. Leaf nitrogen sets the log transformed V_{cmax} parameter using the relationships presented above (slope – 0.6 & intercept – 3.7), the J_{max} to V_{cmax} intercept was maintained at 1.51. The values of leaf nitrogen were chosen to preserve top leaf nitrogen values as those for the single leaf Farquhar model using Beer's Law scaling and an LAI of 5.

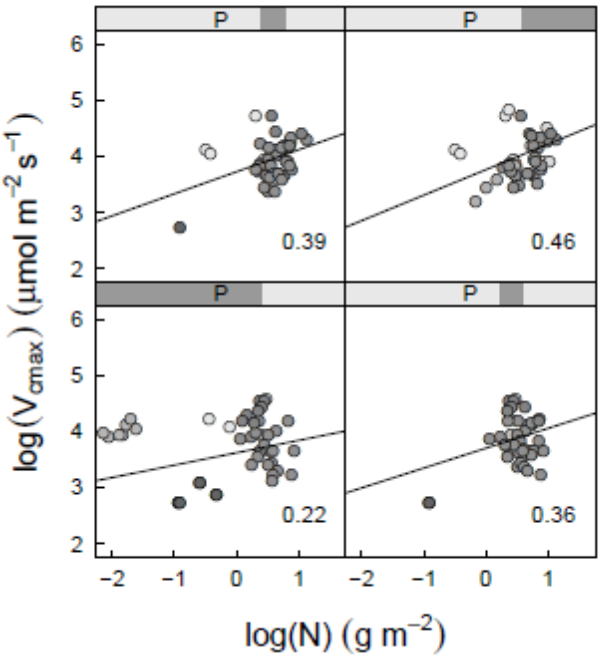

Figure 5-8.The relationship of V_{cmax} to leaf nitrogen as modified by leaf phosphorus. Numbers in each panel represent the slope of the regression line calculated using the minimum adequate model as presented in Table 5-3. Panels are separated by increasing values of phosphorus (left to right, bottom to top). The separation of data was carried out to leave an equal number of points in each panel allowing overlap so a single data point can appear in more than one panel. The header at the top of each panel represents the full range of values of phosphorus and the dark grey fill in the header represents the range of phosphorus values in the particular panel.

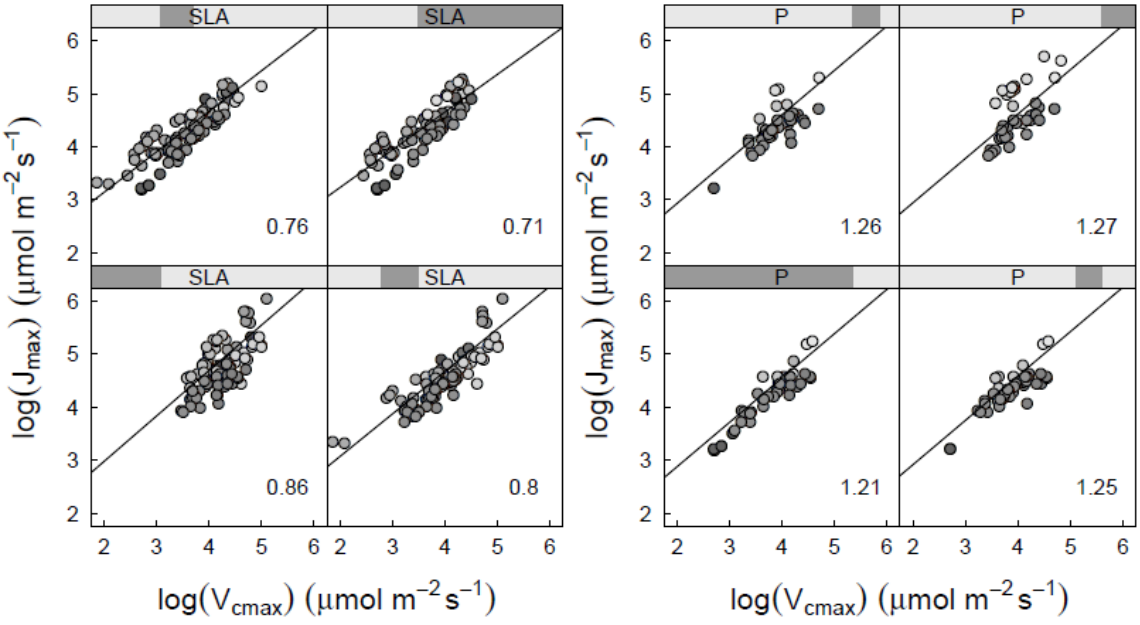

Figure 5-9. The relationship of J_{max} to V_{cmax} as modified by SLA (right 4 panels) and leaf phosphorus (left 4 panels). Panels are separated by increasing values (left to right, bottom to top) of either SLA or phosphorus. Numbers in each panel represent the slope (SLA – top panels) or intercept (phosphorus – bottom panels) of the regression line calculated using the minimum adequate models as presented in Table 5-3. See Figure 5-8 for further explanation of the Figures.

Conclusions

V_{cmax} was most strongly correlated to leaf nitrogen. Leaf phosphorus, in interaction with nitrogen, had a significant relationship with V_{cmax}, and increasing leaf phosphorus increased the sensitivity of V_{cmax} to leaf nitrogen. We tentatively suggest that the differences in slope of the V_{cmax} to leaf nitrogen relationships developed by Kattge et al. (2009) may be explained by differences in leaf phosphorus and it will be interesting to test further as more leaf phosphorus data becomes available.

There was an indication that SLA reduced the sensitivity of J_{max} to V_{cmax} although the J_{max} to V_{cmax} relationship remained tight. Higher than expected values of the J_{max} to V_{cmax} slope parameter, based solely on optimisation of leaf carbon assimilation considered alone, were observed. We suggest that this may be due to investment in electron transport capacity to produce ATP and NADPH for biochemical pathways other than the PCA cycle.

Phosphorus and SLA were only significant regression model variables in interaction with the primary driving variables and future studies are advised to be cautious when basing conclusions on additive models alone. The data and analysis presented in this Chapter suggest that interactions need to be considered and that considering the effect of nitrogen and phosphorus on V_{cmax} in terms of limiting factors may not be suitable for global scale analysis.

Coefficients of the relationship between V_{cmax}, leaf nitrogen and leaf phosphorus and between J_{max}, V_{cmax} and SLA, are tentatively presented. Although much of the data came from studies that manipulated leaf nitrogen and phosphorus and therefore present a good range of leaf nutrient concentrations, it is recognised that more data needs collection and from a more diverse range of biomes. This work builds on that of others and for the first time presents the significance of phosphorus and SLA in relation to V_{cmax} and J_{max} in a global study. The relationships presented in this study can be used to parameterise V_{cmax} and J_{max} in a more empirical and rigorous fashion using data-derived relationships, moving their parameterisation away from simple methods with limited variation (in some models they are fixed by PFT e.g. JULES) or limited grounding in the literature (there is evidence to suggest they have been used as model tuning parameters).

Chapter 6 Simulating terrestrial vegetation with revised V_{cmax} parameterisation

Introduction

Global carbon cycle models are highly sensitive to V_{cmax} and J_{max} parameterisation and often, therefore, leaf nitrogen parameterisation. In a global study Bonan et al. (2011a) demonstrated the sensitivity of Gross Primary Productivity (GPP) in CLM4 (the US Community Land Model) to V_{cmax}, the structure of the photosynthesis scheme and the structure of the canopy radiation scheme. Bonan et al. (2011a) showed that revisions of the photosynthesis scheme (which included the addition of a J_{max} term to the Collatz et al. (1991) formulation) and the canopy radiation and nitrogen scaling scheme reduced GPP from 165 Pg C yr^{-1} to 130 Pg C yr^{-1}. Kattge et al. (2009) developed a dataset of V_{cmax} by biome based on biome specific leaf nitrogen distributions and the relationship of V_{cmax} to leaf nitrogen in that biome—determined using a data assimilation technique. Kattge et al. (2009) showed that their V_{cmax} parameterisation, compared to the Beerling and Quick (1995) V_{cmax} parameterisation, reduced GPP in the tropics by 800 to >1600 g C m^{-2} yr^{-1} (a decrease of up to 30%) and increased GPP in the boreal region by 100 to 400 g C m^{-2} yr^{-1} (an increase of up to 80%).

The version of CLM4 used by Bonan et al. (2011a) reduces V_{cmax} according to soil nitrogen availability and they showed that releasing V_{cmax} from this constraint increased GPP to 161 Pg C yr^{-1}. While this increase in GPP appeared to support the V_{cmax} constraint in CLM4, they also showed that the substitution of the CLM4 V_{cmax} parameterisation with that of Kattge et al. (2009) maintained GPP in CLM4 at 164 Pg C yr^{-1}, close to the non-nitrogen limited value.

The revision of the canopy light scheme in CLM4 showed that simulation of GPP was also sensitive to light levels. In an Amazonian FLUXNET site, under conditions that were not limited by soil water, Mercado et al. (2007) demonstrated the sensitivity of NPP in JULES (Joint UK Land Environment Simulator) to the canopy radiation scheme, and therefore light levels. Mercado et al. (2007) also demonstrated the sensitivity to top leaf values of V_{cmax} but relative insensitivity to the scaling of V_{cmax} through the canopy.

Chapter 4 demonstrated that SDGVM under-predicted leaf nitrogen and had low parameterisation of V_{cmax} (and hence J_{max}) at the Oak Ridge and Duke FACE experiments

located in the south-eastern US. It was also shown that PAR was over-predicted by SDGVM at Oak Ridge and Duke and that model predictions of NPP were highly sensitive to changes in these variables. Accurate PAR, canopy nitrogen and photosynthetic rate limiting parameters significantly improved the simulation of NPP in SDGVM.

The photosynthesis scheme is at the heart of SDGVM, driving Net Primary Productivity (Chapter 4) and water use efficiency (De Kauwe et al. In Prep). Driving the photosynthesis scheme are Photosynthetically Active Radiation (PAR—a model forcing variable), canopy nitrogen and the relationships of the Farquhar et al. (1980) model rate limiting parameters —V_{cmax} and J_{max}—to leaf nitrogen (Chapter 3).

This Chapter assesses the impact of updated V_{cmax} and J_{max} parameterisation, higher leaf nitrogen and short wave radiation driving data in SDGVM on a global scale and in response to future CO_2 and climate change projections. The impact on the global carbon cycle of leaf phosphorus as a variable in the empirical calculation of V_{cmax} and J_{max} was also assessed, to our knowledge for the first time. In contrast to Kattge et al. (2009) and Bonan et al. (2011b) who set V_{cmax} and J_{max} as a PFT specific parameter, the study in this Chapter used an empirical approach (Reich et al. 2007, Ordonez et al. 2009) within the model to prognostically simulate leaf trait values. Top leaf values of nitrogen and phosphorus were based on empirical functions of climate (irradiance and precipitation) and soil carbon to nitrogen ratio. Subsequently leaf nitrogen and phosphorus were used in empirical equations of V_{cmax} as determined in Chapter 5. As J_{max} was calculated as a function of V_{cmax}, leaf nitrogen and phosphorus also had an impact on J_{max}.

Chapter 4 demonstrated that in the South-Eastern US, SDGVM under-predicted V_{cmax} and it was proposed that this under-prediction compensated for over-prediction of PAR by SDGVM. This Chapter tests this in global scale simulations by correcting the under-prediction of V_{cmax} (and J_{max}) using a trait regression method, and drives SDGVM with a global PAR dataset. It is hypothesised that SDGVM will over-predict GPP with the new V_{cmax} scheme but this will be corrected by using the new PAR dataset.

This Chapter investigates how the evolution of atmospheric carbon is affected by the new V_{cmax} parameterisation and the PAR dataset, asking the question: does improved representation of V_{cmax} and PAR improve our confidence in predictions of the carbon cycle over the coming century? Confidence in predictions of the carbon cycle is assessed by

comparing simulated GPP and plant biomass with observed datasets. Soil carbon pools and dynamics are also analysed.

Key to the simulated trajectory of atmospheric CO_2 will be the capacity of the terrestrial biosphere to sequester carbon in biomass (Houghton 2009). This Chapter compares SDGVM predictions of biomass with a number of global biomass datasets and asks whether corrected V_{cmax} and PAR improve the simulation of biomass. To explain errors in biomass predictions, general relationships between biomass and GPP, biomass and NPP and the autotrophic respiration fraction of GPP and temperature were compared with observed datasets.

Methods

The 7th June 2007 version of SDGVM was used as the baseline model for comparison and for investigation of alternative methods to simulate PAR, canopy nitrogen and the V_{cmax} and J_{max} parameters. SDGVM was coupled to the Integrated Model Of Global Effects of climatic aNomalies (IMOGEN) (Huntingford and Cox 2000) General Circulation Model (GCM) analogue to generate scenarios of future climate change based on the patterns projected by a number of GCMs.

IMOGEN uses an energy balance model to predict global temperature change based on the increase of CO_2 and other greenhouse gases. Huntingford et al. (2010) showed that for a given GCM the predicted change in a climatic variable at a particular point on the globe was related to the predicted change in global temperature by a linear approximation. With a baseline climate and globally gridded fields of the relationship between a climatic variable and global temperature increase, IMOGEN mimics the climate predictions of a GCM at a fraction of the computational expense. Global temperatures predicted by IMOGEN are driven by global values of atmospheric CO_2 which are augmented annually by the sum of a CO_2 emissions scenario, the SDGVM predicted terrestrial biosphere CO_2 flux and the CO_2flux from a simple ocean model. IMOGEN couples the SDGVM CO_2 flux with predicted climate change which allows for feedback between the carbon-cycle and climate change, but not other land surface processes (e.g. evapotranspiration/latent heat flux).

Modification of SDGVM

V_{cmax}, J_{max}, leaf nitrogen and leaf phosphorus

For the revised version of SDGVM (SDGVM-Vc) leaf nitrogen, phosphorus, V_{cmax} and J_{max} were simulated using a leaf trait regression method. All leaf traits were calculated on an area basis and for the topleaf. For SDGVM, V_{cmax} and J_{max} were already calculated using trait regression (Eq 4-5 & 4-6) and SDGVM-Vc used the empirical, linear equations, determined in Chapter 5, to calculate new values of V_{cmax} and J_{max}. V_{cmax} was calculated as a function of leaf nitrogen and leaf phosphorus, and J_{max} was calculated as a function of V_{cmax}:

$$V_{cmax} = e^{(3.96+0.78\ln(N)+0.12\ln(P)+0.19\ln(N)\ln(P))} \quad (6\text{-}1)$$

$$J_{max} = e^{(1.51+0.79\ln(V_{cmax}))}$$

(6-2)

Where V_{cmax} and J_{max} are the maximum carboxylation velocity of RuBisCO and the maximum rate of electron transport (µmol m^{-2} s^{-1});*N* is leaf nitrogen (gm^{-2}) and *P* is leaf phosphorus in (gm^{-2}).Leaf nitrogen and leaf phosphorus were calculated in SDGVM-Vc using empirical relationships to the soil carbon to nitrogen ratio, mean annual short wave radiation and mean annual precipitation updated from the Ordonez et al. (2009) data:

$$N = 10^{(-14.03+4.00\log(MAP)+7.94\log(C:N_s)+0.05\mathrm{MASWR}-int1-int2-int3)}$$

(6-3)

$$P = 10^{0.67\log(N)-0.37\log(MAP))}$$

(6-4)

Where:-

$$int1 = 1.87\log(MAP)\log(C:N_s)$$

(6-5)

$$int2 = 0.01\log(MAP)\,MASWR$$

(6-6)

$$int3 = 0.01\log(C:N_s)\,MASWR$$

(6-7)

where *MAP* is the 10 year mean annual precipitation (mm), $C{:}N_s$ is the soil C:Nratio and *MASWR* is the 30 year mean annual downwards shortwave radiation (Wm^{-2}). Soil carbon to nitrogen ratio was obtained from the ISRIC-WISE soils database (ver3.0) (Batjes 2005). Ordonez et al. (2009) used mean annual short wave radiation from New et al. (1999), obtainable from IPCC (2011), in their regression analysis and so these data were used in this study. To avoid extrapolation of the Ordonez et al. (2009) equations, they were only applied in the model when the independent variables of the equations fell within the calibration range of these variables. In practice, at sites where shortwave radiation exceeded 192 Wm^{-2} or precipitation fell short of 300 mm yr^{-1}, the default SDGVM method was used to calculate leaf nitrogen and V_{cmax}. Effectively this exclusion removed the desert regions of the world

from having leaf nitrogen etc calculated using the trait regression method (Figure 6-1). As climate changed over the years of the experiment, SDGVM-Vc sites could switch between the original and the trait regression method but in practice there was little change.

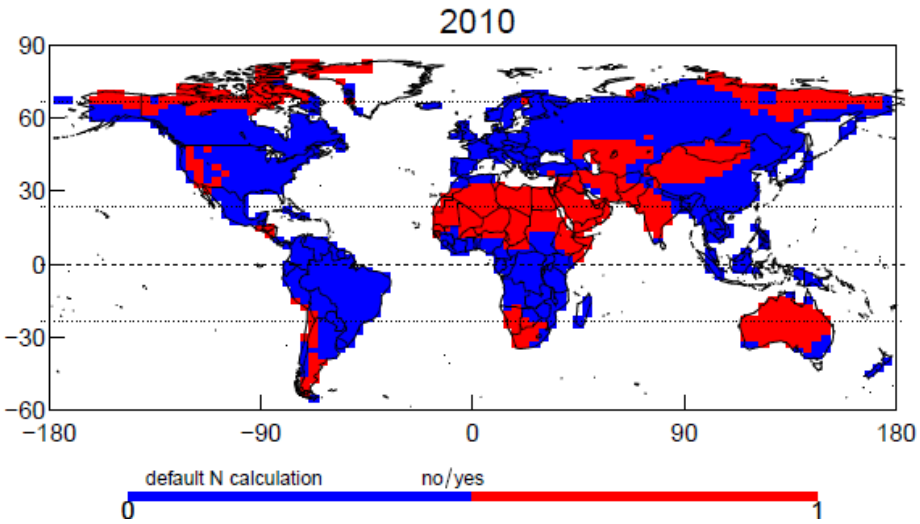

Figure 6-1. Gridpoints which used either the SDGVM default method (red) or the trait regression method (blue) to calculate leaf nitrogen and V_{cmax} in 2010.

Chapter two showed that a general plant response to increased CO_2 was a decrease in leaf nitrogen concentration and a decrease in leaf nitrogen per unit area. To simulate this effect, an empirical equation was derived from the meta-analysis in Chapter two. When broken down by plant functional type (PFT), only leaf nitrogen in grasses was significantly affected by elevated CO_2 so the function was fit only to grasses. Leaf nitrogen for grasses was calculated as:

$$N_g = N(1.2144 - 0.0056C_a) \quad (6\text{-}8)$$

Where N_g is top-leaf nitrogen for grasses and C_a is atmospheric CO_2 (Pa). The function preserved leaf nitrogen at a CO_2 concentration of 38Pa dropping to 0.89 at a CO_2 concentration of 57.5 Pa. For comparison, a reduction in leaf nitrogen across all PFTs was implemented using the 4% reduction calculated in Chapter two:

$$N = N(1.0780 - 0.0021C_a) \quad (6\text{-}9)$$

Lloyd et al. (2010) demonstrated the similarity of canopy nitrogen and canopy phosphorus scaling. Therefore, canopy nitrogen and phosphorus were calculated from LAI and top leaf nitrogen, or phosphorus, by an inversion of the Beer's Law canopy scaling function assuming a linear relationship of leaf nitrogen to light (Haxeltine and Prentice 1996). Although Lloyd et al. (2010) showed that the coefficient of the scaling function was likely to be somewhat lower than the Beer's Law coefficient, investigating canopy scaling was not the purpose of this study and the Beer's Law coefficient was maintained for consistent comparison with the standard version of SDGVM.

Short wave radiation forcing data

SDGVM normally calculates short wave radiation as a function of latitude and in Chapter 3 it was shown that, at the two simulated FACE sites located in the south eastern US, SDGVM over-predicted Photosynthetically Active Radiation (PAR). As described above, the leaf trait regressions of Ordonez et al. (2009) were based on the New et al. (1999) dataset of downward short wave radiation, therefore these data were necessary to accurately predict leaf nitrogen according to Ordonez et al. (2009). The globally gridded downward shortwave dataset from New et al. (1999), available to download at (IPCC 2011), was used as the baseline for IMOGEN, from where it was used to drive SDGVM. Figure 6-2 shows the difference between the SDGVM calculation of downwards short wave radiation and the New et al. (1999) dataset.

The New et al. (1999) dataset provides monthly mean shortwave radiation. To smooth daily shortwave radiation from the stepped monthly values the mean preserving interpolation algorithm of Rymes and Myers (2001) was used. The algorithm uses recursive averaging to smooth the data and correction to preserve the mean. Initially the daily values within a month were set to the mean monthly values. The algorithm then cycled through each day as follows:

$$SWR_{(m\ d)i+1} = \frac{SWR_{(m\ d-1)i} + SWR_{(m\ d)i} + SWR_{(m\ d+1)i}}{3} \quad (6\text{-}10)$$

Where $SWR_{(m\,d)i}$ is the value of shortwave radiation on day *d* in month *m* and iteration step *i*. The daily data over a given month were corrected by the mean deviation from the initial monthly mean value:

$$C_m = \sum_{d=1}^{n} (SWR_m - SWR_{m\,d})/360 \quad (6\text{-}11)$$

Where C_m is the correction for month *m*, SWR_m is the original mean value of short wave radiation in month *m*, *n* is the number of days in month *m* (for SDGVM in global monthly climate mode this happens to be 30 for all months) and $SWR_{m\,d}$ are the daily values of shortwave radiation in month *m*. 360 is the total number of days in the SDGVM year. The final step of the algorithm applied the correction, C_m, to the daily values:

$$SWR_{m\,d} = SWR_{m\,d} + C_m \quad (6\text{-}12)$$

The iteration was carried out for the number of daily values in the year, in this case 360.

Global simulations

Simulations were run on a 3.75^{o} x 2.5^{o} grid. For each modified version of SDGVM a separate spin up run was conducted over 500 years. Land cover was fixed using the GLC2000 database (GLC2000 database 2003), interpreted for the SDGVM Plant Functional Types (PFTs) (Appendix B). CO_2 concentration was fixed at 28.60 Pa. All spin-ups used the 1901–1910 mean monthly precipitation, temperature and humidity of the CRU dataset (New et al. 2000). Downwards shortwave radiation was either calculated by SDGVM as a function of latitude or forced using the New et al. (1999) data, as appropriate to the configuration of the model.

Transient simulations were run from 1860–2100 forcing IMOGEN-SDGVM with historical fossil fuel and land-use change CO_2 emissions until 2010 from the CDIAC database (Boden 2011). Ten variants of the model were run to test the effects of the new leaf trait and photosynthesis schemes. The original model (SDGVM) and the new model (SDGVM-Vc) were run three times, each with no decrease in leaf nitrogen due to CO_2 (SDGVM/SDGVM-Vc none), a decrease of leaf nitrogen in grasses only (SDGVM grass/SDGVM-Vc) and a decrease

of leaf nitrogen in all PFTs (SDGVM all/SDGVM-Vc all) according to the linear equations above. Four runs were conducted with leaf trait schemes that were intermediate between the standard version of SDGVM and the modified version; two with short wave radiation calculated by SDGVM, one with the standard SDGVM nitrogen calculation and modified V_{cmax} calculation (newV) and another with both nitrogen and V_{cmax} calculated by the modified scheme (newNV) and two with the New et al. (1999) data, one with the standard SDGVM nitrogen calculation and modified V_{cmax} calculation (newSWV) and another with both nitrogen and V_{cmax} calculated by the original SDGVM scheme (newSW).

Simulations for the ten variants in model structure were conducted using the SRES A1F1 CO_2 emissions scenario (Nakicenovic et al. 2000) from 2010–2100 as we are currently following this emissions trajectory (Le Quere et al. 2009). The HadGEM1 climate patterns were used to predict climate in these runs as this represents a more up-to-date GCM version than HadCM3, the GCM pattern model used in previous IMOGEN studies (Sitch et al. 2008, Huntingford et al. 2009).

In a climate prediction uncertainty analysis SDGVM and SDGVM-Vc were run using two emissions scenarios—SRES A1F1 & B2 (Nakicenovic et al. 2000) and the patterns from six GCMs—BCCR-BCMv2.0, CSIRO-mk3.5, MPI-ECHAM5, NCAR-CCSM3.0, UKMO-HadCM3 and UKMO-HadGEM1—derived by Zelazowski et al. (2011). The GCM patterns were chosen to give a representative range of the uncertainty in prediction of temperature and precipitation change (Appendix C).

Validation data and statistics

Climate data and productivity data from Earth's major forest biomes were taken from Tables 3–5 in Luyssaert et al. (2007). Mean annual temperatures were not presented by Luyssaert et al. (2007), only mean summer and winter temperatures. Mean annual temperatures were calculated as the mean of the summer and winter temperature for the Luysseart et al. (2007) data based on the assumption that spring and autumn temperatures add little variability to the mean annual temperature. Plant biomass was calculated as the sum of aboveground and belowground biomass and due to correlation between the two, the standard deviation of the aboveground biomass was used as the standard deviation for total plant biomass.

Due to the non-normal distributions of climate data and model outputs (Appendix D), Spearman's rank correlations and partial correlations (ρ) were used to establish correlations

between climate data and model outputs. All figures relating to carbon pools and fluxes are presented in carbon units.

Results

Revised short wave radiation & photosynthetic parameters

In comparison with the New et al. (1999) dataset, SDGVM over-predicted shortwave radiation across almost all regions of the globe (Figure 6-2). Globally, SDGVM over-predicted incident shortwave radiation by 6.5 PW or 32%. Regions especially affected were most of the tropics, particularly the rainforest regions, and south eastern China. Figure 6-2 clearly shows an over-prediction of >100 Wm^{-2}, or nearly 100%, in short wave radiation over the rainforest regions of the world. The over-prediction was due to the simple cloud cover scheme adopted by SDGVM due to the complexity of data needed to accurately simulate the interaction of cloud with radiation and the importance of solar zenith angle (Kazantzidis et al. 2011) which is not applicable to a model with a daily timestep. Indeed, the New et al. (1999) data were derived using a model and appears to be low in comparison with another global calculation of incident shortwave radiation (Hatzianastassiou et al. 2005).

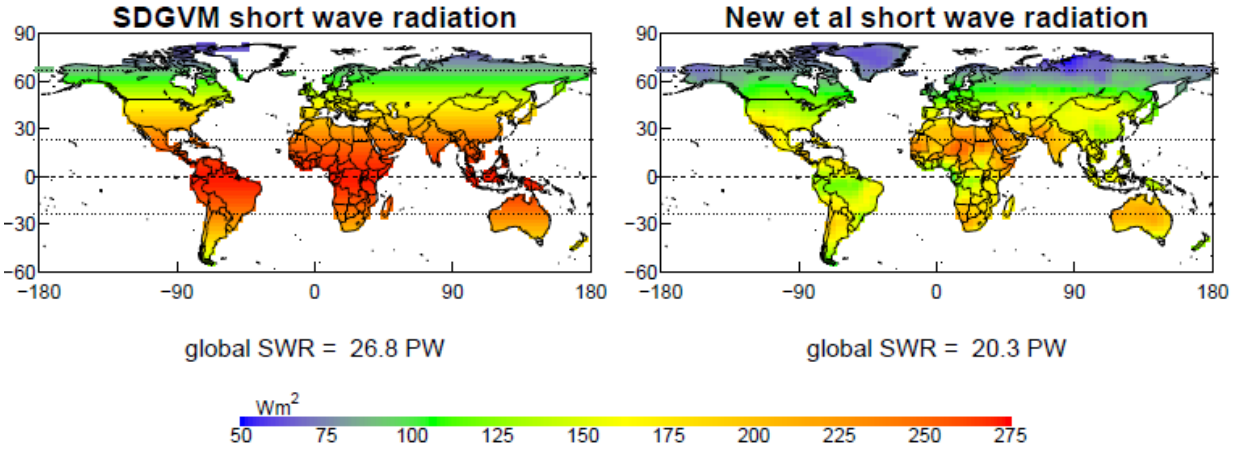

Figure 6-2. Global downwards short wave radiation as calculated by SDGVM (left) and by (New et al. 1999) (right).

However, simulation of GPP was unchanged by driving SDGVM with the New et al. (1999) dataset (124.1 Pg compared to 126.7 Pg—

Figure 6-3). The revised parameterisation of V_{cmax} and J_{max} resulted in a large increase in these variables, more so for V_{cmax}, leading to a very large increase in global GPP from 124.1 Pg to 213.4 Pg from SDGVM to newV. Simulated GPP was reduced, but only to 192.2 Pg in newSWV. The majority of the reduction in GPP was in the tropical rainforest regions where SDGVM strongly over-predicted incident short wave radiation.

No change in GPP from SDGVM to the newSW simulation (Figure 6-3) demonstrates that SDGVM was not light limited in its standard configuration. It was not possible to disentangle the effect of V_{cmax} on J_{max} and the consequent impact of J_{max} on GPP. However, the large intercept of the Wullschleger (1993) J_{max} to V_{cmax} relationship (which SDGVM uses by default) and the low values of V_{cmax} as predicted by SDGVM, meant that values of J_{max} were relatively much larger than V_{cmax} in the standard version of SDGVM than with the new parameterisations of these photosynthetic variables. Given low values of leaf nitrogen in SDGVM (Figure 6-4) and the relatively insensitive parameterisation of V_{cmax} to leaf nitrogen (low slope coefficient), it appears that V_{cmax} was limiting photosynthesis in SDGVM and newV. However, once V_{cmax} became more realistic light became an important limiting factor, particularly in the tropics.

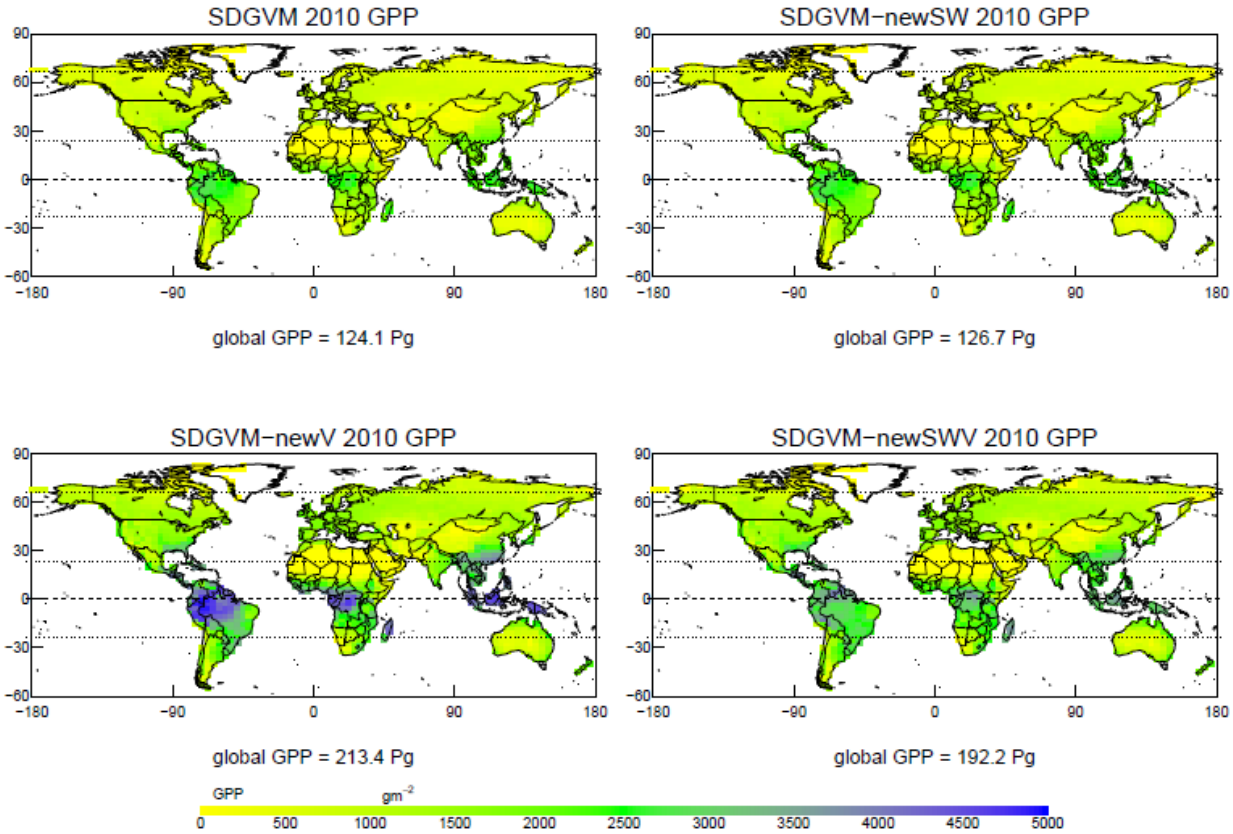

Figure 6-3. Global GPP in 2010 simulated by SDGVM in its default state (topleft); with the (New et al. 1999) shortwave radiation data (topright); with the revised relationship of V_{cmax} to leaf nitrogen and J_{max} to V_{cmax} (bottomleft) and both the revised photosynthetic parameters and the (New et al. 1999) dataset (bottomright).

Model prediction of leaf nitrogen and phosphorus

With its standard canopy nitrogen scheme, SDGVM predicted maximum top-leaf nitrogen around 1.5 gm^{-2} which compares with observations from the TRY database of mean leaf nitrogen values by biome of 1.4 to 3.1 gm^{-2} with maxima above 6 gm^{-2} (Kattge et al. 2011). As demonstrated in the previous section these low values of leaf nitrogen contributed to a large insensitivity to light of SDGVM.

Leaf nitrogen concentrations in SDGVM-Vc were increased by the trait regression method, especially in northern Russia, Scandinavia, Eastern Canada and much of the tropics, particularly Amazonia (Figure 6-4). Consequently, V_{cmax} and $J_{max}$of SDGVM-Vc were much higher in these regions although this was against a general background of increased V_{cmax} and J_{max}. Maximum top-leaf values of V_{cmax} were below 20 µmol m^{-2} s^{-1} for SDGVM, while SDGVM-Vc predicted values up to 60 µmol m^{-2} s^{-1}. The difference in J_{max} was less apparent due to the high intercept term of the Wullschleger (1993) equations (Equation 4-6) compared to the intercept used in SDGVM-Vc.

Top-leaf values of phosphorus were predicted between 0.04 and 0.2 g m^{-2} and showed similar distribution to leaf nitrogen in the temperate regions. In the tropics, leaf phosphorus was low, particularly in the Asian tropics. This had some impact on V_{cmax} predictions, lowering V_{cmax} in the tropics compared to expectations based solely on leaf nitrogen (compare south east China with the Asian tropics in Figure 6-4). Due to the lack of a global soil phosphorus map, leaf phosphorus was simulated as a function of leaf nitrogen and mean annual precipitation (Equation 6-4). Poor prediction of leaf phosphorus in the tropics was likely a result of using empirical equations that were not a function of soil phosphorus(Ordonez et al. 2009).

Prediction of current GPP, respiration and NPP

SDGVM-Vc predicted global GPP at 150 Pg C yr^{-1}, 25.8 Pg C (20.8%) higher than SDGVM (Figure 6-5). NPP was predicted at 82.1 Pg C yr^{-1} and this was 15.7 Pg C (23.6%) higher than SDGVM. Plant respiration (less canopy respiration) was 9.7 Pg C yr^{-1} (19.7%) higher in SDGVM-Vc and canopy respiration was 8.6 Pg C yr^{-1} for SDGVM and 9 Pg C yr^{-1} for SDGVM-Vc (4.7% higher than SDGVM). The predicted increase in GPP of 192.2 Pg C yr^{-1} by the newSWV simulation was far higher than that of SDGVM-Vc, the only major difference between the two model runs being that nitrogen in SDGVM-Vc was calculated using the trait regression.

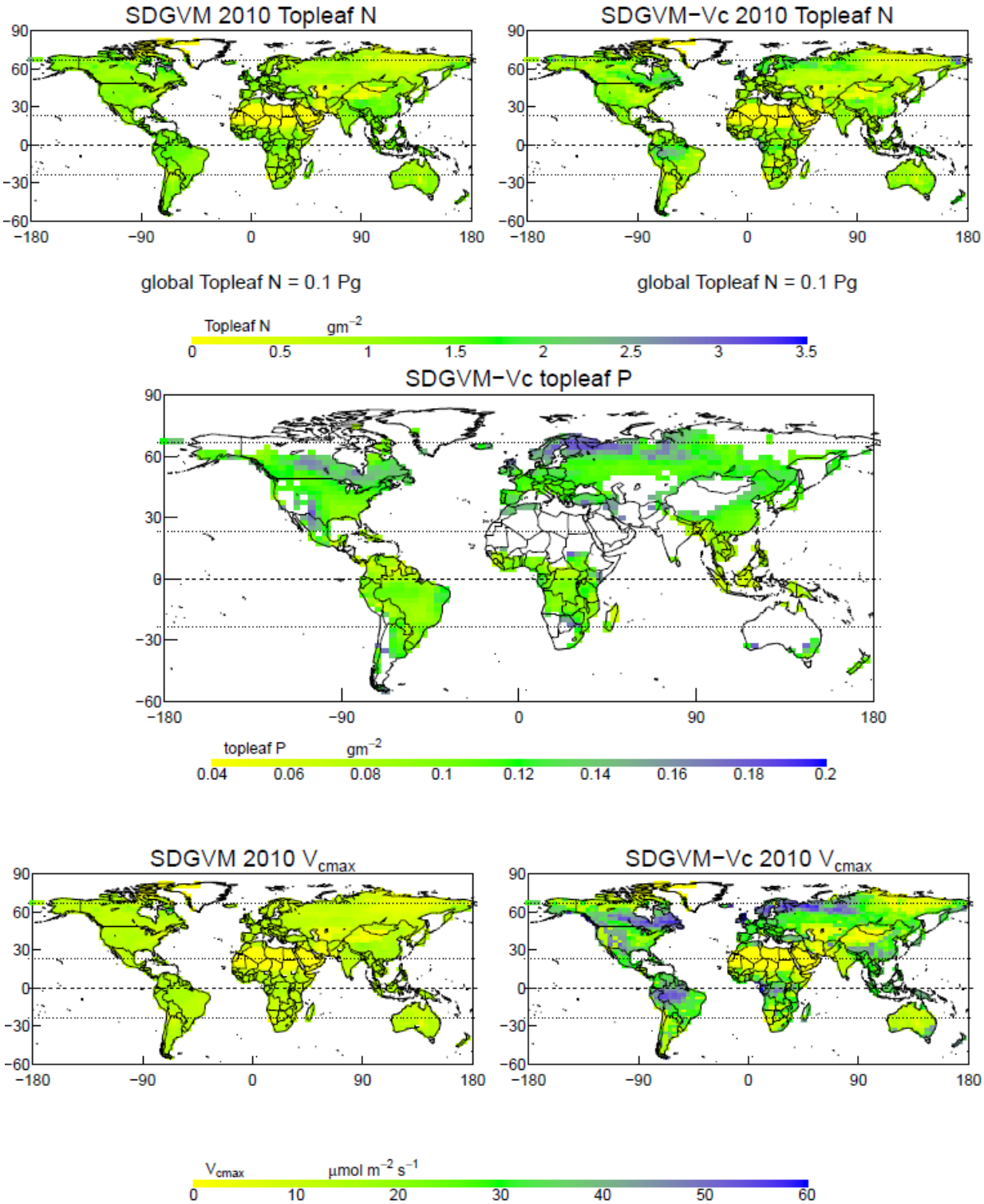

Figure 6-4. Global values of topleaf nitrogen (top panels), topleaf phosphorus (centre panel) and J_{max} (bottom panels) as predicted in 2010 by SDGVM in its standard form (left panels) and with the revised parameterisation determined in Chapter 4 (right panels). Values are annual means for the top leaf and V_{cmax} values are at 25°C and are not adjusted for leaf age or soil water stress. Missing values of leaf phosphorus are because SDGVM has no default method to calculate leaf phosphorus.

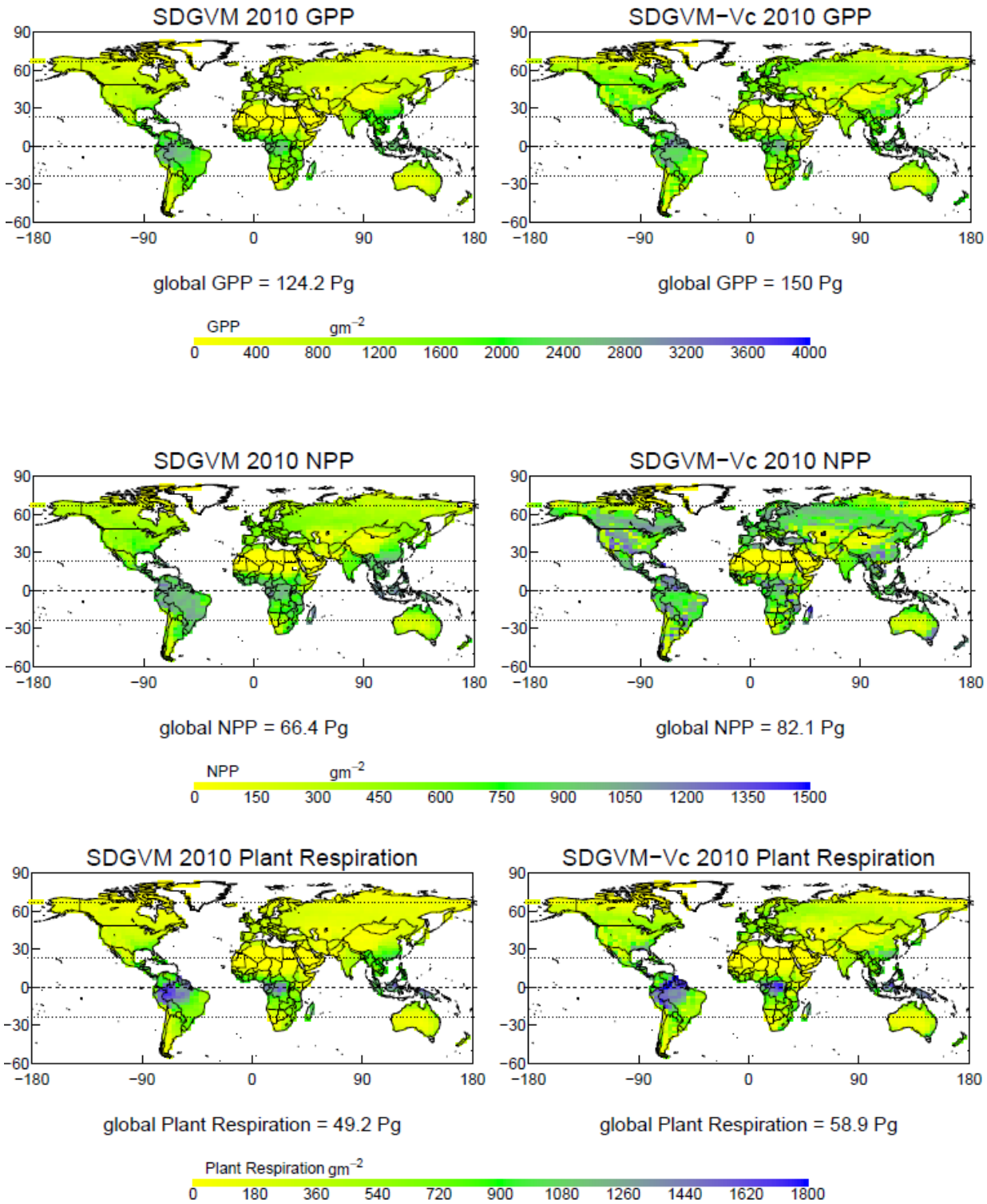

Figure 6-5. Predictions of GPP (upper panels), NPP (middle panels) and plant respiration (not including canopy night time respiration—lower panels) in 2010 by SDGVM (left panels) and SDGVM-Vc (right panels).

SDGVM optimises carbon gain by incrementing maximum LAI up or down based on the carbon balance of the previous year's lowest leaf layer. In the light limited lower canopy, high nitrogen causes higher respiration without increasing assimilation and therefore decreases the optimal LAI. LAI was significantly lower in the tropics for SDGVM-Vc compared with newSWV (Appendix F) and therefore GPP was lower for SDGVM-Vc, mainly in the tropics.

Projections of CO_2 increase

The various versions of the model predicted atmospheric CO_2 concentrations in 2010 with a range from 377–405 µmol mol^{-1} (Figure 6-6). SDGVM predicted atmospheric CO_2 at the lower end of the range with 385 µmol mol^{-1} while SDGVM-Vc predicted CO_2, at the highest value of all the model versions, at 405 µmol mol^{-1}. By 2100 the predicted range was from 987–1155µmol mol^{-1} with SDGVM predicting 992µmol $mol^{-1}$and SDGVM-Vc 1155 µmol mol^{-1}. All the SDGVM-Vc runs were similar in their predictions of CO_2 concentrations as were all of the SDGVM runs until a third of the way into the 20th century where SDGVM (with no down-regulation of nitrogen) began to sequester CO_2 at a greater rate than all of the other models.

The insets in Figure 6-6 show that all the models with the new nitrogen calculation scheme were in the upper range of predicted CO_2 values indicating that canopy nitrogen was a major driver of net CO_2 exchange. Contrary to expectations, higher canopy nitrogen led to decreased sequestration of carbon by terrestrial vegetation (and this is discussed below). Variability within the range of predictions from models using the same nitrogen scheme was caused by the different radiation fields (inset Figure 6-6). As expected, the higher predictions of incident short wave radiation by SDGVM caused greater draw-down of carbon by global vegetation than the New et al. (1999) radiation fields. Despite much greater values of GPP in the newV simulations (

Figure 6-3), predicted CO_2 increase by newV was very similar to that of SDGVM indicating that autotrophic and heterotrophic respiration were largely driven by GPP and that there may be a maximum rate of CO_2 drawdown, a rate largely independent of GPP and dependent upon the internal structure and parameterisation of the model. Key determinants within the model would be parameters and structure that influence residence times of carbon such as the fractions of live biomass required for maintenance respiration and the minimum biomass increment of the self-thinning algorithm.

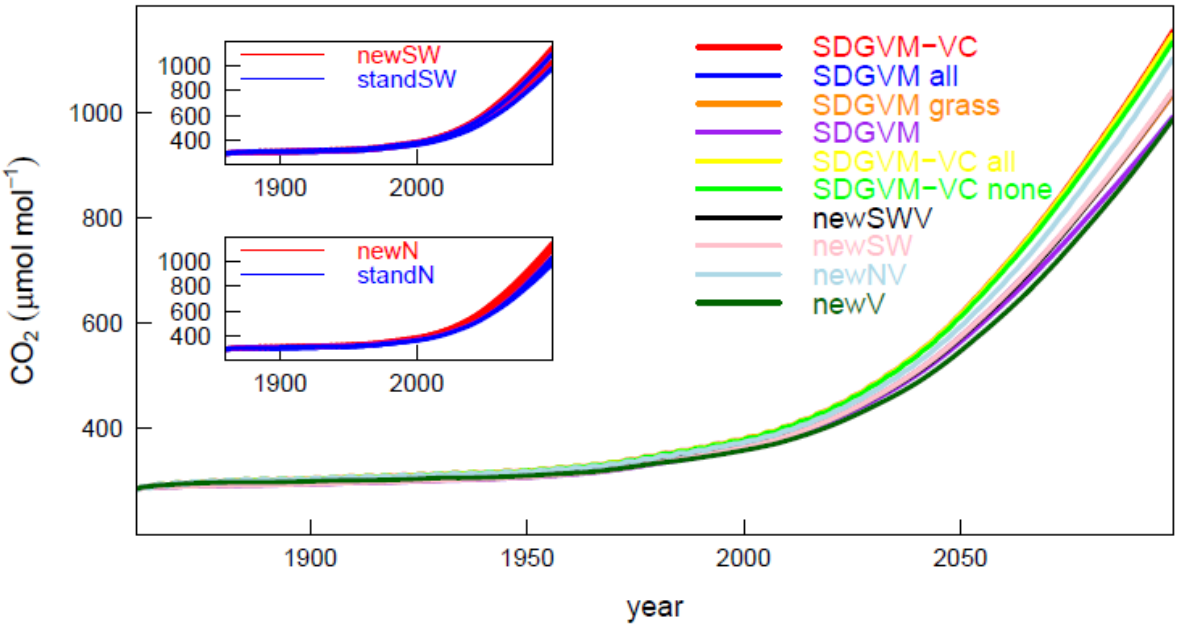

Figure 6-6. CO_2 increase from 1860–2100 as predicted by IMOGEN and various configurations of SDGVM driven with the A1F1 emissions scenario and Had-GEM1 climate change patterns. CO_2 trajectories in the main panel are coloured by model configuration. Trajectories in the inset are coloured by model configuration, the upper panel showing models that use the standard short wave radiation calculation and the (New et al. 1999) dataset and the lower panel showing models that use the default leaf nitrogen calculation and the revised leaf nitrogen calculation (newN). Hidden by the other lines, the black (newSWV), orange (SDGVM grass) and blue (SDGVM all) lines lie under the pink line (newSW).

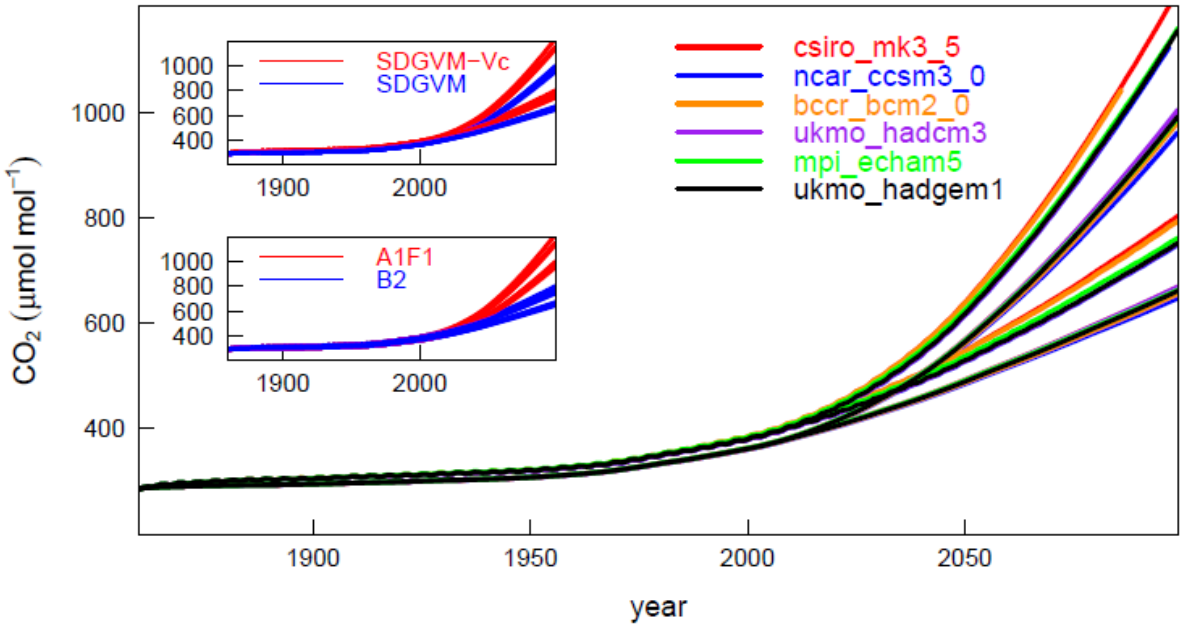

Figure 6-7. CO_2increase from 1860–2100 as predicted by IMOGEN and either SDGVM or SDGVM-Vc. Simulations were driven with either the A1F1 or the B2 emissions scenario and the climate change patterns from 6 GCMS. CO_2 trajectories in the main panel are coloured by the GCM pattern. Trajectories in the inset are coloured by model and emissions scenario.

Table 6-1. Mean and range of predicted atmospheric CO_2 in 2100 by model version and emissions scenario.

model	Emissions Scenario	mean	range
SDGVM	A1F1	988	42
	B2	661	22
SDGVM-Vc	A1F1	1182	74
	B2	768	55

The CO_2 emissions scenario was the main determinant of variability in predictions of CO_2 increase in the uncertainty ensemble. The ensemble predicted mean CO_2 (±1SD) in 2100 at 1052 ± 100 µmol mol^{-1} for the A1F1 scenario and 714 ±59 µmol mol^{-1} for the B2 scenario. When analysed by model, mean CO_2 was 824 ±171 µmol mol^{-1} for SDGVM and 905 ±209 µmol mol^{-1} for SDGVM-Vc,

Biomass accumulation

Carbon in grass and crop biomass has a shorter residence time than in trees and as expected, plant biomass was higher at sites dominated by tree PFTs across all years of the simulation (Figure 6-8). Sites dominated by grass PFTs showed little change in biomass over the years of the simulation. For this reason, most of the following results and discussion focus on sites dominated by tree PFTs.

Due to higher GPP, SDGVM-Vc simulated global plant biomass 337 Pg higher than SDGVM, putting the predictions of SDGVM-Vc outside the range of global vegetation carbon stocks estimated by (Houghton et al. 2009) (Table 6-2) and approaching three times the global forest carbon stock estimate of the Global Forest Resource Assessment (GFRA—FAO 2010). SDGVM-Vc simulated biomass 50 Pg higher than SDGVM in the tropics putting SDGVM-Vc outside the estimated range of Houghton et al. (2009) and again far higher than the GFRA estimate, while SDGVM was at the upper end of the Houghton et al. (2010) and Saatchi et al. (2011) estimates but 50% higher than the GFRA estimate.

Most of the difference in biomass prediction between the two models was in the northern latitudes (>45^{o} latitude) where SDGVM-Vc predicted vegetation biomass 212 Pg higher than SDGVM. The prediction of biomass in the northern latitudes by SDGVM-Vc was over 250 Pg higher than GFRA and McGuire et al. (2010) estimates of biomass in northern latitudes (Table 6-2).

High northern latitude biomass in SDGVM-Vc was a consequence of higher leaf nitrogen, V_{cmax} and therefore productivity. The over-prediction of northern latitude biomass by SDGVM-Vc yet reasonable simulation by SDGVM supports the negative feedback on plant nitrogen caused by increasing organic soil carbon (Woodward et al. 1995). However, leaf nitrogen values of SDGVM-Vc in the north were similar to those of Kattge et al. (2009)suggesting that the soil carbon feedback on plant nitrogen in SDGVM may be misrepresenting stoichiometric nitrogen limitation with photosynthetic nitrogen limitation. Also at these northern sites SDGVM and SDGVM-Vc inaccurately simulate the respiration fraction of GPP and this is discussed below.

The relationship of biomass to productivity

For tree sites, simulated biomass was shown to increase in a linear fashion with GPP (Figure 6-9) and the sensitivity of the relationship in the SDGVM-Vc simulation varied by PFT, particularly for evergreen broadleaved trees. Biomass also followed a linear trend with NPP for both simulations. The different relationships between biomass and GPP across PFTs in the SDGVM-Vc simulation was not apparent in the relationships of biomass to NPP, indicating that it was differences in plant respiration which accounted for the variation in relationships to GPP. Causes of variability in PFT respiration will be discussed below. Biomass in SDGVM (and SDGVM-Vc etc) is the result of flows into the biomass pool, namely NPP, and flows out of the biomass pool by mortality. Therefore steady-state biomass is determined by the simple equation:

$$B = NPP \times MRT$$

where *B* is biomass and *MRT* is the mean residence time of the biomass pool in question. Wood biomass is the major biomass pool due to the long MRT compared with that of leaves and roots (in SDGVM only fine roots are considered roots) and the MRT of wood is determined by wood mortality. In SDGVM wood mortality is caused by age and self thinning (described in Chapter 1).

An increase in NPP will lead to a new equilibrium biomass and that was demonstrated by the linear trend of simulated biomass to NPP. The global, linear trend suggests that NPP was the main driver of biomass at a site and was more important than tree height and density in determining equilibrium biomass. Over the years of the simulation, the response of biomass

to NPP did not appear to saturate although there did appear to be a drop in biomass at some evergreen needleleaved sites by 2100 (Figure 6-9 & Figure AE-1).

Table 6-2.Estimates and predictions of vegetation carbon pools. All values are in Pg C and except where stated are for above and below ground biomass. Unless stated, estimated values are for tree/forest biomass only while simulated values are for the sum of forests, grasslands and croplands. Values in parentheses in the tropics are for Amazonia only. * – values for temperate and boreal forests, and boreal forests only in square brackets; † – Northern hemisphere value; ‡ – cryosphere values (>50° in the Americas and >45° in Europe and Asia) including non-tree biomass; ₣ –values are for aboveground biomass only. Data from Goodale et al. (2002), Malhi et al. (2006), Houghton et al. (2009), McGuire et al. (2010) and Saatchi et al. (2011). Goodale et al. (2002) and McGuire et al. (2010) provide values for northern latitudes and Europe while Malhi et al. (2006) and Saatchi et al. (2011) provide values in the tropics.

Region	Estimate				Model	Year					
	GFRA	Houghton	Saatchi/ Goodale	Malhi/ Mcguire		2000	1860	2100	change	Model difference	Change in last decade
Tropics	203 (74)	175-340	222-271 (105-134)	(83-92) ₣	SDGVM	294 (145)	243 (121)	441 (202)	198 (81)		7 (0)
					SDGVM-Vc	344 (167)	311 (150)	412 (197)	101 (47)	97 (34)	0 (-4)
North	79	63-195 [55]*	90†	60-70 ‡	SDGVM	115	95	182	77		6
					SDGVM-Vc	327	290	383	93	-16	-5
Europe	11	na	8.7		SDGVM	45	39	49	10		-2
					SDGVM-Vc	120	113	81	-32	42	-10
Globe	293	387-650			SDGVM	484	402	733	331		16
					SDGVM-Vc	821	742	952	210	121	-6

With notable exceptions, the simulated biomass to GPP or NPP relationships compared well with a comprehensive observed dataset (Luyssaert et al. 2007) of carbon pools and fluxes across the global range of forest biomes (Figure 6-9). The standard deviation of the observations for each biome was far higher for biomass than for GPP or NPP suggesting that although a global relationship between biomass and GPP and NPP may exist, there are likely to be more important factors affecting biomass variability within a particular biome. The biomass data also compared well with the dataset of Keeling and Phillips (2007). Keeling and Phillips (2007) show a hump-backed, quadratic relationship between biomass and NPP while for SDGVM the relationship is linear. However, the maximum biomass of the Keeling and Phillips (2007) relationship is at NPP values around 2400 gm^{-2} and the maximum NPP simulated by SDGVM is around 1500 gm^{-2}; the Keeling and Phillips (2007) relationship is similar to the SDGVM relationship for values of NPP up to 1500 gm^{-2}.

In comparison with global FLUXNET data, SDGVM-Vc over-predicted tropical GPP. However, in comparison with the Luyssaert et al. (2007) dataset both SDGVM and SDGVM-Vc under-predicted GPP and over-predicted the biomass response to GPP of evergreen broadleaved trees in comparison with observations of the tropical humid evergreen biome. Both models over-estimated NPP for tropical humid evergreen forests. Other evergreen biomes of Luyssaert et. al. (2007)—temperate semi-arid evergreen and Mediterranean evergreen—are not categorised as broadleaved evergreen by GLC2000 (Appendix B) but observations for these biomes did fall within the overall spread of simulated data.

SDGVM under-predicted GPP and was in the lower range of NPP and biomass observations for deciduous needleleaf forest (boreal semiarid deciduous in the Luyssaert et al. 2007 classification), while SDGVM-Vc fell within the observed range of GPP but over-predicted biomass and NPP. As with sites predominantly composed of the tropical evergreen PFT, the ability to capture only GPP or NPP suggested a misrepresentation of respiration for deciduous needleleaf sites. That deciduous needleleaf biomass and NPP were accurately simulated by SDGVM was demonstrated by Quegan et al. (2011) and their estimates are similar to those of Luyssaert et al. (2007). However, Quegan et al. (2011) do not present estimates of GPP and it may be that SDGVM was capturing NPP and biomass at the expense of accurate GPP simulation.

Evergreen needleleaves were represented by three of the biome classifications of Luyssaert et al. (2007)—boreal humid evergreen, boreal semiarid evergreen and temperate humid evergreen. SDGVM predicted the range of GPP and NPP at these sites well and captured the low biomass of the boreal sites, however biomass was predicted below the observed mean. On the other hand SDGVM-Vc reasonably captured GPP and biomass for the temperate evergreens (somewhat over-predicting NPP) but strongly over-predicted biomass, NPP and GPP of the boreal sites.

Both SDGVM and SDGVM-Vc simulated a strong linear dependence of the fraction of GPP allocated to autotrophic respiration on mean annual temperature, and the relationship was invariant across PFTs (Figure 6-10) i.e. the temperature sensitivity of RuBisCO kinetic parameters did not offset the increase in respiration due to temperature. Maintenance respiration (of root and stem biomass) is simulated as a fraction of live biomass (invariant across PFTs) and temperature. Canopy maintenance respiration is simulated as a function of

canopy nitrogen. Canopy respiration was a smaller fraction of overall respiration and hence the strong global relationship of the respiration fraction of GPP to temperature was expected.

As indicated by the Luyssaert et al. (2007) data in Figure 6-9, respiration was not accurately simulated for boreal or tropical evergreen forests. In particular, the fraction of GPP allocated to respiration was inaccurate, highlighted in the boreal zone by the ability of SDGVM to accurately simulate biomass while over-predicting NPP and under-predicting GPP. The comparison of the respiration fraction of GPP as a function of temperature shows that both versions of the model strongly under-predicted the respiration fraction of GPP at cold boreal sites, especially the semi-arid and deciduous sites (Figure 6-10).

Both models under-predicted GPP for the tropical evergreen humid sites of Luyssaert et al. (2007) yet over-predicted NPP. Figure 6-10 shows that the respiratory fraction of GPP was under-predicted by both models but not as severely as at arid boreal sites. However, there were a number broadleaved evergreen sites where it appears that the general respiratory fraction to temperature relationship of the model did not apply and it was these sites where NPP was most strongly over-predicted. Even the revised photosynthesis parameterisation of SDGVM-Vc could not predict GPP observed by Luyssaert et al. (2007). Given the relatively slight reduction necessary for models to meet NPP observations and reasonable prediction of biomass, the measured GPP of Luyssaert et al. (2007) may be high. Indeed, their estimate of the mean at 3551 g C $m^{-2}yr^{-1}$appears to be high when compared with other estimates of GPP from FLUXNET data (Beer et al. 2010, Bonan et al. 2011b, Jung et al. 2011). The measurement scales are different between Luyssaert et. al. (2007) and Jung et. al. (2011) and the coarser resolution of the global grid generated by Jung et. al. (2011) would lead to reduction of high point-values of GPP. Despite this the mean Luyssaert et. al. (2007) value of 3551 g C m^{-2} yr^{-1} seems high.

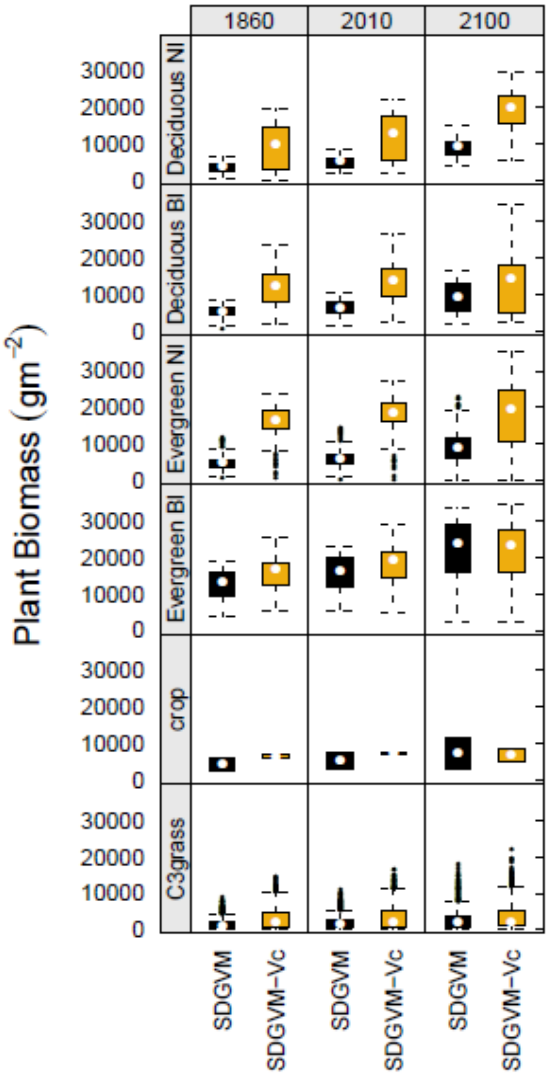

Figure 6-8.Distribution of plant biomass simulated by SDGVM and SDGVM-Vc broken down by PFT dominance and simulation year.

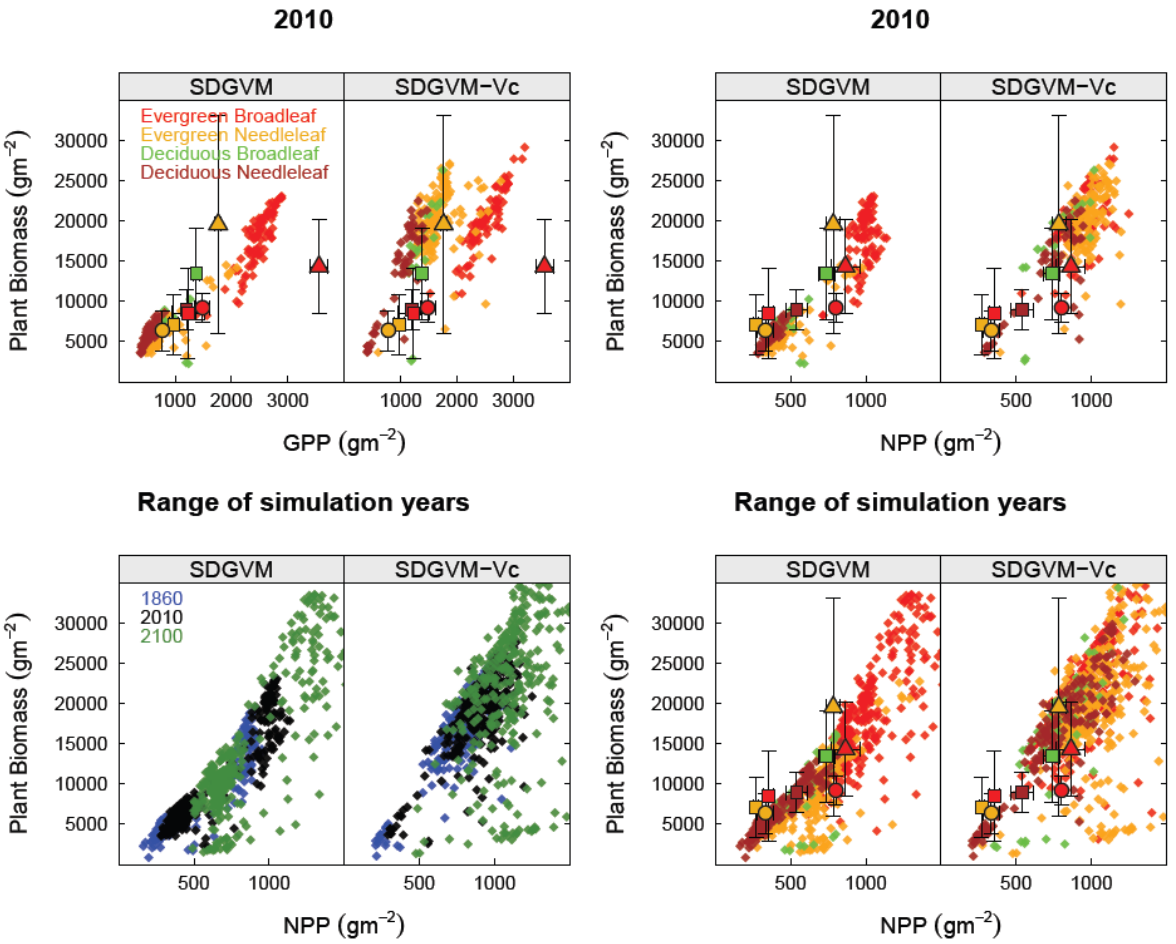

Figure 6-9.The relationship of plant biomass to GPP (topleft plots) and NPP (other 3 plots) for SDGVM and SDGVM-Vc in 2010 (top panels) and 1860, 2010 and 2100 (bottom panels). Data are taken from sites dominated by tree PFTs and are colour coded by SDGVM PFT (based on phenology and leaf type). Superimposed on the plots are observed data (mean ±1SD) for various biomes from (Luyssaert et al. 2007) colour coded by SDGVM PFT, symbols represent the biome—boreal humid evergreen (yellow squares), boreal semiarid evergreen (yellow circles), boreal semiarid deciduous (brown squares), temperate humid evergreen (yellow triangles), temperate humid deciduous (green squares), temperate semiarid evergreen (red squares), Mediterranean evergreen (red circles) and tropical humid evergreen (red triangles).

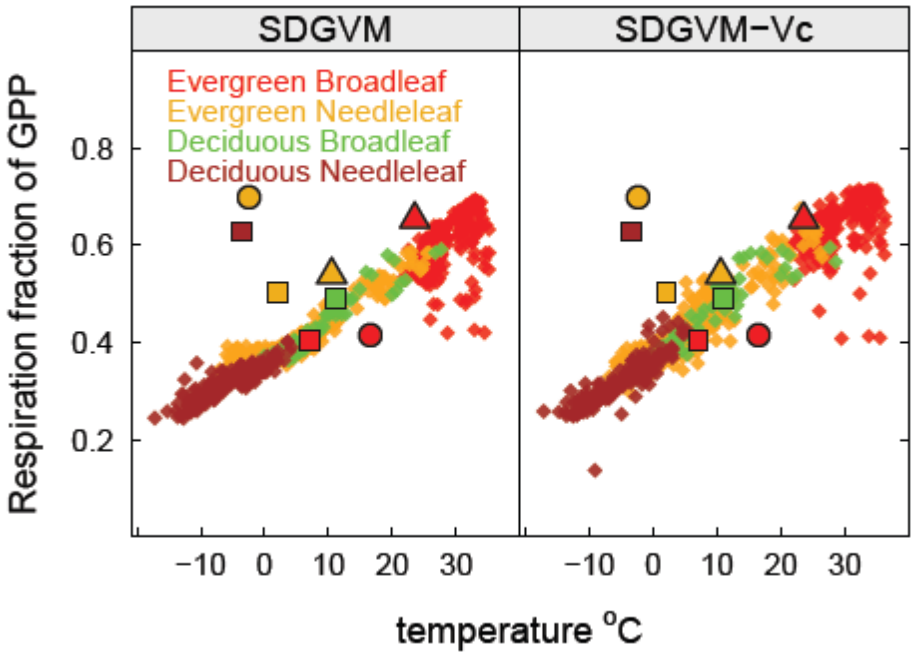

Figure 6-10. Respiration as a fraction of GPP, broken down by PFT, as simulated by SDGVM and SDGVM-Vc. Superimposed on the plots are observed data (mean) for various biomes from (Luyssaert et al. 2007) colour coded by SDGVM PFT, symbols represent the biome—boreal humid evergreen (yellow squares), boreal semiarid evergreen (yellow circles), boreal semiarid deciduous (brown squares), temperate humid evergreen (yellow triangles), temperate humid deciduous (green squares), temperate semiarid evergreen (red squares), Mediterranean evergreen (red circles) and tropical humid evergreen (red triangles).

By 2100 both models showed a large, and similar, increase in broadleaf evergreen biomass and while both models showed an increase in deciduous needleleaf vegetation biomass, SDGVM-Vc showed a larger increase (Figure 6-8). The increase in deciduous needleleaf biomass in both models was due to increased NPP arising from increased growing season length and higher CO_2. At evergreen needleleaf and deciduous broadleaf sites biomass increased from 1860 to 2010 for SDGVM-Vc but not between 2010 and 2100 (although the upper quartile increased for evergreen needleleaf forests) while the opposite was the case for SDGVM. All increases in biomass were also associated with increases in the range in biomass such that the first biomass quartile only increased between 1860 and 2100 for deciduous boreal forests and actually decreased for evergreen broadleaved forests. These predictions suggest that deciduous boreal sites and tropical evergreen sites will be the strongest carbon sinks for atmospheric CO_2 over the coming century although the high land area occupied by evergreen needleleaved forests means that they will also be an important

sink. Deciduous boreal biomass increases were due to increases in growing season length and although the respiration fraction of GPP compared poorly with the Luyssaert et al. (2007) database, GPP prediction by SDGVM-Vc was reasonable and with a revised respiration scheme would still predict increases in biomass.

The increase in biomass by 2100 of evergreen needleleaf trees was within one standard deviation of the mean biomass for temperate humid evergreen forests in Luyssaert et al. (2007) (Figure 6-9) suggesting that the predicted increases were possible. By contrast, some evergreen broadleaved sites were predicted to increase biomass by over two standard deviations from the Luyssaert et al. (2007) mean.

Global biomass trends

There was a steadily increasing trend in vegetation biomass over the course of the SDGVM simulation (Figure 6-11). Rates of biomass accumulation were slower in the SDGVM-Vc simulation but SDGVM-Vc started from higher biomass in 1860, leading to higher plant biomass in a given simulation year than SDGVM. Higher initial biomass was due to higher rates of photosynthesis in the spin-up, resulting from the higher values of V_{cmax} and J_{max}.

Biomass in both simulations increased with increasing CO_2 concentration, and began to saturate at high CO_2. Biomass increased proportionally with GPP, shown by their linear relationship (Figure 6-11), and saturation of biomass in response to CO_2 was likely due to the saturation of the CO_2 effect on photosynthesis, hence GPP. However, for the SDGVM-Vc simulation, the relationship between biomass and GPP was not completely linear. There was some variability in the response caused by an oscillation in grass growth and mortality (Appendix G). More interestingly, global biomass response to GPP showed some saturation at values around 950 Pg (Figure 6-11).

Saturation of biomass accumulation in SDGVM-Vc was not a consequence of feedback at higher rates of GPP as both SDGVM and SDGVM-Vc approached 180 Pg yr^{-1} GPP towards the end of the simulation. Global biomass did not saturate, even at 1100+ Pg for the newSWV simulation. In the last decade of the SDGVM-Vc simulation, global biomass began to decrease, despite a continued increase in GPP. As discussed above, the determinants of simulated biomass in 2010 were NPP as calculated by GPP and the respiratory fraction of GPP which was a function of temperature. NPP in 2100 was generally higher due to high CO_2 and biomass maintained a linear relationship with NPP at these higher values of NPP.

However, there were sites with much lower biomass than expected by their NPP (Figure 6-9—note in the lower plots the sites with biomass below 10,000 gm^{-2} and NPP over 1,000 gm^{-2}).

These, predominantly evergreen needleleaf, sites appear to have suffered mortality events which strongly reduced biomass. These sites were European and the loss in biomass towards the end of the SDGVM-Vc simulation was wholly attributable to a dieback of European forest (Table 6-2), particularly in Scandinavia (Appendix E). Similar mortality events appear to have occurred by 2100 with SDGVM (Figure 6-9) although their impact was not detected globally (Figure 6-11) probably as a result of their lower NPP and hence lower biomass 'expected' by the linear biomass to NPP relationship (Figure 6-9). The Scandinavian dieback was likely due to strong decreases in precipitation predicted by the Had-GEM1 model (Appendix C).

The CO_2 concentration at which SDGVM-Vc stopped accumulating and began to lose plant biomass indicates a 'tipping-point' where biomass accumulation became de-coupled from the CO_2 response of GPP, possibly readjusting to a new relationship. However, given the locality of the dieback in Scandinavia and that the majority of the region's biomass was lost by 2100, the biomass decrease may not continue unless dieback was triggered in another region. Had-GEM1 predicts a strong drying of the Amazon and there was a hint of the initial stages of Amazon dieback, a subject of much previous study (Cox et al. 2000, Huntingford et al. 2004, Huntingford et al. 2008), in SDGVM-Vc and a levelling of the Amazonian biomass increase in SDGVM (Table 6-2).

Soil respiration

In addition to lower rates of biomass accumulation in SDGVM-Vc, soil carbon decreased by the end of the SDGVM-Vc simulation. SDGVM predicted soil carbon in 1860 at 1364 Pg and in 2100 at 1494 Pg, a net gain of 130 Pg carbon; while SDGVM-Vc predicted soil carbon in 1860 at 1966 Pg and in 2100 at 1800 Pg, a net loss of 166 Pg. By the end of the simulation, the difference between the two models in soil carbon sequestration was 296 Pg, more than double the differences in plant biomass sequestration. Predicted soil carbon stocks by SDGVM-Vc were higher than early estimates by Post et al. (1982) who placed global soil carbon at 1395 Pg although the upper limit of their cited 'intermediate' range was 2070 Pg.

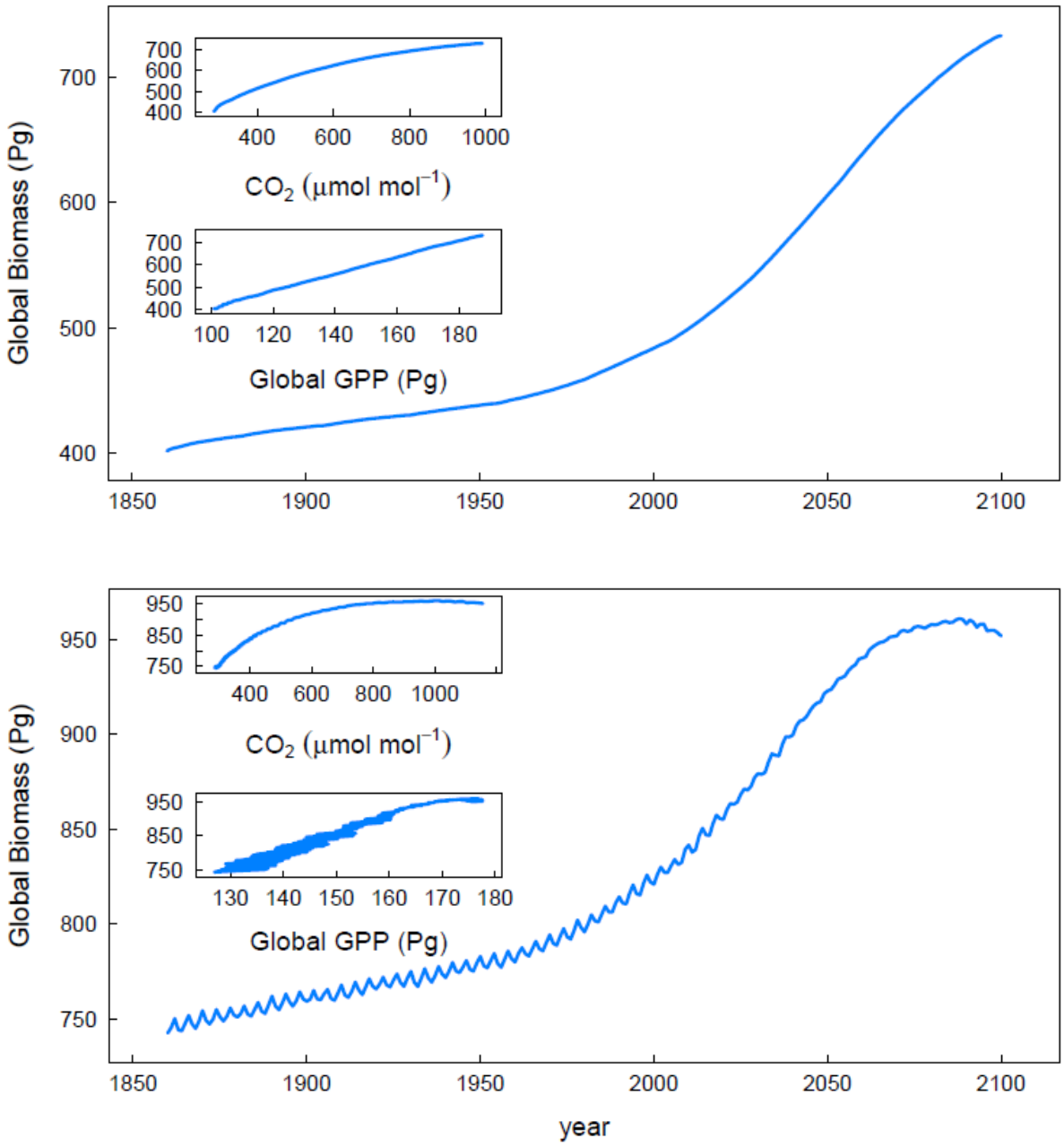

Figure 6-11. Global biomass trend in Pg C for SDGVM (upper) and SDGVM-Vc (lower) over the course of the simulation (main plot). The relationship of global biomass to atmospheric CO_2 concentration over the period (inset top) and the relationship of global biomass to global GPP over the period (inset bottom). Note the difference in scale of the y-axis.

More recently, McGuire et al. (2010) placed an estimate of soil carbon in the northern cryosphere alone at 1400–1850 Pg. The highest values of soil carbon predicted by SDGVM-Vc were in northern regions and reached 50 kg C m^{-2} which were more than double the highest values measured by Lindroth et al. (2008) in Swedish Spruce forest. However, a recent UNEP estimate of global carbon distribution suggests that maximum values of soil carbon are between 30–105 kg C m^{-2} and show a distribution similar to that of SDGVM-Vc (Scharlemann et al. 2010).

The loss of soil carbon in SDGVM-Vc was due to generally higher rates of soil respiration at a given GPP (Figure 6-12). Figure 6-12 shows that there was no obvious difference in the relationship of soil respiration to the soil carbon pool (on a log-log basis) between the two models and the reason for higher soil respiration rates was simply a matter of higher soil carbon at sites dominated by tree PFTs. It appeared that higher biomass in SDGVM-Vc was leading to higher soil carbon pools. However, the newSWV simulation had higher biomass than SDGVM-Vc yet maintained lower values of atmospheric CO_2 which indicated that the trait regression for simulating canopy nitrogen must have affected soil respiration. Correlation analysis showed that for tree dominated sites SDGVM and newSWV had a negative correlation between plant biomass and soil carbon and that this correlation was removed by SDGVM-Vc (Figure 6-13). The trait regression of SDGVM-Vc removed the negative feedback of plant biomass on soil carbon in SDGVM, leading to higher soil respiration at high biomass, tree dominated sites and causing increased rates of atmospheric CO_2 accumulation.

Plant biomass and soil respiration were decoupled in SDGVM-Vc but not SDGVM nor newSWV due to the decoupling of leaf nitrogen from organic soil carbon in SDGVM-Vc. In SDGVM high soil carbon decreases plant nitrogen uptake (Woodward et al. 1995) leading to decreased rates of photosynthesis which reduces GPP and hence biomass, according to the relationship in Figure 6-9, and therefore reducing soil carbon inputs. A negative feedback loop exists between plant biomass and soil biomass. Using trait regression decoupled this feedback, allowing plant biomass to increase, leading to higher soil carbon at sites where plant biomass was a driver of soil carbon. This in turn led to the higher soil respiration rates in SDGVM-Vc and consequent higher rates of rising atmospheric CO_2. It was likely that the increased rates of soil respiration leading to greater rates of CO_2 increase and concomitant climate change was the factor restricting plant biomass accumulation in SDGVM-Vc.

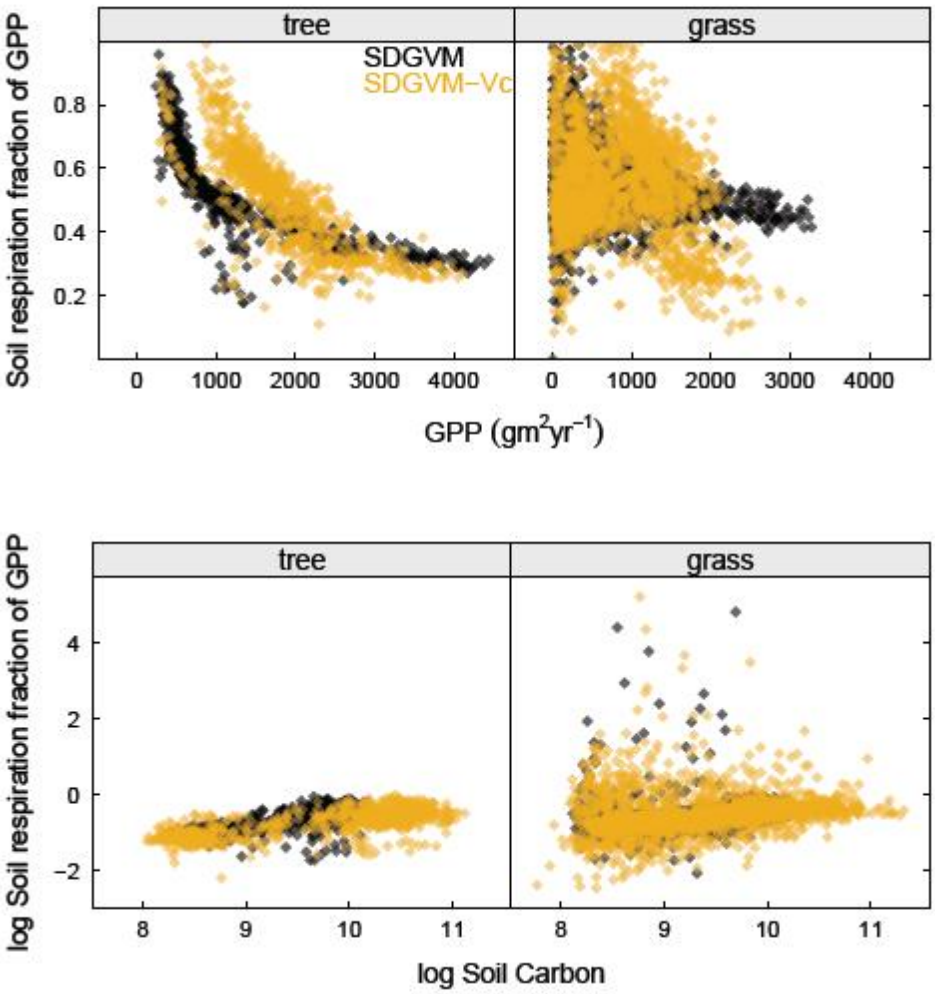

Figure 6-12. Soil respiration as a fraction of GPP in relation to GPP (top panels), and the log-log relationship to soil carbon (bottom panels) for tree and grass dominated sites; as predicted by the SDGVM and SDGVM-Vc simulations.

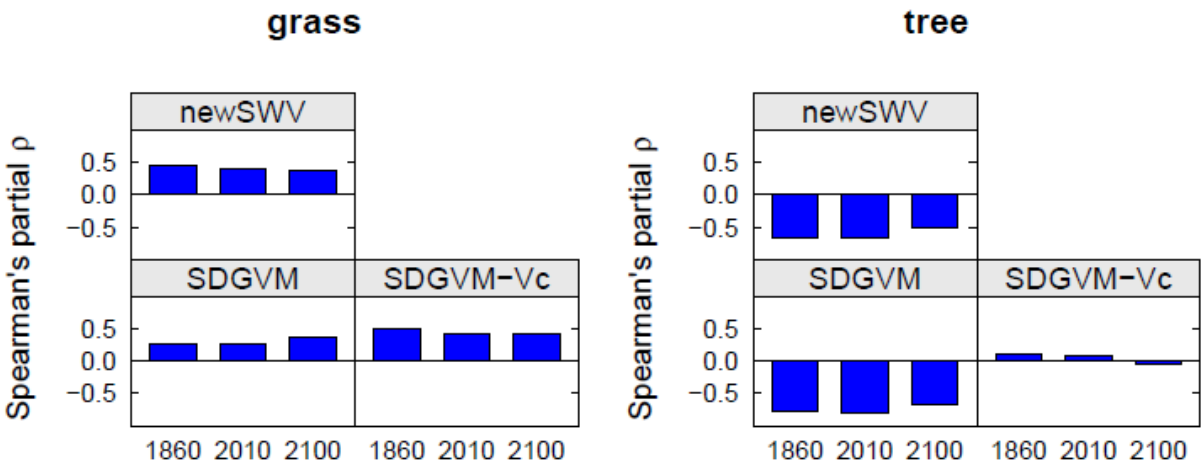

Figure 6-13. Spearman's rank correlation coefficients (ρ) between vegetation biomass and soil carbon for grass dominated sites (left panels) and tree dominated sites (right panels) for the SDGVM, SDGVM-Vc and newSWV simulations and across three simulation years.

Drivers of GPP and plant respiration

LAI was strongly correlated with NPP and GPP. As mentioned above, LAI is adjusted by SDGVM to optimise NPP and therefore carbon fluxes, GPP and NPP, and LAI are highly correlated. For this reason LAI was left out of driving variable analyses.

There were differences between PFT growth habit, either tree or grass/crop, and the response of GPP to driving variables (Figure 6-14). For SDGVM, Spearman's rank partial correlation showed that GPP of grasses and crops was most strongly correlated to precipitation with no changes in correlations over the years of the experiment. Tree GPP was most strongly correlated with temperature and to a lesser extent, leaf nitrogen. The strong correlation to temperature at tree dominated sites suggests that growing season was more important than annual precipitation. In contrast to grasses, the correlation to all driving variables analysed increased over the course of the simulation. In particular, the correlation to top-leaf nitrogen and short wave radiation increased in proportion to temperature indicating the increasing importance of the photosynthetic response.

Grasses occupy regions of the planet with lower rainfall than trees and it could be supposed that the difference between the correlations of the two growth habits was due to grasses occurring only at sites where water limitation was important. However, separation of sites into wet and dry, using a rainfall cut-off at 500 mm yr^{-1} demonstrated somewhat different correlations to the tree and grass habits respectively. As expected, for low precipitation sites GPP was strongly correlated to precipitation with top-leaf nitrogen also showing high correlations ($\rho>0.5$), for wet sites GPP was still strongly correlated with precipitation but shortwave radiation and temperature showed similar correlations.

When analysed for SDGVM-Vc, tree growth habit showed very similar correlations of GPP to driving variables as SDGVM. Grass dominated sites were still strongly correlated to precipitation but top-leaf nitrogen also showed strong correlation and top-leaf nitrogen was the strongest correlate of GPP across the wet sites of SDGVM-Vc. Maintenance respiration was shown to be mostly driven by GPP although other driving variables were significant (Appendix H). However, and as shown above (Figure 6-10), the proportion of GPP that was maintenance respiration increased as a linear function of temperature for the tree growth habit.

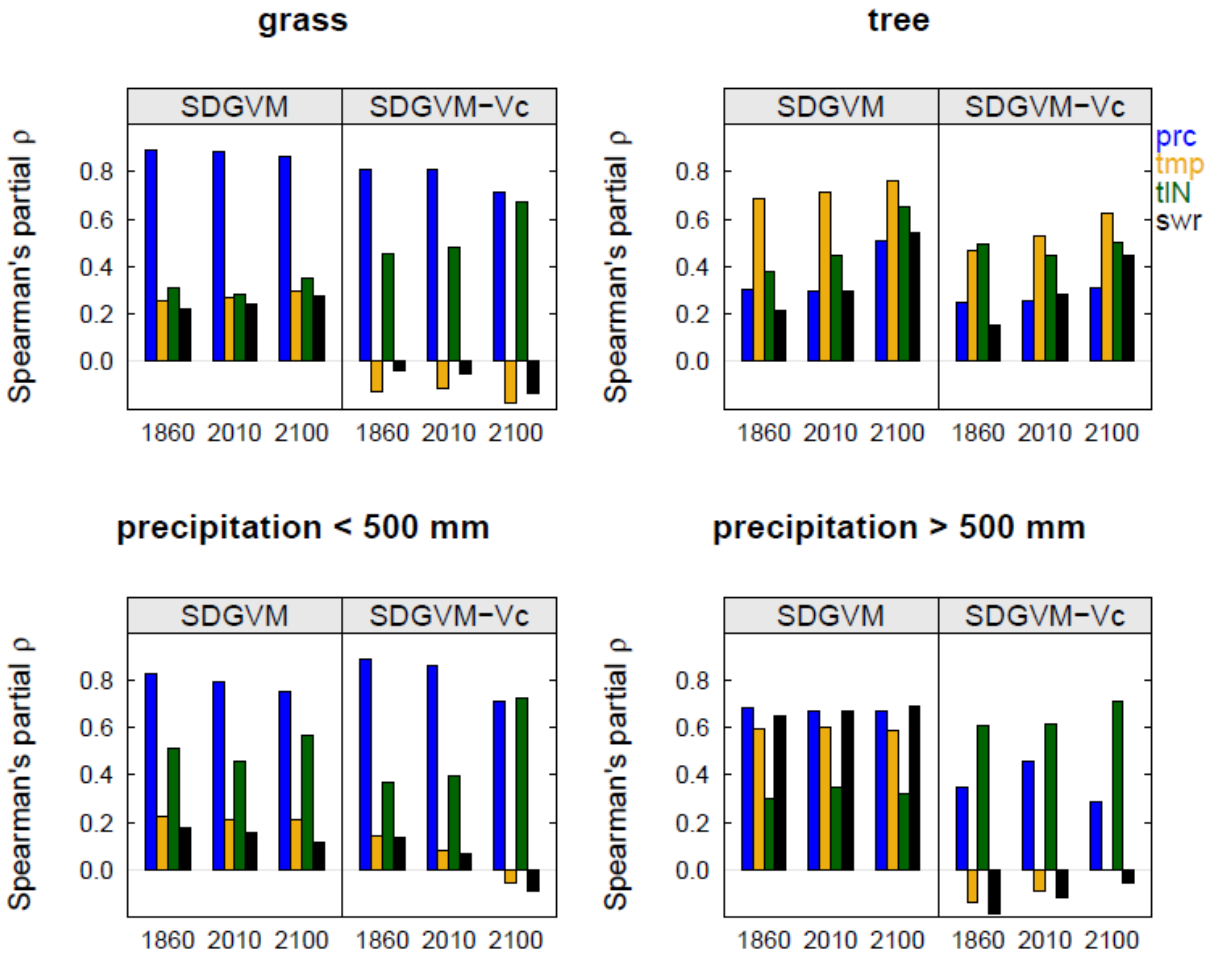

Figure 6-14. Barplots showing the Spearman's partial rank correlation coefficient (ρ) of GPP with model driving variables—precipitation (blue bars), temperature (yellow bars), top leaf nitrogen (green bars) and shortwave radiation (black bars). Each panel shows correlations at the beginning and end of the simulation (1860 and 2100 respectively) and for the modern day (2010). The top row shows ρ for all sites subdivided by PFT growth habit. The bottom row shows ρ for dry sites (annual precipitation below 500 mm yr^{-1}) and wet sites (annual precipitation above 500 mm yr^{-1}). Each plot also shows the results from the SDGVM simulation and the SDGVM-Vc simulation.

Discussion

In comparison with recent estimates (Beer et al. 2010, Bonan et al. 2011b, Jung et al. 2011), global GPP was accurately predicted by SDGVM while SDGVM-Vc strongly over-predicted GPP, predicting values similar to the empirical MIAMI modelling approach of Beer et al. (2010) which related GPP to climate. Similar to Bonan et al. (2011a) using CLM4, realistic values of V_{cmax} and J_{max} contributed to extremely high values of GPP suggesting that V_{cmax} can be used as a parameter to down-tune global GPP. Bonan et al. (2011a) demonstrated that the canopy light scheme of CLM4 needed further re-formulation leading to estimates of GPP that were revised down.

When compared with global GPP of Jung et. al. (2011) much of the over-prediction in GPP of SDGVM-Vc was due to over-prediction of GPP in the boreal and grassed regions of the planet. However, values of leaf nitrogen and V_{cmax} in the boreal zone were similar to those calculated by Kattge et al. (2009) and the over prediction of GPP was perhaps due to poor simulation of canopy structure and scaling of photosynthesis in boreal forests. For SDGVM-Vc the tropics were a hotspot of GPP and in comparison with values of V_{cmax} calculated by Kattge et al. (2009), SDGVM-Vc over-predicted tropical V_{cmax}. Kattge et al. (2009) calculated the V_{cmax} based on observed distributions of leaf nitrogen within a biome and data-assimilated, biome specific relationships of V_{cmax} to leaf nitrogen. Kattge et al. (2009) saw decreased GPP in the tropics with their updated V_{cmax} parameterisation.

The V_{cmax} calculation of SDGVM-Vc used a global multiple-regression of V_{cmax} to leaf nitrogen and leaf phosphorus, where increasing values of leaf phosphorus increase the sensitivity of V_{cmax} to leaf nitrogen (Chapter 5). Predicted values of top-leaf nitrogen in the Amazon appeared reasonable in comparison with the tropical trees in the TRY database (Kattge et al. 2009). The over-prediction of GPP in the tropics by SDGVM-Vc was likely a result of inaccurate representation of the impact of phosphorus on V_{cmax}. Top-leaf phosphorus concentrations in the Amazon were predicted to be between 0.1 and 0.2 gm^{-2} compared to an observed range of 0.05 to 0.15 gm-2 (Mercado et al. 2011) and prediction of leaf phosphorus would be improved with a global soil phosphorus database to drive the leaf phosphorus trait regression (Ordonez et al. 2009). Also, due to the shortage of data measuring V_{cmax}, leaf nitrogen and leaf phosphorus simultaneously the regressions were calculated with a limited dataset and could have under-predicted the sensitivity to leaf phosphorus.

Higher GPP meant that SDGVM-Vc predicted over one and a half times the vegetation biomass of SDGVM, pushing SDGVM-Vc predictions of global vegetation biomass outside the range of estimates of Houghton et al. (2009). Both SDGVM and SDGVM-Vc simulated carbon stocks far greater than the GFRA estimates (FAO 2010). GFRA estimates were forest biomass while model results were total biomass; however, for non-forest biomass account for the difference between SDGVM results and GFRA estimates, non-forest biomass would have to account for 40% of total biomass globally, which is unrealistic (Denman et al. 2007).

If GFRA estimates are accurate then SDGVM over-predicts global biomass and SDGVM-Vc strongly over-predicts global biomass. The GFRA estimates of global biomass were low compared to other estimates (Table 6-2) and with no uncertainty bounds they are hard to compare. The results of SDGVM did fall within the range of the Houghton et al. (2009) estimates of biomass; however, Houghton et al. (2009) estimates were high compared to all other estimates of biomass (FAO 2010, Saatchi et al. 2011, Goodale et al. 2002) and non-forest biomass would have to account for >50% of total global and northern latitude biomass to account for the difference between Houghton et al. (2009) and the GFRA. The importance of biomass carbon stocks in the global carbon cycle and large differences between these datasets highlights the need for accurate and precise, repeatable measurements of biomass stocks to enable monitoring and model validation.

In comparison with the global forest database of Luyssaert et al. (2007), SDGVM-Vc also tended to over-predict vegetation biomass. However, there was some discrepancy between the globally gridded estimates of GPP (Beer et al. 2010) and the Luyssaert et al. (2007) dataset with SDGVM-Vc capturing the high rates of site based GPP of Luyssaert et al. (2007) but over-predicting GPP on a global grid. Both SDGVM and SDGVM-Vc captured the relationship of biomass to NPP across biomes observed by Luyssaert et al. (2007) but within biomes, biomass was still related to NPP, an effect not observed by Luyssaert et al. (2007). Indeed, SDGVM had to predict unrealistically high values of NPP to capture realistically high values of biomass (Figure 6-9).

That within biome variability in NPP was much higher for the models than the Luyssaert et al. (2007) data could be due to more definite classification of sites by Luyssaert et al. (2007). On the other hand, NPP is very difficult to measure in the field requiring large inputs of labour. Allometric equations are necessary to measure aboveground NPP; belowground NPP

is difficult to assess due to turnover and heterogenous distribution of roots, mycorrhiza and root exudation and changes in stored carbon are also necessary to properly assess NPP. The low variance in observed NPP within a biome may reflect these difficulties and may not be a true representation of the range in NPP. While the database is the best we have on properties of mature forest ecosystems, it is still limited in its extent compared with the total forested land surface of the globe. In contrast to NPP, model predicted biomass tended to under-predict the range and often could not capture high biomass values at a given NPP. This was likely to be a result of the difficulty in accurately representing all of the processes, in particular mortality, which influence biomass at a given site (Goetz et al. 2005, Zhang et al. 2008,Liu et al. 2009).

Contrary to the results presented here, in a model (ORCHIDEE) data analysis of the NPP to biomass relationship in Amazon forests, Delbart et al. (2010) showed that observed wood NPP varied more than modelled wood NPP and vice versa for wood biomass. However, they also found a strong linear relationship between modelled biomass and NPP that was not apparent in the observed data. Delbart et al. (2010) demonstrated that the observed decoupling of biomass from NPP was due to variable rates of mortality and they implemented variable mortality rates as a function of NPP which improved the model-data comparison.

The Delbart et al. (2010) function relating turnover to NPP was empirical and they caution that their function was unlikely to apply across biomes. In a global analysis in which all important forest biomes were represented, Keeling and Phillips (2007) demonstrated that the relationship between above-ground biomass (AGB) and above-ground productivity (AGNPP) was best explained by a hump-backed quadratic model. AGB reached a maximum of 30 kg m^{-2} at an AGNPP value of 2400 g m^{-2} yr^{-1}, both of which are higher than any predictions of total biomass and NPP in 2010 by SDGVM and SDGVM-Vc which suggests that the model was close to reality in predicting a linear relationship between biomass and NPP. However, the difference between these model predictions and the values in Keeling and Phillips (2007) are probably due to the scale mismatch between the plot scale measurements of Keeling and Philips (2007) and the regional scale predictions of the model. Averaging plot scale data over a region comparable to that simulated by SDGVM would likely lower the maximum AGB and the maximum AGNPP found in the Keeling and Phillips (2007) data, also reducing the AGNPP at which the AGB maximum occurs. Were the data of a

comparable scale then SDGVM and SDGVM-Vc should probably be simulating a hump-backed relationship between biomass and NPP. Regional-scale, observed datasets of the relationship between biomass and productivity will help to validate a develop how carbon cycle models simulate biomass.

Process based models of mortality, including factors like disease, wind-throw, predation and xylem cavitation, would be ideal for accurate prediction of changes in vegetation biomass over the coming century, particularly in response to climate change as many of these factors are sensitive to climate. However ,process based models of mortality will be complex and empirical relationships between biomass and productivity, like that of Keeling and Phillips (2007), could serve to modify the implicit linear relationship between biomass and productivity that currently exists in SDGVM and other DGVMs in order to make biomass predictions more accurate. However, without empirical data existing at a comparable scale with simulated data, it will be difficult to introduce the correct empirical relationship into the models.

Both SDGVM and SDGVM-Vc, showed a very similar relationship between the autotrophic respiration fraction of GPP and mean annual temperature and this relationship was consistent with observations byLuyssaert et al. (2007) at sites with a mean annual temperature above $0^{o}C$. Below $0^{o}C$, the models strongly under-estimated the respiratory fraction of GPP yet SDGVM-Vc reasonably predicted GPP, suggesting that the updated V_{cmax} parameterisation was necessary but that the respiration algorithm in boreal biomes needed re-evaluation. Hogg et al. (2008) demonstrated the importance of summer drought in Canadian boreal forest plots while Zhang et al. (2008) demonstrated the impact of drought on NPP across the whole of the boreal zone and Ma et al. (2007) demonstrated the reduction in biomass increment caused by summer drought in Canada. Winter ecosystem respiration was also shown to make up 5-10% of the annual total in boreal ecosystems (Wang et al. 2011) although the autotrophic component was not resolved. Boreal sites were important drivers of increasing biomass, particularly in SDGVM-Vc and the re-parameterisation of the respiration algorithm would impact the global capacity to absorb atmospheric CO_2.

Variability in projections of CO_2 increase was mostly determined by the emissions scenario as previously demonstrated by Sitch et al. (2008), followed by the model—SDGVM or

SDGVM-Vc—and finally by the GCM pattern used to simulate climate change in response to CO_2. Higher GPP in SDGVM-Vc led to higher carbon accumulation in live plant biomass leading to higher soil carbon. The trait regression method to calculate leaf nitrogen decoupled a negative relationship between plant biomass and soil carbon which resulted in higher soil carbon and consequently higher rates of soil respiration. Soil carbon pools were higher in SDGVM-Vc due to decoupling of a negative feedback loop between soil carbon and GPP. The loading of soil carbon in the SDGVM-Vc runs during the spin up phase meant that SDGVM-Vc was left with a legacy of higher soil respiration rates which accelerated climate change and restricted biomass accumulation despite higher GPP than SDGVM.

Both SDGVM-Vc and SDGVM predicted a drop in plant biomass in Europe, particularly in the last decade of the simulation and the drop in biomass was sufficient to reduce global biomass in the final decade of the SDGVM-Vc simulation. The possibility of tipping points was illustrated where the effect of CO_2 on GPP and biomass accumulation was superseded by climate induced mortality. HadGEM1 predicts a decrease in European precipitation which leads to an almost complete loss in European forest biomass by the end of 2100, albeit that European forest carbon stocks were over-estimated by SDGVM-Vc.

Houghton et al. (2009) emphasise the role of biomass change in predicting the role of vegetation in the global carbon cycle. The response of global biomass to CO_2 in SDGVM was different to that of SDGVM-Vc, accumulating vegetation carbon at a slower rate despite higher GPP. Higher atmospheric CO_2, caused by higher soil respiration, led to accelerated climate change and the associated impacts on plant respiration. Much of the soil carbon losses of SDGVM-Vc were from the high soil carbon, northern boreal regions. The biggest soil carbon losses occur in the Western US and this is where the pattern of SDGVM-Vc soil carbon deviates most from the Scharlemann et al. (2010) map. The stocks and therefore losses of soil carbon may be a product of the trait regression however, the consequences highlight an important issue—SDGVM accumulates soil carbon while SDGVM-Vc loses soil carbon. The impact of land-use change on soil carbon losses is well established and has long been recognised as a significant contributor to global CO_2 emissions(Houghton 2003). However, the loss, or accumulation, of soil carbon in natural ecosystems under current climate change is less well established (Lal 2008). The major difference between SDGVM and SDGVM-Vc was in their predictions of soil carbon dynamics which led to a mean difference of 150 $\mu mol\ mol^{-1}$in atmospheric CO_2 by 2100.

Conclusions

With higher leaf nitrogen and a more sensitive V_{cmax} and J_{max} response to leaf nitrogen, as expected SDGVM-Vc had higher GPP than SDGVM. However, and similar to previous studies, more accurate representation of photosynthetic parameters did not improve the simulation of GPP and GPP was strongly over-predicted when compared with estimates for the contemporary period. This was partly due to over-prediction of V_{cmax} in the tropics by SDGVM-Vc resulting from poor prediction of leaf phosphorus. Improvement of leaf phosphorus simulation requires a global soil phosphorus database.

It was hypothesised that the use of a PAR dataset would compensate the over-prediction of GPP, however this was not the case, even in regions where V_{cmax} was accurately predicted. Accurate PAR fields could not restore GPP accuracy in simulations with accurate V_{cmax} parameteristation suggesting that the old V_{cmax} parameteristation was also compensating for misrepresented processes, most likely canopy scaling of photosynthesis i.e. nitrogen and light.

SDGVM-Vc predicted a higher rate of atmospheric CO_2 increase than SDGVM. However, confidence in predictions of the CO_2 trajectory over the coming century was not improved by SDGVM-Vc mainly because of over-prediction of GPP and plant biomass. Over-prediction of plant biomass led to high predictions of soil carbon, which although difficult to validate, appeared to compare well with some recent estimates of soil carbon. High soil carbon led to higher rates of soil respiration, increasing the rate of atmospheric CO_2 increase, accelerating climate change, slowing biomass accumulation and accelerating soil respiration, demonstrating the potential positive feedback loop between atmospheric CO_2 and soil respiration.

Corrected V_{cmax} and PAR led to over-prediction of plant biomass resulting from over-prediction of GPP and perhaps, mis-representation of mortality. The simulated relationship of plant biomass to NPP was a linear relationship, similar to that observed in Luyssaert et al. (2007) and Keeling a Phillips et al. (2007) suggesting that mortality was accurately simulated. However, Keeling and Phillips (2007) observed a decline in biomass above NPP values of 2400 gm^{-2}. Maximum SDGVM values of NPP were 1500 gm^{-2}, 900 gm^{-2} less that the Keeling and Phillips (2007) value at which biomass peaked. However, lower NPP values in SDGVM were probably due to a scale mismatch between the plot-scale observed data and the

regional-scale model data. Correction of this mis-match would probably suggest that the simulated linear relationship across the whole range of NPP and biomass by SDGVM should have looked more like the Keeling and Phillips (2007) relationship, although this is only conjecture without datasets of biomass and NPP at a comparable scale to the model data. Regional datasets of biomass and NPP are necessary for validation of the biomass to productivity relationship and to accurately parameterise mortality in the absence of detailed process based models of mortaility.

Chapter 7 General Discussion

Discussion

The aim of this study was to use data from Free Air CO_2 Enrichment (FACE) experiments to validate and inform the simulation of vegetation CO_2responses with global carbon cycle models, primarily the Sheffield Dynamic Global Vegetation Model (SDGVM) and also the Joint UK Land Environment Simulator (JULES). FACE experiments are the most natural experiments on ecosystem responses to elevated CO_2 (Arp 1991, Hendrey et al. 1993, Hendrey and Kimball 1994, Ainsworth and Long 2005) and their spatio-temporal scale is appropriate for comparison with terrestrial carbon cycle/ecosystem models. As discussed in Chapter 1, FACE experiments provide us with an excellent opportunity to validate carbon cycle models at the stand scale and to inform their development. However, quantification of experimental error is important for model-data comparison and FACE experiments are not without artefact. Chiefly, CO_2 concentrations oscillate around the elevated target (Nagy et al. 1994, Hendrey et al. 1997, Miglietta et al. 2001b, Pepin and Körner 2002) and experimentation to understand the effects of oscillating CO_2 has determined that carbon assimilation was increased (Evans and Hendrey 1992, Cardon et al. 1995), unaffected (at oscillation frequencies similar to FACE experiments;Hendrey et al. 1997) and decreased (Holtum and Winter 2003).

The study in Chapter 3 investigated the effect of CO_2 oscillating in concentration (with a similar amplitude and frequency as FACE experiments) on leaf carbon assimilation and water loss. The results demonstrated that over 10 minutes of oscillating CO_2carbon assimilation increased, similar to Evans and Hendrey (1992), while there was no change in stomatal conductance and hence transpiration. It was hypothesised that the increase in assimilation observed in Chapter 3 was explained by a synergy of shifting between V_{cmax}/CO_2 limited assimilation and electron transport/J_{max} limited assimilation and this hypothesis requires testing.

Previously observed reductions in carbon assimilation (A) due to CO_2 oscillations(Hendrey et al. 1997, Holtum and Winter 2003)were previously hypothesised to be caused by the non-linearity of the A-C_i curve. However, modelling of assimilation based on A-C_a/C_i curves showed that reductions in A caused by the non-linearity of the A-C_i curve were of insufficient

magnitude to explain the reductions in carbon assimilation observed byHendrey et al. (1997) andHoltum and Winter (2003).

Calculating assimilation was dependent upon several corrections of the raw data, however these corrections were shown to improve the accuracy of assimilation calculations in control experiments. Experiments were conducted at the leaf scale over tens of minutes making it difficult to translate observed increases in assimilation to changes in plant growth. It would be of interest to test the effect of oscillating CO_2 at the growth chamber scale over a growing season to assess the impact of oscillating CO_2 on plant growth. We caution that, as yet, we do not fully understand the reasons behind plant responses to oscillating CO_2 and that any new FACE experiments should attempt to quantify the effects of oscillating CO_2 on carbon assimilation and plant growth.

The results of this study suggest that a standardised method should be developed to test the effects of oscillating CO_2 on species used in future FACE experiments. The uncertainty in this potentially systematic error in FACE experiments highlights the need to be aware of experimental error, as well as sampling error, in observations when comparing them to model outputs. The results in Chapter 3 and of others (Evans and Hendrey 1992, Cardon et al. 1995, Hendrey et al. 1997, Holtum and Winter 2003) suggested that oscillating CO_2 can affect short-term carbon assimilation although no agreement in the sign of this response and difficulty in scaling this response to longer term and larger scale productivity make it difficult to apply systematically and accurately to validation of annual model productivity.

Site-scale model validation

In their standard versions and with some site specific parameters, both SDGVM and JULES captured some of the inter-annual variability in Net Primary Productivity (NPP) at the Oak Ridge and Duke FACE sites (Figure 4-4, Table 4-3 & Table 4-5), as did a suite of other Carbon Cycle models and ecosystem models (Figure 4-7 & Table 4-7). Measured NPP at the sites was more a measure of growth than complete NPP due to difficulties in measurement and scaling of root exudates and carbon allocated to mycorrhiza. Therefore models were expected to over-predict NPP. Although JULES and SDGVM did over-predict NPP when driven with observations of canopy nitrogen and photosynthetic parameters, there was no general over-prediction of NPP across all the models.

NPP at Duke was relatively high (Inter Quartile Range IQR 944–1074gC m^{-2} yr^{-1}) showing no trend over the course of the experiment while at Oak Ridge NPP was lower (IQR 698–954 g C m^{-2} yr^{-1})with a declining trend in NPP, particularly in the latter half of the experiment. Reasonable prediction of the inter-annual variability in NPP at Duke was encouraging as it suggested that models were responding in a similar way to drivers of inter-annual variability in the Duke forest. However, annual NPP at Duke appeared not to be related to annual climatic drivers in any simple way and different models were sensitive to different drivers which allowed them to be grouped into three general categories—those driven by nitrogen uptake, those driven by photosynthesis and those driven by climate.

Model predictions were less successful at Oak Ridge reflecting the strong progressive nitrogen limitation at that site (Norby et al. 2010, Garten et al. 2011). For the few models that captured some of the inter-annual variability in NPP at Oak Ridge, NPP was correlated with temperature rather than nitrogen uptake (Table 4-4, Table 4-6 & Table 4-8) indicating that the decline in NPP may have been partly driven by climate or that the models may have been getting NPP right for the wrong reasons. OCN, CLM and GDAY captured the lower values of NPP and the lower response to CO_2 at the end of the experiment, suggesting that while they could not reproduce the decline in NPP, they may have captured the longer term, sustainable rate of NPP and the CO_2 response.

Driving SDGVM and JULES with observed data that were non-standard inputs to the models improved the simulation of NPP at Duke and NPP was closer to expectations at Oak Ridge (i.e NPP was over-predicted due to the two models not simulating stoichiometric growth limitation). Observed data on canopy nitrogen, the relationship of V_{cmax} to leaf nitrogen and Photosynthetically Active Radiation (PAR—for SDGVM, JULES takes PAR as a standard input) used to drive the models demonstrated the importance of accurate representation of these leaf traits, and radiation, in accurate simulation of the carbon cycle. Future work needs to build on previous work to determine factors driving variation in leaf nitrogen(Reich et al. 2007, Ordonez et al. 2009, Poorter et al. 2009), determining accurate global methods to simulate V_{cmax} and J_{max} in relation to leaf traits (Chapter 5,Beerling and Quick 1995, Kattge et al. 2009) and accurate representation of incoming PAR and canopy PAR (Haxeltine and Prentice 1996, Mercado et al. 2007, Bonan et al. 2011b).

The NPP response to elevated CO_2 proved to be more difficult to simulate. Many models captured the higher response at Duke compared with Oak Ridge but few models captured the median and the range of responses (Figure 4-8). Model predictions of annual CO_2 responses were broad and, similar to the global study of Sitch et al. (2008), demonstrated the variability across models in simulating the CO_2 response in relation to climate variability. However, few models captured inter-annual variability in the responses (Table 4-9) which at Duke was shown to be related to nitrogen availability and the water balance (McCarthy et al. 2010) and to the response of nitrogen availability at Oak Ridge (Garten et al. 2011). Although the NPP responses at Duke were shown to correlate with common values of nitrogen and the water balance across CO_2 treatments, it was likely the response of nitrogen and soil water that determined the NPP response. Indeed, Drake et al. (2011) showed that elevated CO_2 increased decomposition rates of soil organic matter allowing greater access to soil nitrogen under elevated CO_2. Although a response of soil water to elevated CO_2 was undetected at Duke, Schafer et al. (2002) hypothesised that soil water was higher under elevated CO_2, probably due to reduced soil evaporation resulting from a deeper litter layer.

In agreement with observations, regression showed that the key drivers of the NPP response to CO_2in SDGVM and JULES were the response of canopy nitrogen and the response of soil water limitation, with SDGVM primarily driven by nitrogen and JULES primarily soil water (Figure 4-10). It was surprising that despite the importance of the role of nitrogen in both the observed and SDGVM responses, SDGVM could not capture any of the inter-annual variability in response seven when driven with the observed values of canopy nitrogen. On the other hand, when driven with canopy nitrogen JULES reproduced some of the inter-annual variability in the NPP response at Duke. For the JULES simulations LAI was a constant under both CO_2 treatments while in SDGVM LAI varied by treatment and year according to the LAI scheme and the inability of SDGVM to capture the NPP response to CO_2 was possibly related to the variability in simulated LAI.

Responses to FACE and global carbon cycle simulation

In a meta-analysis of FACE experiments, Chapter 2 built on the previous work of Luo et al. (2006b) and Ainsworth et al. (2008) using the most up-to-date results from FACE experiments to detect any changes in the CO_2 response over longer-term enrichment. In lab and greenhouse experiments, CO_2 responses have often been shown to ‘acclimate’ (be down-regulated) (Stitt 1991), often as a consequence of restricted soil volumes (Arp 1991),

but also due to competition between the carbon assimilation and nitrite assimilation pathways (Searles and Bloom 2003).

The meta-analysis in Chapter 2 had a greater sample of data from forest FACE experiments than Ainsworth and Long (2005) and showed less reduction in photosynthetic capacity than Ainsworth and Long (2005), manifested in lower decreases in leaf nitrogen and V_{cmax}, and no decrease in J_{max} or leaf chlorophyll when expressed on a leaf area basis. When leaf nitrogen was analysed by Plant Functional Type (PFT) the decrease in grasses was far greater than for trees and was similar to that reported by (Ainsworth and Long 2005). In the global carbon cycle analysis of Chapter 6, it was demonstrated that the decrease in leaf nitrogen under elevated CO_2 made very little difference to prediction of atmospheric CO_2 increase over the coming century.

Chapter 2 also demonstrated a recovery in the response of V_{cmax} to elevated CO_2, such that V_{cmax} was unchanged between 4–9 years after CO_2 enrichment began. This was reflected by what appeared to be increases in the response of aboveground biomass in years 7–9 after enrichment compared to earlier years. Although total biomass was not significantly increased in year 7–9 after enrichment, the mean response ratio was similar to that in previous years and the 95% confidence interval only just included no response. The variability in the response of total biomass after 7–9 years of CO_2 enrichment, despite maintained photosynthetic rates, demonstrates the need for further experimentation to illuminate environmental and ecological factors that determine the longevity of the CO_2 response.

Using non-structural carbohydrates as a measure of tree carbon limitation,Körner (2003) argued that trees are not generally limited by carbon and that CO_2 would have little lasting impact on the terrestrial carbon cycle. Nitrogen was shown to be a factor limiting the response of NPP to CO_2 (McCarthy et al. 2010, Norby et al. 2010, Garten et al. 2011) and the theory of Progressive Nitrogen Limitation (PNL) under elevated CO_2 (Johnson 2006, Luo et al. 2006b) was backed up by Garten et al. (2011), albeit in a strongly nitrogen limited system. However, PNL was shown not to be a consequence of CO_2 enrichment at Duke and Rheinlander FACE with increased plant carbon leading to access to nitrogen unavailable to plants at ambient CO_2 concentrations (Drake et al. 2011, Zak et al. 2011). Without proper understanding of these factors, the role of terrestrial vegetation in the global carbon cycle

under future global change will be difficult to quantify accurately. Chapter 6 demonstrated that reductions in leaf nitrogen observed in FACE experiments, and their consequent impact on photosynthesis, made little impact on the simulated trend in global atmospheric CO_2 increases over the coming century.

Chapter 2 showed stronger reductions in leaf traits on a mass basis compared to an area basis and a decrease in Specific Leaf Area (SLA) in response to elevated CO_2. Chapter 5 showed little impact of SLA on V_{cmax} when traits were expressed on a leaf area basis but SLA was significant when traits were expressed on a concentration basis. These results hint that modifying SLA may be a central strategy of plants to optimise photosynthesis in response to increasing CO_2. Indeed, SLA has been shown to respond to many environmental stimuli (Niinemets 1999, Poorter et al. 2009) and may be a central plant response to optimise canopy processes.

Leaf traits and photosynthetic parameters

The key photosynthetic parameters of the Farquhar et al. (1980) model have been shown to bear a strong relationship to leaf nitrogen (Field and Mooney 1984, Wullschleger 1993). Simulation of the FACE experiments in Chapter 4 demonstrated that accurate simulation of V_{cmax} and J_{max}, and therefore leaf nitrogen, was necessary to accurately simulate NPP.A number of studies have generated biome averaged values of V_{cmax} and J_{max} (Beerling and Quick 1995, Kattge et al. 2009) demonstrating clear differences between biomes in the relationship of V_{cmax} to leaf nitrogen.Kattge et al. (2009) demonstrated different relationships of V_{cmax} to leaf nitrogen in the tropics on low or high phosphorus soils. Recent studies demonstrated that leaf phosphorus modified the relationship of carbon assimilation to leaf nitrogen (Reich et al. 2009) and that V_{cmax} and J_{max} were, in some cases, more strongly correlated with leaf phosphorus or even SLA (Domingues et al. 2010).

It was hypothesised that the different relationships of V_{cmax} and J_{max} to leaf nitrogen could be explained by leaf phosphorus and SLA. Chapter 5 shows the results of a meta-analysis which for the first time produced global relationships of V_{cmax} and J_{max} to leaf nitrogen, phosphorus and SLA. In a mixed-model multiple-regression, measured on both a leaf area and concentration basis, much of the variation in V_{cmax} and J_{max} was explained by variation inleaf nitrogen, leaf phosphorus and SLA. On a leaf area basis, V_{cmax} was most strongly related to leaf nitrogen with decreasing leaf phosphorus significantly reducing the slope of the

relationship. As the results of Kattge et al. (2009) andDomingues et al. (2010) suggested, leaf phosphorus was an important global determinant of V_{cmax}.

The strongest correlate of J_{max} was V_{cmax} with some indication that SLA modified this relationship. Both parameters were expected to be strongly related due to their mutual interaction through their photosynthetic coupling. Investigating the slope of the J_{max} to V_{cmax} relationship with the Farquhar et al. (1980) model showed that the slope was higher than expected assuming that resources used to determine these biochemical capacities were allocated to V_{cmax} and J_{max} in order to maximise carbon gain. Specifically J_{max} was higher than expected and it is proposed that this may be due to use of the products from electron transport in biochemical processes other than carbon assimilation.

These relationships augment existing global data on the V_{cmax} and J_{max} parameters (Wullschleger 1993, Beerling and Quick 1995, Kattge et al. 2009)and it is recommended that these relationships are used to accurately simulate terrestrial vegetation and in model development exercises to illuminate model biases and compensating factors. Although the data came from all over the globe, limited published data on all five leaf traits meant that the relationships were limited in their extent and sample size and future meta-analyses will help to develop and refine these relationships.

Compensating factors and missing processes

SDGVM

Simulating the FACE experiments revealed that SDGVM over-predicted Photosynthetically Active Radiation (PAR) and under-predicted leaf nitrogen. Leaf nitrogen was used to calculate V_{cmax} so under-prediction of leaf nitrogen would be expected to under-predict V_{cmax}. Additionally, the results in Chapter 4 demonstrate that V_{cmax} was also under-predicted due to low sensitivity to leaf nitrogen. Driving the model with observed values PAR, leaf nitrogen and the V_{cmax} relationship to leaf nitrogen improved model skill in simulating Net Primary Productivity (NPP).

Modelled NPP was far higher than observed NPP when using observations of nitrogen and V_{cmax} but model calculated PAR (Figure 4-4), revealing that the under-prediction of leaf nitrogen and low parameterisation of V_{cmax} were compensating the over-prediction of PAR. Observed values of PAR brought simulated NPP close to observations and showed very

strong model skill at Duke. Despite closer mean values of NPP at Oak Ridge, all model skill was lost due to simulated NPP responding to strong inter-annual variability in PAR. The main driver of NPP at Oak Ridge was declining soil nitrogen (Norby et al. 2010, Garten et al. 2011) resulting from progressively larger amounts of ecosystem nitrogen being locked away in plant tissue(Johnson 2006), in this case roots and then less accessible soil organic matter (Franklin 2007), a process not simulated by SDGVM. SDGVM does not simulate a mass balanced nitrogen cycle and therefore could not be expected to simulate the Oak Ridge FACE experiment as accurately as Duke. Although Duke FACE experiment was nitrogen limited (McCarthy et al. 2010), the long lived root system of *Pinus taeda* was less demanding of soil nitrogen (Franklin 2007) and was able to increase access to soil nitrogen at elevated CO_2 (Drake et al. 2011) reducing the strength of the nitrogen limitation. The importance of soil nitrogen in the FACE experiments and simulating the experiments highlights the need for multi-factorial experiments of elevated CO_2 and increased temperature as the increased temperatures expected with increased CO_2 would accelerate soil nitrogen mineralisation (Sardans et al. 2008a, Sardans et al. 2008b).

In a global analysis of CLM4 and similar to SDGVM, Bonan et al. (2011b) found that V_{cmax} was also low in comparison to values calculated from an observed, global dataset of leaf nitrogen and light saturated carbon assimilation (Kattge et al. 2009). Similar to SDGVM, Bonan et al. (2011b) found that realistic values of V_{cmax} strongly over-predicted productivity compared to observations (albeit GPP and not NPP) and Bonan et al. (2011a) demonstrated the sensitivity of the GPP prediction to scaling of canopy light levels. Improving the canopy radiation scheme reduced the over-prediction of GPP by CLM4 and accurate predictions of PAR improved predictions of NPP in SDGVM, although SDGVM was shown to be over-sensitive to variability in PAR (Figure 4-4&Table 2-1).

In comparison with FLUXNET estimates of global GPP (Beer et al. 2010, Jung et al. 2011), SDGVM-Vc (with improved representation of PAR and V_{cmax}) showed that productivity was over-predicted while SDGVM accurately predicted global productivity. Much of the over-prediction in GPP of SDGVM-Vc was due to over-prediction of GPP in the boreal and grassed regions of the planet, although there was some discrepancy between comparison with the globally gridded FLUXNET products of Beer et al. (2010) andJung et al. (2011) and the site based data of Luyssaert et al. (2007). A quantitative comparison with the globally gridded

FLUXNET product and a more detailed comparison with the Luyssaert et al. (2007) data will be useful to further develop SDGVM GPP simulation.

Chapter 6, demonstrated a near linear relationship between modelled tree NPP and biomass, a relationship which was also shown in OCN for sites across the Amazon(Delbart et al. 2010). A global linear relationship was apparent in the Luyssaert et al. (2007) database although within a biome, variability suggested that a linear relationship of biomass to NPP was not apparent (Figure 6-9). However, Keeling and Phillips (2007) demonstrated a hump-backed quadratic relationship between above-ground biomass and above-ground NPP, a relationship not apparent in the model. Keeling and Phillips were cautious in explaining the mechanisms behind the relationship but their relationship demonstrates that biomass is not a simple, linear function of NPP and that this needs attention in SDGVM and global carbon cycle modelling more generally.

Plant mortality is a key driver of site biomass and improved representation of mortality was shown to improve biomass simulation at the Amazon site simulations of Delbart et al. (2010). The empirical relationship observed by Keeling and Phillips could improve model biomass simulations while more mechanistic models of plant mortality are developed. Mortality depends on multiple interacting ecological factors and it will be necessary for experimentalists and ecologists to generate more data and hypotheses on drivers of plant mortality in order to develop mechanistic, process based models of mortality.

Much of the over-prediction of biomass was in the boreal latitudes (Figure 6-11 and Table 6-2) and Chapter 6 showed that, as a fraction of GPP, respiration was strongly under-predicted in boreal forests compared with the Luyssaert et al. (2007) dataset which led to over-prediction of biomass, despite accurate prediction of GPP in SDGVM-Vc. Growth in these forests is limited stoichiometrically by nitrogen (Wang et al. 2007b) and the high observed respiration fraction may be related to this stoichiometric limitation. With SDGVM missing a full nitrogen cycle it is likely that, at the global scale and particularly in boreal regions where soil carbon is relatively high (McGuire et al. 2010), the empirical negative feedback of soil carbon on leaf nitrogen in SDGVM (Woodward and Smith 1994, Woodward et al. 1995) represents the complex process of nitrogen limited growth.

JULES

There was evidence to suggest that there were also compensating factors in JULES. As with SDGVM, driving JULES with observations of canopy nitrogen increased carbon assimilation and improved the simulation of NPP. However, in 2003 JULES simulated an extremely high value of NPP because the combination of low temperature and high precipitation in that year resulted in JULES predicting very little soil water limitation. Further investigation revealed that soil water limitation reduced NPP by 27%, compared to 5% in SDGVM. The high value of NPP in 2003 suggested that under conditions not limited by soil water, JULES over-predicted NPP and the generally strong effect of soil water limitation was compensating the over-prediction of potential NPP.

JULES uses the Collatz et al. (1991) formulation of C3 photosynthesis which has no biochemical limit to light limited photosynthesis—i.e. no J_{max} term. CLM4 also uses the Collatz et al. (1991) formulation and Bonan et al. (2011b) demonstrated that CLM4 over-predicted global GPP which was corrected by the inclusion of a J_{max} term as well as a number of corrections to canopy light scaling. In the Amazon, Mercado et al. (2007) found no over-prediction of NPP by JULES under conditions that were not soil water limited demonstrating that compensating over-prediction of potential NPP by strong soil water limitation is likely to apply only in certain regions.

General conclusions, key advances, limitations and future work

Accurate prediction of changing biomass over the coming century will be the key to predicting the impact of terrestrial vegetation on the global carbon cycle (Houghton et al. 2009) and results from a meta-analysis of FACE experiments in Chapter 2 showed that increases in forest biomass were maintained over a decade of CO_2 enrichment. Chapter 2 also showed that acclimation of photosynthetic rates (reductions in assimilation at a common CO_2 concentration and V_{cmax}) under elevated CO_2 observed in years 1-3 of enrichment disappeared in years 6-9 after enrichment.

However, not all forest age classes and types have been subjected to FACE experiments. Therefore, mature forests were not represented in the meta-analysis nor were tropical or boreal systems. Mature forests, tropical forests and boreal forests will be key to determining the response of the land surface to future elevated CO_2 concentrations. Long-term FACE experiments are urgently needed in these systems to understand their responses to CO_2.

Net Primary Productivity feeds into plant biomass pools. Chapter 4 showed that NPP and the mean CO_2 response were accurately simulated at the Duke FACE experiment by SDGVM, JULES and a number of other carbon cycle models although inter-annual variability in the responses proved difficult for the models to reproduce. The variability in model simulations of the NPP response to CO_2 and the difficulty in reproducing inter-annual variability in the CO_2 response suggested that the large range in predicted atmospheric CO_2 concentrations over the coming century (Cramer et al. 2001, Friedlingstein et al. 2006, Sitch et al. 2008) is unlikely to be reduced.

Therefore, model benchmarking exercises should be developed to weight model predictions and help to reduce uncertainty in multi-model predictions of future Earth System dynamics. Due to data availability and time constraints, the model validation of plant CO_2 responses in Chapter four used data from only two FACE experiments – both in similar systems with similar climates. Expansion of this benchmarking exercise to other FACE experiments would make the benchmarking more broadly applicable to global studies.

In Chapter 4, similar to another study of model bias (Bonan et al. 2011b), simulation of NPP at the FACE experiments demonstrated that both SDGVM and JULES were subject to biases that were compensated for by parameterisation bias. However, correction of the Photosynthetically Active Radiation bias and the compensating V_{cmax} parameterisation bias

in SDGVM led to over-prediction of global GPP. This suggests that the V_{cmax} bias was also representing the process of stoichiometric nitrogen limitation to plant growth. Difficulties in representing stoichiometric nitrogen limitation were highlighted by the poorer simulation of Oak Ridge FACE compared with Duke by a number of carbon (and nitrogen) cycle models and further research into the development and validation of ecosystem nitrogen dynamics is needed. JULES and SDGVM had very different strengths of soil water limitation and experimental quantification of the strength of soil water limitation on plant growth is necessary.

Model bias and compensation by model parameters shows the strong need for global parameter datasets and parameter relationships to be sure unrealistic parameter values are not used to tune models, potentially hiding model structural, parameter or driving data errors. Bonan et al. (2011b) suggested that improved simulation of canopy structure was necessary to correct the over-prediction of GPP in CLM4 and this may be the case with SDGVM; however, nitrogen limits NPP both photosynthetically and stoichiometrically and both SDGVM and CLM4 (in the work of Bonan et al. 2011b) do not include stoichiometric nitrogen limitation. DGVMs should include a full nitrogen cycle to be sure to capture the separate but inter-related processes of photosynthetic and stoichiometric nitrogen limitation to NPP.

Chapter 3 showed that experiments, not only models, were biased. Assimilation was increased under oscillations in CO_2 similar to those found in FACE experiments. It was hypothesised that this stimulation was due to switching between electron transport and carboxylation as the rate limiting cycles of carbon assimilation, preventing depletion of substrates supplying each cycle. Previous hypotheses explaining reductions in assimilation under oscillating CO_2 were shown to be insufficient and we hypothesise that stomatal responses to a step change in CO_2 may have been important in explaining these reductions. Experiments were conducted at the leaf scale over tens of minutes making it difficult to translate observed increases in assimilation to changes in plant growth. It would be of interest to test the effect of oscillating CO_2 at the growth chamber scale over a growing season to assess the impact of oscillating CO_2 on plant growth.

Chapter 5 demonstrated the importance of phosphorus in modifying V_{cmax} and therefore limiting photosynthesis. It is cautiously suggested that the inclusion of leaf phosphorus with

leaf nitrogen in a multiple regression of V_{cmax} could provide a single empirical relationship suitable for modelling V_{cmax} at the global scale. Caution is applied due to the limited nature of the dataset and future work should broaden the dataset to cover more biomes. However, data were collected from natural systems and from nutrient manipulation experiments covering a wide range of leaf nitrogen and phosphorus concentrations.

Similar to previous studies, Chapter 5 demonstrated tight coupling between J_{max} and V_{cmax}, showing J_{max} to be higher than expected assuming the relationship was optimised with regards to carbon assimilation. It was proposed that this may be due to the use of ATP and NADPH generated by electron transport in biochemical cycles other than the PCR/PCO cycle i.e. non-carbon photosynthesis. It would be interesting to see future work on the ratio of ATP and NADPH produced by electron transport used in the PCR/PCO cycle compared to use in other biochemical cycles.

In Chapter 6, the trait regression method to simulate canopy nitrogen in SDGVM-Vc, decoupled an empirical relationship between soil carbon and plant productivity. The decoupling of this relationship led to high soil carbon stocks, soil respiration and accelerated rates of atmospheric CO_2 increase. However, general conclusions about model structure and relationships between state variables could be drawn.

More accurate representation of leaf nitrogen and photosynthetic parameters in SDGVM-Vc led to over-predictions of GPP suggesting that more work needs to be done on the photosynthesis scheme within SDGVM. V_{cmax} was over-predicted in the tropics by SDGVM-Vc and was probably due to over-prediction of leaf phosphorus due to the lack of a global soil phosphorus map to drive empirical equations of leaf phosphorus. Phosphorus is the major limiting nutrient in the tropics (Quesada et al. 2011) and probably also limits growth stoichiometrically. DGVMs should also consider representation of the phosphorus cycle as Wang et al. (2007b) has done, and work needs to be done to generate a global soil phosphorus map and to establish plant tissue phosphorus stoichiometry to parameterise DGVMs.

Linear relationships were also shown between biomass and NPP and between the autotrophic respiration fraction of GPP and temperature. In the literature these relationships have been shown to be quadratic in nature. Modelled biomass showed a linear relationship to NPP (Chapter 6), a relationship that was maintained under CO_2 increase leading to higher

global biomass by 2100. Indeed, Luyssaert et al. (2010) found a strong linear relationship between biomass and productivity for European forests. However, results from a global forest database (Luyssaert et al. 2007) suggested that within a biome, biomass appeared not to be related to NPP, albeit that the data were collected at a smaller spatial scale than the simulation scale of the global model. Keeling and Phillips (2007) showed that the relationship between biomass and NPP saturated and that biomass decreased at high values of NPP. It is likely that SDGVM should be demonstrating a similar non-linear relationship between biomass and productivity similar to that of Keeling and Phillips (2007). Future research is necessary to compare observed and simulated biomass to productivity relationships at the correct scale.

The large variance in biomass and relatively small variance in NPP within a biome (Luyssaert et al. 2007) suggested that mortality played a central role in determining plant biomass. Delbart et al. (2010) showed a similar linear relationship of modelled biomass to NPP and demonstrated that improved representation of mortality improved predictions of biomass across a range of sites in the Amazon. Biotic and abiotic factors that underlie plant and tree mortality at the landscape scale are often stochastic disturbance events such as windthrow, fire, pest and pathogen outbreaks. Processes underlying the cause of death resulting from these factors are multiple as are the triggers of these events making modelling complex with resulting parameter and structural uncertainty. Mortality operates over long timescales (although some events can be extremely rapid, the frequency of their occurrence can be low) meaning that the data from observations and experimental manipulations are few. However, work needs to be done to improve the representation of mortality within SDGVM/carbon cycle models.

While good progress is being made to estimate biomass at the landscape scale (Malhi et al. 2006, Saatchi et al. 2007, Saatchi et al. 2011) much of this work focuses on the tropics. This study demonstrates the need to accurately map biomass carbon in Boreal forests as well as in the tropics. Until globally accurate maps of biomass are available, with repeatable accuracy and precision, it will be difficult to properly validate and develop algorithms that simulate terrestrial plant biomass. Accurate simulation of biomass and its determining factors will be essential for confidence in model predictions of future terrestrial vegetation responses to changing atmospheric CO_2 and climate.

References

Abramowitz, G., R. Leuning, M. Clark, and A. Pitman. 2008. Evaluating the Performance of Land Surface Models. Journal of Climate **21**:5468-5481.

Ainsworth, E. A., P. A. Davey, G. J. Hymus, C. P. Osborne, A. Rogers, H. Blum, J. Nosberger, and S. P. Long. 2003. Is stimulation of leaf photosynthesis by elevated carbon dioxide concentration maintained in the long term? A test with Lolium perenne grown for 10 years at two nitrogen fertilization levels under Free Air CO2 Enrichment (FACE). Plant Cell and Environment **26**:705-714.

Ainsworth, E. A., A. D. B. Leakey, D. R. Ort, and S. P. Long. 2008. FACE-ing the facts: inconsistencies and interdependence among field, chamber and modeling studies of elevated [CO2] impacts on crop yield and food supply. New Phytologist **179**:5-9.

Ainsworth, E. A. and S. P. Long. 2005. What have we learned from 15 years of free-air CO2 enrichment (FACE)? A meta-analytic review of the responses of photosynthesis, canopy. New Phytologist **165**:351-371.

Ainsworth, E. A. and A. Rogers. 2007. The response of photosynthesis and stomatal conductance to rising [CO2]: mechanisms and environmental interactions. Plant Cell and Environment **30**:258-270.

Ainsworth, E. A., A. Rogers, A. D. B. Leakey, L. E. Heady, Y. Gibon, M. Stitt, and U. Schurr. 2007. Does elevated atmospheric [CO2] alter diurnal C uptake and the balance of C and N metabolites in growing and fully expanded soybean leaves? Journal of Experimental Botany **58**:579-591.

Allen, M. R., D. J. Frame, C. Huntingford, C. D. Jones, J. A. Lowe, M. Meinshausen, and N. Meinshausen. 2009. Warming caused by cumulative carbon emissions towards the trillionth tonne. Nature **458**:1163-1166.

Anderson, J. W. and J. Done. 1978.Light-dependent assimilation of nitrite by isolated Pea chloroplasts. Plant Physiology **61**:692-697.

Aranda, X., C. Agusti, R. Joffre, and I. Fleck. 2006. Photosynthesis, growth and structural characteristics of holm oak resprouts originated from plants grown under elevated CO2. Physiologia Plantarum **128**:302-312.

Arp, W. J. 1991. Effects of Source-Sink Relations on Photosynthetic Acclimation to Elevated Co2. Plant Cell and Environment **14**:869-875.

Asshoff, R., G. Zotz, and C. Korner. 2006. Growth and phenology of mature temperate forest trees in elevated CO2. Global Change Biology **12**:848-861.

Baldocchi, D., E. Falge, L. H. Gu, R. Olson, D. Hollinger, S. Running, P. Anthoni, C. Bernhofer, K. Davis, R. Evans, J. Fuentes, A. Goldstein, G. Katul, B. Law, X. H. Lee, Y. Malhi, T. Meyers, W. Munger, W. Oechel, K. T. P. U, K. Pilegaard, H. P. Schmid, R. Valentini, S. Verma, T. Vesala, K. Wilson, and S. Wofsy. 2001. FLUXNET: A new tool to study the temporal and spatial variability of ecosystem-scale carbon dioxide, water vapor, and energy flux densities. Bulletin of the American Meteorological Society **82**:2415-2434.

Batjes, N. H. 2005. ISRIC-WISE -- Global data set of derived soil proerties on a 0.5 by 0.5 degree grid (ver. 3.0).*in* I.-W. S. Information, editor., Wageningen.

Beer, C., M. Reichstein, E. Tomelleri, P. Ciais, M. Jung, N. Carvalhais, C. Roedenbeck, M. A. Arain, D. Baldocchi, G. B. Bonan, A. Bondeau, A. Cescatti, G. Lasslop, A. Lindroth, M. Lomas, S. Luyssaert, H. Margolis, K. W. Oleson, O. Roupsard, E. Veenendaal, N. Viovy, C. Williams, F. I. Woodward, and D. Papale. 2010. Terrestrial Gross Carbon Dioxide Uptake: Global Distribution and Covariation with Climate. Science **329**:834-838.

Beerling, D. J. and W. P. Quick. 1995. A new technique for estimating rates of carboxylation and electron-transport in leaves of C-3 plants for use in dynamic

global vegetation models. Global Change Biology **1**:289-294.
Beier, C., B. A. Emmett, J. Penuelas, I. K. Schmidt, A. Tietema, M. Estiarte, P. Gundersen, L. Llorens, T. Riis-Nielsen, A. Sowerby, and A. Gorissen. 2008. Carbon and nitrogen cycles in European ecosystems respond differently to global warming. Science of the Total Environment **407**:692-697.
Bell, J. E., Y. Luo, and E. Weng. 2007. Impact of climate change on prairie soil water dynamics. Ecological Society of America Annual Meeting Abstracts.
Beniston, M., D. B. Stephenson, O. B. Christensen, C. A. T. Ferro, C. Frei, S. Goyette, K. Halsnaes, T. Holt, K. Jylha, B. Koffi, J. Palutikof, R. Schoell, T. Semmler, and K. Woth. 2007. Future extreme events in European climate: an exploration of regional climate model projections. Climatic Change **81**:71-95.
Benson, A. A., J. A. Bassham, M. Calvin, T. C. Goodale, V. A. Haas, and W. Stepka. 1950. THE PATH OF CARBON IN PHOTOSYNTHESIS .5. PAPER CHROMATOGRAPHY AND RADIOAUTOGRAPHY OF THE PRODUCTS. Journal of the American Chemical Society **72**:1710-1718.
Bernacchi, C. J., D. M. Rosenthal, C. Pimentel, S. P. Long, and G. D. Farquhar. 2009. Modeling the Temperature Dependence of C-3 Photosynthesis. Pages 231-246 *in* A. N. L. G. X. Laisk, editor. Photosynthesis in silico: Understanding Complexity from Molecules to Ecosystems.
Best, M. J., M. Pryor, D. B. Clark, G. G. Rooney, R. L. H. Essery, C. B. Menard, J. M. Edwards, M. A. Hendry, A. Porson, N. Gedney, L. M. Mercado, S. Sitch, E. Blyth, O. Boucher, P. M. Cox, C. S. B. Grimmond, and R. J. Harding. 2011. The Joint UK Land Environment Simulator (JULES), model description - Part 1: Energy and water fluxes. Geoscientific Model Development **4**:677-699.
Blyth, E., D. B. Clark, R. Ellis, C. Huntingford, S. Los, M. Pryor, M. Best, and S. Sitch. 2011. A comprehensive set of benchmark tests for a land surface model of simultaneous fluxes of water and carbon at both the global and seasonal scale. Geoscientific Model Development **4**:255-269.
Boden, T. A., G. Marland, and R.J. Andres. 2011. Global, Regional, and National Fossil-Fuel CO2 Emissions. .*in* O. R. N. L. Carbon Dioxide Information Analysis Center, U.S. Department of Energy, Oak Ridge, Tenn., U.S.A., editor.
Bonan, G., K. Oleson, and R. Fisher. 2011a. Improving canopy processes in the Community Land Model using FLUXNET data: Assessing nitrogen limitation and canopy radiation. iLEAPS 3rd Science Conference.
Bonan, G. B., P. J. Lawrence, K. W. Oleson, S. Levis, M. Jung, M. Reichstein, D. M. Lawrence, and S. C. Swenson. 2011b. Improving canopy processes in the Community Land Model version 4 (CLM4) using global flux fields empirically inferred from FLUXNET data. Journal of Geophysical Research-Biogeosciences **116**.
Bown, H. E., M. S. Watt, P. W. Clinton, E. G. Mason, and B. Richardson. 2007. Partititioning concurrent influences of nitrogen and phosphorus supply on photosynthetic model parameters of Pinus radiata. Tree Physiology **27**:335-344.
Cadule, P., P. Friedlingstein, L. Bopp, S. Sitch, C. D. Jones, P. Ciais, S. L. Piao, and P. Peylin. 2010. Benchmarking coupled climate-carbon models against long-term atmospheric CO(2) measurements. Global Biogeochemical Cycles **24**.
Calfapietra, C., B. Gielen, M. Sabatti, P. De Angelis, G. Scarascia-Mugnozza, and R. Ceulemans. 2001. Growth performance of Populus exposed to "Free Air Carbon dioxide Enrichment" during the first growing season in the POPFACE experiment. Annals of Forest Science **58**:819-828.
Calvin, M. 1989. 40 YEARS OF PHOTOSYNTHESIS AND RELATED ACTIVITIES. Photosynthesis Research **21**:3-16.
Canadell, J. G., C. Le Quere, M. R. Raupach, C. B. Field, E. T. Buitenhuis, P. Ciais, T. J.

Conway, N. P. Gillett, R. A. Houghton, and G. Marland. 2007. Contributions to accelerating atmospheric CO2 growth from economic activity, carbon intensity, and efficiency of natural sinks. Proceedings of the National Academy of Sciences of the United States of America **104**:18866-18870.

Cao, M. K. and F. I. Woodward. 1998. Dynamic responses of terrestrial ecosystem carbon cycling to global climate change. Nature **393**:249-252.

Cardon, Z. G., J. A. Berry, and I. E. Woodrow. 1995. Fluctuating [CO2] drives species-specific changes in water use efficiency. Journal of Biogeography **22**:203-208.

Cernusak, L. A., L. B. Hutley, J. Beringer, J. A. M. Holtum, and B. L. Turner. 2011. Photosynthetic physiology of eucalypts along a sub-continental rainfall gradient in northern Australia. Agricultural and Forest Meteorology **151**:1462-1470.

Ceulemans, R., G. Taylor, C. Bosac, D. Wilkins, and R. T. Besford. 1997. Photosynthetic acclimation to elevated CO2 in poplar grown in glasshouse cabinets or in open top chambers depends on duration of exposure. Journal of Experimental Botany **48**:1681-1689.

Chen, J. L., J. F. Reynolds, P. C. Harley, and J. D. Tenhunen. 1993. Coordination Theory of Leaf Nitrogen Distribution in a Canopy. Oecologia **93**:63-69.

Clark, D. B., L. M. Mercado, S. Sitch, C. D. Jones, N. Gedney, M. J. Best, M. Pryor, G. G. Rooney, R. L. H. Essery, E. Blyth, O. Boucher, R. J. Harding, C. Huntingford, and P. M. Cox. 2011. The Joint UK Land Environment Simulator (JULES), model description - Part 2: Carbon fluxes and vegetation dynamics. Geoscientific Model Development **4**:701-722.

Collatz, G. J., J. T. Ball, C. Grivet, and J. A. Berry. 1991. PHYSIOLOGICAL AND ENVIRONMENTAL-REGULATION OF STOMATAL CONDUCTANCE, PHOTOSYNTHESIS AND TRANSPIRATION - A MODEL THAT INCLUDES A LAMINAR BOUNDARY-LAYER. Agricultural and Forest Meteorology **54**:107-136.

Collatz, G. J., M. Ribas-Carbo, and J. A. Berry. 1992. Coupled Photosynthesis-Stomatal Conductance Model for Leaves of C4 Plants. Australian Journal of Plant Physiology **19**:519-538.

Cox, P. 2001. Hadley Centre technical note 24: Description of the TRIFFID Dynamic Global Vegetation Model. Hadley Centre, Met Office, , Bracknell, Berks.

Cox, P. M., R. A. Betts, C. D. Jones, S. A. Spall, and I. J. Totterdell. 2000. Acceleration of global warming due to carbon-cycle feedbacks in a coupled climate model. Nature **408**:184-187.

Cramer, W., A. Bondeau, F. I. Woodward, I. C. Prentice, R. A. Betts, V. Brovkin, P. M. Cox, V. Fisher, J. A. Foley, A. D. Friend, C. Kucharik, M. R. Lomas, N. Ramankutty, S. Sitch, B. Smith, A. White, and C. Young-Molling. 2001. Global response of terrestrial ecosystem structure and function to CO2 and climate change: results from six dynamic global vegetation models. Global Change Biology **7**:357-373.

Crous, K. Y., M. B. Walters, and D. S. Ellsworth. 2008. Elevated CO2 concentration affects leaf photosynthesis-nitrogen relationships in Pinus taeda over nine years in FACE. Tree Physiology **28**:607-614.

Cullingham, C. I., J. E. K. Cooke, S. Dang, C. S. Davis, B. J. Cooke, and D. W. Coltman. 2011. Mountain pine beetle host-range expansion threatens the boreal forest. Molecular Ecology **20**:2157-2171.

Curtis, P. S. 1996. A meta-analysis of leaf gas exchange and nitrogen in trees grown under elevated carbon dioxide. Plant Cell and Environment **19**:127-137.

Curtis, P. S. and X. Z. Wang. 1998. A meta-analysis of elevated CO2 effects on woody plant mass, form, and physiology. Oecologia **113**:299-313.

De Kauwe, M., B. E. Medlyn, M. Dietze, P. Hanson, T. Hickler, A. Jain, Y. Luo, R. J. Norby, R. Oren, P. E. Thornton, Y.-P. Wang, D. Wårlind, B. Parton, S. Wang, E. Weng, and S.

Zäehle. In Prep. Modelled water use efficiency response to CO2 is directly proportional to the CO2 increase.

Del Grosso, S. J., D. S. Ojima, W. J. Parton, E. Stehfest, M. Heistermann, B. DeAngelo, and S. Rose. 2009. Global scale DAYCENT model analysis of greenhouse gas emissions and mitigation strategies for cropped soils. Global and Planetary Change **67**:44-50.

Del Pozo, A., P. Perez, D. Gutierrez, A. Alonso, R. Morcuende, and R. Martinez-Carrasco. 2007. Gas exchange acclimation to elevated CO2 in upper-sunlit and lower-shaded canopy leaves in relation to nitrogen acquisition and partitioning in wheat grown in field chambers. Environmental and Experimental Botany **59**:371-380.

Delbart, N., P. Ciais, J. Chave, N. Viovy, Y. Malhi, and T. Le Toan. 2010. Mortality as a key driver of the spatial distribution of aboveground biomass in Amazonian forest: results from a dynamic vegetation model. Biogeosciences **7**:3027-3039.

Denman, K. L., G. Brasseur, A. Chidthaisong, P. Ciais, P.M. Cox, R.E. Dickinson, D. Hauglustaine, C. Heinze, E. Holland, D. Jacob, U. and S. R. Lohmann, P.L. da Silva Dias, S.C. Wofsy and X. Zhang,. 2007. Couplings Between Changes in the Climate System and Biogeochemistry. Pages 499 - 587 *in* S. Solomon, D. Qin, M. Manning, Z. Chen, M. Marquis, K.B. Averyt, M.Tignor and a. H. L. Miller, editors. Climate Change 2007: The Physical Science Basis. Contribution of Working Group I to the Fourth Assessment Report of the Intergovernmental Panel on Climate Change. Cambridge University Press, Cambridge, United Kingdom and New York, NY, USA.

Domingues, T. F., P. Meir, T. R. Feldpausch, G. Saiz, E. M. Veenendaal, F. Schrodt, M. Bird, G. Djagbletey, F. Hien, H. Compaore, A. Diallo, J. Grace, and J. Lloyd. 2010. Co-limitation of photosynthetic capacity by nitrogen and phosphorus in West Africa woodlands. Plant Cell and Environment **33**:959-980.

Drake, B. G., J. Azcon-Bieto, J. Berry, J. Bunce, P. Dijkstra, J. Farrar, R. M. Gifford, M. A. Gonzalez-Meler, G. Koch, H. Lambers, J. Siedow, and S. Wullschleger. 1999. Does elevated atmospheric CO2 concentration inhibit mitochondrial respiration in green plants? Plant Cell and Environment **22**:649-657.

Drake, B. G., M. A. GonzalezMeler, and S. P. Long. 1997. More efficient plants: A consequence of rising atmospheric CO2? Annual Review of Plant Physiology and Plant Molecular Biology **48**:609-639.

Drake, J. E., A. Gallet-Budynek, K. S. Hofmockel, E. S. Bernhardt, S. A. Billings, R. B. Jackson, K. S. Johnsen, J. Lichter, H. R. McCarthy, M. L. McCormack, D. J. P. Moore, R. Oren, S. Palmroth, R. P. Phillips, J. S. Pippen, S. G. Pritchard, K. K. Treseder, W. H. Schlesinger, E. H. DeLucia, and A. C. Finzi. 2011. Increases in the flux of carbon belowground stimulate nitrogen uptake and sustain the long-term enhancement of forest productivity under elevated CO(2). Ecology Letters **14**:349-357.

Easterling, D. R., G. A. Meehl, C. Parmesan, S. A. Changnon, T. R. Karl, and L. O. Mearns. 2000. Climate extremes: Observations, modeling, and impacts. Science **289**:2068-2074.

Elser, J. J., M. E. S. Bracken, E. E. Cleland, D. S. Gruner, W. S. Harpole, H. Hillebrand, J. T. Ngai, E. W. Seabloom, J. B. Shurin, and J. E. Smith. 2007. Global analysis of nitrogen and phosphorus limitation of primary producers in freshwater, marine and terrestrial ecosystems. Ecology Letters **10**:1135-1142.

Evans, J. R. 1989. PHOTOSYNTHESIS AND NITROGEN RELATIONSHIPS IN LEAVES OF C-3 PLANTS. Oecologia **78**:9-19.

Evans, L. S. and G. R. Hendrey. 1992. Responses of Cotton Foliage to Short-Term Fluctuations in Co-2 Partial Pressures. Critical Reviews in Plant Sciences **11**:203-212.

FAO. 2010. Global forest resources assessment, 2010-Main report. FAO Forestry Paper **163**. Rome, Italy.

Farquhar, G. D., S. V. Caemmerer, and J. A. Berry. 1980. A Biochemical-Model of Photosynthetic Co2 Assimilation in Leaves of C-3 Species. Planta **149**:78-90.

Farrar, J. F. 1985. THE RESPIRATORY SOURCE OF CO2. Plant Cell and Environment **8**:427-438.

Field, C. and H. A. Mooney. 1984. The photosynthesis-nitrogen relationship in wild plants.*in* T. J. Givnish, editor. On the economy of form and function. Cambridge University Press, Cambridge.

Finzi, A. C., D. J. P. Moore, E. H. DeLucia, J. Lichter, K. S. Hofmockel, R. B. Jackson, H.-S. Kim, R. Matamala, H. R. McCarthy, R. Oren, J. S. Pippen, and W. H. Schlesinger. 2006. PROGRESSIVE NITROGEN LIMITATION OF ECOSYSTEM PROCESSES UNDER ELEVATED CO2 IN A WARM-TEMPERATE FOREST. Ecology **87**:15-25.

Finzi, A. C., R. J. Norby, C. Calfapietra, A. Gallet-Budynek, B. Gielen, W. E. Holmes, M. R. Hoosbeek, C. M. Iversen, R. B. Jackson, M. E. Kubiske, J. Ledford, M. Liberloo, R. Oren, A. Polle, S. Pritchard, D. R. Zak, W. H. Schlesinger, and R. Ceulemans. 2007. Increases in nitrogen uptake rather than nitrogen-use efficiency support higher rates of temperate forest productivity under elevated CO2. Proceedings of the National Academy of Sciences of the United States of America **104**:14014-14019.

Flexas, J., M. Ribas-Carbo, A. Diaz-Espejo, J. Galmes, and H. Medrano. 2008. Mesophyll conductance to CO2: current knowledge and future prospects. Plant Cell and Environment **31**:602-621.

Franklin, O. 2007. Optimal nitrogen allocation controls tree responses to elevated CO2. New Phytologist **174**:811-822.

Franklin, O., R. E. McMurtrie, C. M. Iversen, K. Y. Crous, A. C. Finzi, D. T. Tissue, D. S. Ellsworth, R. Oren, and R. J. Norby. 2009. Forest fine-root production and nitrogen use under elevated CO(2): contrasting responses in evergreen and deciduous trees explained by a common principle. Global Change Biology **15**:132-144.

Friedlingstein, P., P. Cox, R. Betts, L. Bopp, W. Von Bloh, V. Brovkin, P. Cadule, S. Doney, M. Eby, I. Fung, G. Bala, J. John, C. Jones, F. Joos, T. Kato, M. Kawamiya, W. Knorr, K. Lindsay, H. D. Matthews, T. Raddatz, P. Rayner, C. Reick, E. Roeckner, K. G. Schnitzler, R. Schnur, K. Strassmann, A. J. Weaver, C. Yoshikawa, and N. Zeng. 2006. Climate-carbon cycle feedback analysis: Results from the (CMIP)-M-4 model intercomparison. Journal of Climate **19**:3337-3353.

Friend, A. D., A. K. Stevens, R. G. Knox, and M. G. R. Cannell. 1997. A process-based, terrestrial biosphere model of ecosystem dynamics (Hybrid v3.0). Ecological Modelling **95**:249-287.

Fuhrer, J., M. Beniston, A. Fischlin, C. Frei, S. Goyette, K. Jasper, and C. Pfister. 2006. Climate risks and their impact on agriculture and forests in Switzerland. Climatic Change **79**:79-102.

Garten, C. T., Jr., C. M. Iversen, and R. J. Norby. 2011. Litterfall (15)N abundance indicates declining soil nitrogen availability in a free-air CO(2) enrichment experiment. Ecology **92**:133-139.

Gill, R. A., L. J. Anderson, H. W. Polley, H. B. Johnson, and R. B. Jackson. 2006. POTENTIAL NITROGEN CONSTRAINTS ON SOIL CARBON SEQUESTRATION UNDER LOW AND ELEVATED ATMOSPHERIC CO2. Ecology **87**:41-52.

Gill, R. A., H. W. Polley, H. B. Johnson, L. J. Anderson, H. Maherali, and R. B. Jackson. 2002. Nonlinear grassland responses to past and future atmospheric CO2. Nature **417**:279-282.

GLC2000 database. 2003. The Global Land Cover Map for the Year 2000.*in* E. C. J. R.

Centre, editor.
Goetz, S. J., A. G. Bunn, G. J. Fiske, and R. A. Houghton. 2005. Satellite-observed photosynthetic trends across boreal North America associated with climate and fire disturbance. Proceedings of the National Academy of Sciences of the United States of America **102**:13521-13525.
Goodale, C. L., M. J. Apps, R. A. Birdsey, C. B. Field, L. S. Heath, R. A. Houghton, J. C. Jenkins, G. H. Kohlmaier, W. Kurz, S. R. Liu, G. J. Nabuurs, S. Nilsson, and A. Z. Shvidenko. 2002. Forest carbon sinks in the Northern Hemisphere. Ecological Applications **12**:891-899.
Gurevitch, J. and L. V. Hedges. 1999. Statistical issues in ecological meta-analyses. Ecology **80**:1142-1149.
Gutschick, V. P. 2007. Plant acclimation to elevated CO2- Frorn simple regularities to biogeographic chaos. Ecological Modelling **200**:433-451.
Haehnel, W. 1984. PHOTOSYNTHETIC ELECTRON-TRANSPORT IN HIGHER-PLANTS. Annual Review of Plant Physiology and Plant Molecular Biology **35**:659-693.
Hatzianastassiou, N., C. Matsoukas, A. Fotiadi, K. G. Pavlakis, E. Drakakis, D. Hatzidimitriou, and I. Vardavas. 2005. Global distribution of Earth's surface shortwave radiation budget. Atmospheric Chemistry and Physics **5**:2847-2867.
Haxeltine, A. and I. C. Prentice. 1996. A general model for the light-use efficiency of primary production. Functional Ecology **10**:551-561.
Heinen, R. B., Q. Ye, and F. Chaumont. 2009. Role of aquaporins in leaf physiology. Journal of Experimental Botany **60**:2971-2985.
Hendrey, G. R. 1992. Global Greenhouse Studies - Need for a New Approach to Ecosystem Manipulation. Critical Reviews in Plant Sciences **11**:61-74.
Hendrey, G. R. and B. A. Kimball. 1994. The Face Program. Agricultural and Forest Meteorology **70**:3-14.
Hendrey, G. R., K. F. Lewin, and J. Nagy. 1993. Free Air Carbon-Dioxide Enrichment - Development, Progress, Results. Vegetatio **104**:17-31.
Hendrey, G. R., S. P. Long, I. F. McKee, and N. R. Baker. 1997. Can photosynthesis respond to short-term fluctuations in atmospheric carbon dioxide? Photosynthesis Research **51**:179-184.
Hickler, T., I. C. Prentice, B. Smith, M. T. Sykes, and S. Zaehle. 2006. Implementing plant hydraulic architecture within the LPJ Dynamic Global Vegetation Model. Global Ecology and Biogeography **15**:567-577.
Hickler, T., B. Smith, I. C. Prentice, K. Mjofors, P. Miller, A. Arneth, and M. T. Sykes. 2008. CO2 fertilization in temperate FACE experiments not representative of boreal and tropical forests. Global Change Biology **14**:1531-1542.
Hickler, T., B. Smith, M. T. Sykes, M. B. Davis, S. Sugita, and K. Walker. 2004. Using a generalized vegetation model to simulate vegetation dynamics in northeastern USA. Ecology **85**:519-530.
Hogg, E. H., J. P. Brandt, and M. Michaellian. 2008. Impacts of a regional drought on the productivity, dieback, and biomass of western Canadian aspen forests. Canadian Journal of Forest Research-Revue Canadienne De Recherche Forestiere **38**:1373-1384.
Holtum, J. A. M. and K. Winter. 2003. Photosynthetic CO2 uptake in seedlings of two tropical tree species exposed to oscillating elevated concentrations of CO2. Planta **218**:152-158.
Houghton, R. A. 2003. Revised estimates of the annual net flux of carbon to the atmosphere from changes in land use and land management 1850-2000. Tellus Series B-Chemical and Physical Meteorology **55**:378-390.
Houghton, R. A., F. Hall, and S. J. Goetz. 2009. Importance of biomass in the global carbon

cycle. Journal of Geophysical Research-Biogeosciences **114**.
Hungate, B. A., J. S. Dukes, M. R. Shaw, Y. Q. Luo, and C. B. Field. 2003. Nitrogen and climate change. Science **302**:1512-1513.
Huntingford, C., B. B. B. Booth, S. Sitch, N. Gedney, J. A. Lowe, S. K. Liddicoat, L. M. Mercado, M. J. Best, G. P. Weedon, R. A. Fisher, M. R. Lomas, P. Good, P. Zelazowski, A. C. Everitt, A. C. Spessa, and C. D. Jones. 2010. IMOGEN: an intermediate complexity model to evaluate terrestrial impacts of a changing climate. Geoscientific Model Development **3**:679-687.
Huntingford, C. and P. M. Cox. 2000. An analogue model to derive additional climate change scenarios from existing GCM simulations. Climate Dynamics **16**:575-586.
Huntingford, C., P. M. Cox, L. M. Mercado, S. Sitch, N. Bellouin, O. Boucher, and N. Gedney. 2011. Highly contrasting effects of different climate forcing agents on terrestrial ecosystem services. Philosophical Transactions of the Royal Society a-Mathematical Physical and Engineering Sciences **369**:2026-2037.
Huntingford, C., R. A. Fisher, L. Mercado, B. B. B. Booth, S. Sitch, P. P. Harris, P. M. Cox, C. D. Jones, R. A. Betts, Y. Malhi, G. R. Harris, M. Collins, and P. Moorcroft. 2008. Towards quantifying uncertainty in predictions of Amazon 'dieback'. Philosophical Transactions of the Royal Society B-Biological Sciences **363**:1857-1864.
Huntingford, C., D. Galbraith, P. Zelazowski, L. M. Mercado, S. Sitch, R. Fisher, M. Lomas, A. Walker, C. D. Jones, B. B. B. Booth, Y. Malhi, P. M. Cox, D. Hemming, G. Kay, P. Good, S. L. Lewis, O. L. Phillips, O. K. Atkin, J. Lloyd, M. Gloor, J. Zaragoza-Castells, P. Meir, R. Betts, P. P. Harris, C. Nobre, and J. Marengo. Submitted. Stability of Tropical Rainforests in a Changing Climate. . Nature Geoscience.
Huntingford, C., P. P. Harris, N. Gedney, P. M. Cox, R. A. Betts, J. A. Marengo, and J. H. C. Gash. 2004. Using a GCM analogue model to investigate the potential for Amazonian forest dieback. Theoretical and Applied Climatology **78**:177-185.
Huntingford, C., J. A. Lowe, B. B. B. Booth, C. D. Jones, G. R. Harris, L. K. Gohar, and P. Meir. 2009. Contributions of carbon cycle uncertainty to future climate projection spread. Tellus Series B-Chemical and Physical Meteorology **61**:355-360.
Idso, S. B. 1999. The long-term response of trees to atmospheric CO2 enrichment. Global Change Biology **5**:493-495.
IPCC. 2007. Climate Change 2007: The Physical Science Basis. Contribution of Working Group I to the Fourth Assessment Report of the Intergovernmental Panel on Climate Change. Cambridge University Press, Cambridge, United Kingdom and New York, NY, USA.
IPCC. 2011. Data Distribution Centre.
Iversen, C. M. 2010. Digging deeper: fine-root responses to rising atmospheric CO(2) concentration in forested ecosystems. New Phytologist **186**:346-357.
Iversen, C. M., T. D. Hooker, A. T. Classen, and R. J. Norby. 2011. Net mineralization of N at deeper soil depths as a potential mechanism for sustained forest production under elevated CO(2). Global Change Biology **17**:1130-1139.
Jain, A. K. and X. J. Yang. 2005. Modeling the effects of two different land cover change data sets on the carbon stocks of plants and soils in concert with CO2 and climate change. Global Biogeochemical Cycles **19**.
Johnson, D. W. 2006. PROGRESSIVE N LIMITATION IN FORESTS: REVIEW AND IMPLICATIONS FOR LONG-TERM RESPONSES TO ELEVATED CO2. Ecology **87**:64-75.
Jordan, D. N., S. F. Zitzer, G. R. Hendrey, K. F. Lewin, J. Nagy, R. S. Nowak, S. D. Smith, J. S. Coleman, and J. R. Seeman. 1999. Biotic, abiotic and performance aspects of the Nevada Desert Free-Air CO2 Enrichment (FACE) Facility. Global Change Biology

5:659-668.

Jung, M., M. Reichstein, H. A. Margolis, A. Cescatti, A. D. Richardson, M. A. Arain, A. Arneth, C. Bernhofer, D. Bonal, J. Chen, D. Gianelle, N. Gobron, G. Kiely, W. Kutsch, G. Lasslop, B. E. Law, A. Lindroth, L. Merbold, L. Montagnani, E. J. Moors, D. Papale, M. Sottocornola, F. Vaccari, and C. Williams. 2011. Global patterns of land-atmosphere fluxes of carbon dioxide, latent heat, and sensible heat derived from eddy covariance, satellite, and meteorological observations. Journal of Geophysical Research-Biogeosciences **116**.

Karl, T. R., R. W. Knight, and N. Plummer. 1995. TRENDS IN HIGH-FREQUENCY CLIMATE VARIABILITY IN THE 20TH-CENTURY. Nature **377**:217-220.

Kattge, J. and S. Diaz and S. Lavorel and C. Prentice and P. Leadley and G. Boenisch and E. Garnier and M. Westoby and P. B. Reich and I. J. Wright and J. H. C. Cornelissen and C. Violle and S. P. Harrison and P. M. van Bodegom and M. Reichstein and B. J. Enquist and N. A. Soudzilovskaia and D. D. Ackerly and M. Anand and O. Atkin and M. Bahn and T. R. Baker and D. Baldocchi and R. Bekker and C. C. Blanco and B. Blonder and W. J. Bond and R. Bradstock and D. E. Bunker and F. Casanoves and J. Cavender-Bares and J. Q. Chambers and F. S. Chapin, III and J. Chave and D. Coomes and W. K. Cornwell and J. M. Craine and B. H. Dobrin and L. Duarte and W. Durka and J. Elser and G. Esser and M. Estiarte and W. F. Fagan and J. Fang and F. Fernandez-Mendez and A. Fidelis and B. Finegan and O. Flores and H. Ford and D. Frank and G. T. Freschet and N. M. Fyllas and R. V. Gallagher and W. A. Green and A. G. Gutierrez and T. Hickler and S. I. Higgins and J. G. Hodgson and A. Jalili and S. Jansen and C. A. Joly and A. J. Kerkhoff and D. Kirkup and K. Kitajima and M. Kleyer and S. Klotz and J. M. H. Knops and K. Kramer and I. Kuehn and H. Kurokawa and D. Laughlin and T. D. Lee and M. Leishman and F. Lens and T. Lenz and S. L. Lewis and J. Lloyd and J. Llusia and F. Louault and S. Ma and M. D. Mahecha and P. Manning and T. Massad and B. E. Medlyn and J. Messier and A. T. Moles and S. C. Mueller and K. Nadrowski and S. Naeem and U. Niinemets and S. Noellert and A. Nueske and R. Ogaya and J. Oleksyn and V. G. Onipchenko and Y. Onoda and J. Ordonez and G. Overbeck and W. A. Ozinga and S. Patino and S. Paula and J. G. Pausas and J. Penuelas and O. L. Phillips and V. Pillar and H. Poorter and L. Poorter and P. Poschlod and A. Prinzing and R. Proulx and A. Rammig and S. Reinsch and B. Reu and L. Sack and B. Salgado-Negre and J. Sardans and S. Shiodera and B. Shipley and A. Siefert and E. Sosinski and J. F. Soussana and E. Swaine and N. Swenson and K. Thompson and P. Thornton and M. Waldram and E. Weiher and M. White and S. White and S. J. Wright and B. Yguel and S. Zaehle and A. E. Zanne and C. Wirth. 2011. TRY - a global database of plant traits. Global Change Biology **17**:2905-2935.

Kattge, J., W. Knorr, T. Raddatz, and C. Wirth. 2009. Quantifying photosynthetic capacity and its relationship to leaf nitrogen content for global-scale terrestrial biosphere models. Global Change Biology **15**:976-991.

Kazantzidis, A., K. Eleftheratos, and C. S. Zerefos. 2011. Effects of cirrus cloudiness on solar irradiance in four spectral bands. Atmospheric Research **102**:452-459.

Körner, C. 2003. Carbon limitation in trees. Journal of Ecology **91**:4-17.

Körner, C. 2009. Biological Carbon Sinks: Turnover Must Not Be Confused with Capital! Gaia-Ecological Perspectives for Science and Society **18**:288-293.

Körner, C., R. Asshoff, O. Bignucolo, S. Hattenschwiler, S. G. Keel, S. Pelaez-Riedl, S. Pepin, R. T. W. Siegwolf, and G. Zotz. 2005. Carbon flux and growth in mature deciduous forest trees exposed to elevated CO2. Science **309**:1360-1362.

Krinner, G., N. Viovy, N. de Noblet-Ducoudre, J. Ogee, J. Polcher, P. Friedlingstein, P. Ciais, S. Sitch, and I. C. Prentice. 2005. A dynamic global vegetation model for studies of

the coupled atmosphere-biosphere system. Global Biogeochemical Cycles **19**.
Kurasova, I., J. Kalina, O. Urban, M. Stroch, and V. Spunda. 2003. Acclimation of two distinct plant species, spring barley and Norway spruce, to combined effect of various irradiance and CO2 concentration during cultivation in controlled environment. Photosynthetica **41**:513-523.
Lal, R. 2008. Soil carbon stocks under present and future climate with specific reference to European ecoregions. Nutrient Cycling in Agroecosystems **81**:113-127.
Lawrence, D. M., K. W. Oleson, M. G. Flanner, P. E. Thornton, N. Swenson, P. J. Lawrence, X. Zeng, Z.-L. Yang, S. Levis, K. Sakaguchi, G. B. Bonan, and A. G. Slater. 2011. Parameterization improvements and functional and struuctural advances in Version $ of the Community Land Model. Journal of advances in Modelling Earth Systems **3**:27.
Lawrence, P. J. and T. N. Chase. 2007. Representing a new MODIS consistent land surface in the Community Land Model (CLM 3.0). Journal of Geophysical Research-Biogeosciences **112**.
Le Quéré, C., M. R. Raupach, J. G. Canadell, G. Marland, L. Bopp, P. Ciais, T. J. Conway, S. C. Doney, R. A. Feely, P. Foster, P. Friedlingstein, K. Gurney, R. A. Houghton, J. I. House, C. Huntingford, P. E. Levy, M. R. Lomas, J. Majkut, N. Metzl, J. P. Ometto, G. P. Peters, I. C. Prentice, J. T. Randerson, S. W. Running, J. L. Sarmiento, U. Schuster, S. Sitch, T. Takahashi, N. Viovy, G. R. van der Werf, and F. I. Woodward. 2009. Trends in the sources and sinks of carbon dioxide. Nature Geoscience **2**:831-836.
Leakey, A. D. B., E. A. Ainsworth, C. J. Bernacchi, A. Rogers, S. P. Long, and D. R. Ort. 2009. Elevated CO2 effects on plant carbon, nitrogen, and water relations: six important lessons from FACE. Journal of Experimental Botany **60**:2859-2876.
Legget, J., W. J. Pepper, R. J. Swart, J. Edmonds, L. G. M. Filho, I. Mintzer, M. X. Wang, and J. Watson. 1992. Emissions scenarios for the IPCC: an update. Climate Change 1992: The Supplementary Report to The IPCC Scientific Assessment. Cambridge University Press, Cambridge.
Leuzinger, S. and C. Korner. 2007. Water savings in mature deciduous forest trees under elevated CO2. Global Change Biology **13**:2498-2508.
Liberloo, M., C. Calfapietra, M. Lukac, D. Godbold, Z. B. Luos, A. Polle, M. R. Hoosbeek, O. Kull, M. Marek, C. Raines, M. Rubino, G. Taylor, G. Scarascia-Mugnozza, and R. Ceulemans. 2006. Woody biomass production during the second rotation of a bio-energy Populus plantation increases in a future high CO2 world. Global Change Biology **12**:1094-1106.
Lindroth, A., L. Klemedtsson, A. Grelle, P. Weslien, and O. Langvall. 2008. Measurement of net ecosystem exchange, productivity and respiration in three spruce forests in Sweden shows unexpectedly large soil carbon losses. Biogeochemistry **89**:43-60.
Liu, S., Y. L. Li, G. Y. Zhou, K. O. Wenigmann, Y. Luo, D. Otieno, and J. Tenhunen. 2009. Applying biomass and stem fluxes to quantify temporal and spatial fluctuations of an old-growth forest in disturbance. Biogeosciences **6**:1839-1848.
Lloyd, J., S. Patino, R. Q. Paiva, G. B. Nardoto, C. A. Quesada, A. J. B. Santos, T. R. Baker, W. A. Brand, I. Hilke, H. Gielmann, M. Raessler, F. J. Luizao, L. A. Martinelli, and L. M. Mercado. 2010. Optimisation of photosynthetic carbon gain and within-canopy gradients of associated foliar traits for Amazon forest trees. Biogeosciences **7**:1833-1859.
Luo, Y., C. B. Field, and R. B. Jackson. 2006a. Does Nitrogen Constrain Carbon Cycling, or Does Carbon Input Stimulate Nitrogen Cycling?1. Ecology **87**:3-4.
Luo, Y., D. Hui, and D. Zhang. 2006b. ELEVATED CO2 STIMULATES NET ACCUMULATIONS OF CARBON AND NITROGEN IN LAND ECOSYSTEMS: A META-ANALYSIS. Ecology **87**:53-63.

Luyssaert, S., P. Ciais, S. L. Piao, E. D. Schulze, M. Jung, S. Zaehle, M. J. Schelhaas, M. Reichstein, G. Churkina, D. Papale, G. Abril, C. Beer, J. Grace, D. Loustau, G. Matteucci, F. Magnani, G. J. Nabuurs, H. Verbeeck, M. Sulkava, G. R. van der Werf, I. A. Janssens, and C.-I. S. Team. 2010. The European carbon balance. Part 3: forests. Global Change Biology **16**:1429-1450.

Luyssaert, S., I. Inglima, M. Jung, A. D. Richardson, M. Reichsteins, D. Papale, S. L. Piao, E. D. Schulzes, L. Wingate, G. Matteucci, L. Aragao, M. Aubinet, C. Beers, C. Bernhoffer, K. G. Black, D. Bonal, J. M. Bonnefond, J. Chambers, P. Ciais, B. Cook, K. J. Davis, A. J. Dolman, B. Gielen, M. Goulden, J. Grace, A. Granier, A. Grelle, T. Griffis, T. Gruenwald, G. Guidolotti, P. J. Hanson, R. Harding, D. Y. Hollinger, L. R. Hutyra, P. Kolar, B. Kruijt, W. Kutsch, F. Lagergren, T. Laurila, B. E. Law, G. Le Maire, A. Lindroth, D. Loustau, Y. Malhi, J. Mateus, M. Migliavacca, L. Misson, L. Montagnani, J. Moncrieff, E. Moors, J. W. Munger, E. Nikinmaa, S. V. Ollinger, G. Pita, C. Rebmann, O. Roupsard, N. Saigusa, M. J. Sanz, G. Seufert, C. Sierra, M. L. Smith, J. Tang, R. Valentini, T. Vesala, and I. A. Janssens. 2007. CO(2) balance of boreal, temperate, and tropical forests derived from a global database. Global Change Biology **13**:2509-2537.

Ma, H. L., J. G. Zhu, Z. B. Xie, G. Liu, Q. Zeng, and Y. Han. 2007. Responses of rice and winter wheat to free-air CO2 enrichment (China FACE) at rice/wheat rotation system. Plant and Soil **294**:137-146.

Malhi, Y., D. Wood, T. R. Baker, J. Wright, O. L. Phillips, T. Cochrane, P. Meir, J. Chave, S. Almeida, L. Arroyo, N. Higuchi, T. J. Killeen, S. G. Laurance, W. F. Laurance, S. L. Lewis, A. Monteagudo, D. A. Neill, P. N. Vargas, N. C. A. Pitman, C. A. Quesada, R. Salomao, J. N. M. Silva, A. T. Lezama, J. Terborgh, R. V. Martinez, and B. Vinceti. 2006. The regional variation of aboveground live biomass in old-growth Amazonian forests. Global Change Biology **12**:1107-1138.

McCarthy, H. R., R. Oren, A. C. Finzi, D. S. Ellsworth, H.-S. Kim, K. H. Johnsen, and B. Millar. 2007. Temporal dynamics and spatial variability in the enhancement of canopy leaf area under elevated atmospheric CO2. Global Change Biology **13**:2479-2497.

McCarthy, H. R., R. Oren, K. H. Johnsen, A. Gallet-Budynek, S. G. Pritchard, C. W. Cook, S. L. LaDeau, R. B. Jackson, and A. C. Finzi. 2010. Re-assessment of plant carbon dynamics at the Duke free-air CO(2) enrichment site: interactions of atmospheric CO(2) with nitrogen and water availability over stand development. New Phytologist **185**:514-528.

McDowell, N. G., D. J. Beerling, D. D. Breshears, R. A. Fisher, K. F. Raffa, and M. Stitt. 2011. The interdependence of mechanisms underlying climate-driven vegetation mortality. Trends in Ecology & Evolution **26**:523-532.

McGroddy, M. E., T. Daufresne, and L. O. Hedin. 2004. Scaling of C : N : P stoichiometry in forests worldwide: Implications of terrestrial redfield-type ratios. Ecology **85**:2390-2401.

McGuire, A. D., R. W. Macdonald, E. A. G. Schuur, J. W. Harden, P. Kuhry, D. J. Hayes, T. R. Christensen, and M. Heimann. 2010. The carbon budget of the northern cryosphere region. Current Opinion in Environmental Sustainability **2**:231-236.

Medlyn, B. E. and P. G. Jarvis. 1999. Design and use of a database of model parameters from elevated CO2 experiments. Ecological Modelling **124**:69-83.

Medlyn, B. E., R. E. McMurtrie, R. C. Dewar, and M. P. Jeffreys. 2000. Soil processes dominate the long-term response of forest net primary productivity to increased temperature and atmospheric CO2 concentration. Canadian Journal of Forest Research-Revue Canadienne De Recherche Forestiere **30**:873-888.

Meir, P., P. E. Levy, J. Grace, and P. G. Jarvis. 2007. Photosynthetic parameters from two contrasting woody vegetation types in West Africa. Plant Ecology **192**:277-287.

Mercado, L. M., N. Bellouin, S. Sitch, O. Boucher, C. Huntingford, M. Wild, and P. M. Cox. 2009. Impact of changes in diffuse radiation on the global land carbon sink. Nature **458**:1014-U1087.

Mercado, L. M., C. Huntingford, J. H. C. Gash, P. M. Cox, and V. Jogireddy. 2007. Improving the representation of radiation interception and photosynthesis for climate model applications. Tellus Series B-Chemical and Physical Meteorology **59**:553-565.

Mercado, L. M., S. Patino, T. F. Domingues, N. M. Fyllas, G. P. Weedon, S. Sitch, C. A. Quesada, O. L. Phillips, L. E. O. C. Aragao, Y. Malhi, A. J. Dolman, N. Restrepo-Coupe, S. R. Saleska, T. R. Baker, S. Almeida, N. Higuchi, and J. Lloyd. 2011. Variations in Amazon forest productivity correlated with foliar nutrients and modelled rates of photosynthetic carbon supply. Philosophical Transactions of the Royal Society B-Biological Sciences **366**:3316-3329.

Migliavacca, M., M. Reichstein, A. D. Richardson, R. Colombo, M. A. Sutton, G. Lasslop, E. Tomelleri, G. Wohlfahrt, N. Carvalhais, A. Cescatti, M. D. Mahecha, L. Montagnani, D. Papale, S. Zaehle, A. Arain, A. Arneth, T. A. Black, A. Carrara, S. Dore, D. Gianelle, C. Helfter, D. Hollinger, W. L. Kutsch, P. M. Lafleur, Y. Nouvellon, C. Rebmann, H. R. da Rocha, M. Rodeghiero, O. Roupsard, M.-T. Sebastia, G. Seufert, J.-F. Soussana, and M. K. van der Molen. 2011. Semiempirical modeling of abiotic and biotic factors controlling ecosystem respiration across eddy covariance sites. Global Change Biology **17**:390-409.

Miglietta, F., M. R. Hoosbeek, J. Foot, F. Gigon, A. Hassinen, M. Heijmans, A. Peressotti, T. Saarinen, N. van Breemen, and B. Wallen. 2001a. Spatial and temporal performance of the MiniFACE (Free Air CO2 Enrichment) system on bog ecosystems in northern and central Europe. Environmental Monitoring and Assessment **66**:107-127.

Miglietta, F., A. Peressotti, F. P. Vaccari, A. Zaldei, P. deAngelis, and G. Scarascia-Mugnozza. 2001b. Free-air CO2 enrichment (FACE) of a poplar plantation: the POPFACE fumigation system. New Phytologist **150**:465-476.

Millard, P., M. Sommerkorn, and G. A. Grelet. 2007. Environmental change and carbon limitation in trees: a biochemical, ecophysiological and ecosystem appraisal. New Phytologist **175**:11-28.

Moorcroft, P. R., G. C. Hurtt, and S. W. Pacala. 2001. A method for scaling vegetation dynamics: The ecosystem demography model (ED). Ecological Monographs **71**:557-585.

Moss, R. H., J. A. Edmonds, K. A. Hibbard, M. R. Manning, S. K. Rose, D. P. van Vuuren, T. R. Carter, S. Emori, M. Kainuma, T. Kram, G. A. Meehl, J. F. B. Mitchell, N. Nakicenovic, K. Riahi, S. J. Smith, R. J. Stouffer, A. M. Thomson, J. P. Weyant, and T. J. Wilbanks. 2010. The next generation of scenarios for climate change research and assessment. Nature **463**:747-756.

Muller, B., F. Pantin, M. Genard, O. Turc, S. Freixes, M. Piques, and Y. Gibon. 2011. Water deficits uncouple growth from photosynthesis, increase C content, and modify the relationships between C and growth in sink organs. Journal of Experimental Botany **62**:1715-1729.

Nagy, J., K. F. Lewin, G. R. Hendrey, E. Hassinger, and R. Lamorte. 1994. Face Facility Co2 Concentration Control and Co2 Use in 1990 and 1991. Agricultural and Forest Meteorology **70**:31-48.

Nagy, J., K. F. Lewin, G. R. Hendrey, F. W. Lipfert, and M. L. Daum. 1992. Face Facility Engineering Performance in 1989. Critical Reviews in Plant Science **11**:165-185.

Nakicenovic, N., J. Alcamo, G. Davis, B. de Vries, J. Fenhann, S. Gaffin, K. Gregory, A. Gr&#xfffd;bler, T. Yong Jung, T. Kram, E. Lebre La Rovere, L. Michaelis, S. Mori, T. Morita,

W. Pepper, H. Pitcher, L. Price, K. Riahi, A. Roehrl, H.-H. Rogner, A. Sankovski, M. Schlesinger, P. Shukla, S. Smith, R. Swart, S. van Rooijen, N. Victor, and Z. Dadi. 2000. IPCC: Special Report on Emissions Scenarios. Cambridge University Press.

New, M., M. Hulme, and P. Jones. 1999. Representing twentieth-century space-time climate variability. Part I: Development of a 1961-90 mean monthly terrestrial climatology. Journal of Climate **12**:829-856.

New, M., M. Hulme, and P. Jones. 2000. Representing twentieth-century space-time climate variability. Part II: Development of 1901-96 monthly grids of terrestrial surface climate. Journal of Climate **13**:2217-2238.

Niinemets, U. 1999. Components of leaf dry mass per area - thickness and density - alter leaf photosynthetic capacity in reverse directions in woody plants. New Phytologist **144**:35-47.

Norby RJ, Warren JM, Iversen CM, M. BE, McMurtrie RE, and H. FM. 2008. Nitrogen limitation is reducing the enhancement of NPP by elevated CO2 in a deciduous forest. Pages B32B-05 *in* Eos Trans. AGU. Fall Meet. Suppl.

Norby, R. J., E. H. DeLucia, B. Gielen, C. Calfapietra, C. P. Giardina, J. S. King, J. Ledford, H. R. McCarthy, D. J. P. Moore, R. Ceulemans, P. De Angelis, A. C. Finzi, D. F. Karnosky, M. E. Kubiske, M. Lukac, K. S. Pregitzer, G. E. Scarascia-Mugnozza, W. H. Schlesinger, and R. Oren. 2005. Forest response to elevated CO2 is conserved across a broad range of productivity. Proceedings of the National Academy of Sciences of the United States of America **102**:18052-18056.

Norby, R. J. and C. M. Iversen. 2006. Nitrogen uptake, distribution, turnover, and efficiency of use in a CO2-enriched sweetgum forest. Ecology **87**:5-14.

Norby, R. J., D. E. Todd, J. Fults, and D. W. Johnson. 2001. Allometric determination of tree growth in a CO2-enriched sweetgum stand. New Phytologist **150**:477-487.

Norby, R. J., J. M. Warren, C. M. Iversen, B. E. Medlyn, and R. E. McMurtrie. 2010. CO(2) enhancement of forest productivity constrained by limited nitrogen availability. Proceedings of the National Academy of Sciences of the United States of America **107**:19368-19373.

Okada, M., M. Lieffering, H. Nakamura, M. Yoshimoto, H. Y. Kim, and K. Kobayashi. 2001. Free-air CO2 enrichment (FACE) using pure CO2 injection: system description. New Phytologist **150**:251-260.

Oleson, K. W., D. M. Lawrence, G. B. Bonan, M. G. Flanner, E. Kluzek, P. J. Lawrence, S. Levis, S. C. Swenson, P. E. Thornton, A. Dai, M. Decker, R. Dickinson, J. Feddema, C. L. Heald, F. Hoffman, J.-F. Lamarque, N. Mahowald, G.-Y. Niu, T. Qian, J. Randerson, S. Running, K. Sakaguchi, A. Slater, R. Stöckli, A. Wang, Z.-L. Yang, X. Zeng, and X. Zeng. 2010. Technical Description of version 4.0 of the Community Land Model (CLM). National Centre for Atmospheric Research, Boulder, CO.

Ordonez, J. C., P. M. van Bodegom, J.-P. M. Witte, I. J. Wright, P. B. Reich, and R. Aerts. 2009. A global study of relationships between leaf traits, climate and soil measures of nutrient fertility. Global Ecology and Biogeography **18**:137-149.

Oren, R., D. S. Ellsworth, K. H. Johnsen, N. Phillips, B. E. Ewers, C. Maier, K. V. R. Schafer, H. McCarthy, G. Hendrey, S. G. McNulty, and G. G. Katul. 2001. Soil fertility limits carbon sequestration by forest ecosystems in a CO2-enriched atmosphere. Nature **411**:469-472.

Pachepsky, L. B., J. D. Haskett, and B. Acock. 1996. An adequate model of photosynthesis .1. Parameterization, validation and comparison of models. Agricultural Systems **50**:209-225.

Papale, D., M. Reichstein, M. Aubinet, E. Canfora, C. Bernhofer, W. Kutsch, B. Longdoz, S. Rambal, R. Valentini, T. Vesala, and D. Yakir. 2006. Towards a standardized processing of Net Ecosystem Exchange measured with eddy covariance technique:

algorithms and uncertainty estimation. Biogeosciences **3**:571-583.
Parry, M. L., O. F. Canziani, J. P. Palutikof, P. J. ven der Linden, and C. E. Hanson, editors. 2007. Contribution of Working Group II to the Fouth Assessment Report of the Intergovernmental Panel on Climate Change, 2007. Cambridge University Press, Cambridge, UK & New York, USA.
Pepin, S. and C. Körner. 2002. Web-FACE: a new canopy free-air CO2 enrichment system for tall trees in mature forests. Oecologia **133**:1-9.
Peters, G. P., G. Marland, C. Le Quere, T. Boden, J. G. Canadell, and M. R. Raupach. 2012. CORRESPONDENCE: Rapid growth in CO2 emissions after the 2008-2009 global financial crisis. Nature Climate Change **2**:2-4.
Pinheiro, J., D. Bates, S. DebRoy, D. Sarkar, and R. D. C. Team. 2011. nlme: Linear and Nonlinear Mixed Effects Models.
Pitman, A. J. 2003. The evolution of, and revolution in, land surface schemes designed for climate models. International Journal of Climatology **23**:479-510.
Pongratz, J., T. Raddatz, C. H. Reick, M. Esch, and M. Claussen. 2009. Radiative forcing from anthropogenic land cover change since AD 800. Geophysical Research Letters **36**.
Pongratz, J., C. H. Reick, T. Raddatz, and M. Claussen. 2010. Biogeophysical versus biogeochemical climate response to historical anthropogenic land cover change. Geophysical Research Letters **37**.
Poorter, H., U. Niinemets, L. Poorter, I. J. Wright, and R. Villar. 2009. Causes and consequences of variation in leaf mass per area (LMA): a meta-analysis (vol 182, pg 565, 2009). New Phytologist **183**:1222-1222.
Post, W. M., W. R. Emanuel, P. J. Zinke, and A. G. Stangenberger. 1982. SOIL CARBON POOLS AND WORLD LIFE ZONES. Nature **298**:156-159.
PPSystems. 2003. CIRAS1 Portable Photosynthesis System. Operators Manual. Version 1.30 edition. PP Systems, Amesbury.
Quesada, C. A., J. Lloyd, L. O. Anderson, N. M. Fyllas, M. Schwarz, and C. I. Czimczik. 2011. Soils of Amazonia with particular reference to the RAINFOR sites. Biogeosciences **8**:1415-1440.
Quesada, C. A., J. Lloyd, M. Schwarz, S. Patino, T. R. Baker, C. Czimczik, N. M. Fyllas, L. Martinelli, G. B. Nardoto, J. Schmerler, A. J. B. Santos, M. G. Hodnett, R. Herrera, F. J. Luizao, A. Arneth, G. Lloyd, N. Dezzeo, I. Hilke, I. Kuhlmann, M. Raessler, W. A. Brand, H. Geilmann, J. O. Moraes Filho, F. P. Carvalho, R. N. Araujo Filho, J. E. Chaves, O. F. Cruz Junior, T. P. Pimentel, and R. Paiva. 2010. Variations in chemical and physical properties of Amazon forest soils in relation to their genesis. Biogeosciences **7**:1515-1541.
Quegan, S., Beer, C., Shvidenko, A., Mccallum, I., Handoh, I. C., Peylin, P., Rödenbeck, C., Lucht, W., Nilsson, S., and Schmullius C. 2011 Estimating the carbon balance of central Siberia using a landscape-ecosystem approach, atmospheric inversion and Dynamic GLobal Vegetation Models. Global Change Biology. **17**:351-365
R Core Development Team. 2011. R: A language and environment for statistical computing. R Foundation for Statistical Computing, Vienna.
Randall, D. A., R.A. Wood, S. Bony, R. Colman, T. Fichefet, J. Fyfe, V. Kattsov, A. Pitman, J. Shukla, J. Srinivasan, R.J. Stouffer, A. Sumi and a. K. E. Taylor. 2007. Cilmate Models and Their Evaluation.*in* S. Solomon, D. Qin, M. Manning, and M. M. Z. Chen, K.B. Averyt, M.Tignor and H.L. Miller, editors. Climate Change 2007: The Physical Science Basis. Contribution of Working Group I to the Fourth Assessment Report of the Intergovernmental Panel on Climate Change. Cambridge University Press, , Cambridge, UK and New York, NY, USA.
Reich, P. B., S. E. Hobbie, T. Lee, D. S. Ellsworth, J. B. West, D. Tilman, J. M. H. Knops, S.

Naeem, and J. Trost. 2006a. Nitrogen limitation constrains sustainability of ecosystem response to CO2. Nature **440**:922-925.

Reich, P. B., J. Knops, D. Tilman, J. Craine, D. Ellsworth, M. Tjoelker, T. Lee, D. Wedin, S. Naeem, D. Bahauddin, G. Hendrey, S. Jose, K. Wrage, J. Goth, and W. Bengston. 2001. Plant diversity enhances ecosystem responses to elevated CO2 and nitrogen deposition. Nature **410**:809-812.

Reich, P. B. and J. Oleksyn. 2004. Global patterns of plant leaf N and P in relation to temperature and latitude. Proceedings of the National Academy of Sciences of the United States of America **101**:11001-11006.

Reich, P. B., J. Oleksyn, and I. J. Wright. 2009. Leaf phosphorus influences the photosynthesis-nitrogen relation: a cross-biome analysis of 314 species. Oecologia **160**:207-212.

Reich, P. B., J. Oleksyn, I. J. Wright, K. J. Niklas, L. Hedin, and J. J. Elser. 2010. Evidence of a general 2/3-power law of scaling leaf nitrogen to phosphorus among major plant groups and biomes. Proceedings of the Royal Society B-Biological Sciences **277**:877-883.

Reich, P. B., M. G. Tjoelker, J. L. Machado, and J. Oleksyn. 2006b. Universal scaling of respiratory metabolism, size and nitrogen in plants. Nature **439**:457-461.

Reich, P. B., I. J. Wright, and C. H. Lusk. 2007. Predicting leaf physiology from simple plant and climate attributes: A global GLOPNET analysis. Ecological Applications **17**:1982-1988.

Rogers, A. and S. W. Humphries. 2000. A mechanistic evaluation of photosynthetic acclimation at elevated CO2. Global Change Biology **6**:1005-1011.

Rosenberg, M. S., J. Gurevitch, and D. C. Adams. 1997. MetaWin: Windows software for ecological meta-analysis. Bulletin of the Ecological Society of America **78**:172.

Running, S. W., R. R. Nemani, F. A. Heinsch, M. S. Zhao, M. Reeves, and H. Hashimoto. 2004. A continuous satellite-derived measure of global terrestrial primary production. Bioscience **54**:547-560.

Ryan, M. G. 1991. EFFECTS OF CLIMATE CHANGE ON PLANT RESPIRATION. Ecological Applications **1**:157-167.

Ryan, M. G. and B. J. Yoder. 1997. Hydraulic limits to tree height and tree growth. Bioscience **47**:235-242.

Rykiel, E. J. 1996. Testing ecological models: The meaning of validation. Ecological Modelling **90**:229-244.

Rymes, M. D. and D. R. Myers. 2001. Mean preserving algorithm for smoothly interpolating averaged data. Solar Energy **71**:225-231.

Saatchi, S. S., N. L. Harris, S. Brown, M. Lefsky, E. T. A. Mitchard, W. Salas, B. R. Zutta, W. Buermann, S. L. Lewis, S. Hagen, S. Petrova, L. White, M. Silman, and A. Morel. 2011. Benchmark map of forest carbon stocks in tropical regions across three continents. Proceedings of the National Academy of Sciences of the United States of America **108**:9899-9904.

Saatchi, S. S., R. A. Houghton, R. Alvala, J. V. Soares, and Y. Yu. 2007. Distribution of aboveground live biomass in the Amazon basin. Global Change Biology **13**:816-837.

Sabine, C. L., R. A. Feely, N. Gruber, R. M. Key, K. Lee, J. L. Bullister, R. Wanninkhof, C. S. Wong, D. W. R. Wallace, B. Tilbrook, F. J. Millero, T. H. Peng, A. Kozyr, T. Ono, and A. F. Rios. 2004. The oceanic sink for anthropogenic CO2. Science **305**:367-371.

Sage, R. F., T. D. Sharkey, and J. R. Seemann. 1989. ACCLIMATION OF PHOTOSYNTHESIS TO ELEVATED CO2 IN 5 C-3 SPECIES. Plant Physiology **89**:590-596.

Sardans, J., J. Penuelas, and M. Estiarte. 2008a. Changes in soil enzymes related to C and N cycle and in soil C and N content under prolonged warming and drought in a

Mediterranean shrubland. Applied Soil Ecology **39**:223-235.
Sardans, J., J. Penuelas, M. Estiarte, and P. Prieto. 2008b. Warming and drought alter C and N concentration, allocation and accumulation in a Mediterranean shrubland. Global Change Biology **14**:2304-2316.
Sato, H., A. Itoh, and T. Kohyama. 2007. SEIB-DGVM: A new dynamic global vegetation model using a spatially explicit individual-based approach. Ecological Modelling **200**:279-307.
Schafer, K. V. R., R. Oren, D. S. Ellsworth, C. T. Lai, J. D. Herrick, A. C. Finzi, D. D. Richter, and G. G. Katul. 2003. Exposure to an enriched CO2 atmosphere alters carbon assimilation and allocation in a pine forest ecosystem. Global Change Biology **9**:1378-1400.
Schafer, K. V. R., R. Oren, C. T. Lai, and G. G. Katul. 2002. Hydrologic balance in an intact temperate forest ecosystem under ambient and elevated atmospheric CO2 concentration. Global Change Biology **8**:895-911.
Scharlemann, J., R. Hiederer, V. Kapos, and C. Ravilious. 2010. Updated global carbon map. UNEP-WCMC.
Scholze, M., W. Knorr, N. W. Arnell, and I. C. Prentice. 2006. A climate-change risk analysis for world ecosystems. Proceedings of the National Academy of Sciences of the United States of America **103**:13116-13120.
Schwalm, C. R., C. A. Williams, K. Schaefer, R. Anderson, M. A. Arain, I. Baker, A. Barr, T. A. Black, G. Chen, J. M. Chen, P. Ciais, K. J. Davis, A. Desai, M. Dietze, D. Dragoni, M. L. Fischer, L. B. Flanagan, R. Grant, L. Gu, D. Hollinger, R. C. Izaurralde, C. Kucharik, P. Lafleur, B. E. Law, L. Li, Z. Li, S. Liu, E. Lokupitiya, Y. Luo, S. Ma, H. Margolis, R. Matamala, H. McCaughey, R. K. Monson, W. C. Oechel, C. Peng, B. Poulter, D. T. Price, D. M. Riciutto, W. Riley, A. K. Sahoo, M. Sprintsin, J. Sun, H. Tian, C. Tonitto, H. Verbeeck, and S. B. Verma. 2010. A model-data intercomparison of CO(2) exchange across North America: Results from the North American Carbon Program site synthesis. Journal of Geophysical Research-Biogeosciences **115**.
Searles, P. S. and A. J. Bloom. 2003. Nitrate photo-assimilation in tomato leaves under short-term exposure to elevated carbon dioxide and low oxygen. Plant Cell and Environment **26**:1247-1255.
Sellers, P. J., J. A. Berry, G. J. Collatz, C. B. Field, and F. G. Hall. 1992. Canopy Reflectance, Photosynthesis, and Transpiration .3. a Reanalysis Using Improved Leaf Models and a New Canopy Integration Scheme. Remote Sensing of Environment **42**:187-216.
Sitch, S., C. Huntingford, N. Gedney, P. E. Levy, M. Lomas, S. L. Piao, R. Betts, P. Ciais, P. Cox, P. Friedlingstein, C. D. Jones, I. C. Prentice, and F. I. Woodward. 2008. Evaluation of the terrestrial carbon cycle, future plant geography and climate-carbon cycle feedbacks using five Dynamic Global Vegetation Models (DGVMs). Global Change Biology **14**:2015-2039.
Sitch, S., B. Smith, I. C. Prentice, A. Arneth, A. Bondeau, W. Cramer, J. O. Kaplan, S. Levis, W. Lucht, M. T. Sykes, K. Thonicke, and S. Venevsky. 2003. Evaluation of ecosystem dynamics, plant geography and terrestrial carbon cycling in the LPJ dynamic global vegetation model. Global Change Biology **9**:161-185.
Sokal, R. R. and F. J. Rohlf. 1995. Biometry. W. H. Freeman and Company, USA.
Solomon, S. D., D. Qin, M. Manning, Z. Chen, M. Marquis, K. B. Averyt, M. Tignor, and H. L. Miller, editors. 2007. Contribution of Working Group I to the Fouth Assessment Report of the Intergovernmental Panel on Climate Change, 2007. Cambridge University Press, Cambridge, UK & New York, USA.
Souza, L., R. T. Belote, P. Kardol, J. F. Weltzin, and R. J. Norby. 2010. CO(2) enrichment accelerates successional development of an understory plant community. Journal

of Plant Ecology-Uk **3**:33-39.
Spitters, C. J. T., H. Toussaint, and J. Goudriaan. 1986. SEPARATING THE DIFFUSE AND DIRECT COMPONENT OF GLOBAL RADIATION AND ITS IMPLICATIONS FOR MODELING CANOPY PHOTOSYNTHESIS .1. COMPONENTS OF INCOMING RADIATION. Agricultural and Forest Meteorology **38**:217-229.
Steffen, W., P. J. Crutzen, and J. R. McNeill. 2007. The Anthropocene: Are humans now overwhelming the great forces of nature. Ambio **36**:614-621.
Stitt, M. 1991. RISING CO2 LEVELS AND THEIR POTENTIAL SIGNIFICANCE FOR CARBON FLOW IN PHOTOSYNTHETIC CELLS. Plant Cell and Environment **14**:741-762.
Sturrock, R. N., S. J. Frankel, A. V. Brown, P. E. Hennon, J. T. Kliejunas, K. J. Lewis, J. J. Worrall, and A. J. Woods. 2011. Climate change and forest diseases. Plant Pathology **60**:133-149.
Tans, P. and R. Keeling. 2012. Trends in Atmospheric Carbon Dioxide. NOAA/ESRL and Scripps Institution of Oceanography.
Taub, D. R., B. Miller, and H. Allen. 2008. Effects of elevated CO2 on the protein concentration of food crops: a meta-analysis. Global Change Biology **14**:565-575.
Taylor, J. A. and J. Lloyd. 1992. Sources and Sinks of Atmospheric Co2. Australian Journal of Botany **40**:407-418.
Thompson Reuters. Web of Knowledge.
Thornley, J. H. M. and M. G. R. Cannell. 2000. Modelling the components of plant respiration: Representation and realism (vol. 85, pg. 55, 2000). Annals of Botany **85**:937-937.
Thornton, P. E., J. F. Lamarque, N. A. Rosenbloom, and N. M. Mahowald. 2007. Influence of carbon-nitrogen cycle coupling on land model response to CO2 fertilization and climate variability. Global Biogeochemical Cycles **21**.
Tjoelker, M. G., J. Oleksyn, and P. B. Reich. 1998. Seedlings of five boreal tree species differ in acclimation of net photosynthesis to elevated CO2 and temperature. Tree Physiology **18**:715-726.
Tjoelker, M. G., J. Oleksyn, and P. B. Reich. 1999. Acclimation of respiration to temperature and CO2 in seedlings of boreal tree species in relation to plant size and relative growth rate. Global Change Biology **5**:679-691.
Tocquin, P., S. Ormenese, A. Pieltain, N. Detry, G. Bernier, and C. Perilleux. 2006. Acclimation of Arabidopsis thaliana to long-term CO2 enrichment and nitrogen supply is basically a matter of growth rate adjustment. Physiologia Plantarum **128**:677-688.
VanOosten, J. J. and R. T. Besford. 1996. Acclimation of photosynthesis to elevated CO2 through feedback regulation of gene expression: Climate of opinion. Photosynthesis Research **48**:353-365.
Venables, W. N. and B. D. Ripley. 2002. Modern Applied Statistics with S. 4th edition. Springer, New York.
Wang, S., A. P. Trishchenko, and X. Sun. 2007a. Simulation of canopy radiation transfer and surface albedo in the EALCO model. Climate Dynamics **29**:615-632.
Wang, T., P. Ciais, S. L. Piao, C. Ottle, P. Brender, F. Maignan, A. Arain, A. Cescatti, D. Gianelle, C. Gough, L. Gu, P. Lafleur, T. Laurila, B. Marcolla, H. Margolis, L. Montagnani, E. Moors, N. Saigusa, T. Vesala, G. Wohlfahrt, C. Koven, A. Black, E. Dellwik, A. Don, D. Hollinger, A. Knohl, R. Monson, J. Munger, A. Suyker, A. Varlagin, and S. Verma. 2011. Controls on winter ecosystem respiration in temperate and boreal ecosystems. Biogeosciences **8**:2009-2025.
Wang, Y. P., B. Z. Houlton, and C. B. Field. 2007b. A model of biogeochemical cycles of carbon, nitrogen, and phosphorus including symbiotic nitrogen fixation and phosphatase production. Global Biogeochemical Cycles **21**.

Warren, J. M., R. J. Norby, and S. D. Wullschleger. 2011. Elevated CO(2) enhances leaf senescence during extreme drought in a temperate forest. Tree Physiology **31**:117-130.

Wolff, E. W. 2011. Greenhouse gases in the Earth system: a palaeoclimate perspective. Philosophical Transactions of the Royal Society a-Mathematical Physical and Engineering Sciences **369**:2133-2147.

Woodward, F. I. 2002. Potential impacts of global elevated CO2 concentrations on plants. Current Opinion in Plant Biology **5**:207-211.

Woodward, F. I. and M. R. Lomas. 2004. Vegetation dynamics - simulating responses to climatic change. Biological Reviews **79**:643-670.

Woodward, F. I. and T. M. Smith. 1994. Global Photosynthesis and Stomatal Conductance - Modeling the Controls by Soil and Climate. Pages 1-41 Advances in Botanical Research, Vol 20.

Woodward, F. I., T. M. Smith, and W. R. Emanuel. 1995. A Global Land Primary Productivity and Phytogeography Model. Global Biogeochemical Cycles **9**:471-490.

Wright, I. J., P. B. Reich, J. H. C. Cornelissen, D. S. Falster, P. K. Groom, K. Hikosaka, W. Lee, C. H. Lusk, U. Niinemets, J. Oleksyn, N. Osada, H. Poorter, D. I. Warton, and M. Westoby. 2005. Modulation of leaf economic traits and trait relationships by climate. Global Ecology and Biogeography **14**:411-421.

Wright, I. J., P. B. Reich, and M. Westoby. 2001. Strategy shifts in leaf physiology, structure and nutrient content between species of high- and low-rainfall and high- and low-nutrient habitats. Functional Ecology **15**:423-434.

Wright, I. J., P. B. Reich, M. Westoby, D. D. Ackerly, Z. Baruch, F. Bongers, J. Cavender-Bares, T. Chapin, J. H. C. Cornelissen, M. Diemer, J. Flexas, E. Garnier, P. K. Groom, J. Gulias, K. Hikosaka, B. B. Lamont, T. Lee, W. Lee, C. Lusk, J. J. Midgley, M. L. Navas, U. Niinemets, J. Oleksyn, N. Osada, H. Poorter, P. Poot, L. Prior, V. I. Pyankov, C. Roumet, S. C. Thomas, M. G. Tjoelker, E. J. Veneklaas, and R. Villar. 2004. The worldwide leaf economics spectrum. Nature **428**:821-827.

Wullschleger, S. D. 1993. BIOCHEMICAL LIMITATIONS TO CARBON ASSIMILATION IN C(3) PLANTS - A RETROSPECTIVE ANALYSIS OF THE A/CI CURVES FROM 109 SPECIES. Journal of Experimental Botany **44**:907-920.

Xiao, G. J., Q. Zhang, Y. B. Yao, H. Zhao, R. Y. Wang, H. Z. Bai, and F. J. Zhang. 2008. Impact of recent climatic change on the yield of winter wheat at low and high altitudes in semi-arid northwestern China. Agriculture Ecosystems & Environment **127**:37-42.

Yong, Z. H., G. Y. Chen, D. Y. Zhang, Y. Chen, J. Chen, J. G. Zhu, and D. Q. Xu. 2007. Is photosynthetic acclimation to free-air CO2 enrichment (FACE) related to a strong competition for the assimilatory power between carbon assimilation and nitrogen assimilation in rice leaf? Photosynthetica **45**:85-91.

Zäehle, S. Pers. Comm.

Zaehle, S., A. Bondeau, T. R. Carter, W. Cramer, M. Erhard, I. C. Prentice, I. Reginster, M. D. A. Rounsevell, S. Sitch, B. Smith, P. C. Smith, and M. Sykes. 2007. Projected changes in terrestrial carbon storage in Europe under climate and land-use change, 1990-2100. Ecosystems **10**:380-401.

Zäehle, S., M. De Kauwe, M. Dietze, P. Hanson, T. Hickler, A. Jain, Y. Luo, B. E. Medlyn, R. J. Norby, R. Oren, P. E. Thornton, Y.-P. Wang, D. Wårlind, B. Parton, S. Wang, and E. Weng. In Prep. Nitrogen drives the NPP response to elevated CO2 when simulating Oak Ridge and Duke FACE

Zaehle, S., P. Friedlingstein, and A. D. Friend. 2010. Terrestrial nitrogen feedbacks may accelerate future climate change. Geophysical Research Letters **37**.

Zaehle, S. and A. D. Friend. 2010. Carbon and nitrogen cycle dynamics in the O-CN land surface model: 1. Model description, site-scale evaluation, and sensitivity to parameter estimates. Global Biogeochemical Cycles **24**.

Zak, D. R., K. S. Pregitzer, M. E. Kubiske, and A. J. Burton. 2011. Forest productivity under elevated CO2 and O3: positive feedbacks to soil N cycling sustain decade-long net primary productivity enhancement by CO2. Ecology Letters **14**:1220-1226.

Zelazowski, P., Y. Malhi, C. Huntingford, S. Sitch, and J. B. Fisher. 2011. Changes in the potential distribution of humid tropical forests on a warmer planet. Philosophical Transactions of the Royal Society a-Mathematical Physical and Engineering Sciences **369**:137-160.

Zhang, K., J. S. Kimball, E. H. Hogg, M. Zhao, W. C. Oechel, J. J. Cassano, and S. W. Running. 2008. Satellite-based model detection of recent climate-driven changes in northern high-latitude vegetation productivity. Journal of Geophysical Research-Biogeosciences **113**.

Zotz, G., Pepin, S. and Körner, C. 2005. No down-regulation of leaf photosynthesis in mature forest trees after three years of exposure to elevated CO2.Plant Biology**7**: 369-374.

Appendix A Additional plots from Chapter 4

Figure AA-1. JULES simulations showing the effect of inter-annual variability in

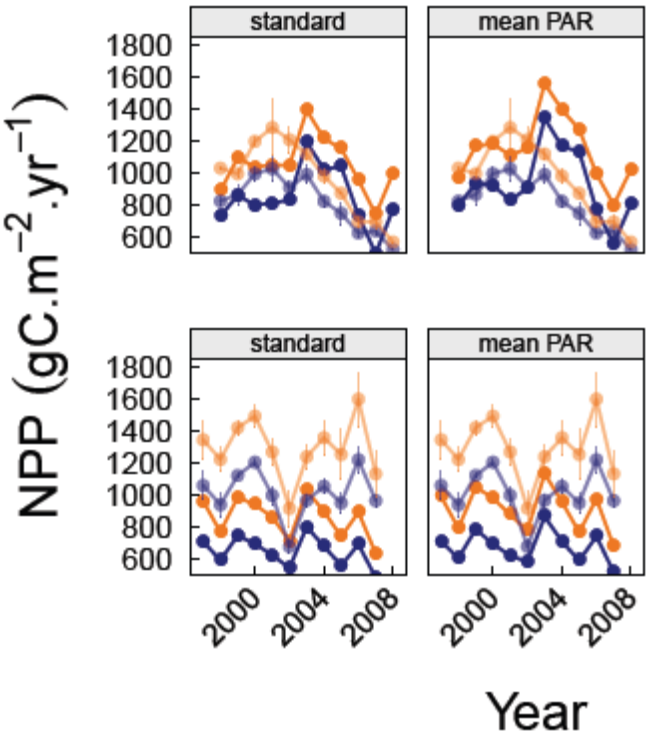

Photosynthetically Active Radiation (PAR—standard run) or no inter-annual variability in PAR (mean PAR) at Oak Ridge (top panels) or Duke (bottom panels).

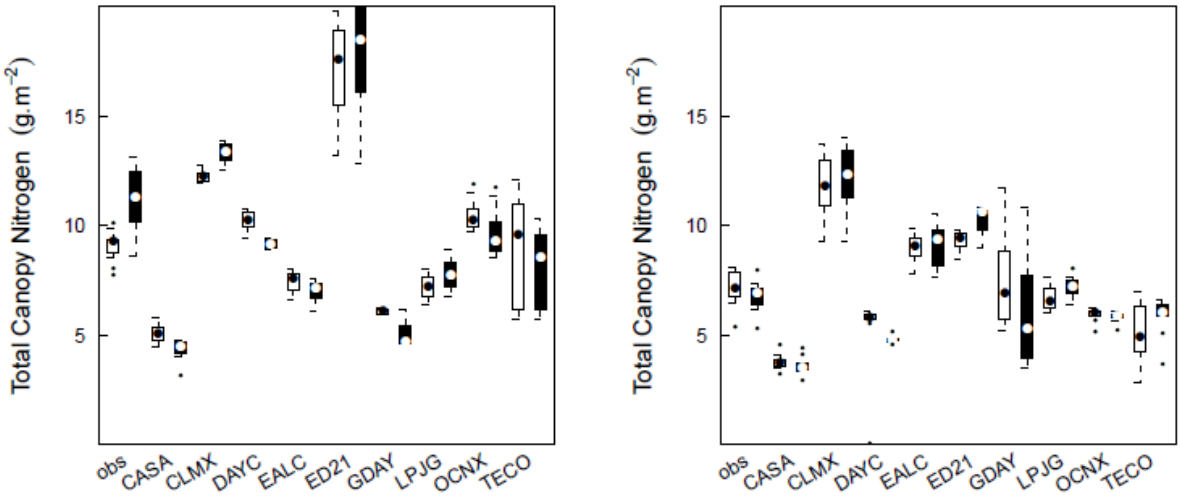

Figure AA-2. Canopy nitrogen at Duke (left panel) and Oak Ridge (right panel) under ambient (white bars) and elevated (black bars) CO_2 for the other LSM simulations of Chapter 4.

Appendix B SDGVM Plant Functional Type coverage from GLC2000

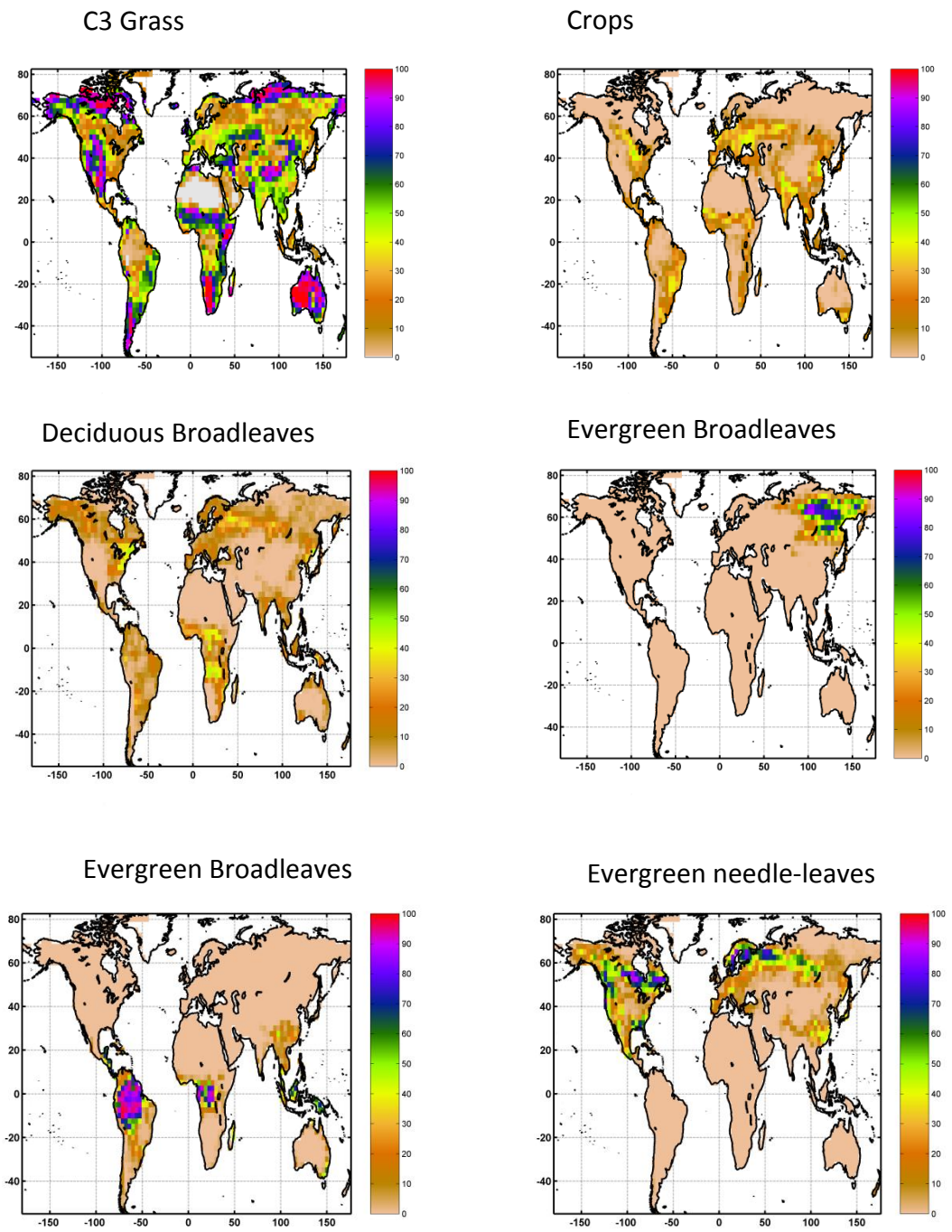

Figure AB-1. Percentage cover of the 6 SDGVM Plant Functional Types interpreted from the GLC2000 database.

Appendix C Climate change of 16 GCMs interpreted by IMOGEN

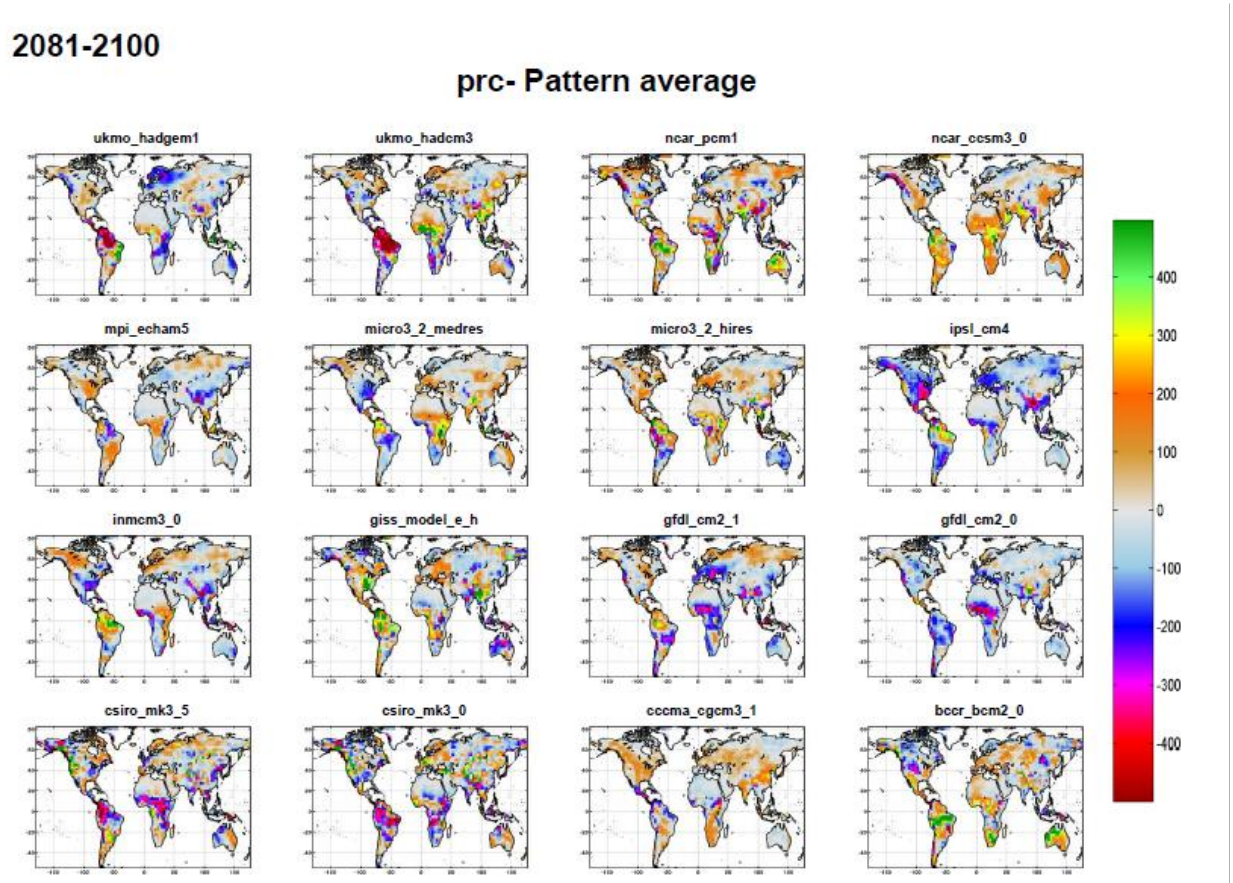

Figure AC-1. 2081-2100 mean precipitation change (mm) for 16 GCMs as interpreted by IMOGEN and SDGVM for the A1F1 SRES scenario.

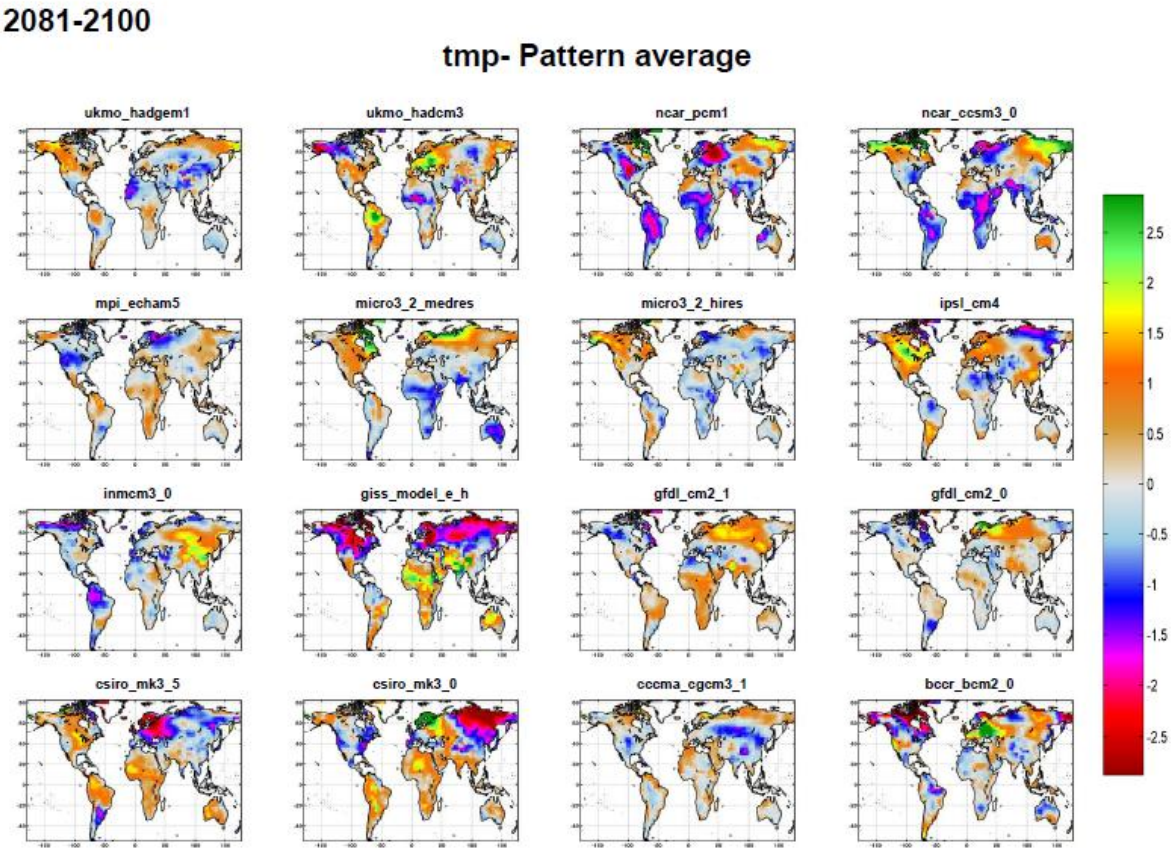

Figure AC-2. 2081-2100 mean temperature change (^{0}C) for 16 GCMs as interpreted by IMOGEN for the A1F1 SRES scenario.

Appendix D Model output and driving variable distributions from Chapter 6

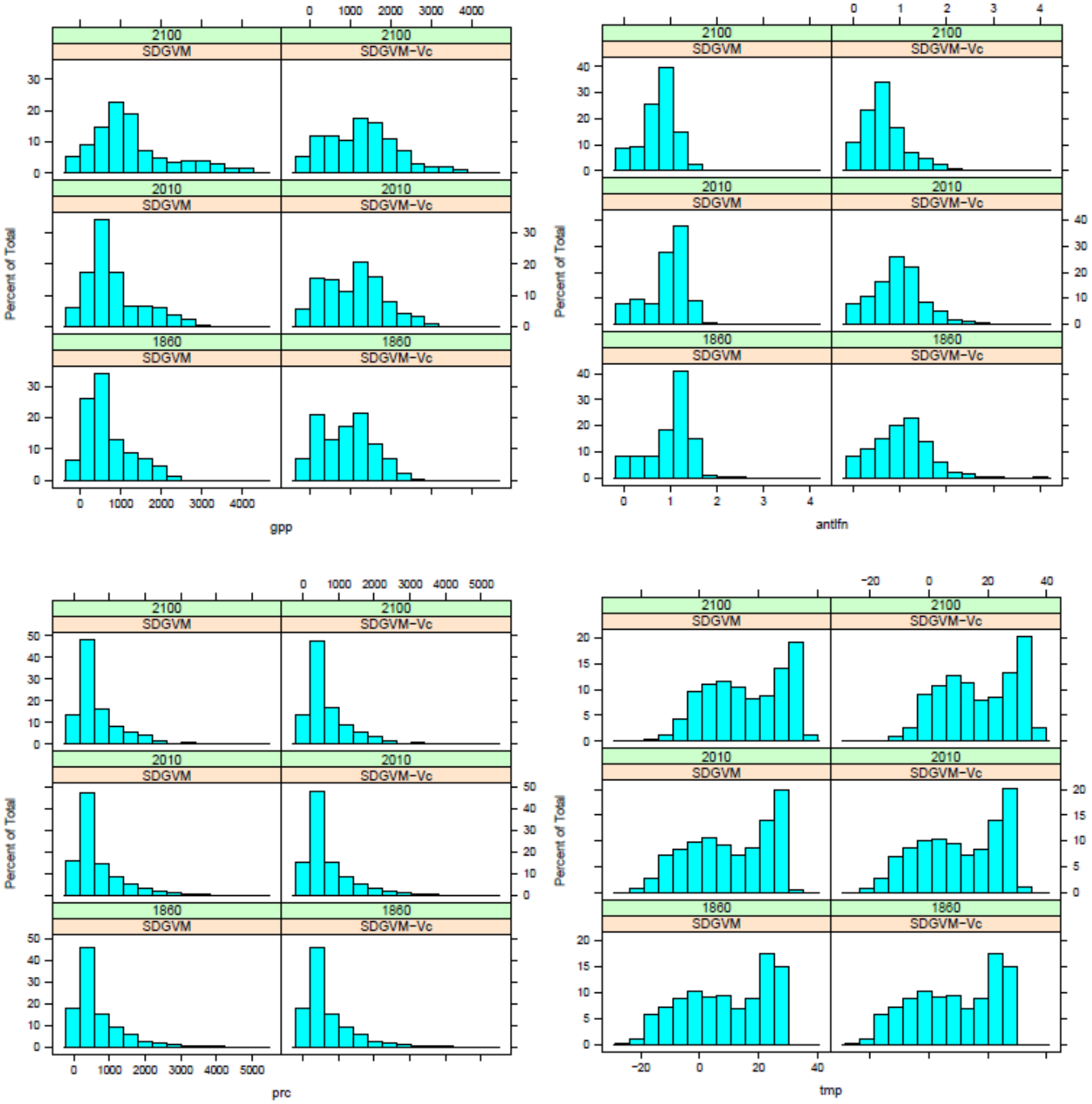

Figure AD-1. Variable distributions for SDGVM and SDGVM-Vc in 1860, 2010 and 2100.GPP (top left), annual average top-leaf nitrogen concentration (antlfn—top right), precipitation (bottom left) and temperature (bottom right).

Appendix E European plant biomass simulated by SDGVM-Vc

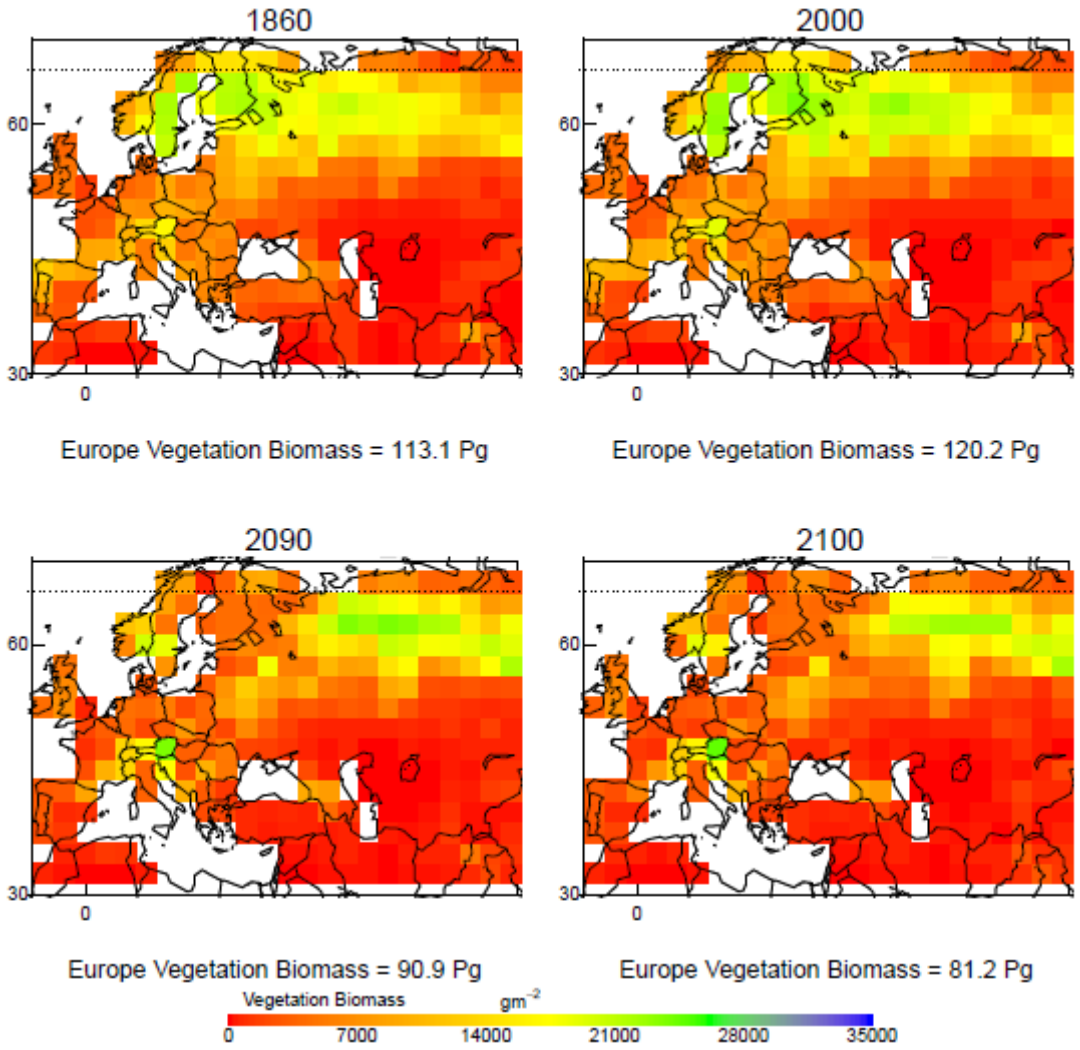

Figure AE-1. Vegetation biomass simulated by SDGVM-Vc in 1860, 2000, 2090 and 2100.

Appendix F SDGVM versus SDGVM-VC LAI

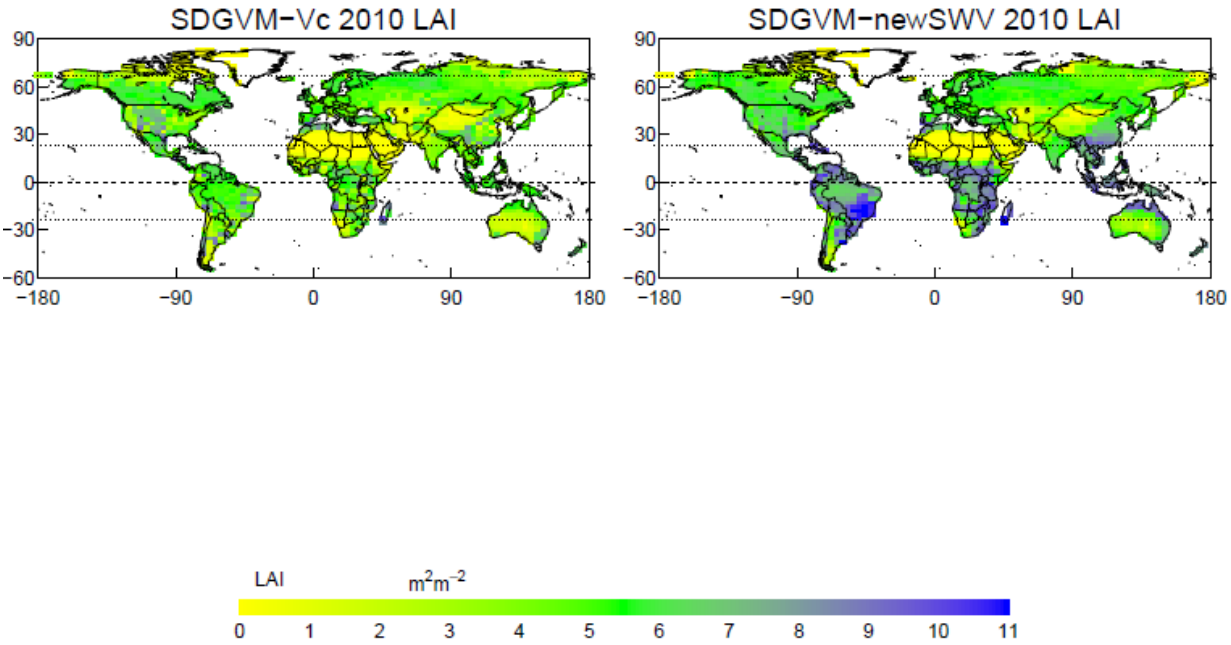

Figure AB-1.Simulated LAI in 2010 for SDGVM-Vc and SDGVM-newSWV.

Appendix G Oscillations in SDGVM-Vc LAI

For all models with the new nitrogen scheme in Chapter 6, the global flux from terrestrial vegetation oscillated with a four year period (Figure 6-6). The fluctuation occurred at points that contained the grass PFT, was most obvious in the tropics (see Figures AC-1-3) and was caused by the leaf area and life history dynamics of the grass PFT.

SDGVM assumes that grasses have a high risk strategy, investing all of their stored carbon from the previous year's productivity in leaf in the following year. With the trait regression nitrogen scheme, canopy nitrogen was higher promoting higher GPP and leading to a large stored pool of carbon for the following year's growth. This led to high canopy investment and consequent LAI, which leads to higher canopy nitrogen and higher GPP leading to even higher carbon stocks which lead to maximal values of LAI (>10 m m^{-2}) in the following year. At this point, instead of increasing GPP, the grass has over invested in LAI and GPP cannot balance respiration in the lower canopy layers.

With no carbon remaining in the store the plant does not have sufficient carbon to supply the following years LAI increment and dies. GPP is therefore stopped and accumulated carbon in its biomass is released into the soil which quickly decomposes returning the bulk of the carbon back to the atmosphere in a single year. While affecting the dynamics over the scale of several years, this oscillation has little effect on the overall long-term dynamics of the system which continues to accumulate carbon.

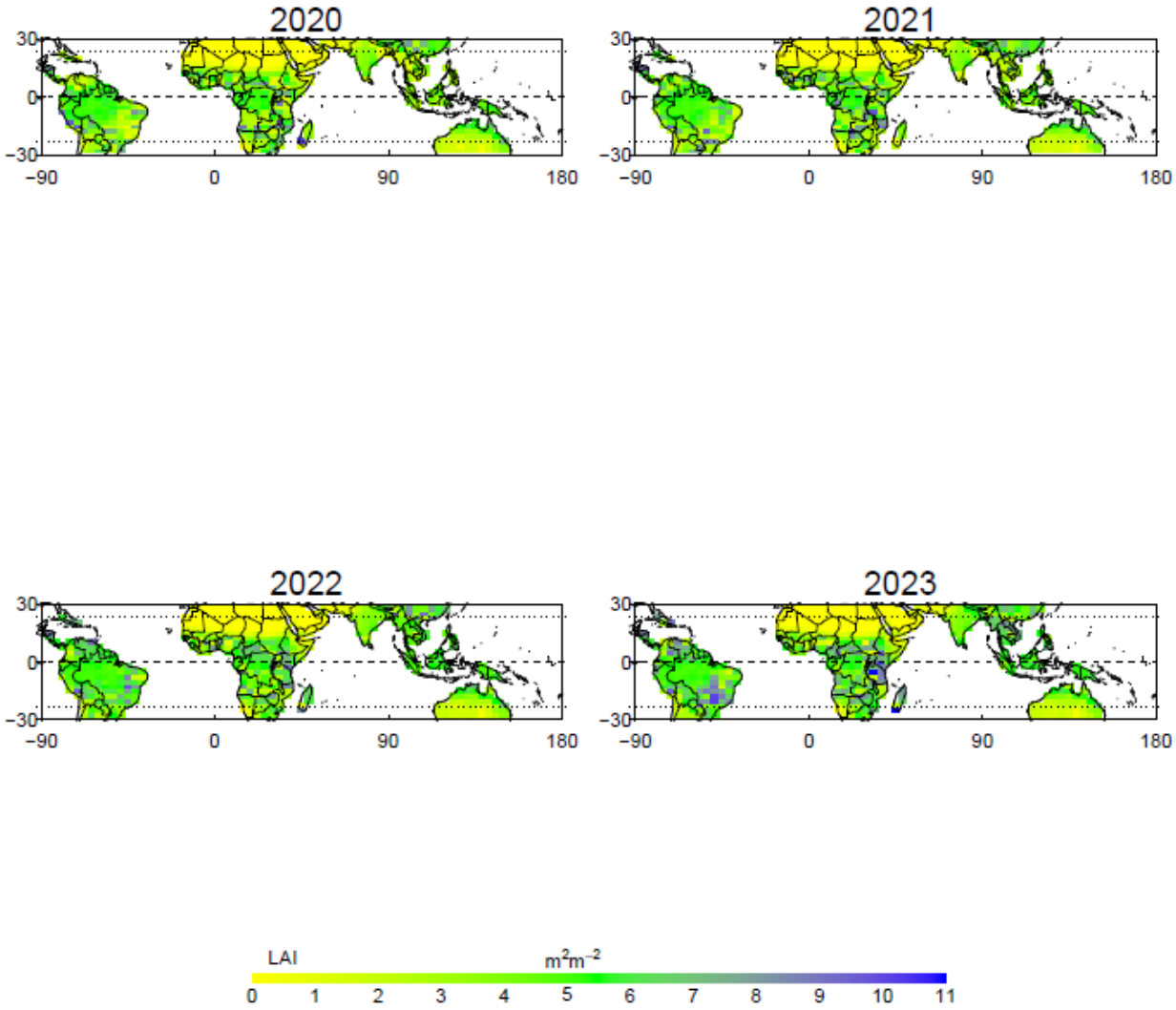

Figure AC-1. Tropical LAI predicted by SDGVM-Vc for 2020 to 2023.

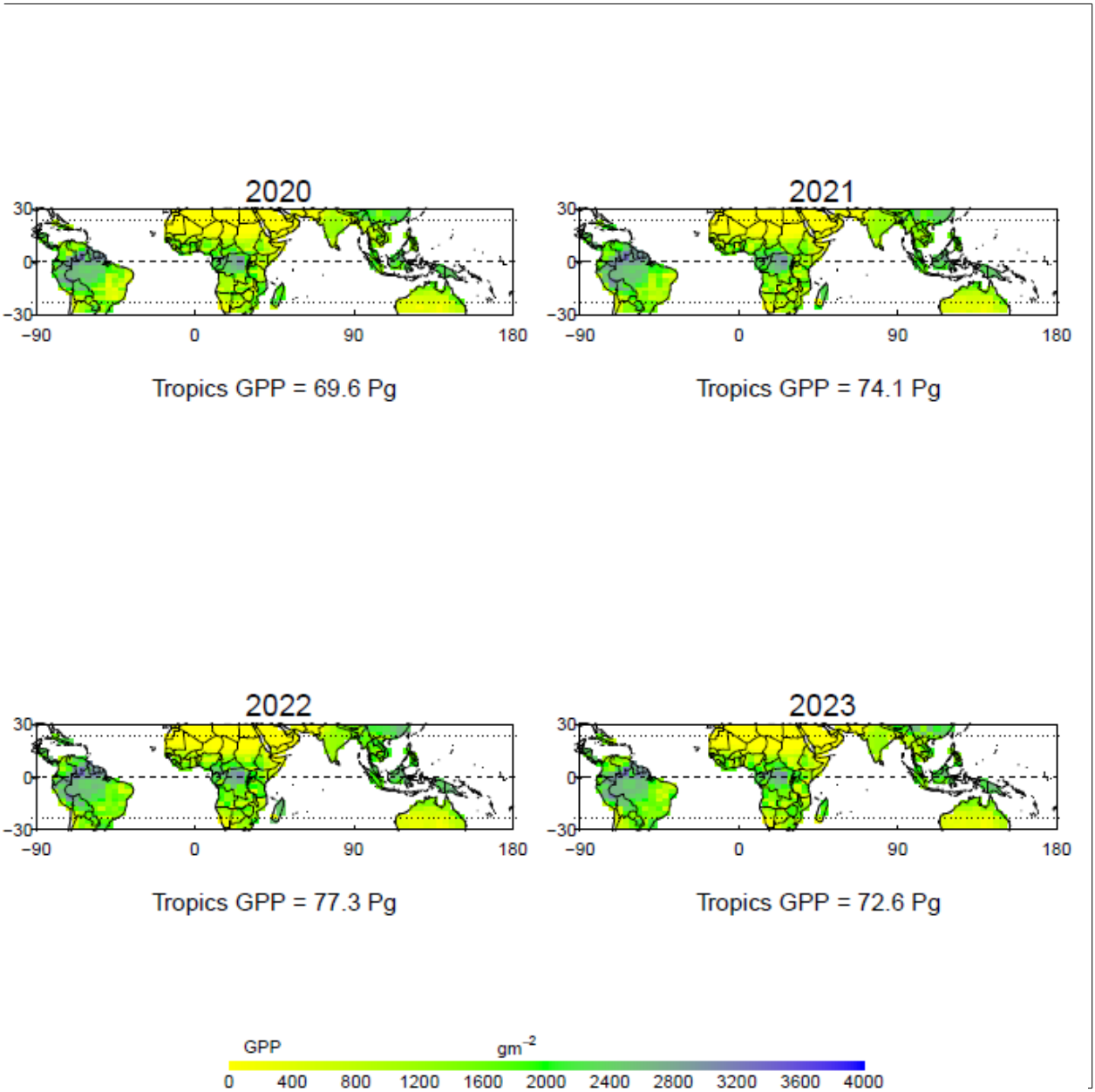

Figure AC-2. Tropical GPP predicted by SDGVM-Vc for 2020 to 2023.

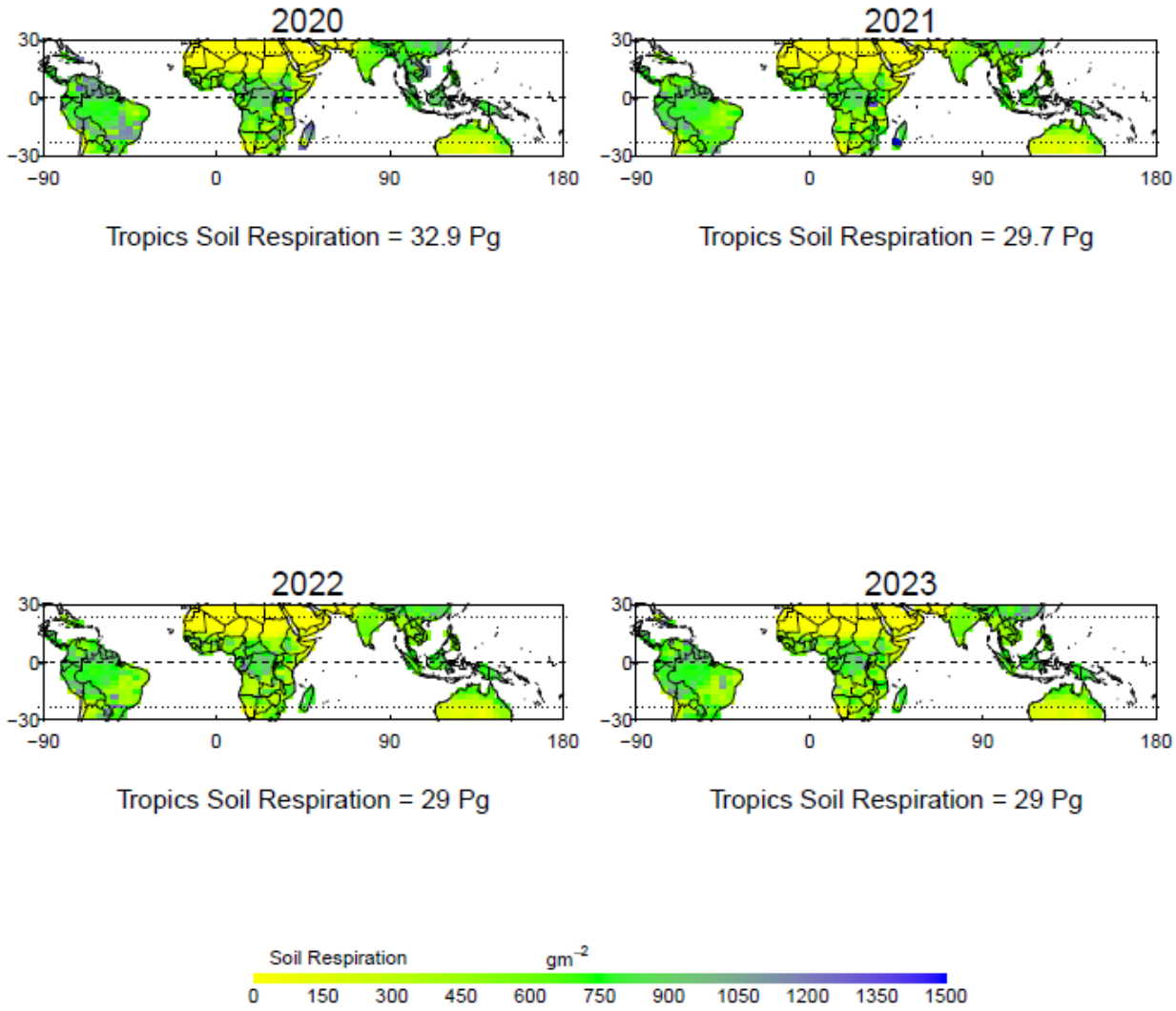

Figure AC-3. Tropical soil respiration predicted by SDGVM-Vc for 2020 to 2023.

Appendix H Correlation analysis of maintenance respiration

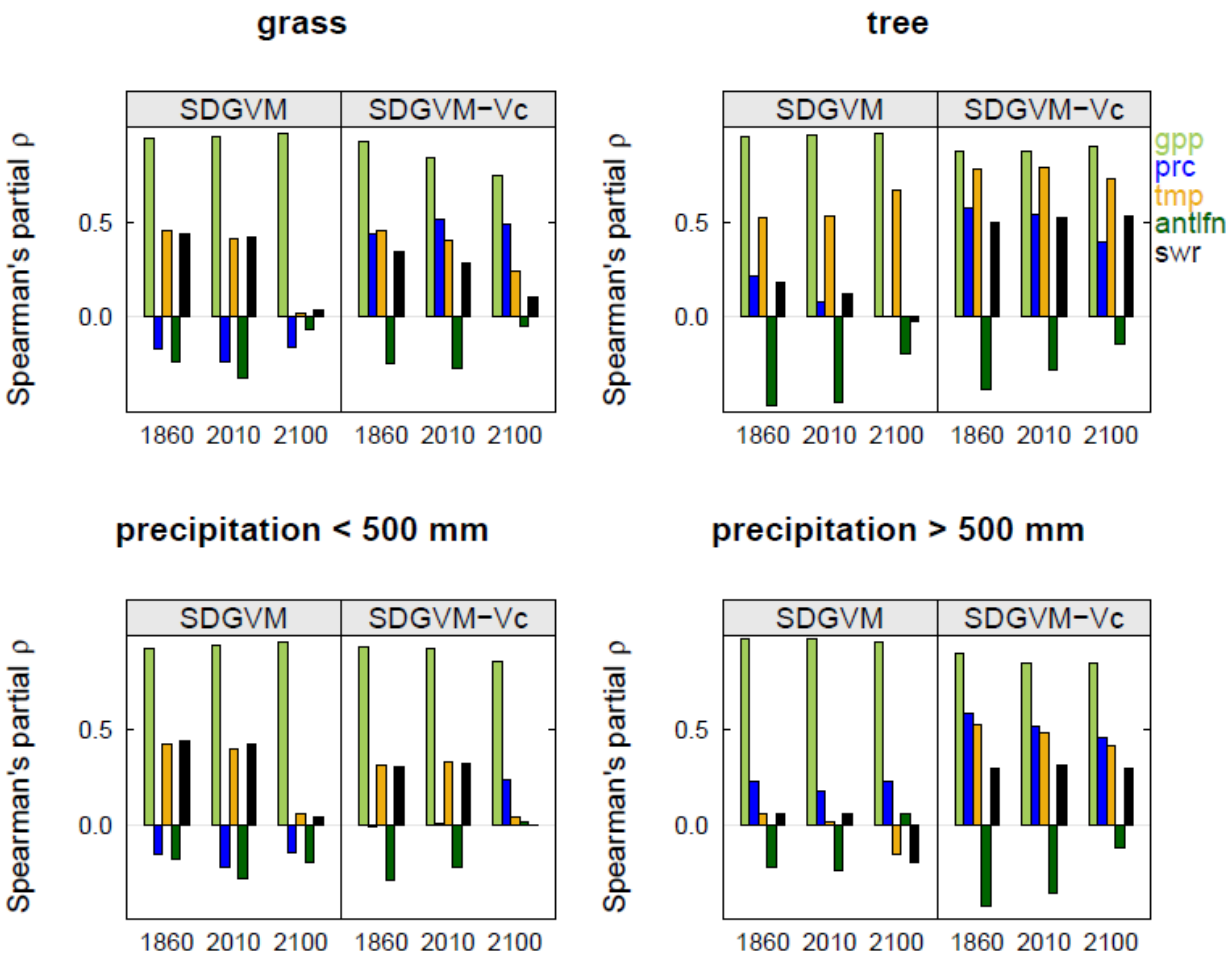

Figure AH-1. Barplots showing the Spearman's partial rank correlation coefficient (ρ) of plant respiration with model driving variables—GPP (pale green bars), precipitation (blue bars), temperature (yellow bars), top leaf nitrogen (green bars) and shortwave radiation (black bars). Each panel shows correlations at the beginning and end of the simulation (1860 and 2100 respectively) and for the modern day (2010). The top row shows Spearman's partial ρ for all sites subdivided by PFT growth habit. The bottom row shows ρ for dry sites (annual precipitation below 500 mm yr^{-1}) and wet sites (annual precipitation above 500 mm yr^{-1}). Each plot also shows the results from the SDGVM simulation and the SDGVM-Vc simulation.

Appendix I References for meta-analysis in Chapter 2

Adam, N. R., G. W. Wall, B. A. Kimball, P. J. Pinter, R. L. LaMorte, D. J. Hunsaker, F. J. Adamsen, T. Thompson, A. D. Matthias, S. W. Leavitt, and A. N. Webber. 2000. Acclimation response of spring wheat in a free-air CO2 enrichment (FACE) atmosphere with variable soil nitrogen regimes. 1. Leaf position and phenology determine acclimation response. Photosynthesis Research **66**:65-77.

Aeschlimann, U., J. Nosberger, P. J. Edwards, M. K. Schneider, M. Richter, and H. Blum. 2005. Responses of net ecosystem CO2 exchange in managed grassland to long-term CO2 enrichment, N fertilization and plant species. Plant Cell and Environment **28**:823-833.

Ainsworth, E. A. and A. Rogers. 2007. The response of photosynthesis and stomatal conductance to rising [CO2]: mechanisms and environmental interactions. Plant Cell and Environment **30**:258-270.

Ainsworth, E. A., A. Rogers, H. Blum, J. Nosberger, and S. P. Long. 2003. Variation in acclimation of photosynthesis in Trifolium repens after eight years of exposure to Free Air CO2 Enrichment (FACE). Journal of Experimental Botany **54**:2769-2774.

Ainsworth, E. A., A. Rogers, R. Nelson, and S. P. Long. 2004. Testing the "source-sink" hypothesis of down-regulation of photosynthesis in elevated [CO2] in the field with single gene substitutions in Glycine max. Agricultural and Forest Meteorology **122**:85-94.

Allard, V., P. C. D. Newton, M. Lieffering, H. Clark, C. Matthew, J. F. Soussana, and Y. S. Gray. 2003. Nitrogen cycling in grazed pastures at elevated CO2: N returns by ruminants. Global Change Biology **9**:1731-1742.

Allard, V., P. C. D. Newton, M. Lieffering, J. F. Soussana, R. A. Carran, and C. Matthew. 2005. Increased quantity and quality of coarse soil organic matter fraction at elevated CO2 in a grazed grassland are a consequence of enhanced root growth rate and turnover. Plant and Soil **276**:49-60.

Allard, V., P. C. D. Newton, M. Lieffering, J. F. Soussana, P. Grieu, and C. Matthew. 2004. Elevated CO2 effects on decomposition processes in a grazed grassland. Global Change Biology **10**:1553-1564.

Allen, A. S., J. A. Andrews, A. C. Finzi, R. Matamala, D. D. Richter, and W. H. Schlesinger. 2000. Effects of free-air CO2 enrichment (FACE) on belowground processes in a Pinus taeda forest. Ecological Applications **10**:437-448.

Anten, N. P. R., T. Hirose, Y. Onoda, T. Kinugasa, H. Y. Kim, M. Okada, and K. Kobayashi. 2004. Elevated CO2 and nitrogen availability have interactive effects on canopy carbon gain in rice. New Phytologist **161**:459-471.

Asshoff, R., G. Zotz, and C. Korner. 2006. Growth and phenology of mature temperate forest trees in elevated CO2. Global Change Biology **12**:848-861.

Bazot, S., L. Ulff, H. Blum, C. Nguyen, and C. Robin. 2006. Effects of elevated CO2 concentration on rhizodeposition from Lolium perenne grown on soil exposed to 9 years of CO2 enrichment. Soil Biology & Biochemistry **38**:729-736.

Belote, R. T., J. F. Weltzin, and R. J. Norby. 2004. Response of an understory plant community to elevated [CO2] depends on differential responses of dominant invasive species and is mediated by soil water availability. New Phytologist **161**:827-835.

Bernacchi, C. J., C. Calfapietra, P. A. Davey, V. E. Wittig, G. E. Scarascia-Mugnozza, C. A. Raines, and S. P. Long. 2003. Photosynthesis and stomatal conductance responses of poplars to free-air CO2 enrichment (PopFACE) during the first growth cycle and immediately following coppice. New Phytologist **159**:609-621.

Bernacchi, C. J., P. B. Morgan, D. R. Ort, and S. P. Long. 2005. The growth of soybean under free air [CO2] enrichment (FACE) stimulates photosynthesis while decreasing in vivo Rubisco capacity. Planta **220**:434-446.

Bernhardt, E. S., J. J. Barber, J. S. Pippen, L. Taneva, J. A. Andrews, and W. H. Schlesinger. 2006. Long-term effects of free air CO2 enrichment (FACE) on soil respiration. Biogeochemistry **77**:91-116.

Billings, S. A., S. F. Zitzer, H. Weatherly, S. M. Schaeffer, T. Charlet, J. A. Arnone, and R. D. Evans. 2003. Effects of elevated carbon dioxide on green leaf tissue and leaf litter quality in an intact Mojave Desert ecosystem. Global Change Biology **9**:729-735.

Bindi, M., L. Fibbi, M. Lanini, and F. Miglietta. 2001. Free Air CO2 Enrichment (FACE) of grapevine (Vitis vinifera L.): I. Development and testing of the system for CO2 enrichment. European Journal of Agronomy **14**:135-143.

Blum, H., G. Hendrey, and J. Nosberger. 1997. Effects of elevated CO2, N fertilization, and cutting regime on the production and quality of Lolium perenne L. shoot necromass. Acta Oecologica-International Journal of Ecology **18**:291-295.

Borjigidai, A., K. Hikosaka, T. Hirose, T. Hasegawa, M. Okada, and K. Kobayashi. 2006. Seasonal changes in temperature dependence of photosynthetic rate in rice under a free-air CO2 enrichment. Annals of Botany **97**:549-557.

Brooks, T. J., G. W. Wall, P. J. Pinter, B. A. Kimball, R. L. LaMorte, S. W. Leavitt, A. D. Matthias, F. J. Adamsen, D. J. Hunsaker, and A. N. Webber. 2000. Acclimation response of spring wheat in a free-air CO2 enrichment (FACE) atmosphere with variable soil nitrogen regimes. 3. Canopy architecture and gas exchange. Photosynthesis Research **66**:97-108.

Bryant, J., G. Taylor, and M. Frehner. 1998. Photosynthetic acclimation to elevated CO2 is modified by source : sink balance in three component species of chalk grassland swards grown in a free air carbon dioxide enrichment (FACE) experiment. Plant Cell and Environment **21**:159-168.

Calfapietra, C., B. Gielen, A. N. J. Galema, M. Lukac, P. De Angelis, M. C. Moscatelli, R. Ceulemans, and G. Scarascia-Mugnozza. 2003. Free-air CO2 enrichment (FACE) enhances biomass production in a short-rotation poplar plantation. Tree Physiology **23**:805-814.

Calfapietra, C., B. Gielen, M. Sabatti, P. De Angelis, G. Scarascia-Mugnozza, and R. Ceulemans. 2001. Growth performance of Populus exposed to "Free Air Carbon dioxide Enrichment" during the first growing season in the POPFACE experiment. Annals of Forest Science **58**:819-828.

Calfapietra, C., I. Tulva, E. Eensalu, M. Perez, P. De Angelis, G. Scarascia-Mugnozza, and O. Kull. 2005. Canopy profiles of photosynthetic parameters under elevated CO2 and N fertilization in a poplar plantation. Environmental Pollution **137**:525-535.

Cech, P. G., S. Pepin, and C. Korner. 2003. Elevated CO2 reduces sap flux in mature deciduous forest trees. Oecologia **137**:258-268.

Chen, G. Y., Z. H. Yong, Y. Liao, D. Y. Zhang, Y. Chen, H. B. Zhang, J. Chen, J. G. Zhu, and D. Q. Xu. 2005. Photosynthetic acclimation in rice leaves to free-air CO2 enrichment related to both ribulose-1,5-bisphosphate carboxylation limitation and ribulose-1,5-bisphosphate regeneration limitation. Plant and Cell Physiology **46**:1036-1045.

Conley, M. M., B. A. Kimball, T. J. Brooks, P. J. Pinter, D. J. Hunsaker, G. W. Wall, N. R. Adam, R. L. LaMorte, A. D. Matthias, T. L. Thompson, S. W. Leavitt, M. J. Ottman, A. B. Cousins, and J. M. Triggs. 2001. CO2 enrichment increases water-use efficiency in sorghum. New Phytologist **151**:407-412.

Cotrufo, M. F., P. De Angelis, and A. Polle. 2005. Leaf litter production and decomposition in a poplar short-rotation coppice exposed to free air CO2 enrichment (POPFACE). Global Change Biology **11**:971-982.

Cousins, A. B., N. R. Adam, G. W. Wall, B. A. Kimball, P. J. Pinter, S. W. Leavitt, R. L. LaMorte, A. D. Matthias, M. J. Ottman, T. L. Thompson, and A. N. Webber. 2001. Reduced photorespiration and increased energy-use efficiency in young CO2-enriched sorghum leaves. New Phytologist **150**:275-284.

Cousins, A. B., N. R. Adam, G. W. Wall, B. A. Kimball, P. J. Pinter, M. J. Ottman, S. W. Leavitt, and A. N. Webber. 2002. Photosystem II energy use, non-photochemical quenching and the xanthophyll cycle in Sorghum bicolor grown under drought and free-air CO2 enrichment (FACE) conditions. Plant Cell and Environment **25**:1551-1559.

Cousins, A. B., N. R. Adam, G. W. Wall, B. A. Kimball, P. J. Pinter, M. J. Ottman, S. W. Leavitt, and A. N. Webber. 2003. Development of C-4 photosynthesis in sorghum leaves grown under free-air CO2 enrichment (FACE). Journal of Experimental Botany **54**:1969-1975.

Crous, K. Y. and D. S. Ellsworth. 2004. Canopy position affects photosynthetic adjustments to long-term elevated CO2 concentration (FACE) in aging needles in a mature Pinus taeda forest. Tree Physiology **24**:961-970.

Crous, K. Y., M. B. Walters, and D. S. Ellsworth. 2008. Elevated CO2 concentration affects leaf photosynthesis-nitrogen relationships in Pinus taeda over nine years in FACE. Tree Physiology **28**:607-614.

Daepp, M., D. Suter, J. P. F. Almeida, H. Isopp, U. A. Hartwig, M. Frehner, H. Blum, J. Nosberger, and A. Luscher. 2000. Yield response of Lolium perenne swards to free air CO2 enrichment increased over six years in a high N input system on fertile soil. Global Change Biology **6**:805-816.

Davey, P. A., H. Olcer, O. Zakhleniuk, C. J. Bernacchi, C. Calfapietra, S. P. Long, and C. A. Raines. 2006. Can fast-growing plantation trees escape biochemical down-regulation of photosynthesis when grown throughout their complete production cycle in the open air under elevated carbon dioxide? Plant Cell and Environment **29**:1235-1244.

DeLucia, E. H., J. G. Hamilton, S. L. Naidu, R. B. Thomas, J. A. Andrews, A. C. Finzi, M. Lavine, R. Matamala, J. E. Mohan, G. R. Hendrey, and W. H. Schlesinger. 1999. Net primary production of a forest ecosystem with experimental CO(2) enrichment. Science **284**:1177-1179.

DeLucia, E. H. and R. B. Thomas. 2000. Photosynthetic responses to CO2 enrichment of four hardwood species in a forest understory. Oecologia **122**:11-19.

Dermody, O., S. P. Long, and E. H. DeLucia. 2006. How does elevated CO2 or ozone affect the leaf-area index of soybean when applied independently? New Phytologist **169**:145-155.

Derner, J. D., H. B. Johnson, B. A. Kimball, P. J. Pinter, H. W. Polley, C. R. Tischler, T. W. Boutton, R. L. Lamorte, G. W. Wall, N. R. Adam, S. W. Leavitt, M. J. Ottman, A. D. Matthias, and T. J. Brooks. 2003. Above- and below-ground responses of C-3-C-4 species mixtures to elevated CO2 and soil water availability. Global Change Biology **9**:452-460.

Dijkstra, F. A., S. E. Hobbie, P. B. Reich, and J. M. H. Knops. 2005. Divergent effects of elevated CO2, N fertilizattion, and plant diversity on soil C and N dynamics in a grassland field experiment. Plant and Soil **272**:41-52.

Edwards, G. R., H. Clark, and P. C. D. Newton. 2001a. The effects of elevated CO2 on seed production and seedling recruitment in a sheep-grazed pasture. Oecologia **127**:383-394.

Edwards, G. R., P. C. D. Newton, J. C. Tilbrook, and H. Clark. 2001b. Seedling performance of pasture species under elevated CO2. New Phytologist **150**:359-369.

Edwards, N. T., T. J. Tschaplinski, and R. J. Norby. 2002. Stem respiration increases in CO2-enriched sweetgum trees. New Phytologist **155**:239-248.

Eguchi, N., R. Funada, T. Ueda, K. Takagi, T. Hiura, K. Sasa, and T. Koike. 2005. Soil moisture condition and growth of deciduous tree seedlings native to northern Japan grown under elevated CO2 with a FACE system. Phyton-Annales Rei Botanicae **45**:133-138.

Ellsworth, D. S. 1999. CO2 enrichment in a maturing pine forest: are CO2 exchange and water status in the canopy affected? Plant Cell and Environment **22**:461-472.

Ellsworth, D. S., R. Oren, C. Huang, N. Phillips, and G. R. Hendrey. 1995. Leaf and Canopy Responses to Elevated Co2 in a Pine Forest under Free-Air Co2 Enrichment. Oecologia **104**:139-146.

Ellsworth, D. S., P. B. Reich, E. S. Naumburg, G. W. Koch, M. E. Kubiske, and S. D. Smith. 2004. Photosynthesis, carboxylation and leaf nitrogen responses of 16 species to elevated pCO(2) across four free-air CO2 enrichment experiments in forest, grassland and desert. Global Change Biology **10**:2121-2138.

Estiarte, M., J. Penuelas, B. A. Kimball, D. L. Hendrix, P. J. Pinter, G. W. Wall, R. L. LaMorte, and D. J. Hunsaker. 1999. Free-air CO2 enrichment of wheat: leaf flavonoid concentration throughout the growth cycle. Physiologia Plantarum **105**:423-433.

Finzi, A. C., A. S. Allen, E. H. DeLucia, D. S. Ellsworth, and W. H. Schlesinger. 2001. Forest litter production, chemistry, and decomposition following two years of free-air CO2 enrichment. Ecology **82**:470-484.

Finzi, A. C., E. H. DeLucia, J. G. Hamilton, D. D. Richter, and W. H. Schlesinger. 2002. The nitrogen budget of a pine forest under free air CO2 enrichment. Oecologia **132**:567-578.

Finzi, A. C., D. J. P. Moore, E. H. DeLucia, J. Lichter, K. S. Hofmockel, R. B. Jackson, H. S. Kim, R. Matamala, H. R. McCarthy, R. Oren, J. S. Pippen, and W. H. Schlesinger. 2006. Progressive nitrogen limitation of ecosystem processes under elevated CO2 in a warm-temperate forest. Ecology **87**:15-25.

Finzi, A. C., R. J. Norby, C. Calfapietra, A. Gallet-Budynek, B. Gielen, W. E. Holmes, M. R. Hoosbeek, C. M. Iversen, R. B. Jackson, M. E. Kubiske, J. Ledford, M. Liberloo, R. Oren, A. Polle, S. Pritchard, D. R. Zak, W. H. Schlesinger, and R. Ceulemans. 2007. Increases in nitrogen uptake rather than nitrogen-use efficiency support higher rates of temperate forest productivity under elevated CO2. Proceedings of the National Academy of Sciences of the United States of America **104**:14014-14019.

Franzaring, J., P. Hoegy, and A. Fangmeier. 2008. Effects of free-air CO2 enrichment on the growth of summer oilseed rape (Brassica napus cv. Campino). Agriculture Ecosystems & Environment **128**:127-134.

Frehner, M., A. Luscher, T. Hebeisen, S. Zanetti, F. Schubiger, and M. Scalet. 1997. Effects of elevated partial pressure of carbon dioxide and season of the year on forage quality and cyanide concentration of Trifolium repens L. from a FACE experiment. Acta Oecologica-International Journal of Ecology **18**:297-304.

Garcia, R. L., S. P. Long, G. W. Wall, C. P. Osborne, B. A. Kimball, G. Y. Nie, P. J. Pinter, R. L. Lamorte, and F. Wechsung. 1998. Photosynthesis and conductance of spring-wheat leaves: field response to continuous free-air atmospheric CO2 enrichment. Plant Cell and Environment **21**:659-669.

Gielen, B., C. Calfapietra, M. Lukac, V. E. Wittig, P. De Angelis, I. A. Janssens, M. C. Moscatelli, S. Grego, M. F. Cotrufo, D. L. Godbold, M. R. Hoosbeek, S. P. Long, F. Miglietta, A. Polle, C. J. Bernacchi, P. A. Davey, R. Ceulemans, and G. E. Scarascia-Mugnozza. 2005. Net carbon storage in a poplar plantation (POPFACE) after three years of free-air CO2 enrichment. Tree Physiology **25**:1399-1408.

Gielen, B., C. Calfapietra, M. Sabatti, and R. Ceulemans. 2001. Leaf area dynamics in a closed poplar plantation under free-air carbon dioxide enrichment. Tree Physiology **21**:1245-1255.

Gielen, B., G. Scarascia-Mugnozza, and R. Ceulemans. 2003. Stem respiration of Populus species in the third year of free-air CO2 enrichment. Physiologia Plantarum **117**:500-507.

Grant, R. F., G. W. Wall, B. A. Kimball, K. F. A. Frumau, P. J. Pinter, D. J. Hunsaker, and R. L. Lamorte. 1999. Crop water relations under different CO2 and irrigation: testing of ecosys with the free air CO2 enrichment (FACE) experiment. Agricultural and Forest Meteorology **95**:27-51.

Gunderson, C. A., J. D. Sholtis, S. D. Wullschleger, D. T. Tissue, P. J. Hanson, and R. J. Norby. 2002. Environmental and stomatal control of photosynthetic enhancement in the canopy of a sweetgum (Liquidambar styraciflua L.) plantation during 3 years of CO2 enrichment. Plant Cell and Environment **25**:379-393.

Guo, J. M., C. M. Trotter, and P. C. D. Newton. 2006. Initial observations of increased requirements for light-energy dissipation in ryegrass (Lolium perenne) when source/sink ratios become high at a naturally grazed Free Air CO2 Enrichment (FACE) site. Functional Plant Biology **33**:1045-1053.

Hamerlynck, E. P., T. E. Huxman, T. N. Charlet, and S. D. Smith. 2002. Effects of elevated CO2 (FACE) on the functional ecology of the drought-deciduous Mojave Desert shrub, Lycium andersonii. Environmental and Experimental Botany **48**:93-106.

Hamerlynck, E. P., T. E. Huxman, R. S. Nowak, S. Redar, M. E. Loik, D. N. Jordan, S. F. Zitzer, J. S. Coleman, J. R. Seemann, and S. D. Smith. 2000. Photosynthetic responses of larrea tridentata to a step-increase in atmospheric CO2 at the Nevada desert FACE facility. Journal of Arid Environments **44**:425-436.

Handa, I. T., C. Korner, and S. Hattenschwiler. 2006. Conifer stem growth at the altitudinal treeline in response to four years of CO2 enrichment. Global Change Biology **12**:2417-2430.

Hansen, R. A., R. S. Williams, D. C. Degenhardt, and D. E. Lincoln. 2001. Non-litter effects of elevated CO2 on forest floor microarthropod abundances. Plant and Soil **236**:139-144.

Hattenschwiler, S., I. T. Handa, L. Egli, R. Asshoff, W. Ammann, and C. Korner. 2002. Atmospheric CO2 enrichment of alpine treeline conifers. New Phytologist **156**:363-375.

Hebeisen, T., A. Luscher, and J. Nosberger. 1997. Effects of elevated atmospheric CO2 and nitrogen fertilisation on yield of Trifolium repens and Lolium perenne. Acta Oecologica-International Journal of Ecology **18**:277-284.

Hendrix, D. L., J. R. Mauney, B. A. Kimball, K. Lewin, J. Nagy, and G. R. Hendrey. 1994. Influence of Elevated Co2 and Mild Water-Stress on Nonstructural Carbohydrates in Field-Grown Cotton Tissues. Agricultural and Forest Meteorology **70**:153-162.

Herrick, J. D. and R. B. Thomas. 1999. Effects of CO2 enrichment on the photosynthetic light response of sun and shade leaves of canopy sweetgum trees (Liquidambar styraciflua) in a forest ecosystem. Tree Physiology **19**:779-786.

Herrick, J. D. and R. B. Thomas. 2003. Leaf senescence and late-season net photosynthesis of sun and shade leaves of overstory sweetgum (Liquidambar styraciflua) grown in elevated and ambient carbon dioxide concentrations. Tree Physiology **23**:109-118.

Hileman, D. R., G. Huluka, P. K. Kenjige, N. Sinha, N. C. Bhattacharya, P. K. Biswas, K. F. Lewin, J. Nagy, and G. R. Hendrey. 1994. Canopy Photosynthesis and Transpiration of Field-Grown Cotton Exposed to Free-Air Co2 Enrichment (Face) and Differential Irrigation. Agricultural and Forest Meteorology **70**:189-207.

Hill, P. W., C. Marshall, G. G. Williams, H. Blum, H. Harmens, D. L. Jones, and J. F. Farrar. 2007. The fate of photosynthetically-fixed carbon in Lolium perenne grassland as modified by elevated CO2 and sward management. New Phytologist **173**:766-777.

Holmes, W. E., D. R. Zak, K. S. Pregitzer, and J. S. King. 2006. Elevated CO2 and O-3 alter soil nitrogen transformations beneath trembling aspen, paper birch, and sugar maple. Ecosystems **9**:1354-1363.

Holton, M. K., R. L. Lindroth, and E. V. Nordheim. 2003. Foliar quality influences tree-herbivore-parasitoid interactions: effects of elevated CO2, O-3, and plant genotype. Oecologia **137**:233-244.

Hoosbeek, M. R., N. van Breemen, F. Berendse, P. Grosvernier, H. Vasander, and B. Wallen. 2001. Limited effect of increased atmospheric CO2 concentration on ombrotrophic bog vegetation. New Phytologist **150**:459-463.

Hoosbeek, M. R., N. Van Breemen, H. Vasander, A. Buttler, and F. Berendse. 2002. Potassium limits potential growth of bog vegetation under elevated atmospheric CO2 and N deposition. Global Change Biology **8**:1130-1138.

Housman, D. C., E. Naumburg, T. E. Huxman, T. N. Charlet, R. S. Nowak, and S. D. Smith. 2006. Increases in desert shrub productivity under elevated carbon dioxide vary with water availability. Ecosystems **9**:374-385.

Hovenden, M. J. 2003. Photosynthesis of coppicing poplar clones in a free-air CO2 enrichment (FACE) experiment in a short-rotation forest. Functional Plant Biology **30**:391-400.

Hovenden, M. J., F. Miglietta, A. Zaldei, J. K. Vander Schoor, K. E. Wills, and P. C. D. Newton. 2006. The TasFACE climate-change impacts experiment: design and performance of combined elevated CO2 and temperature enhancement in a native Tasmanian grassland. Australian Journal of Botany **54**:1-10.

Hovenden, M. J., P. C. D. Newton, R. A. Carran, P. Theobald, K. E. Wills, J. K. V. Schoor, A. L. Williams, and Y. Osanai. 2008. Warming prevents the elevated CO2-induced reduction in available soil nitrogen in a temperate, perennial grassland. Global Change Biology **14**:1018-1024.

Huluka, G., D. R. Hileman, P. K. Biswas, K. F. Lewin, J. Nagy, and G. R. Hendrey. 1994. Effects of Elevated Co2 and Water-Stress on Mineral Concentration of Cotton. Agricultural and Forest Meteorology **70**:141-152.

Hunt, M. G., S. Rasmussen, P. C. D. Newton, A. J. Parsons, and J. A. Newman. 2005. Near-term impacts of elevated CO2, nitrogen and fungal endophyte-infection on Lolium perenne L. growth, chemical composition and alkaloid production. Plant Cell and Environment **28**:1345-1354.

Huxman, T. E., E. P. Hamerlynck, B. D. Moore, S. D. Smith, D. N. Jordan, S. F. Zitzer, R. S. Nowak, J. S. Coleman, and J. R. Seemann. 1998. Photosynthetic down-regulation in Larrea tridentata exposed to elevated atmospheric CO2: interaction with drought under glasshouse and field (FACE) exposure. Plant Cell and Environment **21**:1153-1161.

Huxman, T. E. and S. D. Smith. 2001. Photosynthesis in an invasive grass and native forb at elevated CO2 during an El Nino year in the Mojave Desert. Oecologia **128**:193-201.

Ineson, P., M. F. Cotrufo, R. Bol, D. D. Harkness, and H. Blum. 1996. Quantification of soil carbon inputs under elevated CO2:C-3 plants in a C-4 soil. Plant and Soil **187**:345-350.

Inubushi, K., W. G. Cheng, S. Aonuma, M. M. Hoque, K. Kobayashi, S. Miura, H. Y. Kim, and M. Okada. 2003. Effects of free-air CO2 enrichment (FACE) on CH4 emission from a rice paddy field. Global Change Biology **9**:1458-1464.

Isebrands, J. G., E. P. McDonald, E. Kruger, G. Hendrey, K. Percy, K. Pregitzer, J. Sober, and D. F. Karnosky. 2001. Growth responses of Populus tremuloides clones to interacting elevated carbon dioxide and tropospheric ozone. Environmental Pollution **115**:359-371.

Isopp, H., M. Frehner, J. P. F. Almeida, H. Blum, M. Daepp, U. A. Hartwig, A. Luscher, S. Suter, and J. Nosberger. 2000. Nitrogen plays a major role in leaves when source-sink relations change: C and N metabolism in Lolium perenne growing under free air CO2 enrichment. Australian Journal of Plant Physiology **27**:851-858.

Jasoni, R. L., S. D. Smith, and J. A. Arnone. 2005. Net ecosystem CO2 exchange in Mojave Desert shrublands during the eighth year of exposure to elevated CO2. Global Change Biology **11**:749-756.

Kaakinen, S., K. Kostiainen, F. Ek, P. Saranpaa, M. E. Kubiske, J. Sober, D. F. Karnosky, and E. Vapaavuori. 2004. Stem wood properties of Populus tremuloides, Betula papyrifera and Acer saccharum saplings after 3 years of treatments to elevated carbon dioxide and ozone. Global Change Biology **10**:1513-1525.

Kammann, C., L. Grunhage, U. Gruters, S. Janze, and H. J. Jager. 2005. Response of aboveground grassland biomass and soil moisture to moderate long-term CO2 enrichment. Basic and Applied Ecology **6**:351-365.

Karnosky, D. F. 2003. Impacts of elevated atmospheric CO2 on forest trees and forest ecosystems: knowledge gaps. Environment International **29**:161-169.

Karnosky, D. F., K. S. Pregitzer, D. R. Zak, M. E. Kubiske, G. R. Hendrey, D. Weinstein, M. Nosal, and K. E. Percy. 2005. Scaling ozone responses of forest trees to the ecosystem level in a changing climate. Plant Cell and Environment **28**:965-981.

Keel, S. G., R. T. W. Siegwolf, and C. Korner. 2006. Canopy CO2 enrichment permits tracing the fate of recently assimilated carbon in a mature deciduous forest. New Phytologist **172**:319-329.

Kimball, B. A., P. J. Pinter, R. L. Garcia, R. L. LaMorte, G. W. Wall, D. J. Hunsaker, G. Wechsung, F. Wechsung, and T. Kartschall. 1995. Productivity and water use of wheat under free-air CO2 enrichment. Global Change Biology **1**:429-442.

King, J. S., M. E. Kubiske, K. S. Pregitzer, G. R. Hendrey, E. P. McDonald, C. P. Giardina, V. S. Quinn, and D. F. Karnosky. 2005. Tropospheric O-3 compromises net primary production in young stands of trembling aspen, paper birch and sugar maple in response to elevated atmospheric CO2. New Phytologist **168**:623-635.

Knepp, R. G., J. G. Hamilton, J. E. Mohan, A. R. Zangerl, M. R. Berenbaum, and E. H. DeLucia. 2005. Elevated CO2 reduces leaf damage by insect herbivores in a forest community. New Phytologist **167**:207-218.

Koizumi, H., T. Kibe, S. Mariko, T. Ohtsuka, T. Nakadai, W. H. Mo, H. Toda, N. Seiichi, and K. Kobayashi. 2001. Effect of free-air CO2 enrichment (FACE) on CO2 exchange at the flood-water surface in a rice paddy field. New Phytologist **150**:231-239.

Korner, C., R. Asshoff, O. Bignucolo, S. Hattenschwiler, S. G. Keel, S. Pelaez-Riedl, S. Pepin, R. T. W. Siegwolf, and G. Zotz. 2005. Carbon flux and growth in mature deciduous forest trees exposed to elevated CO2. Science **309**:1360-1362.

Kreuzwieser, J., H. Rennenberg, and R. Steinbrecher. 2006. Impact of short-term and long-term elevated CO2 on emission of carbonyls from adult Quercus petraea and Carpinus betulus trees. Environmental Pollution **142**:246-253.

Kubiske, M. E., V. S. Quinn, W. E. Heilman, E. P. McDonald, P. E. Marquardt, R. M. Teclaw, A. L. Friend, and D. F. Karnosky. 2006. Interannual climatic variation mediates elevated CO2 and O-3 effects on forest growth. Global Change Biology **12**:1054-1068.

Lau, J. A., J. Peiffer, P. B. Reich, and P. Tiffin. 2008a. Transgenerational effects of global environmental change: long-term CO(2) and nitrogen treatments influence offspring growth response to elevated CO(2). Oecologia **158**:141-150.

Lau, J. A., J. Strengbom, L. R. Stone, P. B. Reich, and P. Tiffin. 2008b. Direct and indirect effects of CO2, nitrogen, and community diversity on plant-enemy interactions. Ecology **89**:226-236.

Leakey, A. D. B., C. J. Bernacchi, F. G. Dohleman, D. R. Ort, and S. P. Long. 2004. Will photosynthesis of maize (Zea mays) in the US Corn Belt increase in future [CO2] rich atmospheres? An analysis of diurnal courses of CO2 uptake under free-air concentration enrichment (FACE). Global Change Biology **10**:951-962.

Leakey, A. D. B., C. J. Bernacchi, S. P. Long, and D. R. Ort. 2005. Elevated CO, does not stimulate C-4 photosynthesis directly, but impacts water relations and indirectly enhances carbon gain during drought stress in maize (Zea mays) grown under free-air CO2 enrichment (FACE). Comparative Biochemistry and Physiology a-Molecular & Integrative Physiology **141**:S305-S306.

Leakey, A. D. B., C. J. Bernacchi, D. R. Ort, and S. P. Long. 2006. Long-term growth of soybean at elevated [CO2] does not cause acclimation of stomatal conductance under fully open-air conditions. Plant Cell and Environment **29**:1794-1800.

Leuzinger, S., G. Zotz, R. Asshoff, and C. Korner. 2005. Responses of deciduous forest trees to severe drought in Central Europe. Tree Physiology **25**:641-650.

Liberloo, M., C. Calfapietra, M. Lukac, D. Godbold, Z. B. Luos, A. Polle, M. R. Hoosbeek, O. Kull, M. Marek, C. Raines, M. Rubino, G. Taylor, G. Scarascia-Mugnozza, and R. Ceulemans. 2006. Woody biomass production during the second rotation of a bio-energy Populus plantation increases in a future high CO2 world. Global Change Biology **12**:1094-1106.

Liberloo, M., S. Y. Dillen, C. Calfapietra, S. Marinari, Z. Bin Luo, P. De Angelis, and R. Ceulemans. 2005. Elevated CO2 concentration, fertilization and their interaction: growth stimulation in a short-rotation poplar coppice (EUROFACE). Tree Physiology **25**:179-189.

Liberloo, M., I. Tulva, O. Raim, O. Kull, and R. Ceulemans. 2007. Photosynthetic stimulation under long-term CO2 enrichment and fertilization is sustained across a closed Populus canopy profile (EUROFACE). New Phytologist **173**:537-549.

Lindroth, R. L., B. J. Kopper, W. F. J. Parsons, J. G. Bockheim, D. F. Karnosky, G. R. Hendrey, K. S. Pregitzer, J. G. Isebrands, and J. Sober. 2001. Consequences of elevated carbons dioxide and ozone for foliar chemical composition and dynamics in trembling aspen (Populus tremuloides) and paper birch (Betula papyrifera). Environmental Pollution **115**:395-404.

Liu, L. L., J. S. King, and C. P. Giardina. 2005. Effects of elevated concentrations of atmospheric CO2 and tropospheric O-3 on leaf litter production and chemistry in trembling aspen and paper birch communities. Tree Physiology **25**:1511-1522.

Lukac, M., C. Calfapietra, and D. L. Godbold. 2003. Production, turnover and mycorrhizal colonization of root systems of three Populus species grown under elevated CO2 (POPFACE). Global Change Biology **9**:838-848.

Luo, Y. Q., D. F. Hui, and D. Q. Zhang. 2006. Elevated CO2 stimulates net accumulations of carbon and nitrogen in land ecosystems: A meta-analysis. Ecology **87**:53-63.

Luo, Z.-B., C. Calfapietra, G. Scarascia-Mugnozza, M. Liberloo, and A. Polle. 2008. Carbon-based secondary metabolites and internal nitrogen pools in Populus nigra under Free Air CO2 Enrichment (FACE) and nitrogen fertilisation. Plant and Soil **304**:45-57.

Luscher, A. and J. Nosberger. 1997. Interspecific and intraspecific variability in the response of grasses and legumes to free air CO2 enrichment. Acta Oecologica-International Journal of Ecology **18**:269-275.

Magliulo, V., M. Bindi, and G. Rana. 2003. Water use of irrigated potato (Solanum tuberosum L.) grown under free air carbon dioxide enrichment in central Italy. Agriculture Ecosystems & Environment **97**:65-80.

Maier, C. A., S. Palmroth, and E. Ward. 2008. Short-term effects of fertilization on photosynthesis and leaf morphology of field-grown loblolly pine following long-term exposure to elevated CO2 concentration. Tree Physiology **28**:597-606.

Marchi, S., R. Tognetti, F. P. Vaccari, M. Lanini, M. Kaligaric, F. Miglietta, and A. Raschi. 2004. Physiological and morphological responses of grassland species to elevated atmospheric CO2 concentrations in FACE-systems and natural CO2 springs. Functional Plant Biology **31**:181-194.

Mauney, J. R., B. A. Kimball, P. J. Pinter, R. L. Lamorte, K. F. Lewin, J. Nagy, and G. R. Hendrey. 1994. Growth and Yield of Cotton in Response to a Free-Air Carbon-Dioxide Enrichment (Face) Environment. Agricultural and Forest Meteorology **70**:49-67.

McCarthy, H. R., R. Oren, K. H. Johnsen, A. C. Finzi, S. G. Pritchard, R. B. Jackson, C. W. Cook, and K. K. Treseder. 2007. Reassessment of carbon accumulation at the Duke free air CO2 enrichment site: Interactions of atmospheric CO2 with nitrogen and water availability and stand development. Ecological Society of America Annual Meeting Abstracts.

McElrone, A. J., C. D. Reid, K. A. Hoye, E. Hart, and R. B. Jackson. 2005. Elevated CO2 reduces disease incidence and severity of a red maple fungal pathogen via changes in host physiology and leaf chemistry. Global Change Biology **11**:1828-1836.

Miglietta, F., A. Giuntoli, and M. Bindi. 1996. The effect of free air carbon dioxide enrichment (FACE) and soil nitrogen availability on the photosynthetic capacity of wheat. Photosynthesis Research **47**:281-290.

Miglietta, F., V. Magliulo, M. Bindi, L. Cerio, F. P. Vaccari, V. Loduca, and A. Peressotti. 1998. Free air CO2 enrichment of potato (Solanum tuberosum L.): development, growth and yield. Global Change Biology **4**:163-172.

Mohan, J. E., J. S. Clark, and W. H. Schlesinger. 2007. Long-term CO2 enrichment of a forest ecosystem: Implications for forest regeneration and succession. Ecological Applications **17**:1198-1212.

Myers, D. A., R. B. Thomas, and E. H. Delucia. 1999. Photosynthetic capacity of loblolly pine (Pinus taeda L.) trees during the first year of carbon dioxide enrichment in a forest ecosystem. Plant Cell and Environment **22**:473-481.

Nagel, J. M., T. E. Huxman, K. L. Griffin, and S. D. Smith. 2004. Co-2 enrichment reduces the energetic cost of biomass construction in an invasive desert grass. Ecology **85**:100-106.

Natali, S., S. A. Sanudo-Wilhelmy, and M. Lerdau. 2009. Effects of elevated carbon dioxide and nitrogen fertilization on nitrate reductase activity in sweetgum and loblolly pine trees in two temperate forests. Plant and Soil **314**:197-210.

Natali, S. M., S. A. Sanudo-Wilhelmy, R. J. Norby, H. Zhang, A. C. Finzi, and M. T. Lerdau. 2008. Increased mercury in forest soils under elevated carbon dioxide. Oecologia **158**:343-354.

Naumburg, E. and D. S. Ellsworth. 2000. Photosynthesis sunfleck utilization potential of understory saplings growing under elevated CO2 in FACE. Oecologia **122**:163-174.

Nie, G. Y., S. P. Long, R. L. Garcia, B. A. Kimball, R. L. Lamorte, P. J. Pinter, G. W. Wall, and A. N. Webber. 1995. Effects of Free-Air Co2 Enrichment on the Development of the Photosynthetic Apparatus in Wheat, as Indicated by Changes in Leaf Proteins. Plant Cell and Environment **18**:855-864.

Nijs, I., R. Ferris, H. Blum, G. Hendrey, and I. Impens. 1997. Stomatal regulation in a changing climate: a field study using Free Air Temperature Increase (FATI) and Free Air CO2 enrichment (FACE). Plant Cell and Environment **20**:1041-1050.

Nijs, I., F. Kockelbergh, H. Teughels, H. Blum, G. Hendrey, and I. Impens. 1996. Free air temperature increase (FATI): A new tool to study global warming effects on plants in the field. Plant Cell and Environment **19**:495-502.

Nitschelm, J. J., A. Luscher, U. A. Hartwig, and C. VanKessel. 1997. Using stable isotopes to determine soil carbon input differences under ambient and elevated atmospheric CO2 conditions. Global Change Biology **3**:411-416.

Noormets, A., E. P. McDonald, R. E. Dickson, E. L. Kruger, A. Sober, J. G. Isebrands, and D. F. Karnosky. 2001. The effect of elevated carbon dioxide and ozone on leaf- and branch-level photosynthesis and potential plant-level carbon gain in aspen. Trees-Structure and Function **15**:262-270.

Norby, R. J. and C. M. Iversen. 2006. Nitrogen uptake, distribution, turnover, and efficiency of use in a CO2-enriched sweetgum forest. Ecology **87**:5-14.

Norby, R. J., J. Ledford, C. D. Reilly, N. E. Miller, and E. G. O'Neill. 2004. Fine-root production dominates response of a deciduous forest to atmospheric CO2 enrichment. Proceedings of the National Academy of Sciences of the United States of America **101**:9689-9693.

Norby, R. J., J. D. Sholtis, C. A. Gunderson, and S. S. Jawdy. 2003. Leaf dynamics of a deciduous forest canopy: no response to elevated CO2. Oecologia **136**:574-584.

Norton, L. R., L. G. Firbank, and H. Blum. 1999. Effects of free-air CO2 Enrichment (FACE) on experimental grassland communities. Functional Ecology **13**:38-44.

Novotny, A. M., J. D. Schade, S. E. Hobbie, A. D. Kay, M. Kyle, P. B. Reich, and J. J. Elser. 2007. Stoichiometric response of nitrogen-fixing and non-fixing dicots to manipulations of CO2, nitrogen, and diversity. Oecologia **151**:687-696.

Osborne, C. P., S. P. Long, R. L. Garcia, G. W. Wall, B. A. Kimball, P. J. Pinter, R. L. LaMorte, and G. R. Hendrey. 1995. Do shade and elevated CO2 concentration have an interactive effect on photosynthesis? An analysis using wheat grown under free-air CO2-enrichment (FACE). Photosynthesis: from Light to Biosphere, Vol 5:929-932.

Pang, J., J. G. Zhu, Z. B. Xie, G. Liu, Y. L. Zhang, G. P. Chen, Q. Zeng, and L. Cheng. 2006. A new explanation of the N concentration decrease in tissues of rice (Oryza sativa L.) exposed to elevated atmospheric pCO(2). Environmental and Experimental Botany **57**:98-105.

Parsons, W. F. J., R. L. Lindroth, and J. G. Bockheim. 2004. Decomposition of Betula papyrifera leaf litter under the independent and interactive effects of elevated CO2 and O-3. Global Change Biology **10**:1666-1677.

Phillips, D. L., M. G. Johnson, D. T. Tingey, C. E. Catricala, T. L. Hoyman, and R. S. Nowak. 2006. Effects of elevated CO2 on fine root dynamics in a Mojave Desert community: a FACE study. Global Change Biology **12**:61-73.

Picon-Cochard, C., F. Teyssonneyre, J. M. Besle, and J. F. Soussana. 2004. Effects of elevated CO2 and cutting frequency on the productivity and herbage quality of a semi-natural grassland. European Journal of Agronomy **20**:363-377.

Pregitzer, K. S., A. J. Burton, J. S. King, and D. R. Zak. 2008. Soil respiration, root biomass, and root turnover following long-term exposure of northern forests to elevated atmospheric Co-2 and tropospheric O-3. New Phytologist **180**:153-161.

Prior, S. A., H. H. Rogers, G. B. Runion, and G. R. Hendrey. 1994. Free-Air Co2 Enrichment of Cotton - Vertical and Lateral Root Distribution Patterns. Plant and Soil **165**:33-44.

Reich, P. B., B. A. Hungate, and Y. Q. Luo. 2006. Carbon-nitrogen interactions in terrestrial ecosystems in response to rising atmospheric carbon dioxide. Annual Review of Ecology Evolution and Systematics **37**:611-636.

Reich, P. B., J. Knops, D. Tilman, J. Craine, D. Ellsworth, M. Tjoelker, T. Lee, D. Wedin, S. Naeem, D. Bahauddin, G. Hendrey, S. Jose, K. Wrage, J. Goth, and W. Bengston. 2001. Plant diversity enhances ecosystem responses to elevated CO2 and nitrogen deposition (vol 410, pg 809, 2001). Nature **411**:824-+.

Rogers, A., D. J. Allen, P. A. Davey, P. B. Morgan, E. A. Ainsworth, C. J. Bernacchi, G. Cornic, O. Dermody, F. G. Dohleman, E. A. Heaton, J. Mahoney, X. G. Zhu, E. H. Delucia, D. R. Ort, and S. P. Long. 2004. Leaf photosynthesis and carbohydrate dynamics of soybeans grown throughout their life-cycle under Free-Air Carbon dioxide Enrichment. Plant Cell and Environment **27**:449-458.

Rogers, A. and D. S. Ellsworth. 2002. Photosynthetic acclimation of Pinus taeda (loblolly pine) to long-term growth in elevated pCO(2) (FACE). Plant Cell and Environment **25**:851-858.

Rogers, A., B. U. Fischer, J. Bryant, M. Frehner, H. Blum, C. A. Raines, and S. P. Long. 1998. Acclimation of photosynthesis to elevated CO2 under low-nitrogen nutrition is affected by the capacity for assimilate utilization. Perennial ryegrass under free-air CO2 enrichment. Plant Physiology **118**:683-689.

Rogers, A., Y. Gibon, M. Stitt, P. B. Morgan, C. J. Bernacchi, D. R. Ort, and S. P. Long. 2006. Increased C availability at elevated carbon dioxide concentration improves N assimilation in a legume. Plant Cell and Environment **29**:1651-1658.

Ross, D. J., P. C. D. Newton, and K. R. Tate. 2004. Elevated [CO2] effects on herbage production and soil carbon and nitrogen pools and mineralization in a species-rich, grazed pasture on a seasonally dry sand. Plant and Soil **260**:183-196.

Saarnio, S., S. Jarvio, T. Saarinen, H. Vasander, and J. Silvola. 2003. Minor changes in vegetation and carbon gas balance in a boreal mire under a raised CO2 or NH4NO3 supply. Ecosystems **6**:46-60.

Sasaki, H., T. Hara, S. Ito, S. Miura, M. M. Hoque, M. Lieffering, H. Y. Kim, M. Okada, and K. Kobayashi. 2005. Seasonal changes in canopy photosynthesis and respiration, and partitioning of photosynthate, in rice (Oryza sativa L.) grown under free-air CO2 enrichment. Plant and Cell Physiology **46**:1704-1712.

Sasaki, H., T. Hara, S. Ito, N. Uehara, H. Y. Kim, M. Lieffering, M. Okada, and K. Kobayashi. 2007. Effect of free-air CO2 enrichment on the storage of carbohydrate fixed at different stages in rice (Oryza sativa L.). Field Crops Research **100**:24-31.

Schafer, K. V. R., R. Oren, D. S. Ellsworth, C. T. Lai, J. D. Herrick, A. C. Finzi, D. D. Richter, and G. G. Katul. 2003. Exposure to an enriched CO2 atmosphere alters carbon assimilation and allocation in a pine forest ecosystem. Global Change Biology **9**:1378-1400.

Schafer, K. V. R., R. Oren, C. T. Lai, and G. G. Katul. 2002. Hydrologic balance in an intact temperate forest ecosystem under ambient and elevated atmospheric CO2 concentration. Global Change Biology **8**:895-911.

Schneider, M. K., A. Luscher, M. Richter, U. Aeschlimann, U. A. Hartwig, H. Blum, E. Frossard, and J. Nosberger. 2004. Ten years of free-air CO2 enrichment altered the mobilization of N from soil in Lolium perenne L. swards. Global Change Biology **10**:1377-1388.

Seneweera, S., J. Conroy, and K. Kobayashi. 2002. Photosynthetic acclimation of rice to free air CO2 enrichment (FACE) depend on carbon and nitrogen relationship during ontogeny. Plant and Cell Physiology **43**:S68-S68.

Senock, R. S., J. M. Ham, T. M. Loughin, B. A. Kimball, D. J. Hunsaker, P. J. Pinter, G. W. Wall, R. L. Garcia, and R. L. LaMorte. 1996. Sap flow in wheat under free-air CO2 enrichment. Plant Cell and Environment **19**:147-158.

Shimono, H., M. Okada, Y. Yamakawa, H. Nakamura, K. Kobayashi, and T. Hasegawa. 2007. Lodging in rice can be alleviated by atmospheric CO2 enrichment. Agriculture Ecosystems & Environment **118**:223-230.

Sholtis, J. D., C. A. Gunderson, R. J. Norby, and D. T. Tissue. 2004. Persistent stimulation of photosynthesis by elevated CO2 in a sweetgum (Liquidambar styraciflua) forest stand. New Phytologist **162**:343-354.

Sinclair, T. R., P. J. Pinter, B. A. Kimball, F. J. Adamsen, R. L. LaMorte, G. W. Wall, D. J. Hunsaker, N. Adam, T. J. Brooks, R. L. Garcia, T. Thompson, S. Leavitt, and A. Matthias. 2000. Leaf nitrogen concentration of wheat subjected to elevated [CO2] and either water or N deficits. Agriculture Ecosystems & Environment **79**:53-60.

Singsaas, E. L., D. R. Ort, and E. H. DeLucia. 2000. Diurnal regulation of photosynthesis in understory saplings. New Phytologist **145**:39-49.

Springer, C. J. and R. B. Thomas. 2007. Photosynthetic responses of forest understory tree species to long-term exposure to elevated carbon dioxide concentration at the Duke Forest FACE experiment. Tree Physiology **27**:25-32.

Strengbom, J. and P. B. Reich. 2006. Elevated CO(2) and increased N supply reduce leaf disease and related photosynthetic impacts on Solidago rigida. Oecologia **149**:519-525.

Suter, D., J. Nosberger, and A. Luscher. 2001. Response of perennial ryegrass to free-air CO2 enrichment (FACE) is related to the dynamics of sward structure during regrowth. Crop Science **41**:810-817.

Taylor, G., R. Ceulemans, R. Ferris, S. D. L. Gardner, and B. Y. Shao. 2001. Increased leaf area expansion of hybrid poplar in elevated CO2. From controlled environments to open-top chambers and to FACE. Environmental Pollution **115**:463-472.

Taylor, G., M. J. Tallis, C. P. Giardina, K. E. Percy, F. Miglietta, P. S. Gupta, B. Gioli, C. Calfapietra, B. Gielen, M. E. Kubiske, G. E. Scarascia-Mugnozza, K. Kets, S. P. Long, and D. F. Karnosky. 2008. Future atmospheric CO2 leads to delayed autumnal senescence. Global Change Biology **14**:264-275.

Thayer, S. S., S. B. St Clair, C. B. Field, and S. C. Somerville. 2008. Accentuation of phosphorus limitation in Geranium dissectum by nitrogen: an ecological genomics study. Global Change Biology **14**:1877-1890.

Tissue, D. T., J. D. Lewis, S. D. Wullschleger, J. S. Amthor, K. L. Griffin, and R. Anderson. 2002. Leaf respiration at different canopy positions in sweetgum (Liquidambar styraciflua) grown in ambient and elevated concentrations of carbon dioxide in the field. Tree Physiology **22**:1157-1166.

Tognetti, R., A. Longobucco, A. Raschi, F. Miglietta, and I. Fumagalli. 1999. Responses of two Populus clones to elevated atmospheric CO2 concentration in the field. Annals of Forest Science **56**:493-500.

Tognetti, R., L. Sebastiani, A. Minnocci, and A. Raschi. 2002. Foliar responses of olive trees (Olea europaea L.) under field exposure to elevated CO2 concentration. Proceedings of the Fourth International Symposium on Olive Growing, Vols 1 and 2:449-452.

Tognetti, R., L. Sebastiani, C. Vitagliano, A. Raschi, and A. Minnocci. 2001. Responses of two olive tree (Olea europaea L.) cultivars to elevated CO2 concentration in the field. Photosynthetica **39**:403-410.

Tricker, P. J., H. Trewin, O. Kull, G. J. J. Clarkson, E. Eensalu, M. J. Tallis, A. Colella, C. P. Doncaster, M. Sabatti, and G. Taylor. 2005. Stomatal conductance and not stomatal density determines the long-term reduction in leaf transpiration of poplar in elevated CO2. Oecologia **143**:652-660.

Wall, G. W. 2001. Elevated atmospheric CO2 alleviates drought stress in wheat. Agriculture Ecosystems & Environment **87**:261-271.

Wall, G. W., R. L. Garcia, B. A. Kimball, D. J. Hunsaker, P. J. Pinter, S. P. Long, C. P. Osborne, D. L. Hendrix, F. Wechsung, G. Wechsung, S. W. Leavitt, R. L. LaMorte, and S. B. Idso. 2006. Interactive effects of elevated carbon dioxide and drought on wheat. Agronomy Journal **98**:354-381.

Warwick, K. R., G. Taylor, and H. Blum. 1998. Biomass and compositional changes occur in chalk grassland turves exposed to elevated CO2 for two seasons in FACE. Global Change Biology **4**:375-385.

Weatherly, H. E., S. F. Zitzer, J. S. Coleman, and J. A. Arnone. 2003. In situ litter decomposition and litter quality in a Mojave Desert ecosystem: effects of elevated atmospheric CO2 and interannual climate variability. Global Change Biology **9**:1223-1233.

Wechsung, G., F. Wechsung, G. W. Wall, F. J. Adamsen, B. A. Kimball, R. L. Garcia, P. J. Pinter, and T. Kartschall. 1995. Biomass and growth rate of a spring wheat root system grown in free-air CO2 enrichment (FACE) and ample soil moisture. Journal of Biogeography **22**:623-634.

West, J. B., J. HilleRisLambers, T. D. Lee, S. E. Hobbie, and P. B. Reich. 2005. Legume species identity and soil nitrogen supply determine symbiotic nitrogen-fixation responses to elevated atmospheric [CO2]. New Phytologist **167**:523-530.

Winkler, J. B. and M. Herbst. 2004. Do plants of a semi-natural grassland community benefit from long-term CO2 enrichment? Basic and Applied Ecology **5**:131-143.

Wittig, V. E., C. J. Bernacchi, X. G. Zhu, C. Calfapietra, R. Ceulemans, P. Deangelis, B. Gielen, F. Miglietta, P. B. Morgan, and S. P. Long. 2005. Gross primary production is stimulated for

three Populus species grown under free-air CO2 enrichment from planting through canopy closure. Global Change Biology **11**:644-656.

Wullschleger, S. D. and R. J. Norby. 2001. Sap velocity and canopy transpiration in a sweetgum stand exposed to free-air CO2 enrichment (FACE). New Phytologist **150**:489-498.

Wustman, B. A., E. Oksanen, D. F. Karnosky, A. Noormets, J. G. Isebrands, K. S. Pregitzer, G. R. Hendrey, J. Sober, and G. K. Podila. 2001. Effects of elevated CO2 and O-3 on aspen clones varying in O-3 sensitivity: can CO2 ameliorate the harmful effects of O-3? Environmental Pollution **115**:473-481.

Xu, T., L. White, D. F. Hui, and Y. Q. Luo. 2006. Probabilistic inversion of a terrestrial ecosystem model: Analysis of uncertainty in parameter estimation and model prediction. Global Biogeochemical Cycles **20**.

Yang, L., H. Liu, Y. Wang, J. Zhu, J. Huang, G. Liu, G. Dong, and Y. Wang. 2009a. Impact of elevated CO(2) concentration on inter-subspecific hybrid rice cultivar Liangyoupeijiu under fully open-air field conditions. Field Crops Research **112**:7-15.

Yang, L. X., H. Y. Huang, H. J. Yang, G. C. Dong, H. J. Liu, G. Liu, J. G. Zhu, and Y. L. Wang. 2007. Seasonal changes in the effects of free-air CO2 enrichment (FACE) ion nitrogen (N) uptake and utilization of rice at three levels of N fertilization. Field Crops Research **100**:189-199.

Yang, L. X., J. Y. Huang, H. J. Yang, G. C. Dong, G. Liu, J. G. Zhu, and Y. L. Wang. 2006. Seasonal changes in the effects of free-air CO2 enrichment (FACE) on dry matter production and distribution of rice (Oryza sativa L.). Field Crops Research **98**:12-19.

Yang, L. X., H. J. Liu, Y. X. Wang, J. G. Zhu, J. Y. Huang, G. Liu, G. C. Dong, and Y. L. Wang. 2009b. Impact of elevated CO2 concentration on inter-subspecific hybrid rice cultivar Liangyoupeijiu under fully open-air field conditions. Field Crops Research **112**:7-15.

Zak, D. R., W. E. Holmes, K. S. Pregitzer, J. S. King, D. S. Ellsworth, and M. E. Kubiske. 2007. Belowground competition and the response of developing forest communities to atmospheric CO2 and O-3. Global Change Biology **13**:2230-2238.

Zhang, D. Y., G. Y. Chen, Z. Y. Gong, J. Chen, Z. H. Yong, J. G. Zhu, and D. Q. Xu. 2008. Ribulose-1,5-bisphosphate regeneration limitation in rice leaf photosynthetic acclimation to elevated CO2. Plant Science **175**:348-355.

Zheng, X. H., Z. X. Zhou, Y. S. Wang, J. G. Zhu, Y. L. Wang, J. Yue, Y. Shi, K. Kobayashi, K. Inubushi, Y. Huang, S. H. Han, Z. J. Xu, B. H. Xie, K. Butterbach-Bahl, and L. X. Yang. 2006. Nitrogen-regulated effects of free-air CO2 enrichment on methane emissions from paddy rice fields. Global Change Biology **12**:1717-1732.

Zhu, C. W., J. G. Zhu, Q. Zeng, G. Liu, Z. B. Xie, H. Y. Tang, J. L. Cao, and X. Z. Zhao. 2009. Elevated CO2 accelerates flag leaf senescence in wheat due to ear photosynthesis which causes greater ear nitrogen sink capacity and ear carbon sink limitation. Functional Plant Biology **36**:291-299.

Appendix J References for meta-analysis in Chapter 5

Aranda, X., C. Agusti, R. Joffre, and I. Fleck. 2006. Photosynthesis, growth and structural characteristics of holm oak resprouts originated from plants grown under elevated CO2. Physiologia Plantarum **128**:302-312.

Bauer, G. A., G. M. Berntson, and F. A. Bazzaz. 2001. Regenerating temperate forests under elevated CO2 and nitrogen deposition: comparing biochemical and stomatal limitation of photosynthesis. New Phytologist **152**:249-266.

Bown, H. E., M. S. Watt, P. W. Clinton, E. G. Mason, and B. Richardson. 2007. Partititioning concurrent influences of nitrogen and phosphorus supply on photosynthetic model parameters of Pinus radiata. Tree Physiology **27**:335-344.

Bruck, H. and S. W. Guo. 2006. Influence of N form on growth and photosynthesis of Phaseolus vulgaris L. plants. Journal of Plant Nutrition and Soil Science-Zeitschrift Fur Pflanzenernahrung Und Bodenkunde **169**:849-856.

Carswell, F. E., D. Whitehead, G. N. D. Rogers, and T. M. McSeveny. 2005. Plasticity in photosynthetic response to nutrient supply of seedlings fr

om a mixed conifer-angiosperm forest. Austral Ecology **30**:426-434.

Cernusak, L. A., L. B. Hutley, J. Beringer, J. A. M. Holtum, and B. L. Turner. 2011. Photosynthetic physiology of eucalypts along a sub-continental rainfall gradient in northern Australia. Agricultural and Forest Meteorology **151**:1462-1470.

Deng, X., W. H. Ye, H. L. Feng, Q. H. Yang, H. L. Cao, K. Y. Hui, and Y. Zhang. 2004. Gas exchange characteristics of the invasive species Mikania micrantha and its indigenous congener M. cordata (Asteraceae) in South China. Botanical Bulletin of Academia Sinica **45**:213-220.

Domingues, T. F., P. Meir, T. R. Feldpausch, G. Saiz, E. M. Veenendaal, F. Schrodt, M. Bird, G. Djagbletey, F. Hien, H. Compaore, A. Diallo, J. Grace, and J. Lloyd. 2010. Co-limitation of photosynthetic capacity by nitrogen and phosphorus in West Africa woodlands. Plant Cell and Environment **33**:959-980.

Grassi, G., P. Meir, R. Cromer, D. Tompkins, and P. G. Jarvis. 2002. Photosynthetic parameters in seedlings of Eucalyptus grandis as affected by rate of nitrogen supply. Plant Cell and Environment **25**:1677-1688.

Han, Q. M., T. Kawasaki, T. Nakano, and Y. Chiba. 2008. Leaf-age effects on seasonal variability in photosynthetic parameters and its relationships with leaf mass per area and leaf nitrogen concentration within a Pinus densiflora crown. Tree Physiology **28**:551-558.

Jach, M. E. and R. Ceulemans. 2000. Effects of season, needle age and elevated atmospheric CO2 on photosynthesis in Scots pine (Pinus sylvestris). Tree Physiology **20**:145-157.

Katahata, S. I., M. Naramoto, Y. Kakubari, and Y. Mukai. 2007. Photosynthetic capacity and nitrogen partitioning in foliage of the evergreen shrub Daphniphyllum humile along a natural light gradient. Tree Physiology **27**:199-208.

Kubiske, M. E., D. R. Zak, K. S. Pregitzer, and Y. Takeuchi. 2002. Photosynthetic acclimation of overstory Populus tremuloides and understory Acer saccharum to elevated atmospheric CO2 concentration: interactions with shade and soil nitrogen. Tree Physiology **22**:321-329.

Manter, D. K., K. L. Kavanagh, and C. L. Rose. 2005. Growth response of Douglas-fir seedlings to nitrogen fertilization: importance of Rubisco activation state and respiration rates. Tree Physiology **25**:1015-1021.

Meir, P., P. E. Levy, J. Grace, and P. G. Jarvis. 2007. Photosynthetic parameters from two contrasting woody vegetation types in West Africa. Plant Ecology **192**:277-287.

Merilo, E., K. Heinsoo, O. Kull, I. Soderbergh, T. Lundmark, and A. Koppel. 2006. Leaf photosynthetic properties in a willow (Salix viminalis and Salix dasyclados) plantation in response to fertilization. European Journal of Forest Research **125**:93-100.

Midgley, G. F., S. J. E. Wand, and N. W. Pammenter. 1999. Nutrient and genotypic effects on CO2-responsiveness: Photosynthetic regulation in Leucadendron species of a nutrient-poor environment. Journal of Experimental Botany **50**:533-542.

Norby, R. J., E. H. DeLucia, B. Gielen, C. Calfapietra, C. P. Giardina, J. S. King, J. Ledford, H. R. McCarthy, D. J. P. Moore, R. Ceulemans, P. De Angelis, A. C. Finzi, D. F. Karnosky, M. E.

Kubiske, M. Lukac, K. S. Pregitzer, G. E. Scarascia-Mugnozza, W. H. Schlesinger, and R. Oren. 2005. Forest response to elevated CO2 is conserved across a broad range of productivity. Proceedings of the National Academy of Sciences of the United States of America **102**:18052-18056.

Porte, A. and D. Loustau. 1998. Variability of the photosynthetic characteristics of mature needles within the crown of a 25-year-old Pinus pinaster. Tree Physiology **18**:223-232.

Rodriguez-Calcerrada, J., P. B. Reich, E. Rosenqvist, J. A. Pardos, F. J. Cano, and I. Aranda. 2008. Leaf physiological versus morphological acclimation to high-light exposure at different stages of foliar development in oak. Tree Physiology **28**:761-771.

Sholtis, J. D., C. A. Gunderson, R. J. Norby, and D. T. Tissue. 2004. Persistent stimulation of photosynthesis by elevated CO2 in a sweetgum (Liquidambar styraciflua) forest stand. New Phytologist **162**:343-354.

Tissue, D. T., K. L. Griffin, M. H. Turnbull, and D. Whitehead. 2005. Stomatal and non-stomatal limitations to photosynthesis in four tree species in a temperate rainforest dominated by Dacrydium cupressinum in New Zealand. Tree Physiology **25**:447-456.

Turnbull, T. L., M. A. Adams, and C. R. Warren. 2007. Increased photosynthesis following partial defoliation of field-grown Eucalyptus globulus seedlings is not caused by increased leaf nitrogen. Tree Physiology **27**:1481-1492.

Warren, C. R. 2004. The photosynthetic limitation posed by internal conductance to CO2 movement is increased by nutrient supply. Journal of Experimental Botany **55**:2313-2321.

Wohlfahrt, G., M. Bahn, E. Haubner, I. Horak, W. Michaeler, K. Rottmar, U. Tappeiner, and A. Cernusca. 1999. Inter-specific variation of the biochemical limitation to photosynthesis and related leaf traits of 30 species from mountain grassland ecosystems under different land use. Plant Cell and Environment **22**:1281-1296.

Zhang, S. R. and Q. L. Dang. 2006. Effects of carbon dioxide concentration and nutrition on photosynthetic functions of white birch seedlings. Tree Physiology **26**:1457-1467.